SANDIA REPORT
SAND2017-13084
Unlimited Release
Printed November 2017

Cordova Electric Cooperative Energy Storage Evaluation

Jeremy B Vandermeer, Benjamin Schenkman, Michael Baca, Marc Mueller-Stoffels, Clay Koplin

Prepared by
Sandia National Laboratories
Albuquerque, New Mexico 87185 and Livermore, California 94550

Sandia National Laboratories is a multi-mission laboratory managed and operated by National Technology and Engineering Solutions of Sandia, LLC, a wholly owned subsidiary of Honeywell International, Inc., for the U.S. Department of Energy's National Nuclear Security Administration under contract DE-NA0003525.

Issued by Sandia National Laboratories, operated for the United States Department of Energy by National Technology and Engineering Solutions of Sandia, LLC.

Available to DOE and DOE contractors from
U.S. Department of Energy
Office of Scientific and Technical Information
P.O. Box 62
Oak Ridge, TN 37831

Telephone: (865) 576-8401
Facsimile: (865) 576-5728
E-Mail: reports@osti.gov
Online ordering: http://www.osti.gov/scitech

Available to the public from
U.S. Department of Commerce
National Technical Information Service
5301 Shawnee Rd
Alexandria, VA 22312

Telephone: (800) 553-6847
Facsimile: (703) 605-6900
E-Mail: orders@ntis.gov
Online order: https://classic.ntis.gov/help/order-methods/

SAND2017-
13084130841308413084130841308413084130841308413084130841308413084130841308413084130841308
41308413084130841308413084130841308413084130841308413084130841308413084130841308413084130
84130841308413084130841308413084130841308413084130841308413084130841308413084130841308413
08413084130841308413084130841308413084130841308413084130841308413084130841308413084130841
30841308413084130841308413084130841308413084130841308413084130841308413084130841308413084
13084130841308413084130841308413084130841308413084130841308413084130841308413084130841308
41308413084130841308413084130841308413084130841308413084130841308413084130841308413084130
84130841308413084130841308413084130841308413084130841308413084130841308413084130841308413
08413084130841308413084130841308413084130841308413084130841308413084130841308413084130841
30841308413084130841308413084130841308413084130841308413084130841308413084130841308413084
13084130841308413084130841308413084130841308413084130841308413084130841308413084130841308
41308413084130841308413084130841308413084130841308413084130841308413084130841308413084130
84130841308413084130841308413084130841308413084130841308413084130841308413084130841308413
08413084130841308413084130841308413084130841308413084130841308413084130841308413084130841
30841308413084130841308413084130841308413084130841308413084130841308413084130841308413084
13084130841308413084130841308413084130841308413084130841308413084130841308413084130841308
41308413084130841308413084130841308413084130841308413084130841308413084130841308413084130
84130841308413084130841308413084130841308413084130841308413084130841308413084130841308413
08413084130841308413084130841308413084130841308413084130841308413084130841308413084130841
30841308413084130841308413084130841308413084130841308413084130841308413084130841308413084
13084130841308413084130841308413084130841308413084130841308413084130841308413084130841308
41308413084130841308413084130841308413084130841308413084130841308413084130841308413084130
84130841308413084130841308413084130841308413084130841308413084130841308413084130841308413
08413084130841308413084130841308413084130841308413084130841308413084130841308413084130841
30841308413084130841308413084130841308413084130841308413084130841308413084130841308413084
13084130841308413084130841308413084130841308413084130841308413084130841308413084130841308
41308413084130841308413084130841308413084130841308413084130841308413084130841308413084130
84130841308413084130841308413084130841308413084130841308413084130841308413084130841308413
08413084130841308413084130841308413084130841308413084130841308413084130841308413084130841
30841308413084130841308413084130841308413084130841308413084130841308413084130841308413084
13084130841308413084130841308413084130841308413084130841308413084130841308413084130841308
41308413084130841308413084130841308413084130841308413084130841308413084130841308413084130
84130841308413084130841308413084130841308413084130841308413084130841308413084130841308413
08413084130841308413084130841308413084130841308413084130841308413084130841308413084130841
30841308413084130841308413084130841308413084
Printed September 2017
Unlimited Release

Cordova Electric Cooperative Energy Storage Evaluation

Jeremy B Vandermeer and Marc Mueller-Stoffels
Alaska Center for Energy and Power

P.O. Box 7559-10
Fairbanks, Alaska 99775-5910

Michael Baca and Benjamin Schenkman
Sandia National Laboratories
P. O. Box 5800
Albuquerque, New Mexico 87185-MS1108

Clay Koplin
Cordova Electric Cooperative
P.O. Box 20
Cordova, Alaska 99574

Abstract

The community of Cordova, Alaska currently uses diesel and run-of-river hydro generation for its electricity needs. In the past, 60% of the Cordova summer load was supplied by the run-of-river generation. The majority of the time, the load was supplied only by the run-of-river generation. The bulk of generated electricity is delivered to Cordova's industrial fish processing plants and to other industrial loads. With the expansion of Cordova's fishing industry, the run-of-river generation is less often able to supply 100% of the load demand. When the run-of-river generation is not able to supply 100% of the load demand it has to be supplemented by diesel generation. There are also many times when the load demand is low and the available run-of-river generation has to be curtailed by spilling water which could be stored in an energy storage system. Sandia National Laboratories and Alaska Center for Energy and Power collaborated to evaluate how an energy storage system can be used to capture the spilled water and how it can economically and technically benefit Cordova during the fishing season and other times throughout the year. Results from this study are summarized in this report.

ACKNOWLEDGMENTS

Sandia National Labs and Alaska Center for Energy and Power would like to acknowledge Dr. Imre Gyuk, Program Manager for Energy Storage R&D at the Department of Energy Office of Electricity, and Mr. Clay Koplin, CEO of Cordova Electric Cooperative and Mayor for the City of Cordova. Their support and guidance was invaluable to the successful study. The Alaska Center for Energy and Power performed the energy storage sizing analysis. Sandia National Laboratories performed the dynamic system modeling and analysis.

Table of Contents

Figures

Tables

1. INTRODUCTION

The City of Cordova and the adjacent Native Village of Eyak have a combined population of 2,286 residents as of 2014 and are located between the Southeastern entrance to Prince Williams Sound and the Copper River delta in the Gulf of Alaska. These communities are accessible only by sea and air with regular ferry sailings and daily jet service. A project to convert the former railroad line (closed in 1941) to the copper fields at the Kennecott Mine to a road connection was initiated but never completely. The main economic engine of Cordova is a thriving fishing industry, which ranks the city in the top 20 fishing ports of the nation both by volume and value. The fishing activity regularly nets between $45M and $85M annually and causes the summer population in Cordova to nearly double.

Cordova Electric Cooperative (CEC) serves 1,580 electric customers in the City of Cordova and the Native Village of Eyak. Both supply and demand for electricity follow strong seasonal cycles. The bulk of generated electricity is delivered to industrial fish processing plants and support industry, mostly during the summer months. This causes system loads to peak at nearly 10 MW during the fishing season. In winter months, demand declines and daytime peaks can drop below 3 MW. CEC has two run-of-river hydroelectric power plants with generation capacity totaling 7.125 MW that are capable of supplying the summer load demand as much as 60% of the time. However, recent expansion of the fishing industry has exceeded the supply capability of the hydro units and the additional electricity needs are being met with supplemental diesel generation. At the same time, hydropower capacity exceeds diurnal off-peak and night time demand, resulting in 10 million kWh equivalent of the run-of-river water to be spilled over the dam. Hence, in the current configuration, the benefit from hydropower is limited by a mismatch between variable supply and variable load demand.

There is an opportunity for application of energy storage to maintain adequate levels of frequency and spinning reserve when running solely on hydropower, and to allow available diesel generators to operate more efficiently. Frequency regulation during hydro-only operation is currently accomplished with a custom retrofit governor on both of the run-of-river power plants allowing either one to deflect a selected amount of potential generation and hold it in reserve. This has two effects detrimental to optimal operation. First, the hydropower generators' governor system is subject to excessive wear, as the core hardware was not designed for fast frequency regulation. Second, providing frequency regulation with this prime-generating asset requires curtailing 500kW (17% of nameplate capacity) for spinning reserve. An energy storage system with inverters of suitable size and functionality could resolve both equipment wear and waste of hydropower capacity. Diesel generators at CEC's Orca Power Plant are scheduled and dispatched based on reliability measures empirically driven through past experiences. At any given time, there is always enough generation capacity online, sometimes lightly loaded, so that if one generator fails the other generators online have enough capacity to satisfy the load demand. Operating the diesel generators in this manner is not optimal for fuel consumption. Energy storage can be used as a spinning reserve to allow generators to operate less frequently and at a more optimal set point reducing fuel consumption and maintenance cost.

This report discusses results of the economic and technical analyses conducted by the Alaska Center for Energy and Power (ACEP) and Sandia National Laboratories (Sandia). The report describes the assumptions and models that were used for sizing an energy storage system in the Cordova electrical system to be used as spinning reserve and/or smoothing the load seen by the existing Cordova generation fleet. The Alaska Center for Energy and Power performed the energy storage sizing analysis. Sandia National Laboratories performed the dynamic system modeling and analysis.

2. ESTIMATING SPILLED POWER

To determine the appropriate size range of the energy storage system, we first calculated the amount of spilled water by the hydropower plants. A test was performed by CEC where the amount of water spilled over the dam was varied starting from zero and increased in discrete steps. The water that was not spilled over the dam was run through the turbine generators in the hydropower plants. The total power of the water spilled over the dam was taken to be equivalent to the reduction in output from the turbine generator scaled by the turbine generator efficiency. A physical relationship was developed to calculate the hydro power spilled over the dam at each instance. The power of the water going over the dam can be calculated with Equation 1. For more details on estimating hydro power, refer to Appendix A.

Equation 1

$$P_{spill} = \rho g(h_w+h_p)q\mu_t = \rho \cdot g \cdot (h_w+h_p) \cdot w \cdot c_d \cdot (2/3 \cdot \sqrt{2g} \cdot h_{diff}^{3/2} + v_0 \cdot h_{diff}) \cdot \mu_t$$

Where:

ρ	Density of the water in kg/m^3, assumed to be 1,000 kg/m^3.
g	Gravitational constant, 9.81 m/s^2.
hw	Height of the water in the forebay in m.
h_p	Height of the penstock, estimated to be 87.9 m.
q	*F*low of water over the dam, in m^3/s.
μ_t	Efficiency of the turbine generator, calculated to be 73%.
w	Width of the dam, estimated to be 13 m.
c_d	Coefficient of discharge for an inflatable dam.
h_{diff}	Difference in height between the height of the water in the forebay and the height of the dam, in m.
v_0	Initial velocity of water in the river, in m/s.

The only unknown variables in this equation are c_d, h_{diff} and v_0. An initial estimate for c_d and v_0 were 0.3 and 0.7 m/s respectively. The equation was solved for h_d which is the height of the dam. A relationship for the height of the dam to the dam pressure and water height in the forebay was calculated. Equation 2 shows the relationship.

Equation 2

$$h_d = 0.256 \cdot p_d^3 - 2.500 \cdot p_d^2 + 3.748 \cdot p_d - 1.955 \cdot h_w^2 + 3.460 \cdot h_w + 1.939 \cdot p_d h_w - 4.353$$

Where:

- h_d is the height of the dam in m.
- p_d is the pressure in the dam in psi.
- h_W is the height of the water in the forebay in m.

The water speed v_0 was solved using P_{spill} from Equation 1 and the calculated height of the dam h_d in Equation 2. Water speed did not vary significantly with any of the measured predictors (p_d and h_w); therefore, v_0 was kept constant. Spilled power of the water over the dam (P_{spill}) was calculated using the calculated values for h_d and c_d and the assumed value for v_0. A good fit was obtained with a 99kW standard deviation between the predicted and measured P_{spill}. After calculating and accounting for dam dynamics, as shown in Appendix B, the fit improved to a standard deviation of 87kW shown in Figure 1.

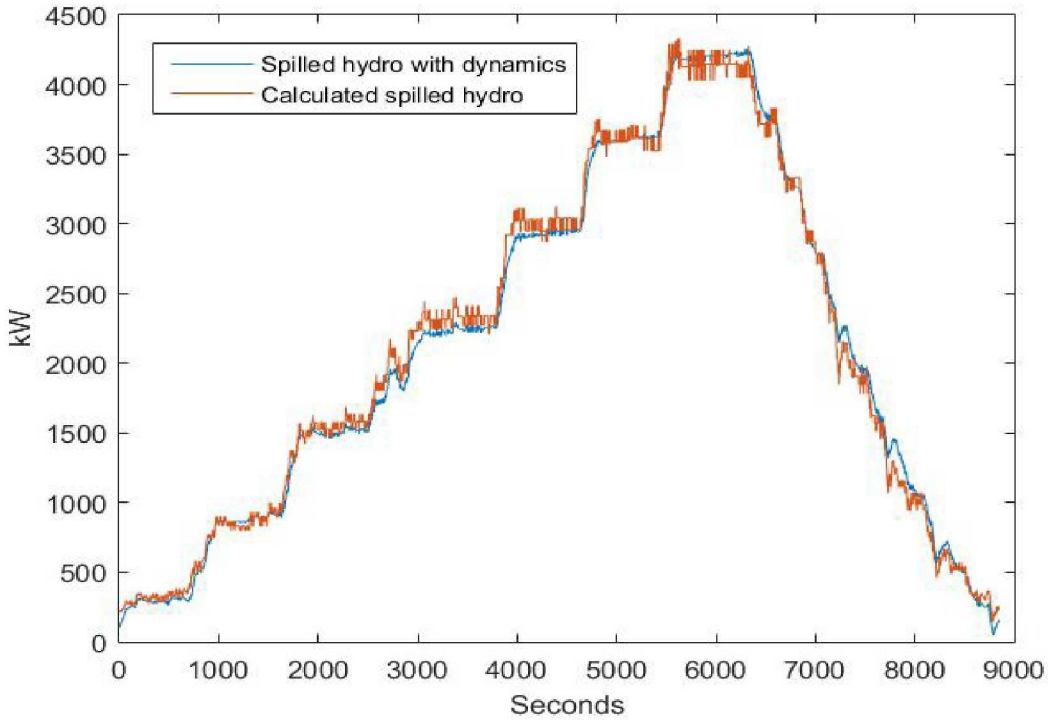

Figure 1 - The compared calculated and measured spilled hydro

There were several challenges applying this fit to the data. First, during the test, no water was deflected at the turbine generator while in actual operation 500kW or more is often deflected. Calculated values from CEC's SCADA system were used for the deflected power. Based on conversations with CEC and from analyzing the data, the calculated deflected hydro often seem to be higher than was is calculated. Second, the forebay water levels and dam pressures used in the test were higher than the values usually seen in normal operation. Thus, the relation between forebay water height, dam pressure and dam height is an extrapolation from the test data for much of the normal operations, which reduces confidence in the fit.

The calculated spilled hydro power seemed high when compared with non-spill hydro power. This could either be because the calculated spilled hydro from Equation 1 is too high or the deflected hydro from the CEC SCADA system during non-spill events is too low. In order to be conservative, the calculated spilled hydro was scaled in half to match the deflected calculations. The calculated available hydro used in this report is considered to be conservative.

3. ENERGY STORAGE SYSTEM SIZING

A range of energy storage system (ESS) power ratings (0.5 to 4.0 MW) and capacity ratings (0.5 to 5.5 MWh) were simulated for determining proper ESS sizing. Multiple simulations with various ESS sizes were performed as well as varying the dispatch control options. Control options included allowing the diesel generators to charge the ESS up to 75%, not allowing diesel generators to charge the ESS, and smoothing the diesel and hydro load profiles.

The performance of the ESS in the CEC grid was analyzed according to diesel savings, as well as diesel operation and ESS operation profiles. Diesel savings correspond to reduced fuel consumption, which can be directly translated into monetary savings. For the diesel operation statistics such as diesel off-times, diesel runtimes, diesel capacity factors, diesel switching (cycling a diesel unit on and off) and diesel ramp rates were collected. Increasing diesel off-time and reducing diesel runtime reduces maintenance costs. Increasing the diesel capacity factor and reducing diesel switching can reduce wear on the diesel generators and increase their life expectancy. Reduction in the load ramp rates on the diesel generator could reduce wear on the diesel generators. The main ESS operation statistic that was recorded throughout the simulations was the cycles per year. By minimizing the number of cycles on the ESS the life expectancy of the ESS is increased. More detail on the sizing of the energy storage is discussed later in this paper.

[PAGE LEFT INTENTIONALLY BLANK]

4. MODEL INPUTS

4.1. Hydro

The calculation for spilled hydro was applied to 2011, 2012 and 2013 operating data from CEC. Data for 2013 was only available up to October 19. The total available hydro is calculated with Equation 3. The total available hydro power equals the power diverted at the turbine generator, the power through the turbine generators and the power spilled over the dam.

Equation 3

$$P_{hydro}{}' = P_{diverted} + P_{turbine} + P_{spill}$$

$$P_{hydro} = \begin{cases} P_{hydro}{}', if\ P_{hydro}{}' < 6MW \\ 6MW, if\ P_{hydro}{}' \geq 6MW \end{cases}$$

The power through the turbine generator was measured and the diverted power at the turbine generator was calculated on the CEC SCADA system. There were several challenges applying the relationship for calculation spilled hydro to the rest of the data, as outlined in Appendix C.

4.2. Load

The load was calculated as the sum of all generation, to include transmission and distribution losses. As described in Appendix D, there were some very high ramp rates in measured data for the different generators. High ramp rates seemed to be the result of oscillation in measurements, blackouts and dropping off a hydro turbine generator to clear a rack. This resulted in 434 instances of 500 to 1500 kW/sec ramp rates in the calculated load. These events can cause grid blackouts in the simulation since there is only 500 kW of spinning reserve required. Therefore, ramp rates over 500kW/s were filtered out.

4.3. Diesel-ESS schedule

The diesel-ESS schedule attempted to minimize diesel consumption. The fuel consumption of the diesel generators was estimated fuel curves and diesel consumption while warming up and cooling down. The diesel schedule could be triggered by a diesel generator approaching its upper or lower bound of operation, less spinning reserve capacity than required, spilled hydro or the presence of a more efficient generator combination. The diesel schedule tried to predict the diesel efficiency of all possible generator combination and would bring online the optimal one.

4.4. Estimated diesel consumption

The diesel consumption was estimated using maximum diesel efficiency estimates from CEC, listed in Table 1 and applied to a generic per unit diesel fuel curve shown in Figure 2. The max efficiencies are best guess estimates for all units in the Orca Power Plant except for Gen7, which has a fuel flow meter. The minimum optimal loading (MOL) and startup times are based on CEC's

grid operation. The cool down times were assumed to be the same as startup times. However, this is too short and the actual cool off time is around 10 minutes.

Table 1: Diesel generator statistics and operation constraints at the Orca Power Plant.

Name	Size[kW]	Max Efficiency[kWh/gal]	Minimum Optimal Loading(MOL)	Start up/cool down time [min]	Min. run time	Diesel consumption during warm up cool down [gal/hr]
G3	2500	14.56	0.5	2	60	77
G4	2450	13.60	0.5	2	60	77
G7	3800	14.40	0.5	2	60	77
G5	1125	14.45	0.3	0.5	60	26
G6	1125	14.45	0.3	0.5	60	26

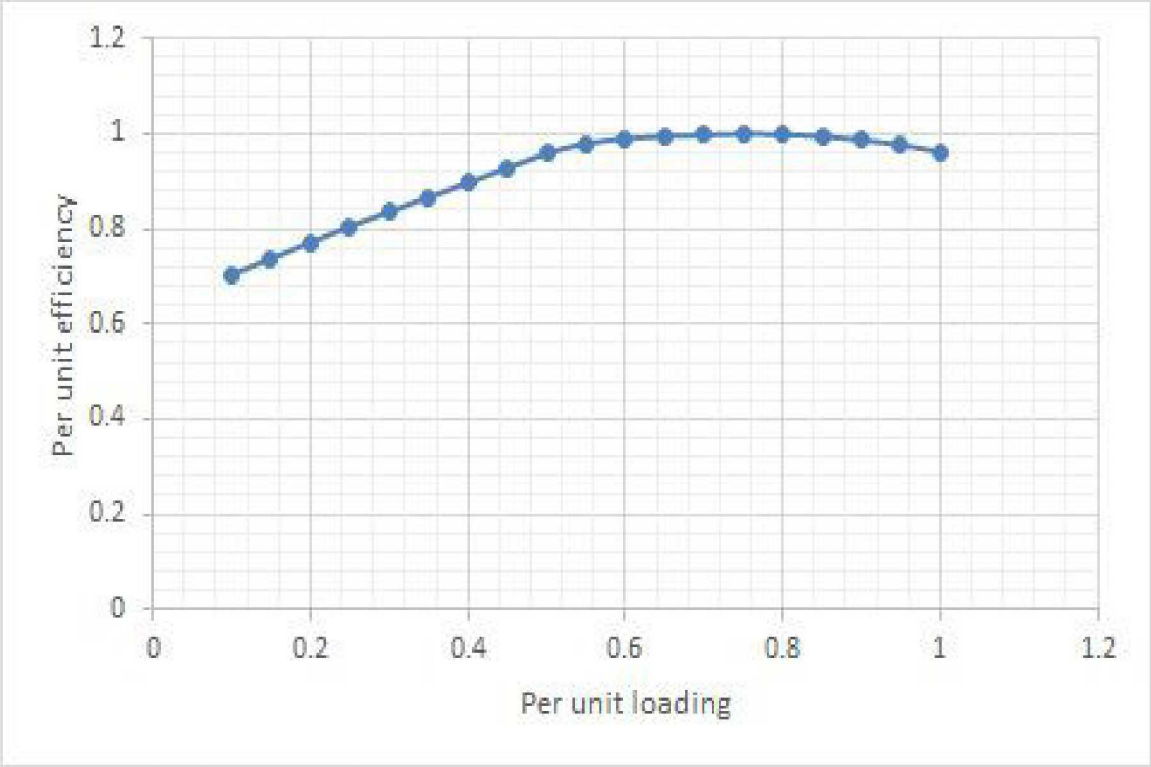

Figure 2 - Generic per unit fuel curve scaled by the recorded maximum efficiency of each generator.

4.5. Calculate next state efficiency

Diesel efficiency of different generating combination was calculated with Equation 4. In this case, diesel efficiency refers to the total kWh supplied (load) divided by gallons consumed. Thus, supplying the load with hydro is the most efficient option. The efficiency of using the ESS depends if it has been charged with hydro or with diesel. A penalty was applied to diesel

switching (turning a generator on or off) to account for additional engine wear and discourage excessive diesel switching operation.

The diesel schedule will try to bring online the most efficient option. If the grid is approaching critical operating bounds, it will bring online any diesel generating option that brings it back under normal operating conditions that can be switched immediately. Rules and triggers for the diesel schedule are listed in Appendix E.

Equation 4

$$\mu_{total}(i)=P_{load\ mean}/[(P_{load\ diff}(i))+c_1 \cdot \text{sum}(P_{sw\ diesel\ effective}(i,:))+c_2 \cdot P_{ESS}(i)/\ \mu_{diesel0}]$$

Where:

μ_{total}	Estimated diesel efficiency if generator combination *i* is brought online. This is the total load divided by the kW equivalent of the total diesel consumed to supply that load and assigns no cost to hydro
$P_{load\ mean}$	Average load over the past 5 minutes
$P_{load\ diff}(i)$	Amount of the load that would be supplied by the diesels if generator combination *i* is brought online. As much hydro as possible will supply the load as possible while maintaining a minimum MOL loading on the diesels. The maximum value is full capacity, after which the ESS will discharge to cover the rest of the load
$\mu_{diesel}(i)$	Efficiency of the diesel generator combination *i at loading* $P_{load\ diff}(i)$
$P_{sw\ diesel\ effective}(i)$	Effective kW value of the diesel consumption required to switch on or off each diesel generator to bring generator combination *i* online.
c_1	Constant that increases the diesel cost of switching to reflect other non-diesel costs of switching and reduce diesel switching. Default value is 3.
c_2	Scaled ratio of the charging of the ESS by diesel by the total charging of the eSS in the past day
$P_{ESS}(i)$	ESS discharge required if the load is higher than generator combination *i* capacity
$\mu_{diesel0}$	Assumed diesel efficiency of 33% (13 kWh/gal)

The effective kW value of the diesel consumption by each diesel generator required to bring diesel generator combination *i* online is given by Equation 5.

Equation 5

$$P_{SW\ diesel\ effective}(i,j) = C_{ON\ S_{sw}}(j) * 39\frac{kWh}{gal} * \frac{t_{sw}(j)}{t_{\min\ run\ time}(j)}$$

Where:

$C_{ON\ Ssw}(j)$	Fuel consumption in gallons required to switch generator *j* in generator combination *i*
$t_{sw}(j)$	Time required to switch generator *j* in generator combination *i*
$t_{min\ run\ time}(j)$	Minimum amount of time required for generator *j* to run for

The ratio of ESS charging by diesel to the total ESS charging, c_2 is given by Equation 6.

Equation 6

$$C_2 = \frac{E_{ch\ diesels}}{E_{ch\ total}}$$

$E_{ch\ diesels}$	Diesel charging of the ESS in the past day (kWh)
$E_{ch\ total}$	Total charging of the ESS in the past day (kWh)

4.6. Hydro Control

At the Power Creek hydro plant, deflectors at the turbine generators control the loading by deflecting water onto or away from the turbine generator. When running in diesel-off mode, an approximate of 500 kW deflection is maintained. When the water head at the dam drops below a certain height, one of the 1,125 kW CAT generators is brought online and loaded at around 500 kW. If the diesel output drops below 400 kW for a minimum of 1 minute, the deflectors reduce the loading on the turbine generator by 100 kW. If the diesel output goes above 700 kW, the deflectors increase the loading on the turbine generator by 100 kW. When the diesel generators are running, the dam is fully inflated. Often, no water is spilling over the dam in this situation, with all excess water diverted at the turbine generator.

If the reserve of deflected water at the turbine generator reaches 1,100 kW, the system will return to running in diesel-off mode. When the system switches to diesel-off, the diverted water is maintained at around 500 kW and the dam is lowered to maintain the water level and excess water is spilled over the dam. When the water height begins to drop below the dam a diesel generator is brought back online.

4.7. Modified control scheme

CEC's current control scheme does not maximize the amount of hydro used in the grid. When a diesel generator is switched online from diesel-off, there is around 500 kW of deflected hydro at the turbine generators. The loading on the generator is maintained between 400 and 700 kW (35 – 60%). If the diesels were loaded around a minimum loading of 400 kW whenever there was available hydro this would result in significant diesel savings approximately 0.5 GWh.

It is possible that this control scheme would require operating the diesel and hydro turbine generator in a way that utility operators are not comfortable with. In this case, adding the ESS could make operating the grid with the control scheme more feasible. The ESS would supply additional back-up and support the diesel and hydro. Based on simulations described later in this report, adding a 1 MWh ESS increased the saved diesel to 1 GWh, twice as much as only modifying the control scheme.

Figure 3 shows an example of the modified control scheme. The measured diesel output (red) and simulated diesel output are shown (green line). The simulated output spend much more time at the minimum loading than the measured. 500 kW of spinning reserve capacity is maintained in both scenarios. The hydro turbine generator and diesel generator outputs both add up to the same in the simulated and measured cases (light blue line). The measured deflected reserve at the hydro turbine generators is shown (yellow line). The simulation allows smaller capacity generators to run online, as shown by the diesel generator capacity (maroon and dark blue lines).

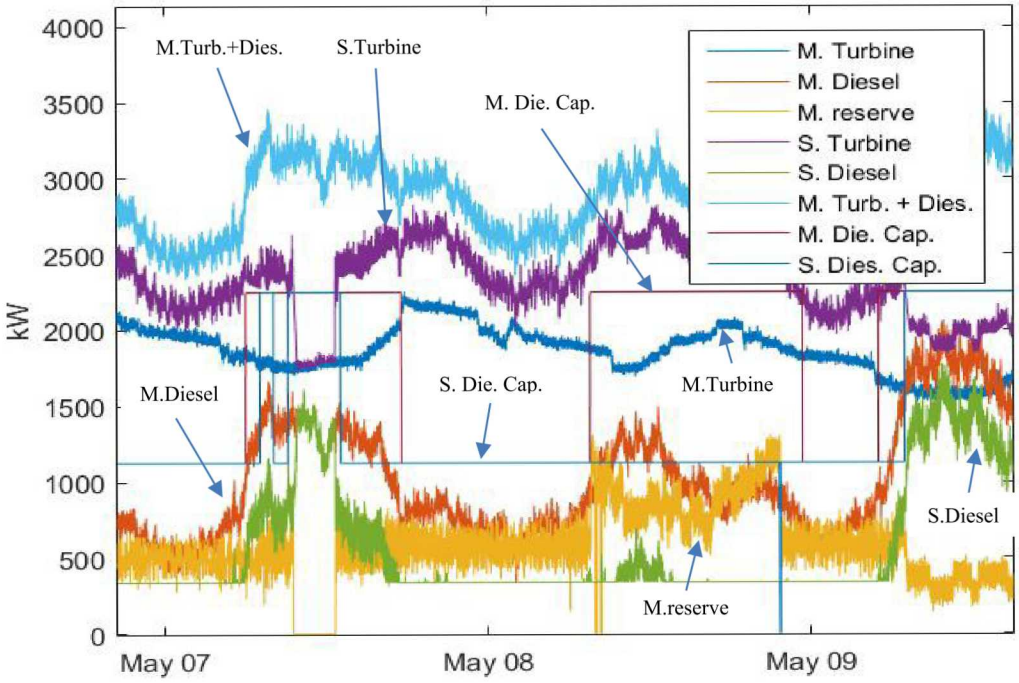

Figure 3 - Comparison of the measured and simulated hydro control

[PAGE LEFT INTENTIONALLY BLANK]

5. ESS CONTROL

5.1. Smoothing

A real time FIR lowpass filter was used in the simulation to load the ESS in order to smooth the loading of the diesel and hydro generators. The filters used were 100th order with a cutoff frequency of 0.001 Hz. Smoothing significantly reduced diesel and hydro ramp rates. Figure 4 shows unsmoothed and smoothed diesel load profiles, it added significant low amplitude cycling on the ESS.

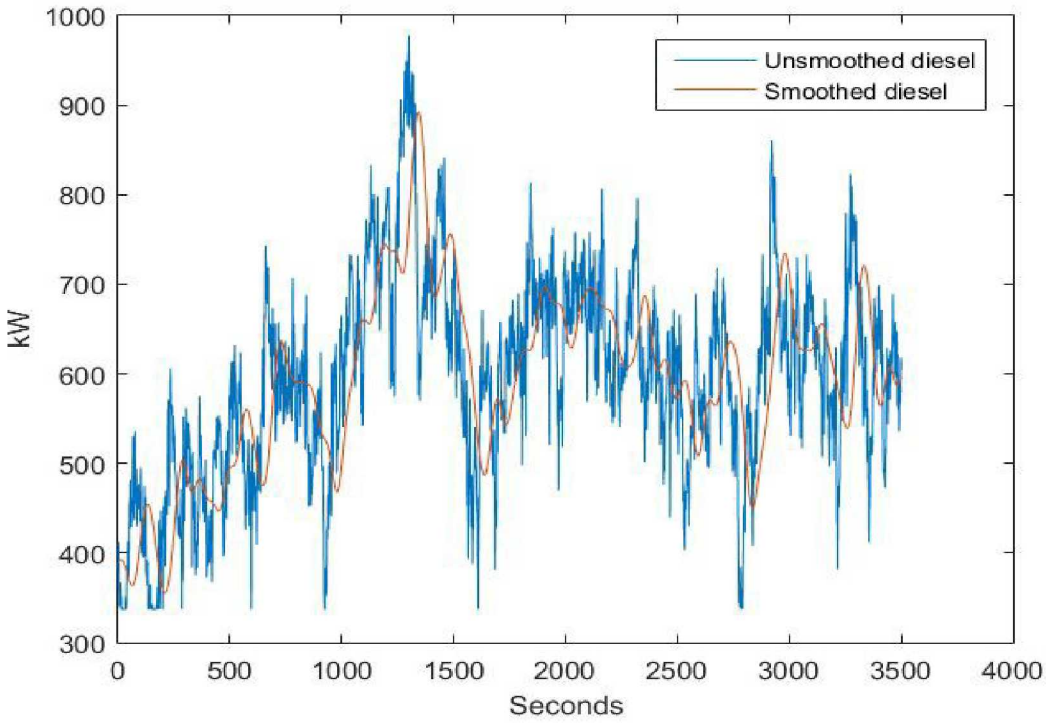

Figure 4 - Smoothed and unsmoothed diesel load profile.

5.2. Diesel charging of ESS

Diesel generators were allowed to charge the ESS under certain conditions. The idea was that a fully charged ESS can supply spinning reserve capacity which allows smaller capacity diesel generators to run online at a higher loading or more hydro into the grid. The diesel generators were allowed to charge the ESS up to a certain maximum state of charge (MaxSOC). Maximums ranging from 0 to 90% were tested and finally a maximum of 75% was chosen. The 75% had the greatest diesel savings.

The diesels were optimally loaded in order to charge the ESS according to Table 2. Maximum that the diesel loading can be increased to in order to charge the ESS depends on the ratio of the state of charge (SOC) of the ESS to the maximum SOC that the diesels are allowed to charge the ESS.

Table 2: The maximum amount that the diesel loading can be increased to in order charge the ESS.

Ratio of ESS SOC to MaxSOC[%]	Max Allowed Diesel Loading [%]
100 to 30	65
30 to 10	75
10 to 0	85

5.3. ESS Discharge Time

The ESS was considered to be a generating source in the diesel dispatch. The SOC of the ESS was required to be high enough to discharge for a certain amount of time at the power it was scheduled at in the diesel schedule. Different values of minimum discharge times were simulated and a value of 10 min was used in the simulations to minimize diesel switching while maximizing hydro utilization.

6. MEASURED DATA

This section summarizes the measured operating stats of the CEC grid for the years 2011 and 2012. These values will be used to compare the results of the simulations. The total diesel fuel consumption calculated for this data was around 6% lower than the measured fuel consumption. Results of the simulation are compared with this calculated fuel consumption since the same assumptions were made for all simulated scenarios. Comparing to a more efficient baseline makes the diesel savings more conservative since each kWh reduction of diesel output results in lower fuel savings.

6.1. 2011 Cordova Operational Stats

Table 3 shows the diesel generator operating statistics for the year 2011. Gen5, Gen6 and Gen7 were the most commonly used diesel generators. A total of 2817 hours were spent operating in diesel-off mode. The diesel generators were switched online a total of 1003 times and the total diesel generator output was 10.38 GWh. Table 3 gives the total load and hydro output for 2011.

The diesel consumption calculated based on the fuel curve in Figure 2 and diesel switching fuel consumption in Table 3 was 730,000 gallons. This is 35,000 gallons less than what was recorded. Table 4 gives the total load and hydro generation for Power Creek (PC) and Humpback Creek (HBC).

Table 3: The statistics of the operating diesel generators for 2011

	Gen5 (1125 kW)	Gen6 (1125 kW)	Gen4 (2450 kW)	Gen3 (2500 kW)	Gen7 (3800 kW)	Overall	Diesel Off
Run Time [hr]	2146	3009	690	1086	1516	8447	2817
Avg. Cap. Factor [%]	54	56	76	71	69	61	
Times Switched Online (#)	291	363	39	124	186	1003	
Total Output [GWh]	1.31	1.90	1.28	1.94	3.95	10.38	
Estimated online Diesel Consumption [kgal]	97.5	140.2	97.1	137.4	255.9	728.0	
Estimated Offline Diesel Consumption [kgal]	0.12	0.16	0.20	0.64	0.95	2.07	

Table 4: The total load and hydro output for 2011 and estimated total available hydro

Total Load [GWh]	27.68
Calculated Total Available PC Hydro [GWh]	21.06
Calculated Total Available HBC Hydro [GWh]	1.61
Total PC Turbine Generator Output[GWh]	15.71
Total HBC Turbine Generator Output [GWh]	1.61

6.2. 2012 Cordova Operational Stats

Table 5 shows the diesel generator operating stats for 2012. There is a more even utilization of the different diesel generators. A total of 2653 hours were spent operating in diesel-off mode. The diesel generators were switched online a total 729 times. The total diesel generator output was 10.67 GWh. The diesel consumption calculated based on the fuel curve in Figure 2 and diesel switching fuel consumption in Table 5 was 755,000 gallons. The recorded engine fuel consumption in 2012 was 811,000 gal, 56,000 gal more than calculated. Table 6 gives the total load and hydro generation and calculated total available hydro.

Table 5: The statistics of the operating diesel generator for 2012

	Gen5 (1125 kW)	**Gen6 (1125 kW)**	**Gen4 (2450 kW)**	**Gen3 (2500 kW)**	**Gen7 (3800 kW)**	**Overall**	**Diesel off**
Run Time [hr]	2139	878	1060	1900	1362	7339	2653
Ave Cap. Factor [%]	75	70	55	54	66	64	
Times Switched Online (#)	232	156	100	85	156	729	
Total Output [GWh]	3.43	1.33	1.83	3.55	0.53	10.67	
Estimated Online Diesel Consumption [kgal]	251.1	139.7	222.6	98.1	39.7	751.1	
Estimated Offline Diesel Consumption [kgal]	0.10	0.07	1.14	0.50	0.21	3.70	

Table 6: The total load and hydro output for 2012 and estimated total available hydro

Total Load [GWh]	27.86
Calculated total available PC hydro [GWh]	19.66
Calculated total available HBC hydro [GWh]	3.52
Total PC Turbine Generator output[GWh]	13.44
Total HBC Turbine Geneartor output [GWh]	3.52

[PAGE LEFT INTENTIONALLY BLANK]

7. RESULTS FOR ENERGY STORAGE SIZING

Calculations were performed to determine the what size of ESS would be required to take advantage of a given percentages of the spilled hydro. Then simulations were performed with no ESS as a benchmark to compare with the measured grid data. Finally, simulations with different ESS sizes were performed.

7.1. ESS Size Required for Reduction in Spilled Hydro

There are two reasons why hydropower is not used. The first is because of spinning reserve capacity (SRC) requirements. SRC is the amount of unused generating power that is online and available. In Cordova, 500 kW of SRC is maintained. When both the diesel generators and the hydro turbines are supplying the load, this often results in spilling or diverting hydropower that could be used. This can be referred to as operating constraints. In 2011, 1 GWh of hydropower went unused as a result of operating constraints.

The second reason is that there are times when there is more hydropower than load. Thus, even when the hydro turbines are supplying the full load, hydropower is not being used. This can be referred to as temporal mismatch. In 2011, 4.35 GWh of hydropower went unused as a result of temporal mismatch.

Energy storage systems can save hydropower by supplying SRC and minimizing operating constraints on the hydro turbines, or by addressing the temporal mismatch by saving hydropower when there is excess and discharging when it is needed (time-shifting). The following section will address the possible savings for each.

7.1.1. Possible savings through time-shifting

The differences between the available hydropower and the load throughout the year represent possible savings through time-shifting with an energy storage system. Figure 5 gives an indication of the power requirements for an energy storage system to perform time-shifting. shows the probability and cumulative distributions of the charging and discharging powers required to cover all differences between the hydro and the load in 2011. Red, yellow and green lines on the curve show, respectively, the charge and discharge powers required to cover 90, 75 and 50% of events.

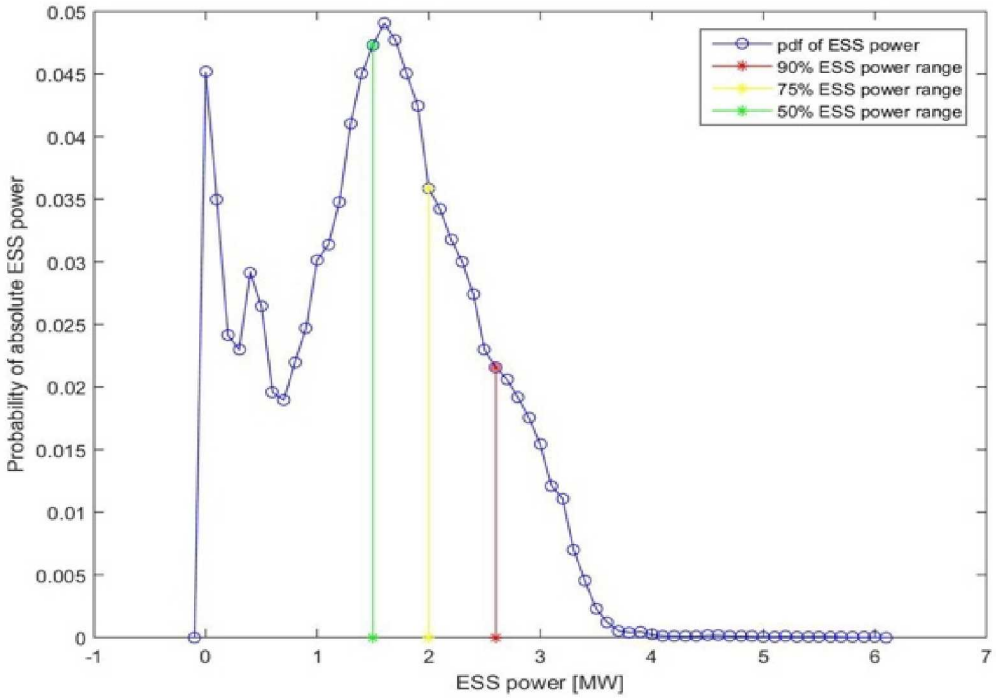

Figure 5 - The probability and cumulative distributions of the charging and discharging powers.

ESS power required for 50% of charge events [MW]	ESS power required for 75% of events [MW]	ESS power required for 90% of events [MW]
1.5	2	2.6

Table 7: ESS Power Requirements to cover a percentage of all charge and discharge events

Figure 6 shows the cumulative difference between the hydro and load over 2011. There is a net negative difference since the load (27.7GWh) is greater than the calculated total hydro. The ESS capacity required to store all excess hydro is the difference between the local minima and maxima, 3.7 GWh, which is three orders of magnitude larger than what can be considered practical.

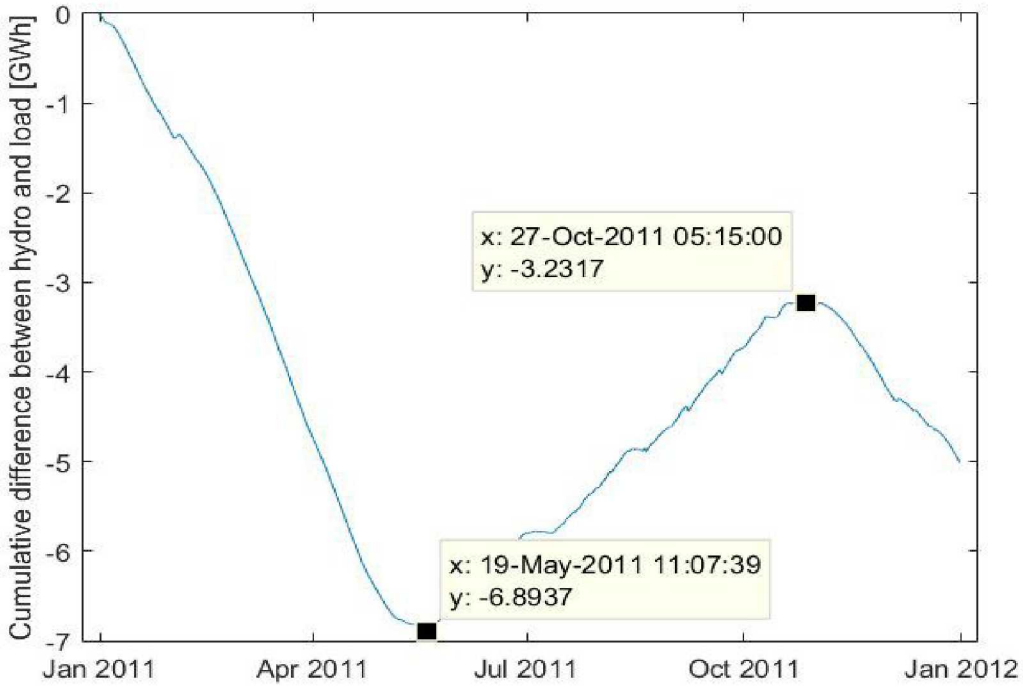

Figure 6 - The cumulative difference between hydro and load for 2011.

Figure 7 shows the possible hydropower savings that can be achieved for a given size of energy storage system. It was calculated using rainflow analysis on the cumulative difference between hydropower and the load, shown in Figure 6. It shows that little savings are possible with reasonably sized energy storage systems. Table 8 shows the possible savings for a range of energy storage sizes.

Table 8: Possible energy storage savings for different energy storage capacities as a result of time-shifting.

Energy storage capacity [kWh]	Possible hydropower savings [MWh]
100	14
1000	50
5000	223
10,000	289

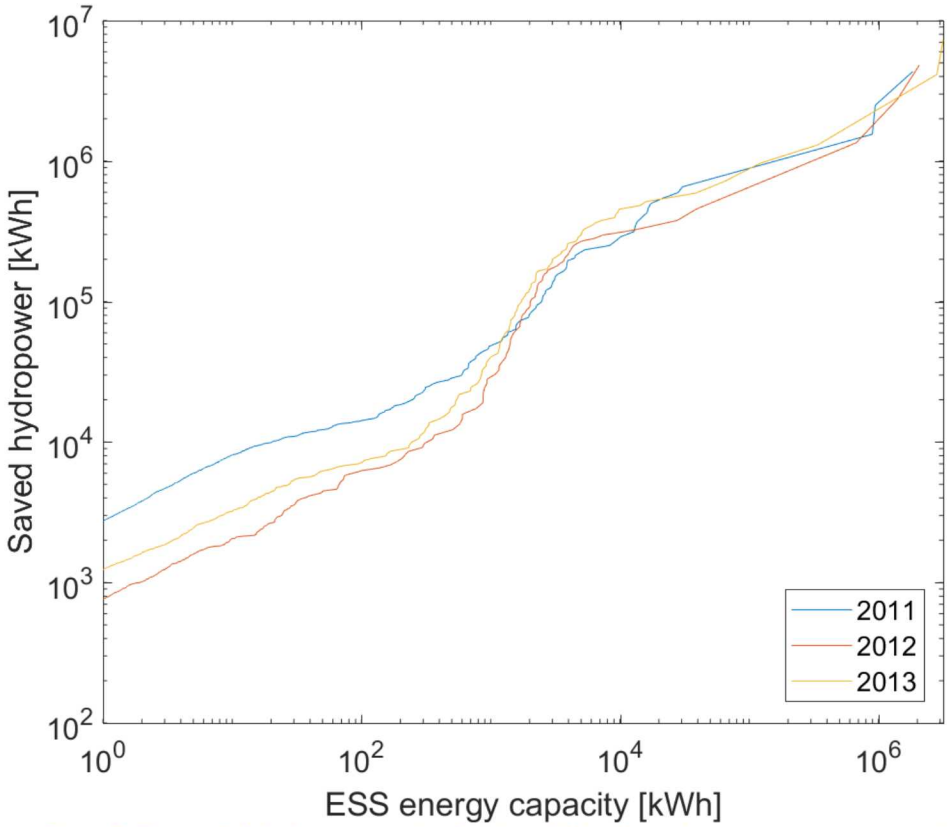

Figure 7: The possible hydropower savings by time-shifting for a given energy storage capacity.

7.1.2. Possible savings through supplying spinning reserve capacity

A total of 1 GWh of hydropower was unused as a result of operating constraints. An energy storage system could supply spinning reserve capacity (SRC) to save some of this hydropower. Only a qualitative analysis is done here to get an idea of what size of energy storage system would be required. A quantitative analysis is difficult without running simulations.

A minimum SRC of 500 kW is maintained on the grid in Cordova. This represents the minimum energy storage system power capability required to come close to saving the 1 GWh of hydropower. The minimum amount of energy capacity required is dictated by how long it takes to bring a diesel generator online. The energy storage system will be need to be able to supply the load until the diesel generator is online. As per Table 1 it takes between 30 seconds and 2 minutes to bring a diesel generator online.

Having additional power and energy capabilities will allow the energy storage system to supply some of the load while continuing to supply SRC and avoid bringing a diesel generator online. This will allow more of the unused hydropower due to operating constraints to be saved. It will also allow the energy storage system to perform time-shifting to capture some of those savings.

8. RESULTS FROM ENERGY BALANCE SIMULATIONS

This section presents the results of the energy balance simulations using data collected every second. Simulations were performed using the collected data from CEC for years 2011 and 2012 with no ESS as a benchmark to compare with the measured data. Finally, simulations with different ESS sizes were performed using 4 different energy management controls and the 2011 data. The 4 energy management controls are:

- Control Scheme 1: ESS is operating as spinning reserve for the hydro generators, smoothing the ramp rates on the hydro and diesel generators and can be charged by the diesel and hydro generators
- Control Scheme 2: ESS is operating as spinning reserve for the hydro generators and can be charged by the diesel and hydro generators
- Control Scheme 3: ESS is operating as spinning reserve for the hydro generators, smoothing the ramp rates on the hydro and diesel generators and can be charged only by the hydro generators
- Control Scheme 4: ESS is operating as spinning reserve and charged only by the hydro generators

Control scheme 4 results are shown below which yielded the highest savings in diesel consumption. All the results for each control scheme is provided in Appendix F.

8.1. 2011: Simulation with Modified Controls and No Energy Storage

Table 9 shows the diesel generator operating statistics and results from the energy balance model for 2011 with modified dispatch controls and no energy storage. Gen5, Gen6 and Gen7 were the most commonly dispatched diesel generators. This simulation had 164 fewer hours in diesel-off mode than measured. Simulated diesel output and fuel consumption were also lower than measured by 0.54 GWh and 47,000 gallons, respectively. There were 196 fewer diesel switching events in the simulation. The diesel capacity factor dropped to 57% from the 61% measured in actual operations.

Table 9: Diesel operating stats for 2011 with modified controls and no energy storage

	Gen5 (1125 kW)	Gen6 (1125 kW)	Gen4 (2450 kW)	Gen3 (2500 kW)	Gen7 (3800 kW)	Overall	Diesel off
Run Time [hr]	3456	1521	18.6	59.9	2726	7782	2653
Ave Cap Factor [%]	47.9	60.1	51.9	69.8	65.9	56.8	
Times Switched Online	423	251	17	9	106	807	
Total Output [GWh]	1.86	1.02	0.02	0.10	6.83	9.84	
Diesel Total Consumption [kgal]						683.4	

Table 10: Total load and simulated hydro output for 2011 and estimated total available hydro

Total Load [GWh]	27.68
Total Available PC Hydro [GWh]	21.06
Total Available HBC Hydro [GWh]	1.61
Total PC Turbine Generator Output [GWh]	16.22
Total HBC Turbine Generator Output [GWh]	1.61

8.2. 2012: Simulation with Modified Controls and No Energy Storage

Table 11 shows the diesel generator operating stats for 2012 with modified controls and no energy storage. Gen5, Gen6 and Gen7 were the most commonly used diesel generators. This simulation had 426 more hours in diesel-off than measured. Diesel output and consumption were reduced by 0.79 GWh and 82,000 gallon respectively. The diesel switching increased by 291 times. The diesel capacity factor dropped to 58% from 64%.

	Gen5(1125 kW)	Gen6(1125 kW)	Gen4(2450 kW)	Gen3(2500 kW)	Gen7(3800 kW)	Overall	Diesel Off
Run Time [hr]	2,608	1,273	65	252	2924	7,119	3,079
Avg. Cap. Factor [%]	51	60	59	66	63	58	
Times Switched Online	612	211	39	9	106	807	
Total Output [GWh]	1.48	0.86	0.10	0.41	7.03	9.88	
Diesel Total Consumption [kgal]	111.6	63.1	7.3	29.5	457.7	673.2	

Table 11: Note that the overall average capacity factor is scaled by the runtime of each generator

Table 12: Total load and simulated hydro output for 2012 and estimated total available hydro.

Total Load [GWh]	27.86
Total Available PC Hydro [GWh]	19.66
Total Available HBC Hydro [GWh]	3.52
Total PC Turbine Generator Output [GWh]	14.45
Total HBC Turbine Generator Output [GWh]	3.51

8.3. 2011: Simulation with No Smoothing and No Diesel Charging

8.3.1. Diesel Output

Figure 8 shows the diesel output for each generator in each of the simulation. Generators Gen7, Gen5 and Gen6 are the most commonly used. Figure 9 show the total diesel output for each simulation and Figure 10 shows the reduction in diesel output. As the ESS capacity and power increases the diesel output reduces.

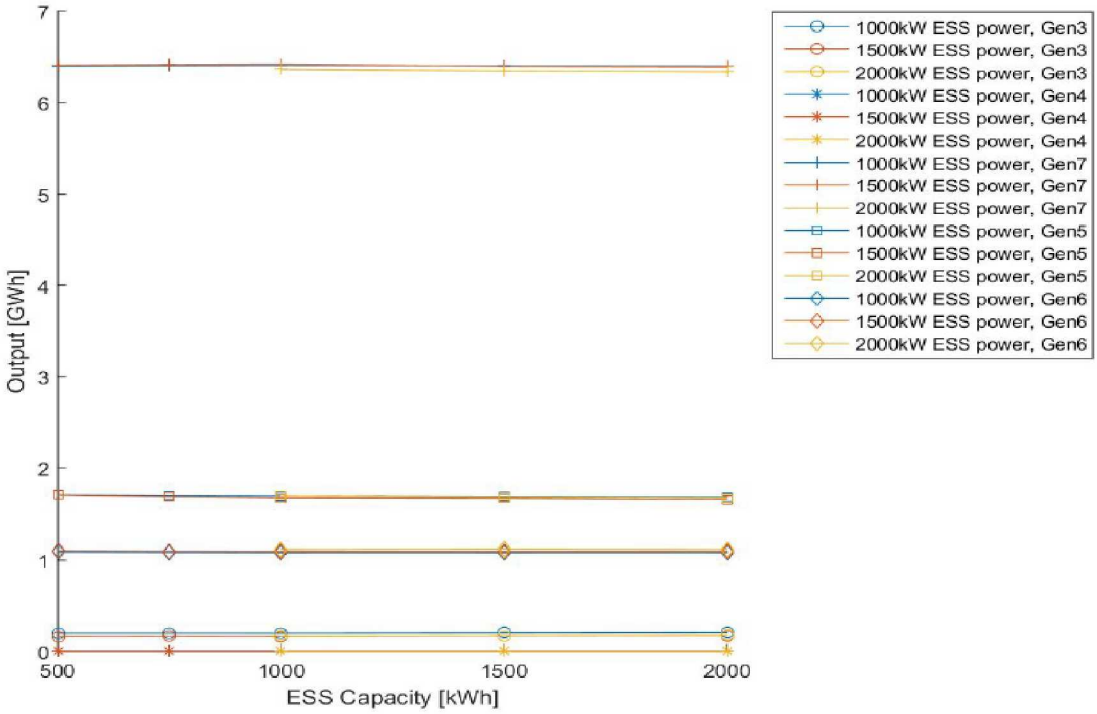

Figure 8 - The output of each diesel generator for different ESS capacities and powers

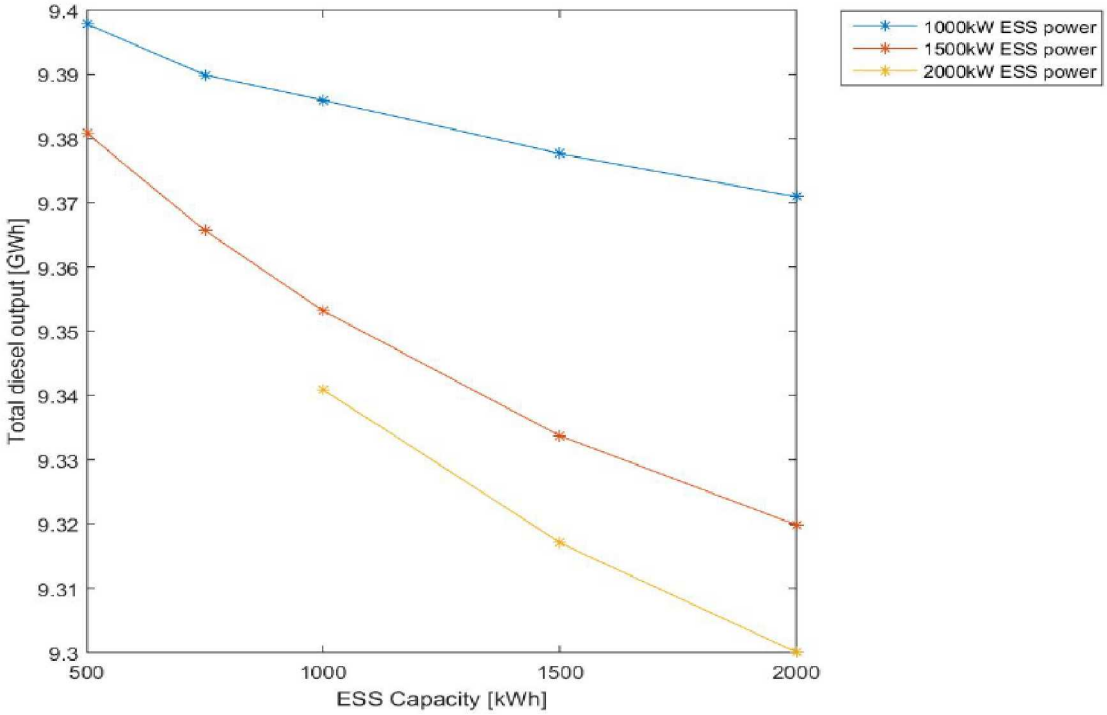

Figure 9 - The total diesel output for different ESS capacities and powers

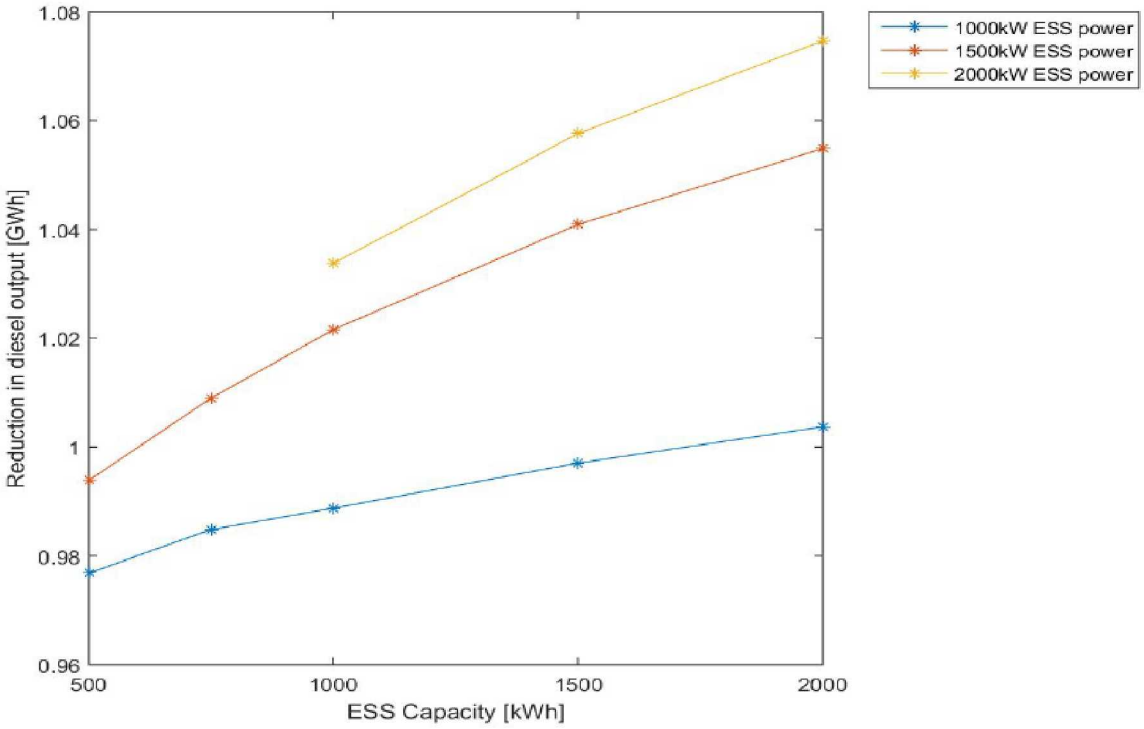

Figure 10 - Reduction in total diesel output for different ESS capacities and powers

8.3.2. Diesel Consumption

Figure 11 shows the diesel consumption for each generator in each simulation. Figure 12 and Figure 13 show the total consumption and reduction in total consumption. Increasing ESS capacity and power reduces diesel consumption. The reduction in consumption is a result of the reduction in diesel output as well as running the diesel generators at a higher and more efficiency loading.

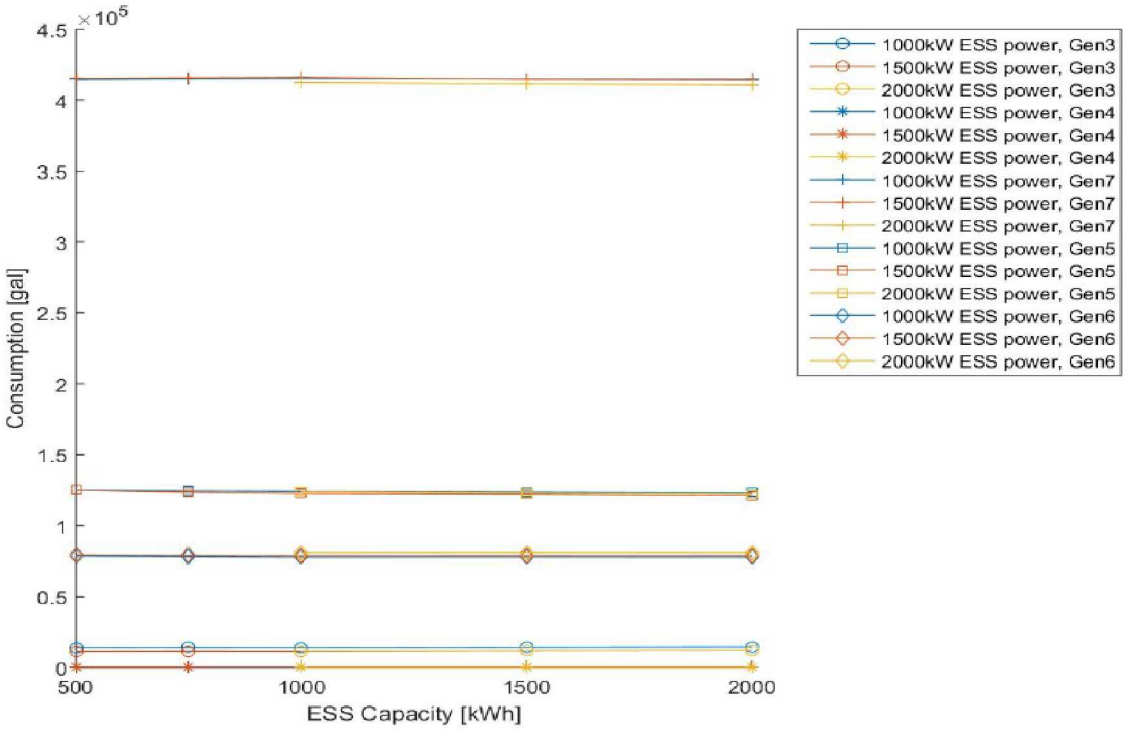

Figure 11 - Diesel consumption of each diesel generator for different ESS capacities and powers

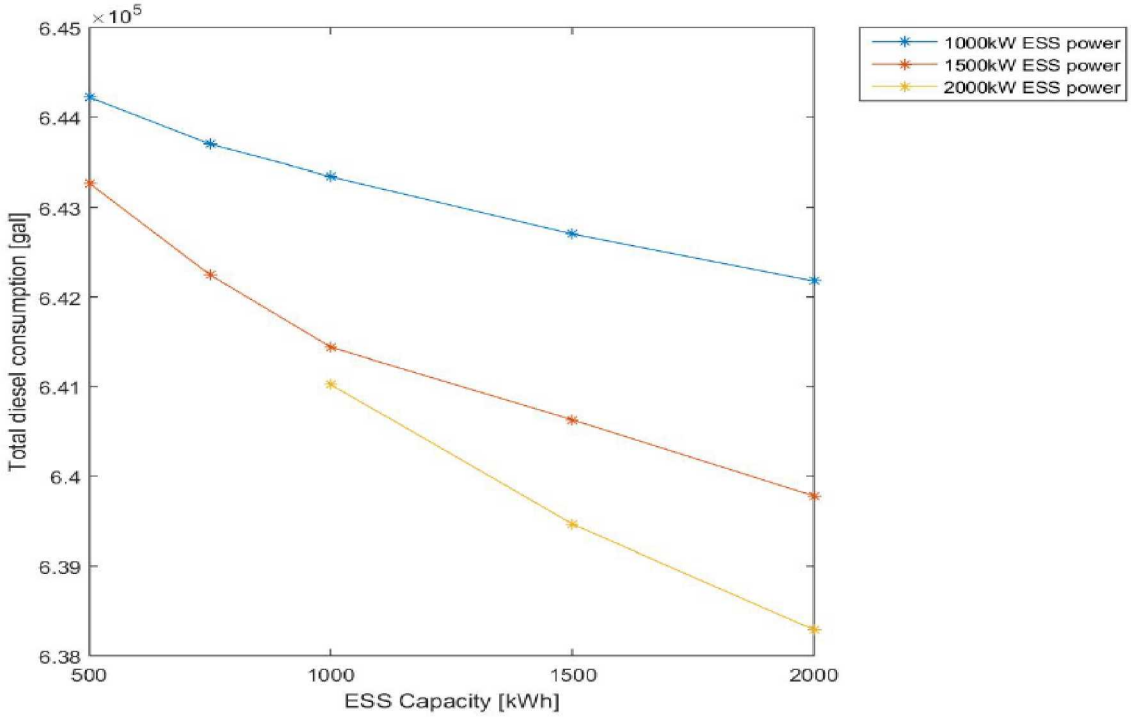

Figure 12 - Total diesel consumption for different ESS capacities and powers

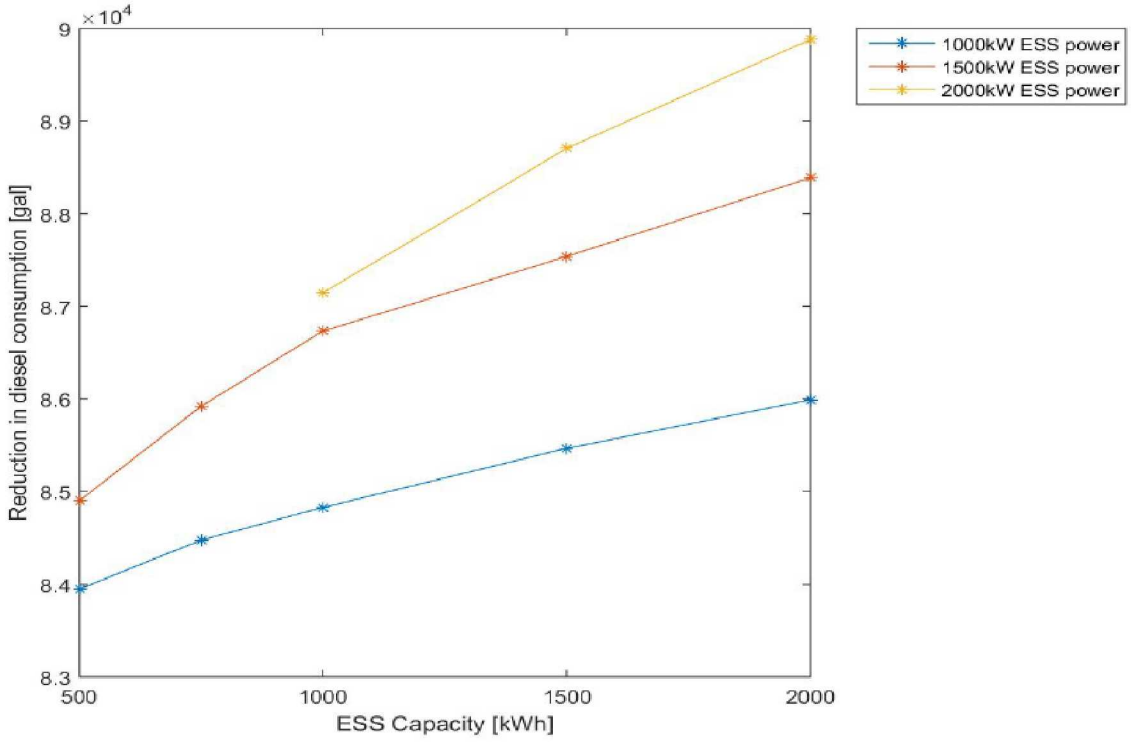

Figure 13 - Reduction in diesel consumption for different ESS capacities and powers

8.3.3. Diesel Off Time

Figure 14 shows the time spent in diesel off in 2011. Figure 15 shows the increase in time spent in diesel off. Increasing ESS capacity and power increases the time spent in diesel off.

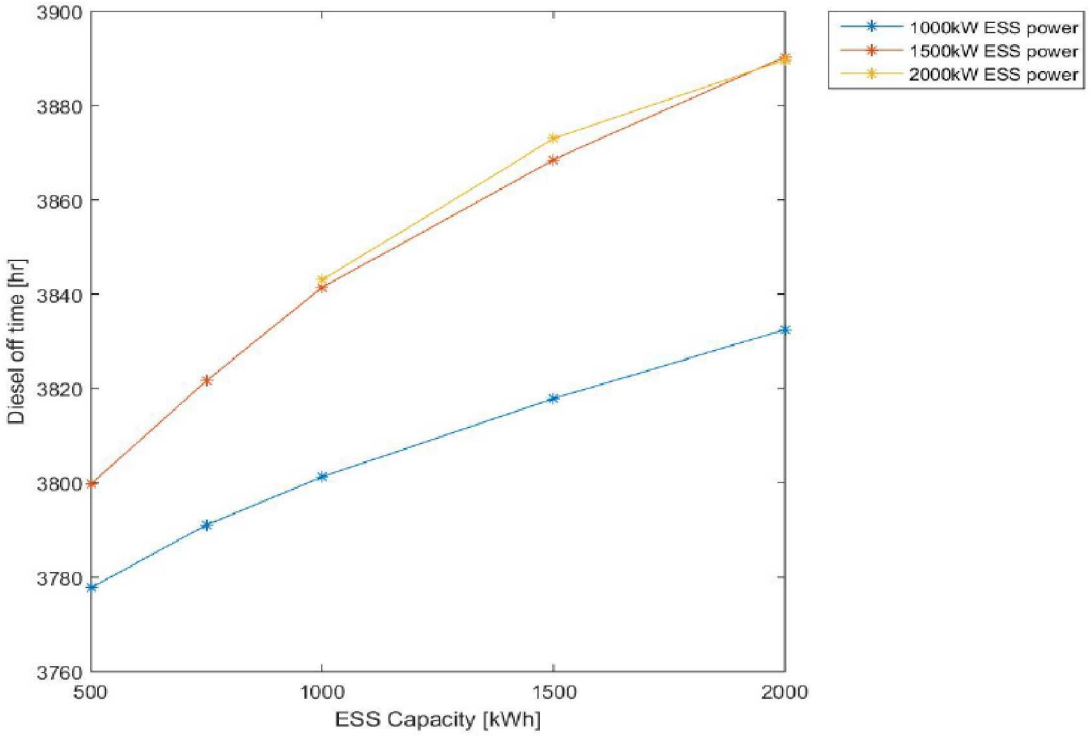

Figure 14 - Time spent in diesel off mode in 2011 for different ESS capacities and powers

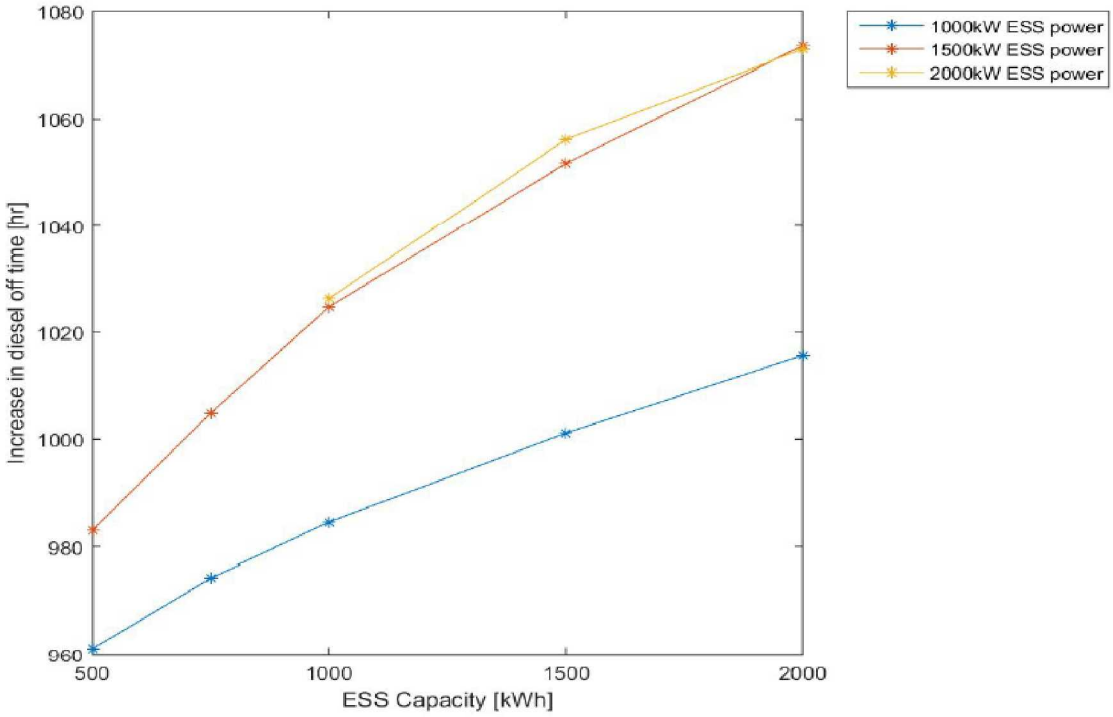

Figure 15 - Increase in time spent in diesel-off mode in 2011 for different ESS capacities and powers

8.3.4. Diesel Run Time

Figure 16 shows the run time for each diesel generator for different ESS capacities and powers. Figure 17 shows the total diesel run time and Figure 18 shows the decrease in diesel run time. Increasing the ESS capacity reduces diesel run time. Changes in diesel-off time are not directly related to changes in diesel run time, since multiple generators can be running online for different lengths of time.

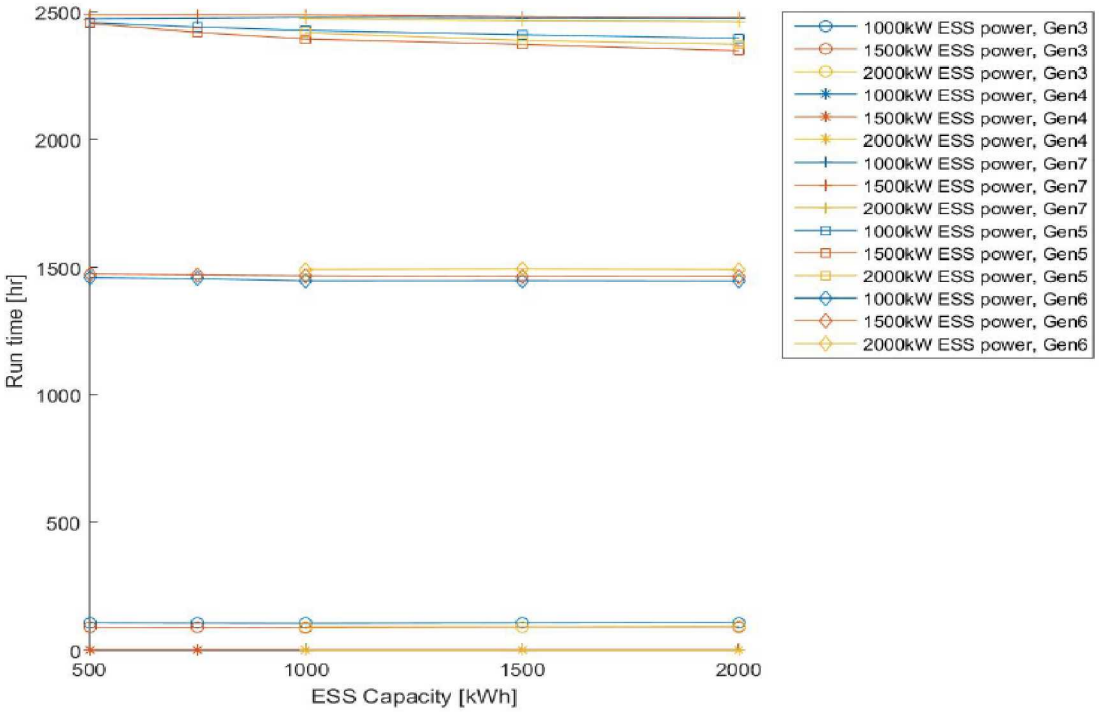

Figure 16 - Run time for each diesel generator for different ESS capacities and powers

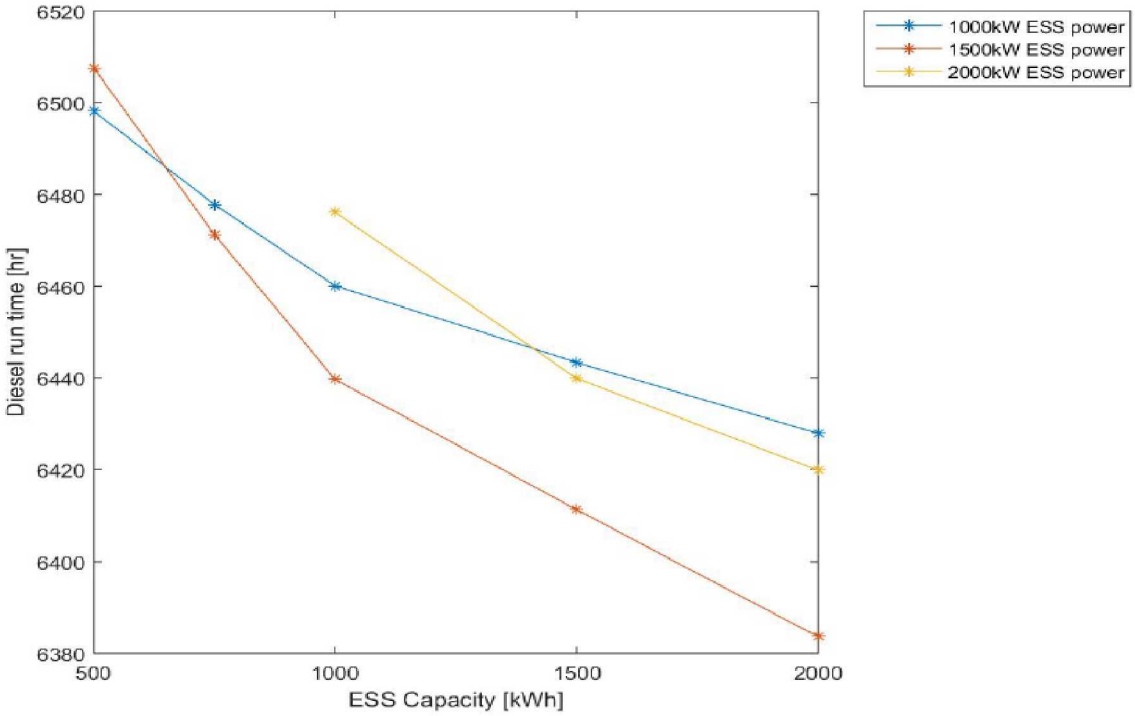

Figure 17 - Total diesel run time for different ESS capacities and powers

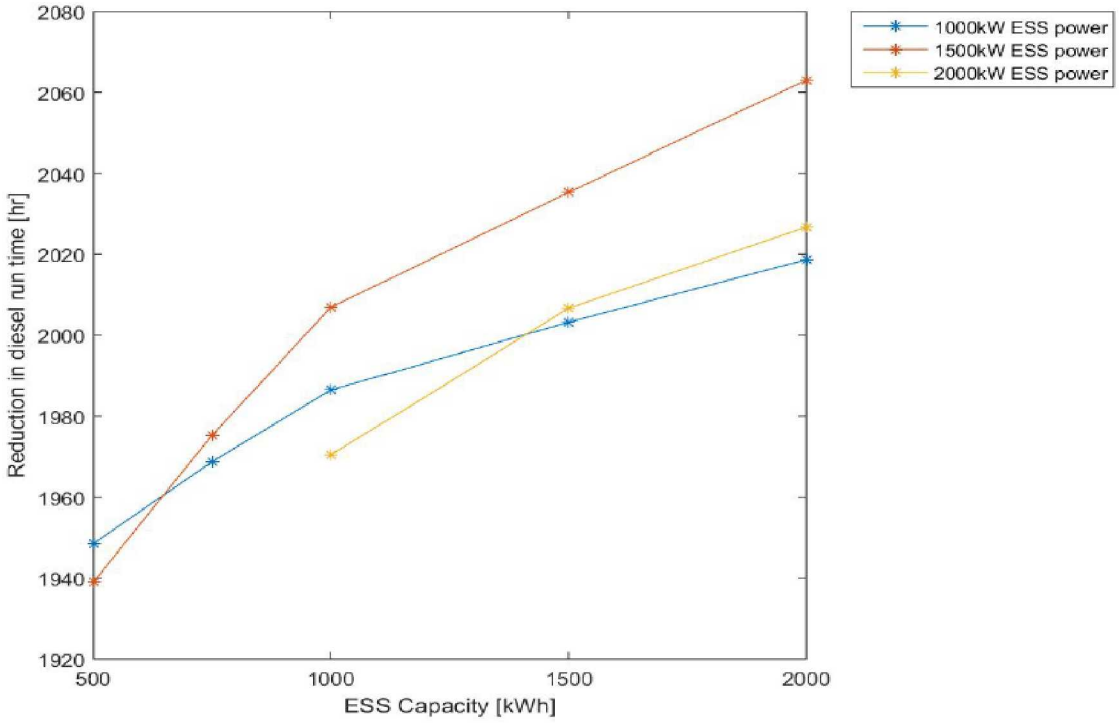

Figure 18 - Reduction in diesel run time for different ESS capacities and powers

8.3.5. Diesel Capacity Factor

Figure 19 and Figure 20 show the diesel capacity factor for each diesel generator and the total diesel capacity factor for different ESS capacities and powers. A higher ESS capacity and power resulted in a higher diesel capacity factor. These simulations show a marginal increase in diesel capacity factor from the measured value for 2011 or 61%.

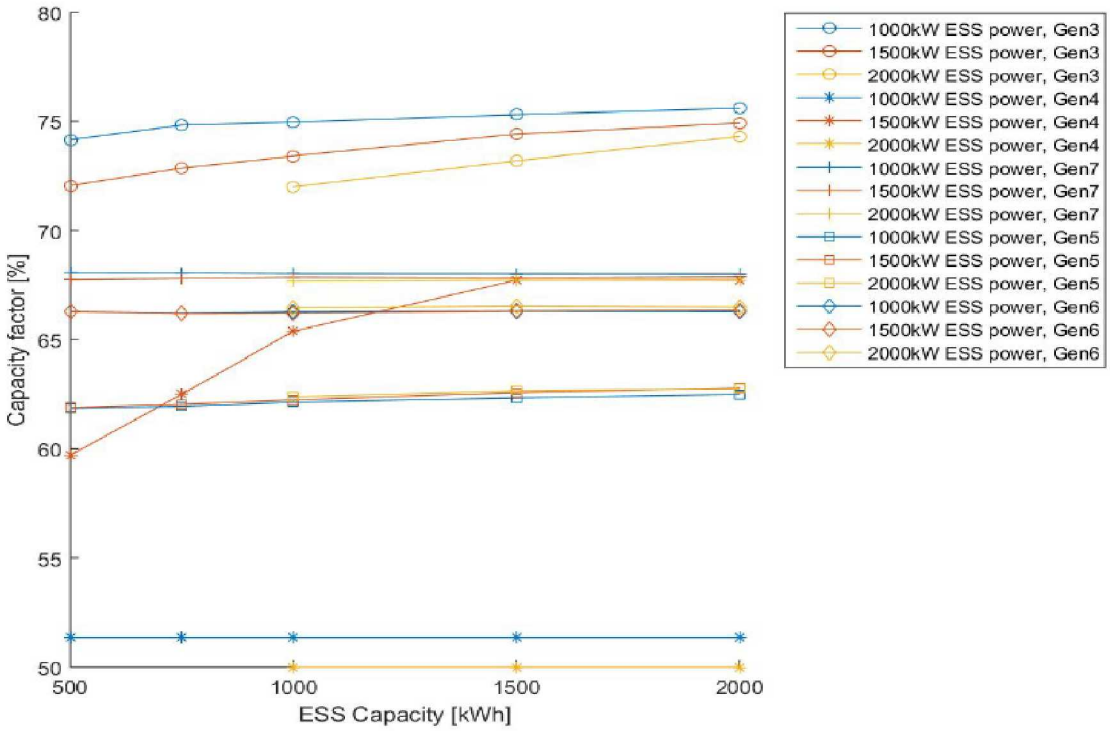

Figure 19 - Capacity factor for each diesel generator for different ESS capacities and powers

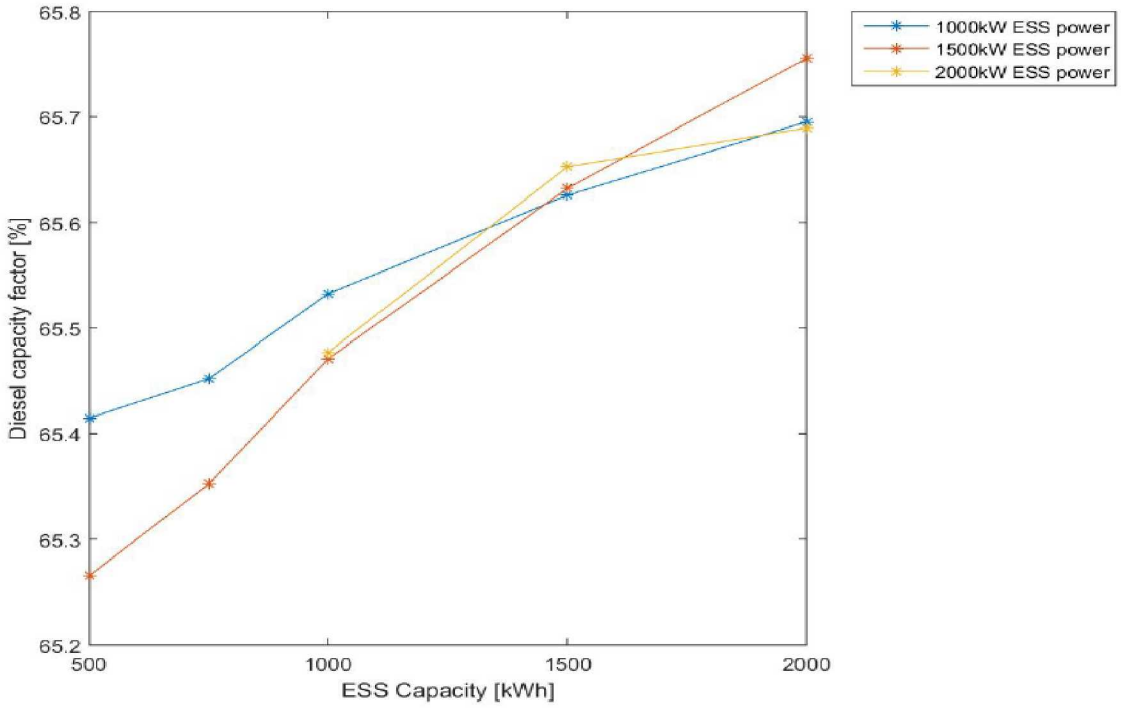

Figure 20 - Overall diesel capacity factor for different ESS capacities and powers

8.3.6. Diesel Switching

Figure 21 and Figure 22 show the number of times each diesel generator and all diesel generators are switched online for different ESS capacities and powers. As seen in the graphs, a decrease in diesel switching compared to the measured value of 1001 times for 2011.

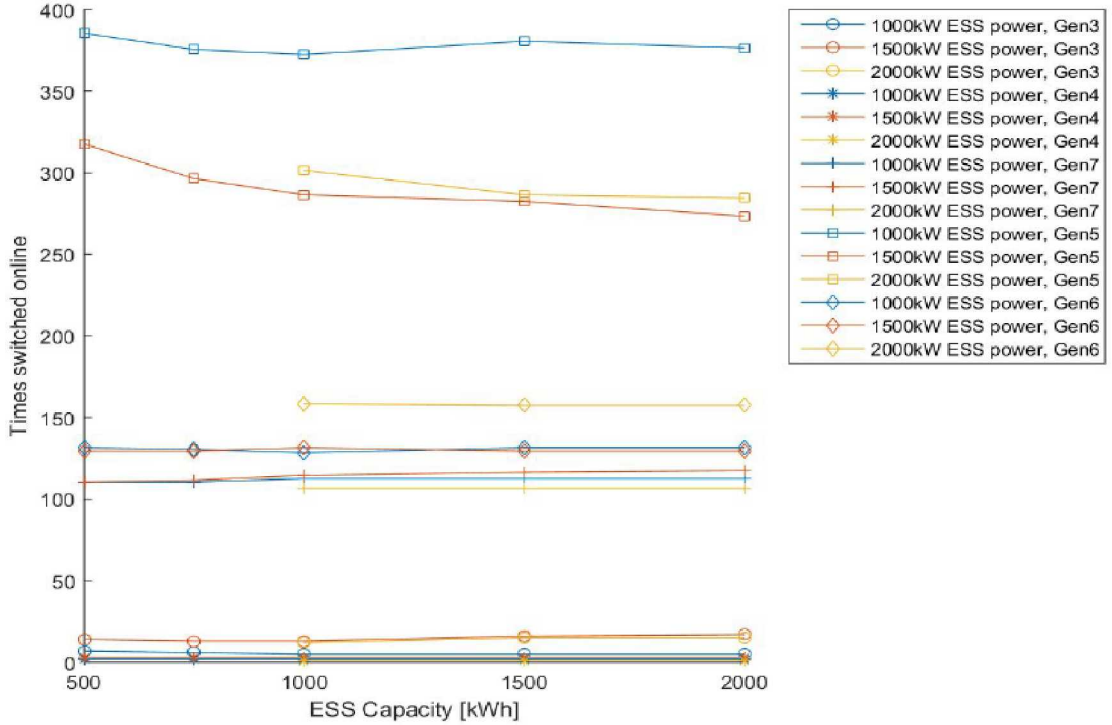

Figure 21 - Number of times each diesel generator is switched online for different ESS capacities and powers

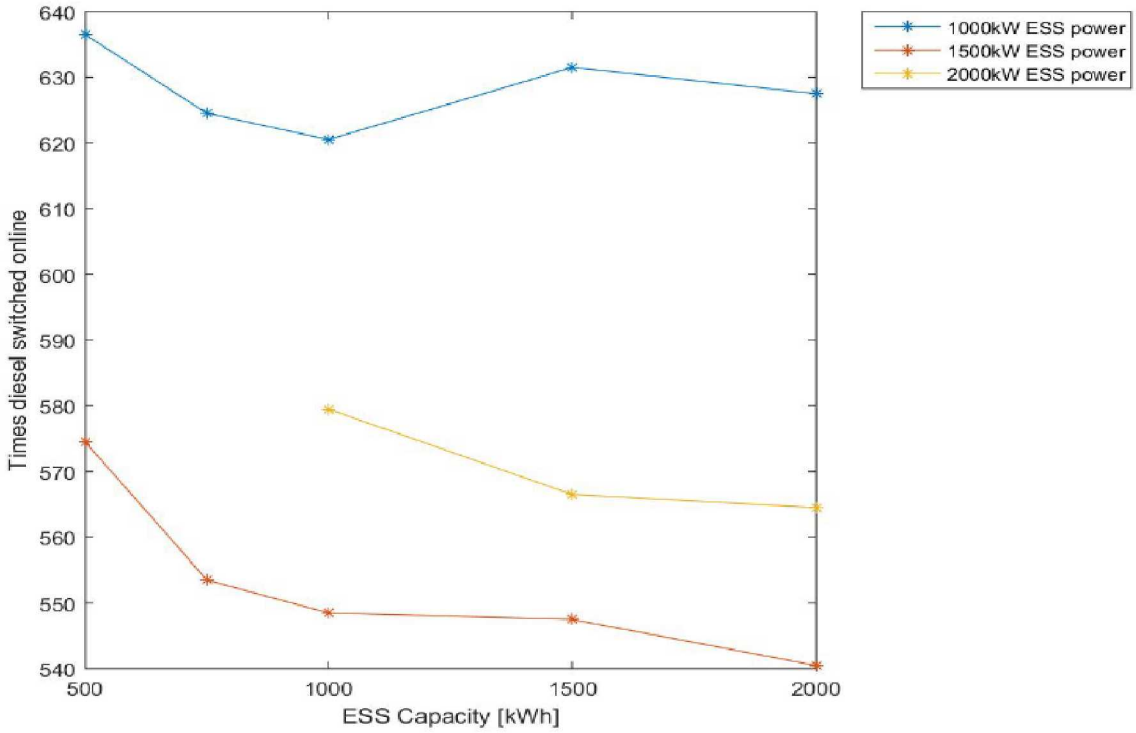

Figure 22 -Total number times diesel generators are switched online for different ESS capacities and powers

8.3.7. Diesel Ramp Rate

Figure 23 shows the probability distribution of diesel ramp rates for different ESS capacities and powers. There is not much difference between the different ESS capacities and powers. The combined ramp rates have a mean value of around 3.9 kW/s which is slightly higher than the average measured value of 3.13 kW/s for 2011.

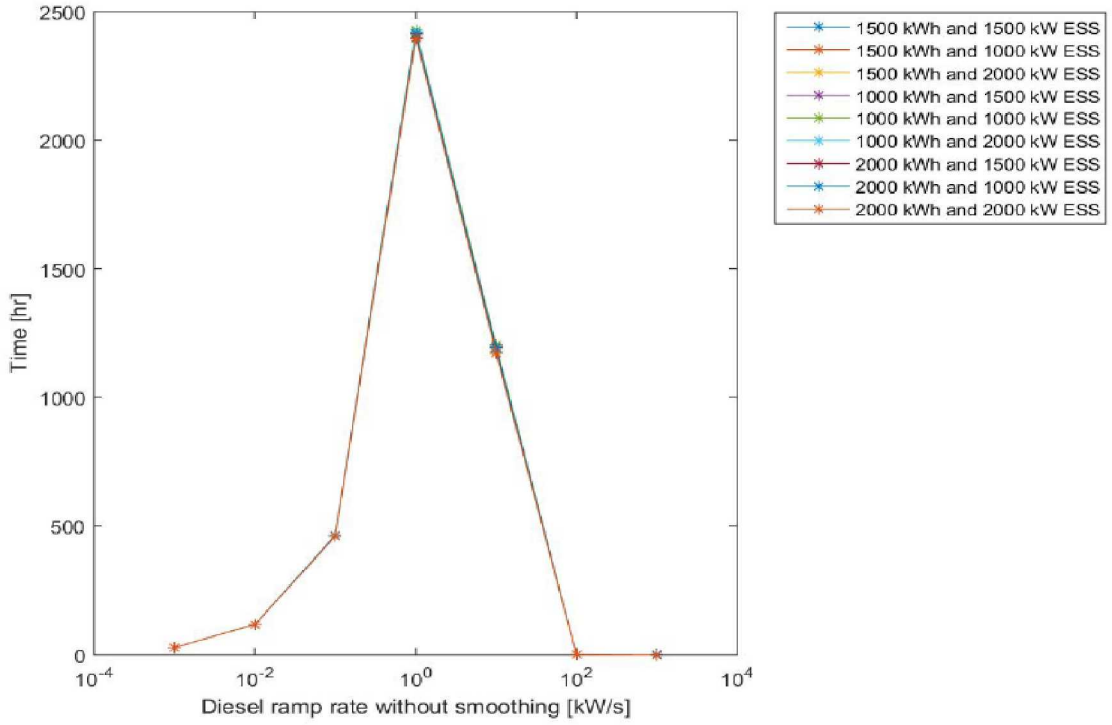

Figure 23 - Probability distribution of diesel ramp rates for different ESS capacities and powers

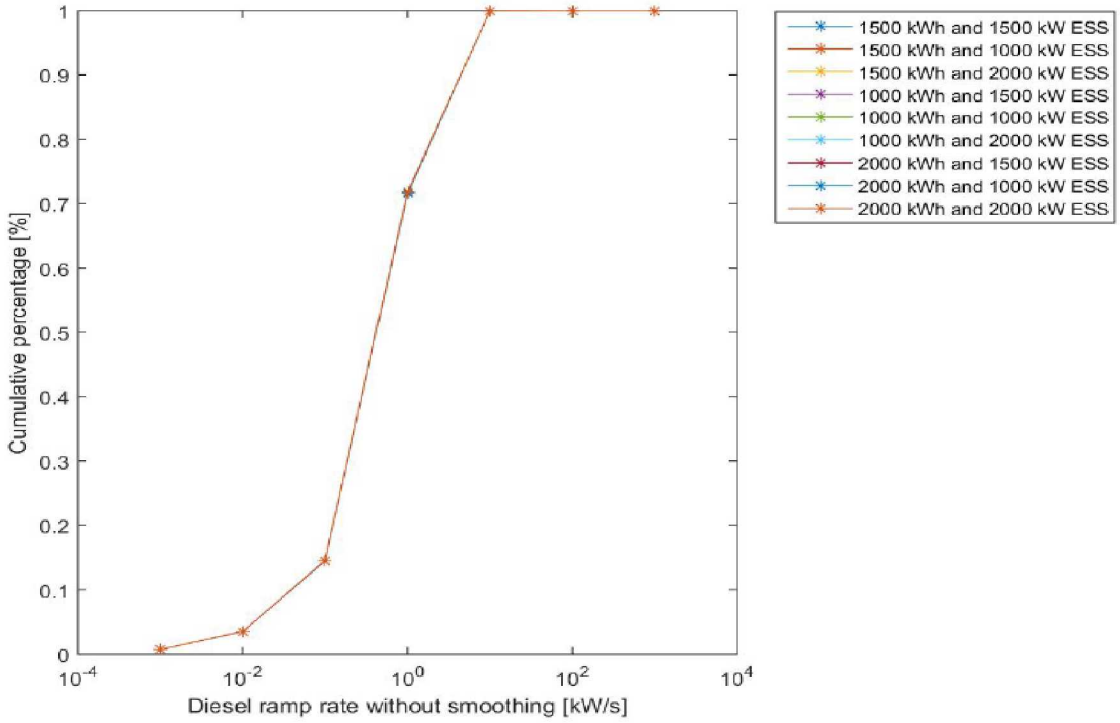

Figure 24 - Cumulative percentage of diesel ramp rate for different ESS capacities and powers

8.3.8. ESS Equivalent Cycles

Figure 25 shows the number of equivalent full ESS cycles. Multiple ESS cycles that add up to the full ESS capacity are considered to be on equivalent ESS cycle. These simulation have low ESS cycling which increases the life of most ESS technologies.

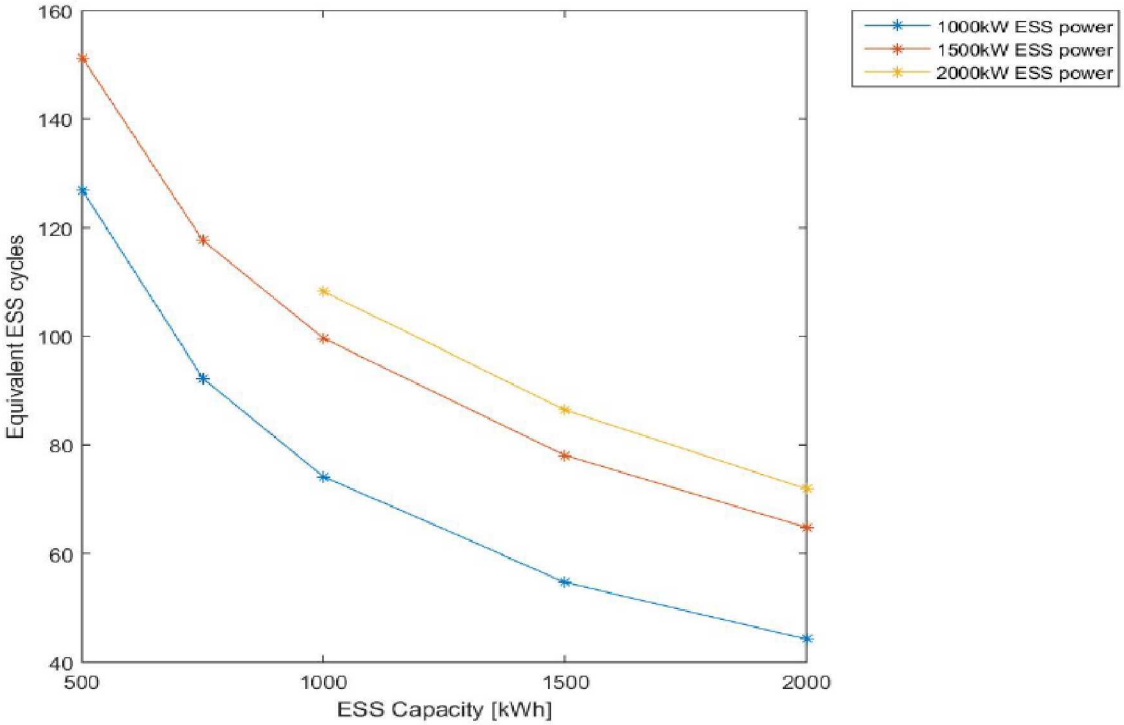

Figure 25 - Number of equivalent full ESS cycles for different ESS capacities and powers

8.3.9. Number of ESS Cycles

Rainflow counting was used to calculate the number of ESS cycles of varying amplitude experienced by the ESS. Figure 26 shows the number of ESS cycles for each cycle amplitude for different ESS capacities and powers. The number of cycles decreases with increasing amplitude.

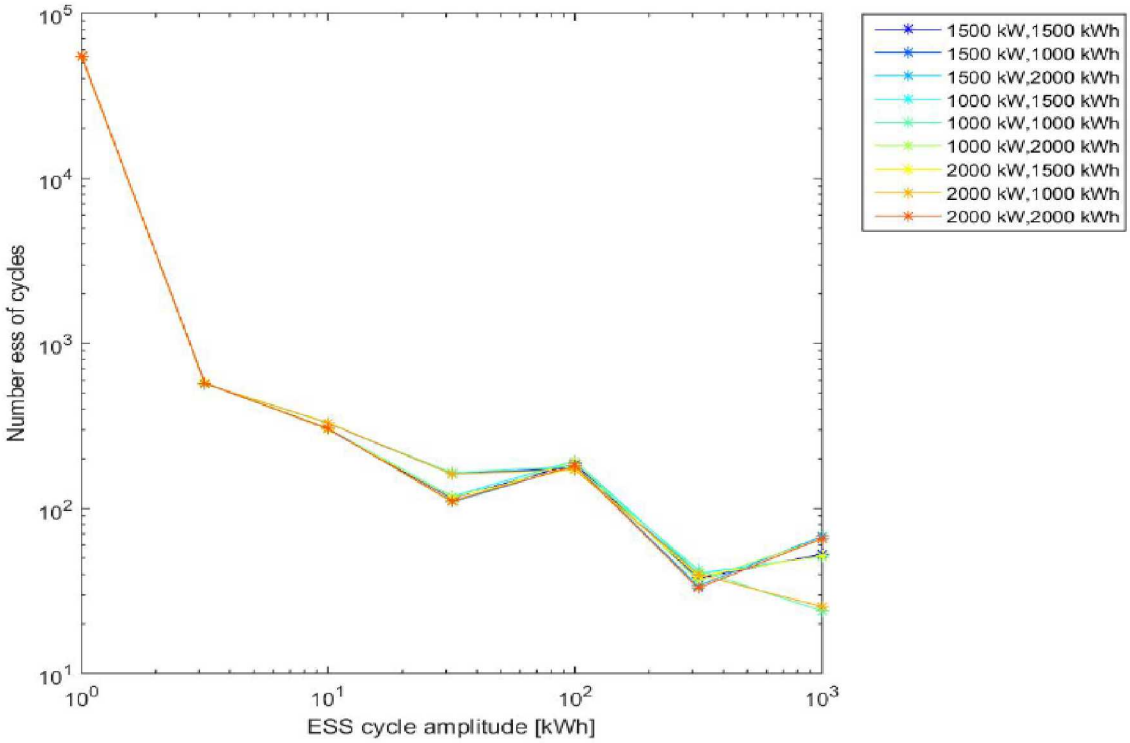

Figure 26 - Number of ESS cycles at different cycle amplitudes for different ESS capacities and powers.

8.3.10. ESS Power Levels

Figure 27 shows the time the ESS spends charging or discharging at different power levels. Since the ESS is being used as spinning reserve capacity and not for smoothing, majority of the ESS cycles are 100 kW or less.

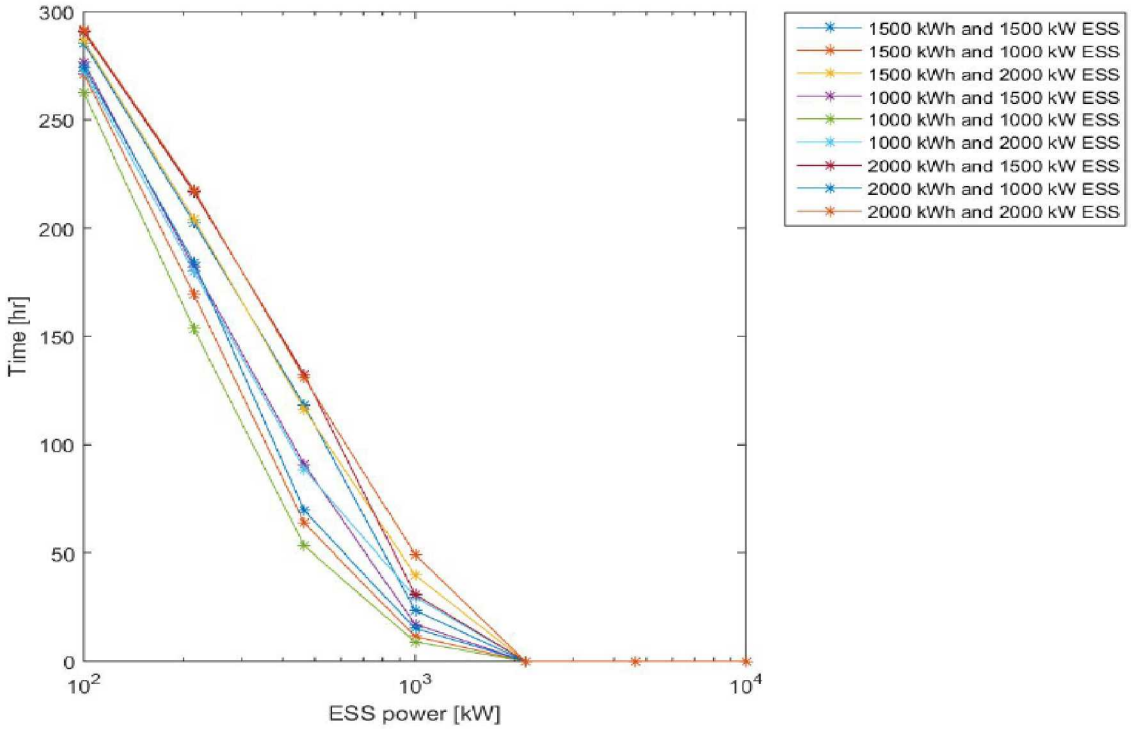

Figure 27 - Time the ESS spent charging or discharging at different power levels

8.3.11. ESS Ramp Rate

Figure 28 shows the probability distribution of ESS ramp rates for different ESS capacities and powers. The mean ramp rate is 1.6 kW/s, which is the lowest among the other simulations.

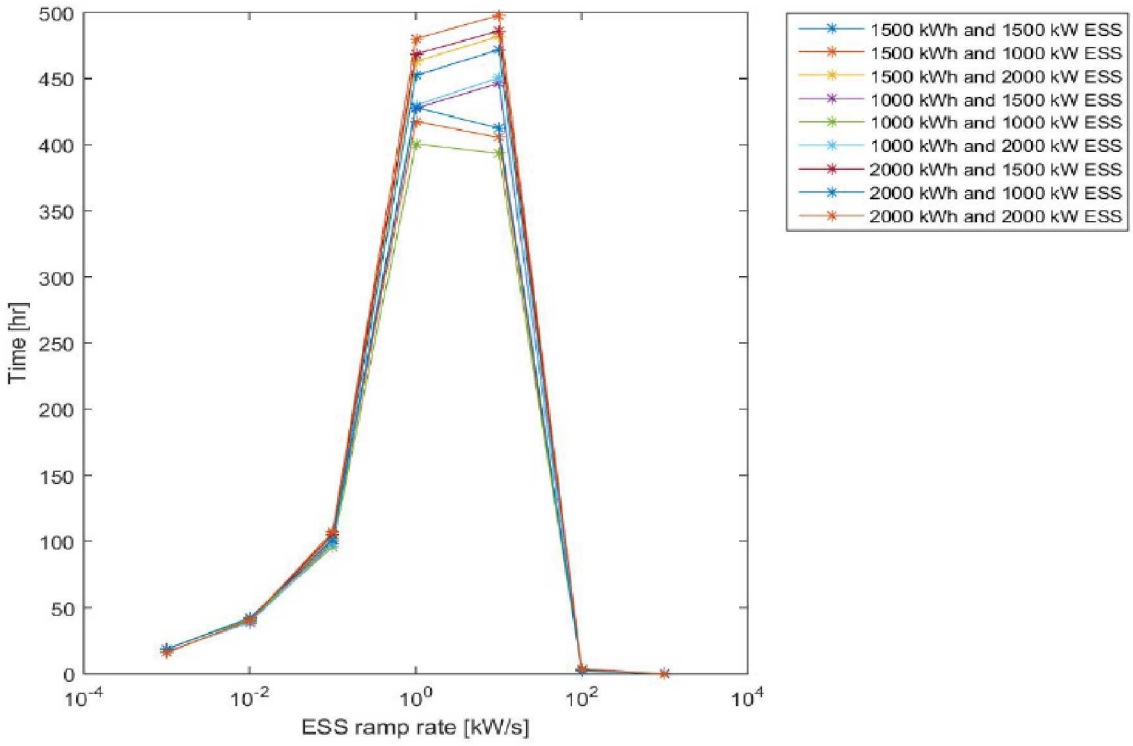

Figure 28 - Probability distribution of ESS ramp rates for different ESS capacities and powers

8.3.12. ESS Throughput

Figure 29 shows the total ESS throughput for different ESS capacities and powers. As the ESS capacity and power increases the throughput increases.

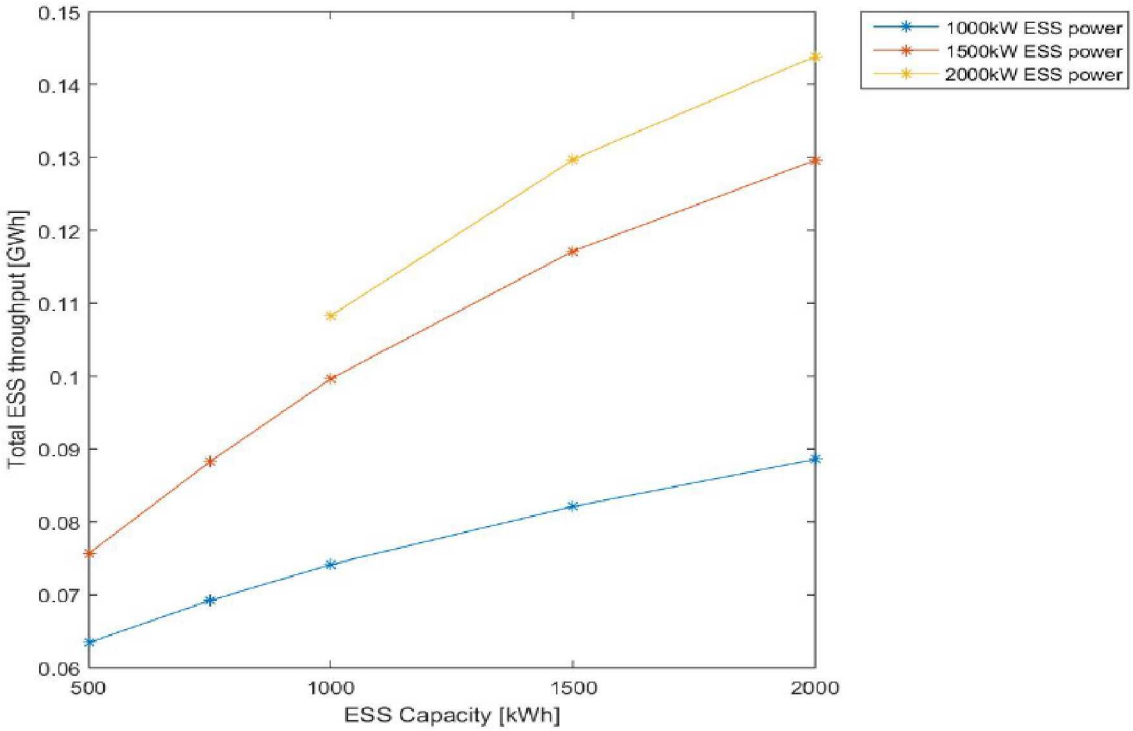

Figure 29 - ESS throughput for different ESS capacities and powers

8.3.13. ESS Contribution to Diesel Reduction

Figure 30 shows the ESS direct contribution to diesel reduction for different ESS capacities and powers. It is calculated as the total reduction in diesel output that did not go through the ESS. In other words, the ESS enabled the reduction of diesel without actually having to charge and discharge.

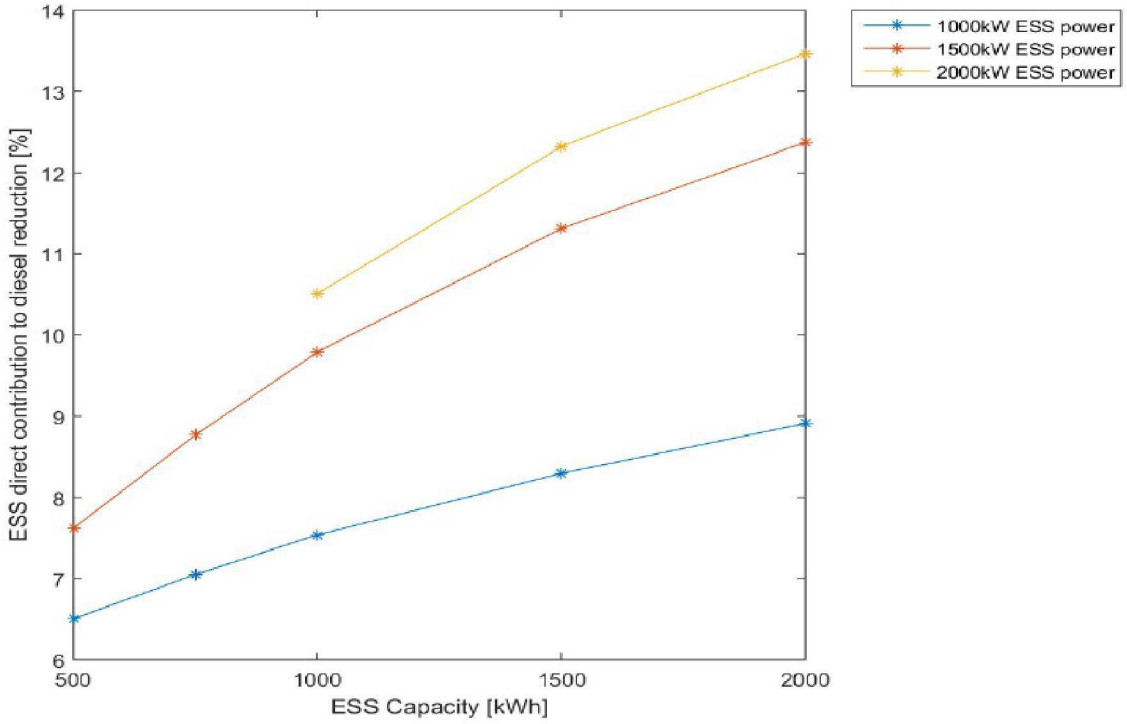

Figure 30 - ESS direct contribution to diesel reduction for different ESS capacities and powers

[PAGE LEFT INTENTIONALLY BLANK]

9. COMPARISON OF SIMULATION RESULTS

The 1.5 MW / 1 MWh ESS is compared for each simulation in this section. It was chosen as a size that performed well although depending on an economic analysis and available technologies, other sizes may be a better fit for CEC. Choosing one ESS size allows the relative comparison of the different control parameters from the different simulations. Simulation #'s in this section are described as follow:

- Simulation 1: ESS is operating as spinning reserve for the hydro generators, smoothing the ramp rates on the hydro and diesel generators, and can be charged by the diesel and hydro generators
- Simulation 2: ESS is operating as spinning reserve for the hydro generators and can be charged by the diesel and hydro generators
- Simulation 3: ESS is operating as spinning reserve for the hydro generators, smoothing the ramp rates on the hydro and diesel generators, and can be charged only by the hydro generators
- Simulation 4: ESS is operating as spinning reserve and charged only by the hydro generators

In each of the simulations, the generator controls were modified that allowed for maximized hydro utilization. Table 13 shows the diesel savings in each of the simulations as well as the base case with only modified generator controls. The diesel output and diesel consumption were reduced by around 10% in simulations 1-4 (with ESS). Simulated data reduced diesel consumption by approximately 5% through changing the control scheme of the diesel generators that maximized hydro utilization and no ESS. Simulation 2 has the highest reduction in diesel consumption which the ESS did not smooth the loading on the hydro and diesel generators and allowed the ESS to be charge by the diesel generators.

Table 13: Diesel Savings on each simulation performed

Project Description	Simulation using 1.5MW / 1MWh ESS				2011 Simulated Data	2011 Measured Data
	1	2	3	4		
Smoothing of Diesel and Hydro Loading by ESS	Yes	No	Yes	No	N/A	N/A
Max SOC charging of ESS by Diesel [%]	75	75	0	0	N/A	N/A
Diesel Output [GWh]	9.40	9.37	9.37	9.35	9.85	10.37
Reduction in Diesel Output[GWh]	0.97	1.01	1.01	1.02	0.53	N/A
Diesel Consumption [kgal]	640.55	638.75	642.98	641.44	683.41	728.17

Reduction in Diesel	87.62	89.42	85.19	86.73	44.76	N/A

Consumption						

Table 14 compares the operation of the diesel generators in each of the simulations. The diesel off time increases by 45% in simulations 1 and 2 and by around 36% in simulations 3 and 4. Total diesel run time was reduced by 32% in simulations 1 - 2 and by around 24% in simulations 3 and 4. Simulations 1and 2 significantly increases the diesel capacity factor, simulations 3 and 4 marginally increased it and the simulated data decreased it.

Diesel switching has fuel cost and maintenance costs. Simulations 1 and 3 significantly reduce the diesel ramp rates as a result of smoothing the hydro and diesel generators loading. The simulations without hydro and diesel generators smoothing show around a 25% increase in the diesel ramp rate. There are several factors that could affect this. In the current operation of the grid the hydro and diesels work together to supply the variations in the load, resulting in reduced ramp rates on each. When there was excess hydro the diesel ran at a minimum loading while the hydro varied with the load, which resulted in lower ramp rates. The standard deviations in the simulations without smoothing were around 9 while in the measured data 7.3 kW/s. Overall there was a slight increase in the mean ramp rate.

Table 14: Diesel Operation

Project Description	Simulation using 1.5MW / 1MWh ESS				2011 Simulated Data	2011 Measured Data
	1	2	3	4		
Smoothing of diesel and hydro loading by ESS	**yes**	**No**	**Yes**	**No**	**n/a**	**n/a**
Max SOC charging of ESS by diesel [%]	**75**	**75**	**0**	**0**	**n/a**	**n/a**
Diesel off time [hr]	4,086.82	4,103.13	3,828.27	3,841.40	2,652.91	2,816.72
Increase in diesel off time [hr]	1,270.10	1,286.41	1,011.55	1024.68	-163.81	n/a
Diesel run time [hr]	5,771.98	5,796.80	6,425.51	6,439.73	7,781.85	8,452.11
Decrease in diesel run time [hr]	2,680.13	2,655.24	2,026.60	2,012.37	670.26	n/a
Diesel capacity factor [%]	74.39	75.06	62.37	65.47	56.75	61.36
Increase in diesel capacity factor [%]	13.03	13.70	1.01	4.11	-4.61	n/a
Times diesel switched online	1,157.50	1,106.50	733.50	548.50	806.50	1,003.00
Reduction in times diesel switched online	-154.50	-103.50	269.50	454.50	196.50	n/a
Mean ramp rate [kW/s]	0.31	3.07	0.55	3.94	3.94	3.13
Decrease in mean ramp rate [kW/s]	2.82	0.06	2.58	-0.81	-0.81	n/a

In summary, simulations 1-4 (with ESS) all resulted in very similar diesel fuel savings. Simulation 1 and 2, which uses the diesel to charge the ESS, has improved diesel operation over simulations 3 and 4 except for the increase in diesel switching. Simulations 2 and 4 (no smoothing) had a higher diesel loading and less diesel switching than simulations 1 and 3, but it had a much higher mean ramp rate.

Simulations 1 and 3 have a much greater utilization of the ESS than the other two simulations, which may be its main detriment. Higher utilization of the ESS reduces the lifecycle of the system and may need to be replaced. Simulations 2 and 4 results in the least utilization of the ESS which would result in a longer ESS life. If the ESS services are purchased, it would result in less expenses. When considering simulations 1 and 2, it needs to be determined if their added benefits outweigh the increased ESS cost. When considering simulations 1-4, their added benefits needs to be compared with the simulated data (no ESS), which may be possible without or with minimal ESS.

10. CORDOVA DYNAMIC STABILITY STUDY OF ENERGY STORAGE PLACEMENT

This section describes how an ESS in the power rating range of 0.5 – 4MW may affect system voltage and frequency dynamics within the CEC grid. Conditions such as line faults and loss of generators were evaluated using a dynamic model. A commercial dynamic power simulation software (General Electric's Positive Sequence Load Flow--PSLF) was used. A PSLF dynamic model allows for analysis of electro-mechanical stability of large power systems.

The model data was extracted from one-line diagrams, generator nameplate data, and load data provided by CEC. In PSLF, two models are used to specify the system: (1) a power flow model which defines the generator and load initial conditions, distribution line parameters, and (2) a dynamic model which specifies parameters for the dynamic behavior of equipment such as the hydro generation and diesel generation exciters and governors.

10.1. PSLF Steady State and Dynamic Model

A power flow model of the generators, loads, and distribution lines was built in PSLF. Loads were placed along the feeder based upon the physical distance of the cables between load sections, to the extent information was available through CEC and Google Earth. Loads with similar dynamic characteristics and located along feeders close to one another were consolidated and represented as one load to simplify the model. Since individual load information was not made available, the relative demand of each load was modeled based upon the transformer kVA rating. For each feeder, the load demands were calculated as the consolidated transformer kVA ratings divided by total transformer kVA ratings and then multiplied by the peak demands provided by CEC. The peak summer conditions were modeled using data provided by CEC, shown in Table 15.

Table 15: Cordova electric feeders and loading

FEEDER	**Peak Demand (MW)**
Main Town	2.33
New Town	0.58
Lake Ave	0.80
13 Mile	0.42
Auxiliary	4.08
Humpback Creek	0.32
TOTAL	**8.53**

During the summer months, the majority of the hydro power is supplied by the large Power Creek hydro units with some additional hydro power coming from the Humpback Creek hydro units. Two of the six Orca Power Plant diesel units are scheduled to supplement power provided by the hydro units. Table 16 show the generator kVA and kW ratings and output power during peak load conditions. This power flow model is used to evaluate the power flow from the generators to the loads through the feeders determining if low voltage or congested feeders exist.

Table 16: Modeled Cordova Generator Power for Summer Peak Conditions

Cordova Generator	Type	Rated (MVA)	Rated (MW)	Modeled (MW)
Power Creek 1	Hydro	3.750	3.00	2.713
Power Creek 2	Hydro	3.750	3.00	2.713
Humpback Creek 1	Hydro	0.625	0.50	0.50
Humpback Creek 2	Hydro	0.625	0.50	0.50
Humpback Creek 3	Hydro	0.3125	0.25	0.25
Orca 3	Diesel	3.250	2.50	0
Orca 4	Diesel	3.004	2.40	0
Orca 5	Diesel	1.406	1.125	0.952
Orca 6	Diesel	1.406	1.125	0.952
Orca 7	Diesel	5.000	4.00	0
Orca 8	Diesel	0.081	0.065	0.00
Total		23.209	18.465	8.587

Standard library PSLF models were utilized to represent the hydro and diesel units. These models included a turbine generator-governor, a synchronous generator and an exciter. The simulations used model parameters from similarly sized hydro and diesel units available in the Western Electricity Coordinating Council (WECC) dynamic model database.

Figure 31 below shows the PSLF model topology. Most of the feeders in the CEC distribution grid are 12.47 kV and underground except for the feeder from the Power Creek Substation to the Eyak Substation which is 25kV. The higher voltage feeder is needed due to the distance of about 7 miles between the substations and this feeder is underwater. Since most of the feeders are underground, the nuisances from the elements such as tree slapping the feeders is avoided and inherently increasing the reliability of delivering power from the generators to the customer. In the CEC distribution grid, all the feeders except the feeder labeled “13 mile” off the Eyak substation are looped such that if the Eyak substation was taken out of service the feeders can be powered from the Orca substation and vice versa. A major load that is off the “13 mile” feeder is the Airport.

In addition to the feeders being looped, the large generation sources being the Orca Power Plant and the Power Creek Power Plant are separated. The Orca Power Plant is attached to the Orca substation which has the capability of supplying the load demand of the Cordova community. Power Creek Power Plant is attached to the Eyak substation which in certain times in the summer is adequate to supply the load demand of the Cordova community. By having the major power plants separated, this increases the availability of a generation source being available to satisfy the load demand of the Cordova community during the summer.

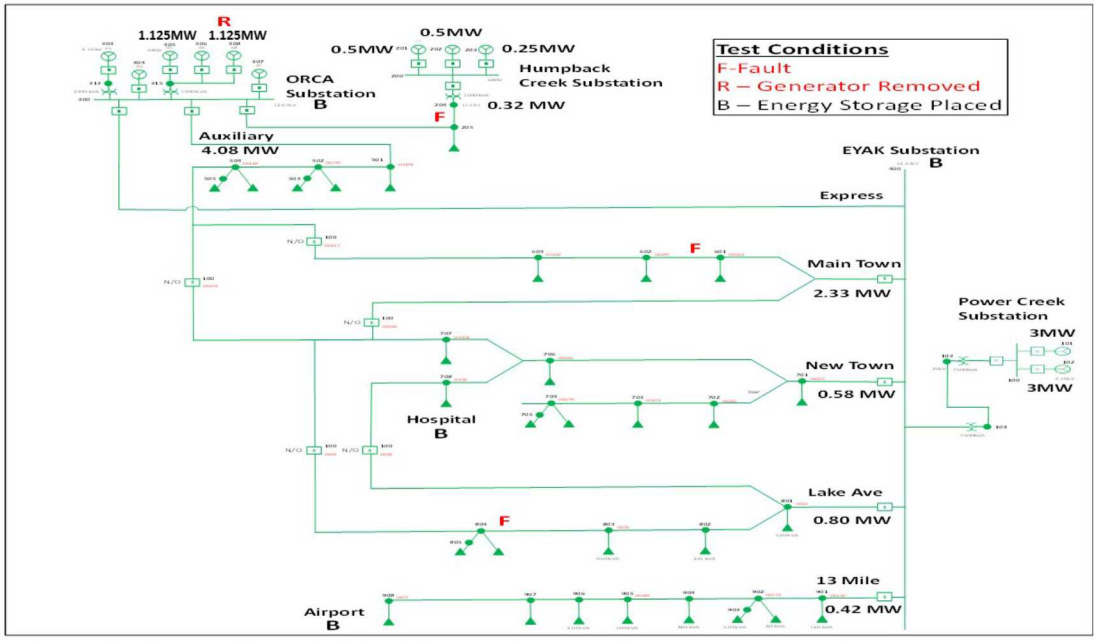

Figure 31 - Cordova Electric PSLF Model Showing Hydro and Diesel Generation and Primary Feeders.

The energy storage system was represented using available PSLF models (estor2 and regc_a) which when combined is representative of a battery connected to the grid through a power conditioning device. This model operates in all 4 quadrants of the real and reactive power spectrum to damp frequency and voltage oscillations by injecting power into the electrical system to restore the system to equilibrium. When the ESS is called upon to supply or absorb both real and reactive power, the control is set to have a priority of providing the required reactive power to stabilize voltage at the bus over providing real power to stabilize frequency. If the MVA rating of the ESS is not exceeded when providing reactive power, the ESS control allows the ESS to provide real power as needed. A sensitivity analysis was performed on the PSLF ESTOR2 controller using a 2 MW ESS and adjusting the droop gain (D), filtering time constant (Tf), voltage output gain (Kv) and power output gain (K) during the Humpback feeder fault and Main town fault. Results for the sensitivity analysis is provided in Appendix G with the parameter D=0, Tf=0.05, Kv=10 and K=1 set based on the analysis. In each of the dynamic simulations the ESS was initialized at 100% SOC and was initialized at approximately -0.3 to -0.4 MVAR output depending on which bus the energy storage system was attached to. Multiple simulations were run for various power ratings of an energy storage system which were 0.5 MVA, 1.0 MVA, 1.5 MVA, 2.0 MVA, 3.0 MVA and 4.0MVA. Energy rating of the energy storage was not included in the dynamic simulation. The transients of interest only last for a second or less which the simulation time for each dynamic run was set to last only 30-40 seconds. Since the simulations are run for short periods of time, this is the reason why the energy rating of the energy storage device was not included. In every simulation, the ESS is connected to the 12.47kV CEC grid through a $480V_{ll}/12.47kV_{ll}$ transformer so behind-the-meter ESSs were not considered in this study.

10.2. Dynamic Test Cases

Dynamic simulations for fault and generation drop events were conducted to demonstrate how an ESS might perform in the CEC system to support voltage and frequency stability. Fault scenarios that were simulated were faults along the Humpback Creek feeder, Main Town feeder, and Lake Avenue feeder. Humpback Creek feeder fault was performed to understand transient behavior of the CEC grid when a loss of a substation connecting generation units to the CEC electrical grid occurs with and without an ESS. The other two faults analyzed were the Main Town feeder fault being cleared by itself and the Lake Avenue feeder fault being cleared by opening the feeder breaker at the Eyak substation. In addition to fault scenarios, we also simulated the loss of a diesel generator at the Orca power plant initially dispatched at 0.952 MW. This event was used to demonstrate that the energy storage system could be used to provide fast voltage and frequency support, thus reducing the risk of cascading loss of load or generation in the CEC grid. The key performance metrics were resultant ESS and generator power, system frequency and system voltage responses at the Orca Substation. Simulations were conducted with the ESS at four locations: Eyak Substation, Orca Substation, the main Hospital, and the Airport. These scenarios were evaluated to determine whether the location of the energy storage system makes a significant difference. Also, multiple scenarios were run at each location with various ESS power ratings to determine if a larger power rating provides improved transient stability. In Figure 31, candidate locations based on CEC's inputs for the energy storage system are indicated with a "B", locations of the simulated faults are indicated with the letter "F", and the location of the generator that was disconnected is indicated with the letter "R".

10.3. Dynamic Simulation Results

Figures in this section show the system frequency, bus voltage at the Orca power plant, and the power output from the ESS in the CEC grid during electrical transients. The following sections only show the results for when the energy storage system is placed at the Orca Substation. Appendix G has all the results for the other 3 locations for the ESS as well as the different sizes.. In each section below, ESS of different sizes 0.5MVA, 1.5MVA, 3.0MVA and 4.0MVA at the Orca Substation were simulated. Results from the figures below, the determination of the kVA rating and location of the ESS effect on the transient stability of the CEC grid is shown.

10.3.1. ESS at Orca Substation and Humpback Creek Fault

In these simulations, at time t=5s a fault occurs along the Humpback Creek feeder causing a disturbance in the CEC electrical grid. This fault occurs along the only feeder which the Humpback Creek Hydro plant facility is tied into the CEC grid. Type of fault simulated is a self-clearing fault which is cleared by time t=5.1s. The simulation is run out to time t=30s to give the CEC electrical grid time to return to a steady state value from the fault. Multiple simulations were conducted with this same fault with one being the base case not including an ESS and the others varying the rating of an ESS. Results are as follow.

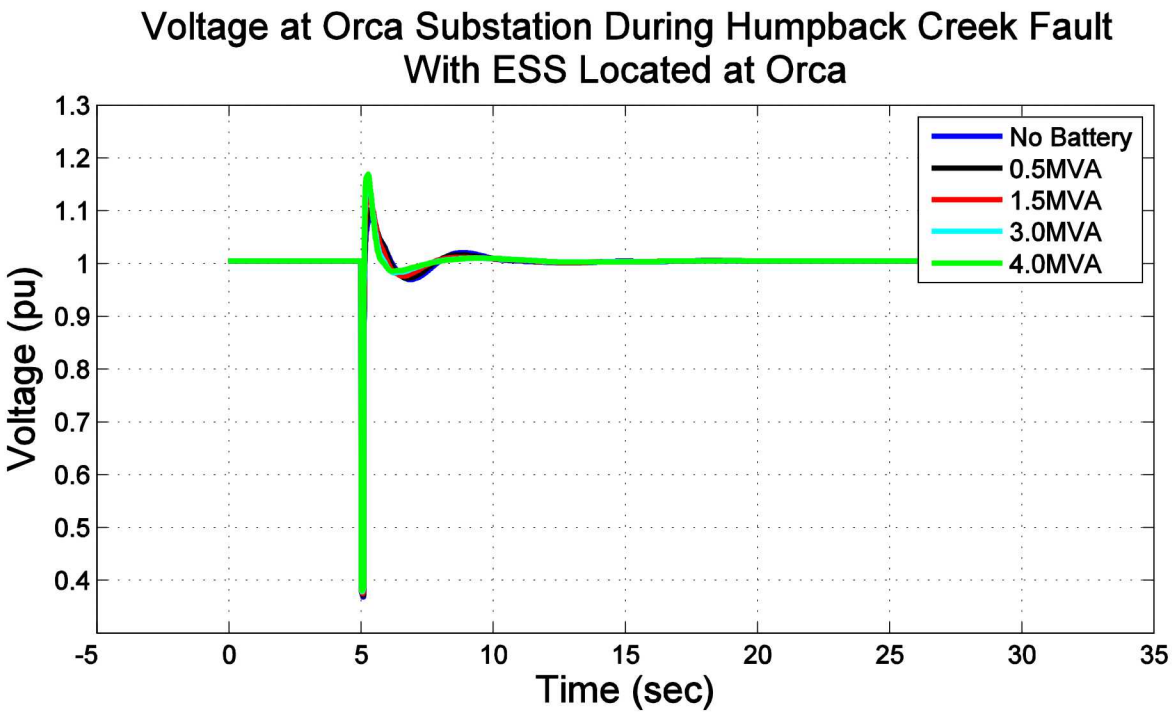

Figure 32 - Voltage at Orca Substation for a fault along Humpback Creek feeder, with energy storage located at Orca Substation

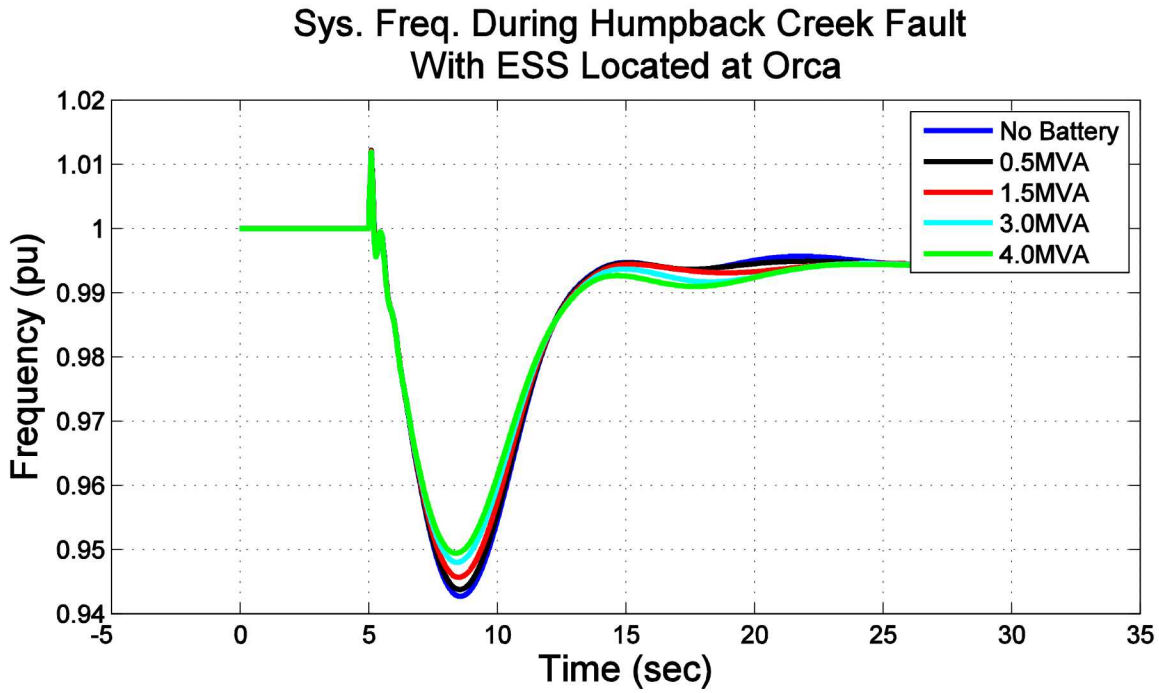

Figure 33 – System Frequency at Orca Substation for a fault along Humpback Creek feeder, with energy storage located at Orca Substation

In Figure 32 and Figure 33 with the ESS at the Orca Substation, the voltage at the Orca Substation and the system frequency are not significantly affected by the ESS in the system. By increasing the size of the ESS the voltage at the Orca Substation and system frequency are

slightly dampened but not enough to determine that a larger rated ESS provides more dampening.

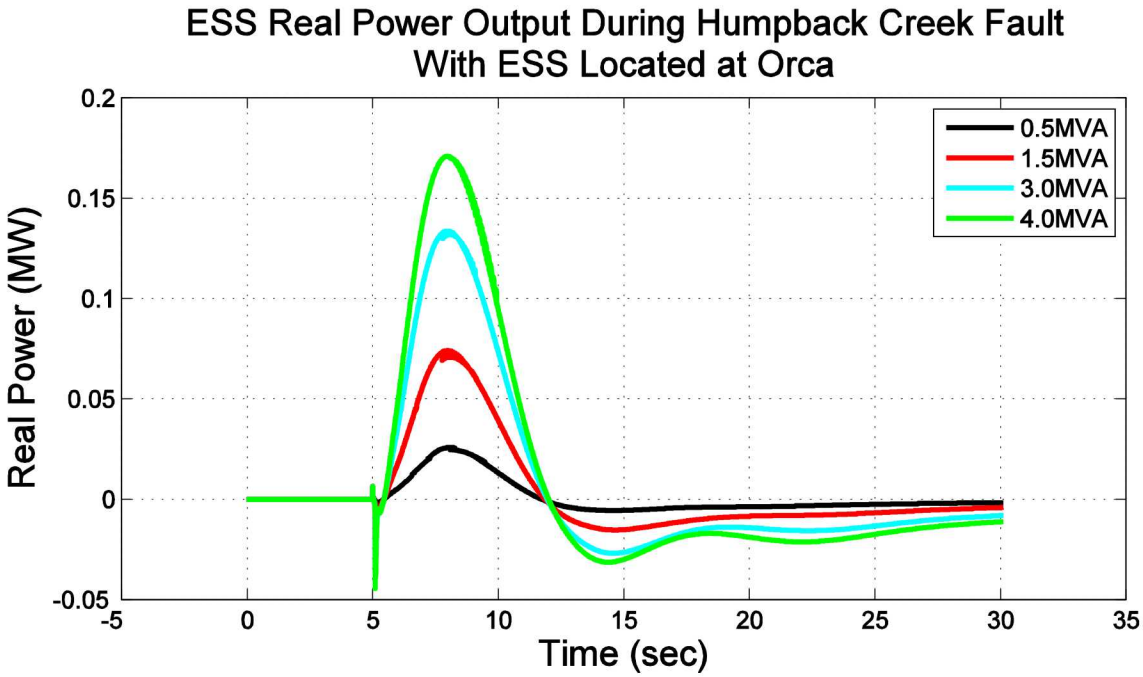

Figure 34 – Real Power Output of energy storage system located at the Orca Substation for a fault along Humpback Creek feeder

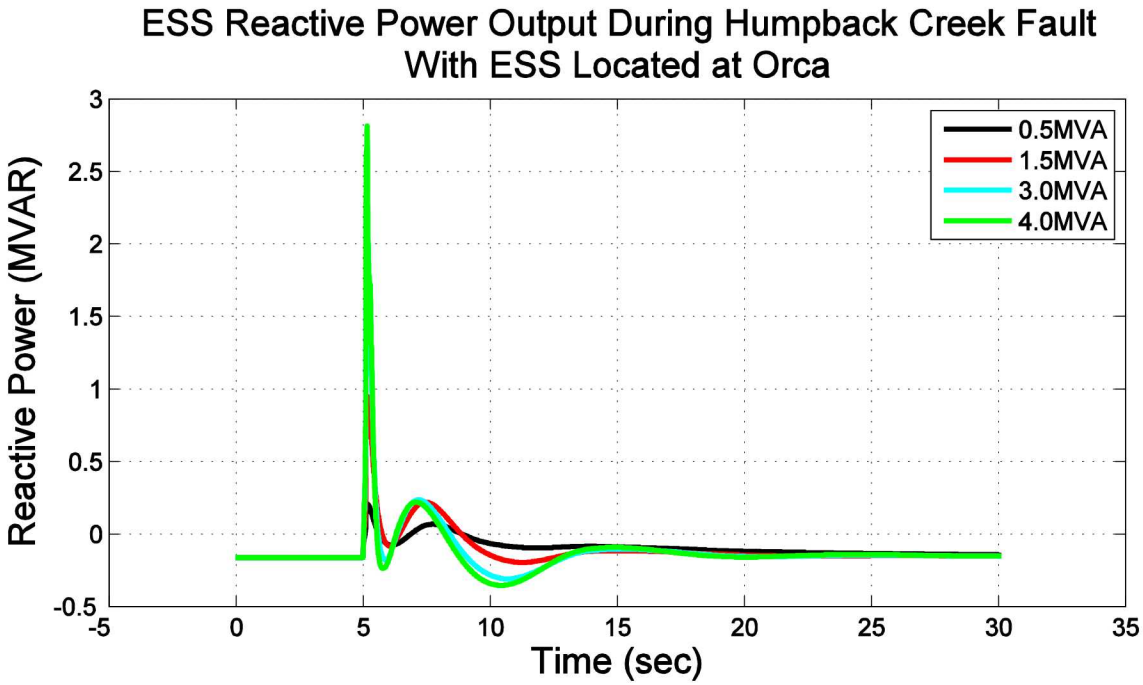

Figure 35 - Reactive Power Output of energy storage system located at the Orca Substation for a fault along Humpback Creek feeder

The figures above show the real and reactive power output from the ESS during the humpback creek fault. Control of the ESS in the PSLF model has priority to provide reactive power when

needed over providing real power but does allow real power to be supplied or absorbed if the rating of the ESS is not exceeded. Reactive power output from the ESS is increased as the rating of the ESS is increased as seen in Figure 35. The 3MVA and 4MVA ESS size have similar reactive power outputs during the fault leading to that no more power output is needed at some ESS rating between 1.5MVA and 3MVA.

10.3.2. ESS at Orca Substation and Main Town Fault

In these simulations, at time t=5s a fault occurs along the Main Town feeder between bus 601 and 602 causing a disturbance in the CEC electrical grid. Type of fault simulated is a 3-phase bolted fault which is only cleared by opening the Eyak Substation breaker isolating the feeder from the rest of the CEC electrical grid. The breaker at the Eyak Substation opens up at time t=5.2s which is the time for a mechanical breaker to detect a fault from the I^2t function and physically open. The simulation is run out to time t=30s to give the CEC electrical grid time to return to a steady state value. Multiple simulations were conducted with one being the base case not including an ESS and the others varying the rating of an ESS. Results are shown below.

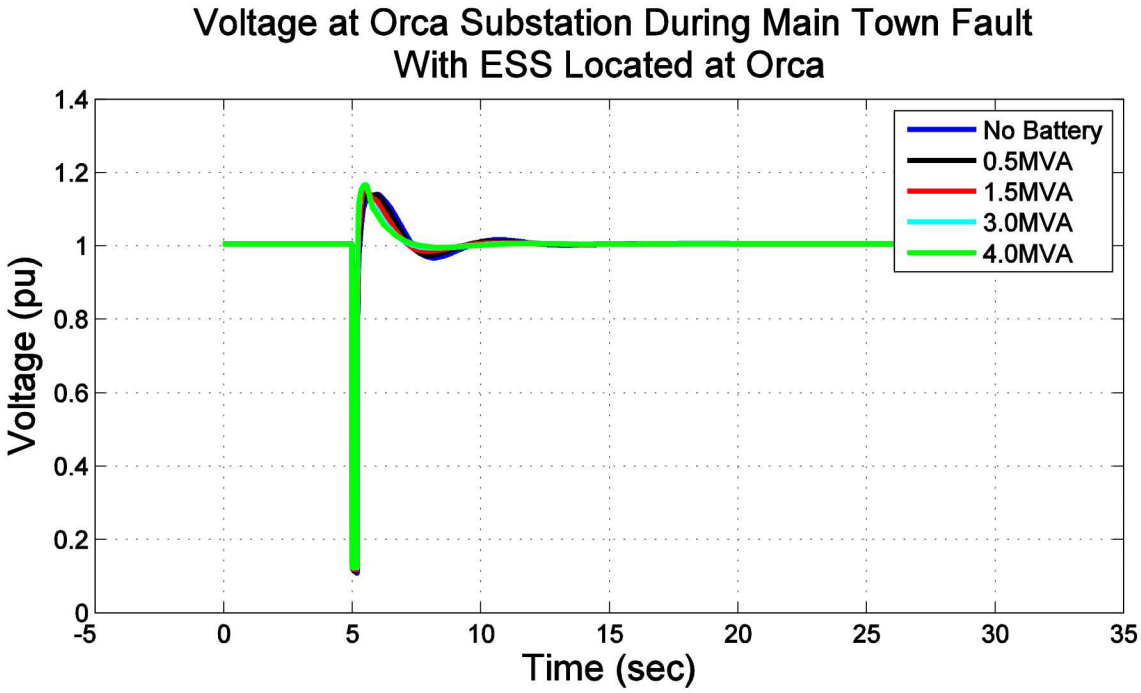

Figure 36 - Voltage at Orca Substation for a fault along Main Town feeder, with energy storage located at Orca Substation

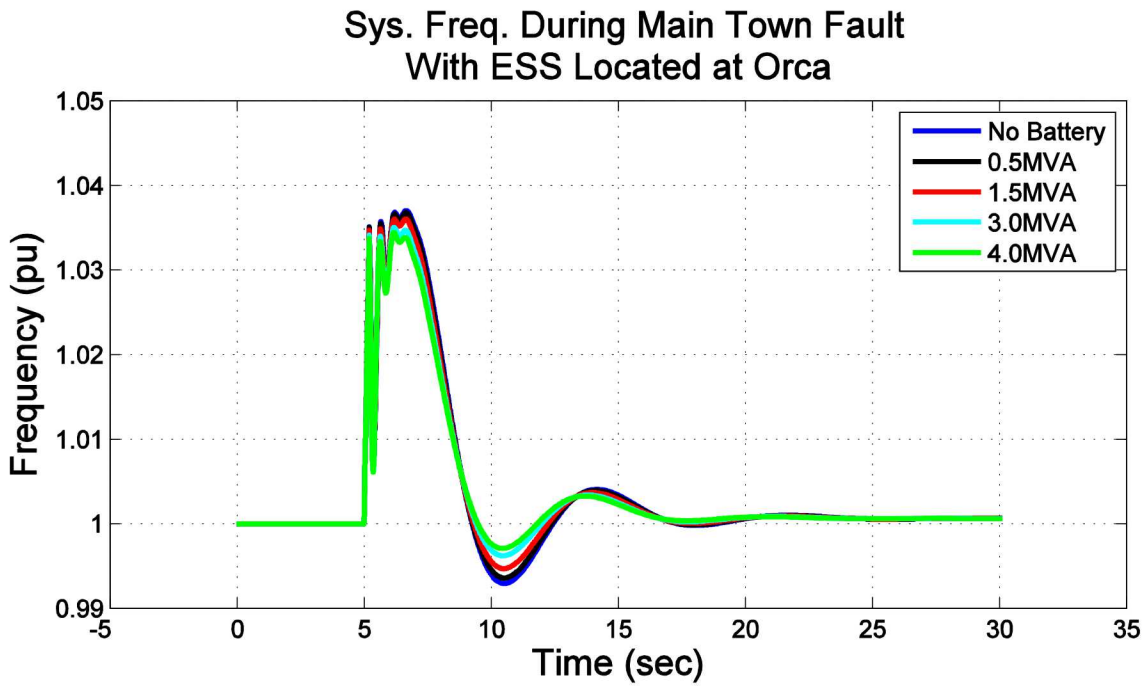

Figure 37 - System Frequency at Orca Substation for a fault along Main Town feeder, with energy storage located at Orca Substation

Voltage and system frequency before and after the Main Town feeder fault are shown in Figure 36 and Figure 37. The results are similar to that of the simulation with the Humpback Creek fault which the ESS did not have a large effect on the dampening of the voltage at the Orca Substation or system frequency. As the rating of the ESS is increased, the Orca Substation voltage and system frequency do show a slight increase in dampening occurs. Since the increase in dampening as the ESS rating is increased is meniscal, it can be concluded that ESS with a larger rating does not provide more transient stability benefit.

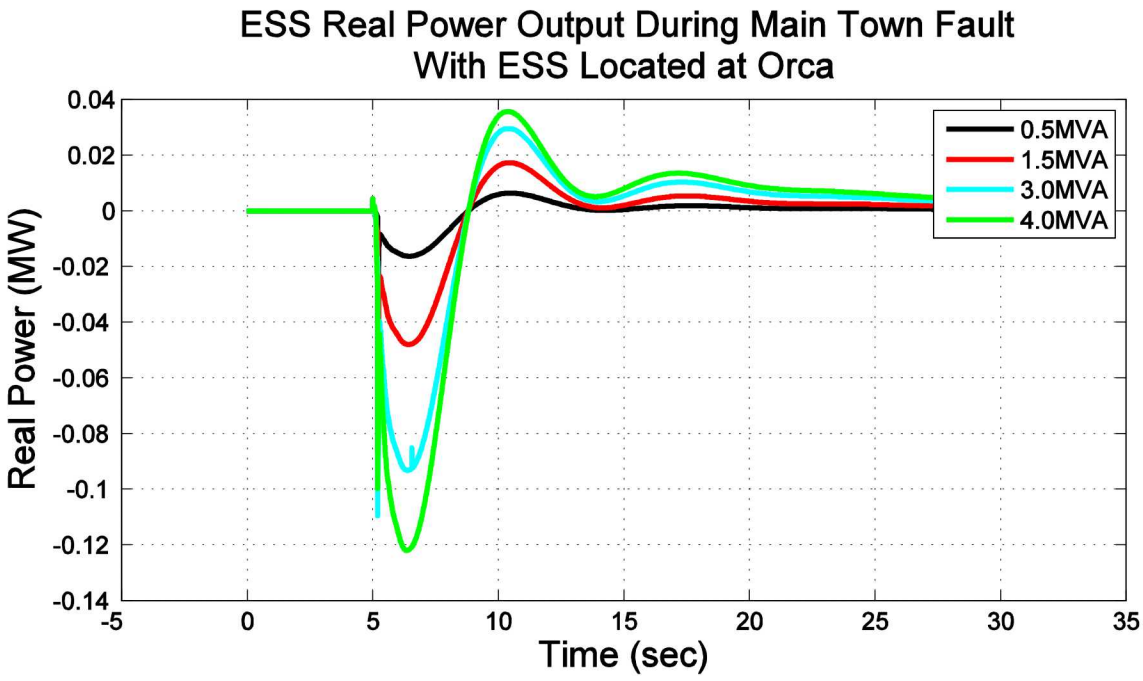

Figure 38 - Real Power Output of energy storage system located at the Orca Substation for a fault along Main Town feeder

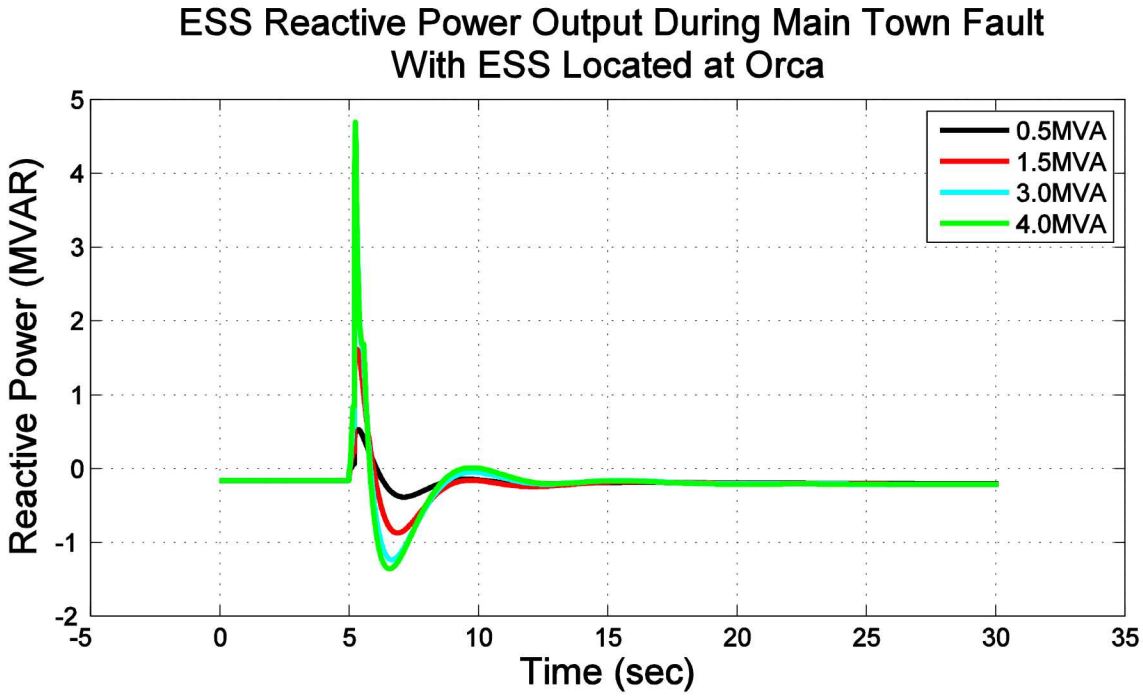

Figure 39 - Reactive Power Output of energy storage system located at the Orca Substation for a fault along Main Town feeder

Power output from the ESS shown in Figure 38 and Figure 39 is increased as the rating of the ESS is increased. As it was for the results from the Humpback Creek feeder fault, the reactive power output of the 3MVA and 4MVA are similar. These results show that a 4MVA ESS does not provide more benefit in providing reactive power than the 3MVA ESS during a fault along the Main Town feeder.

10.3.3. ESS at Orca Substation and Lake Avenue Fault

In these simulations, at time t=5s a fault occurs along the Lake Avenue feeder between bus 803 and 804 causing a disturbance in the CEC electrical grid. This fault occurs along a feeder which is fed off the Eyak substation. Type of fault simulated is a self-clearing fault which is cleared by time t=5.1s. The simulation is run out to time t=30s to give the CEC electrical grid time to return to a steady state value from the fault. Multiple simulations were conducted with this same fault with one being the base case not including an ESS and the others varying the rating of an ESS. Results are as follow.

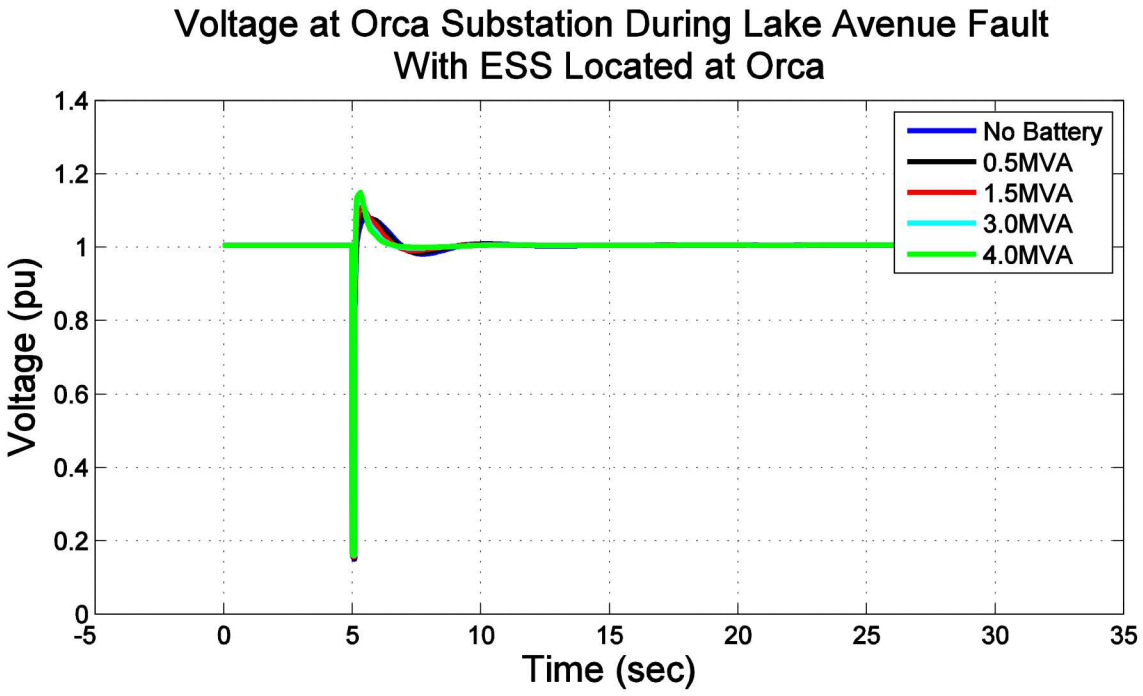

Figure 40 - Voltage at Orca Substation for a fault along Lake Avenue feeder, with energy storage located at Orca Substation

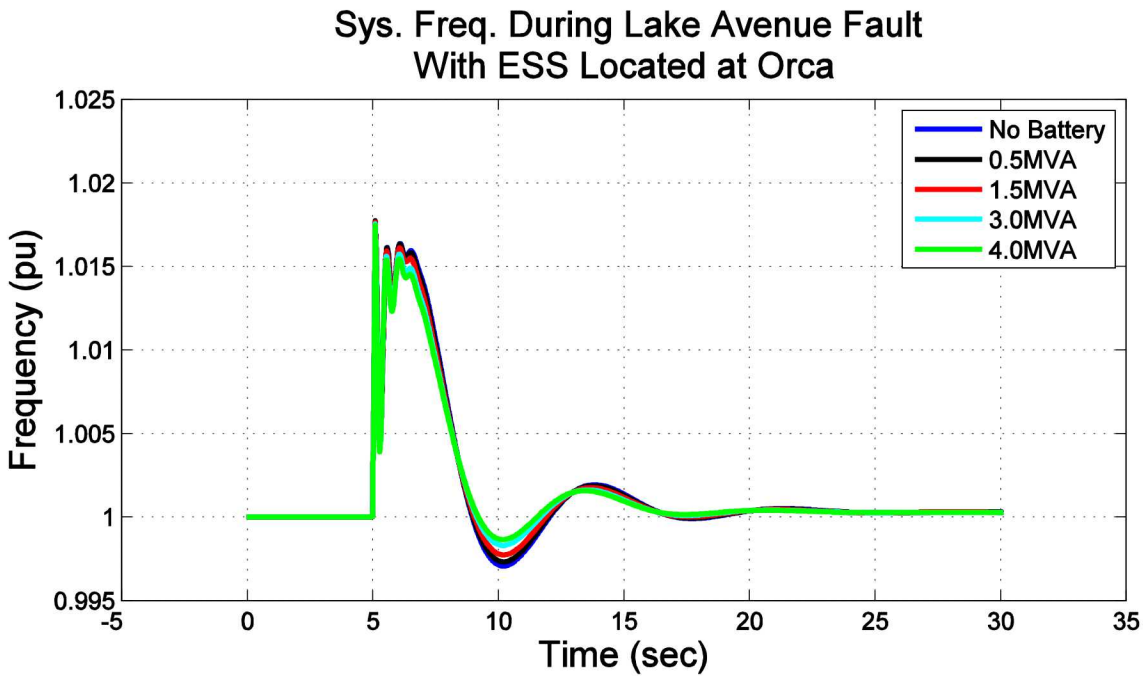

Figure 41 - System Frequency at Orca Substation for a fault along Lake Avenue feeder, with energy storage located at Orca Substation

Voltage and system frequency before and after the Lake Avenue feeder fault are shown in Figure 40 and Figure 41. The results are similar to that of the simulation with the Humpback Creek fault and the Main Town feeder fault which the ESS did not have a large effect on the dampening of the voltage at the Orca Substation or system frequency. As the rating of the ESS is increased, the Orca Substation voltage and system frequency do show a slight increase in dampening occurs. Since the increase in dampening as the ESS rating is increased is meniscal, it can be concluded that ESS with a larger rating does not provide more transient stability benefit.

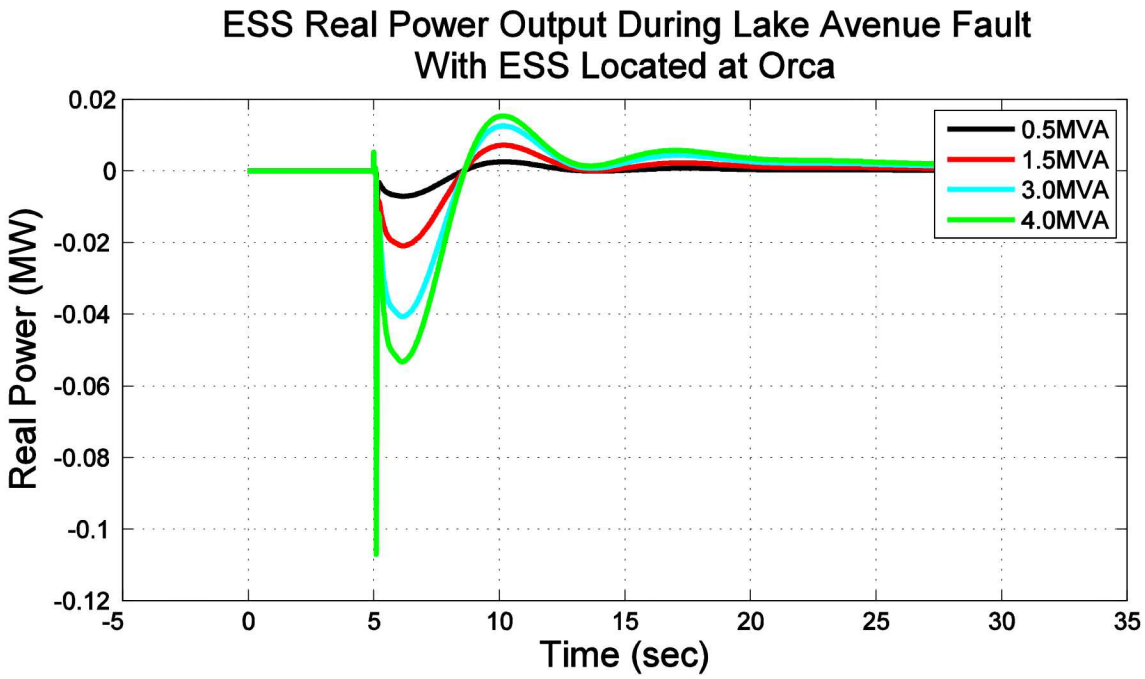

Figure 42 - Real Power Output of energy storage system located at the Orca Substation for a fault along Lake Avenue feeder

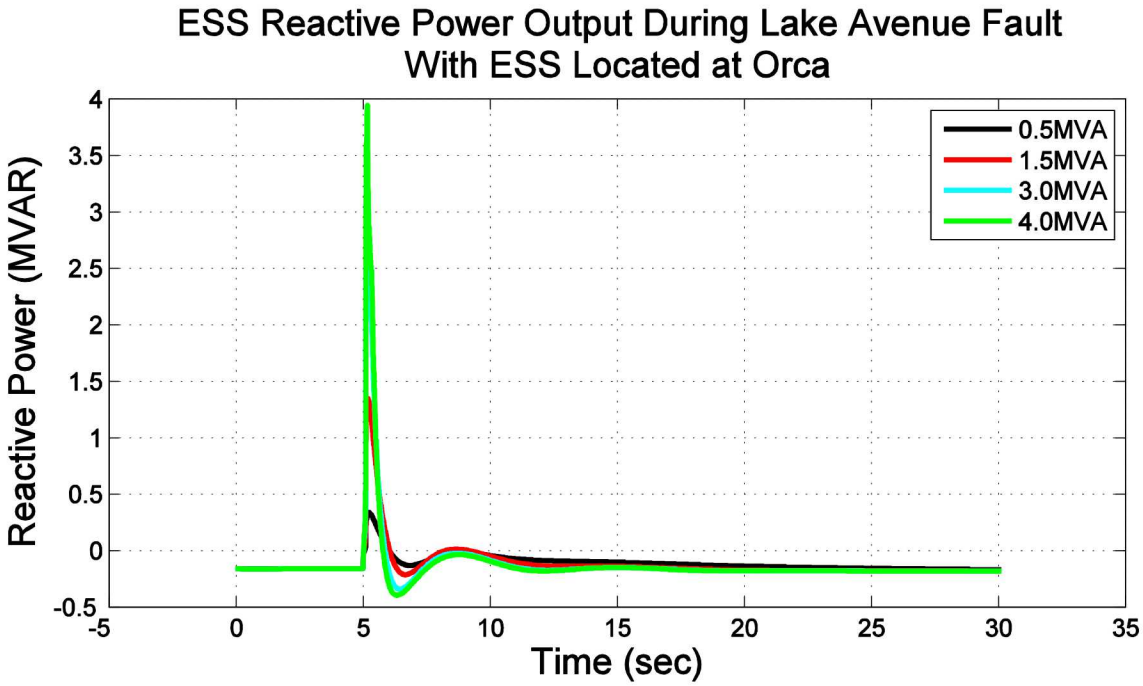

Figure 43 - Reactive Power Output of energy storage system located at the Orca Substation for a fault along Lake Avenue feeder

Power output from the ESS shown in Figure 42 and Figure 43 is increased as the rating of the ESS is increased. As it was for the results from the Humpback Creek feeder fault and Main Town feeder fault, the reactive power output of the 3MVA and 4MVA are similar. These results show that a 4MVA ESS does not provide more benefit in providing reactive power than the 3MVA ESS during a fault along the Main Town feeder.

10.3.4. ESS at Orca Substation and Diesel Generator Trip

In these simulations, at time t=5s the diesel generator Orca 5 (1.406MVA) at the Orca Power Plant trips offline causing a disturbance in the CEC electrical grid. After the generator is tripped, it stays offline for the rest of the simulation. The simulation is run out to time t=30s to give the CEC electrical grid time to return to a steady state value from the generator trip. Multiple simulations were conducted with the same generator tripping offline with one being the base case not including an ESS and the others varying the rating of an ESS. Results are as follow.

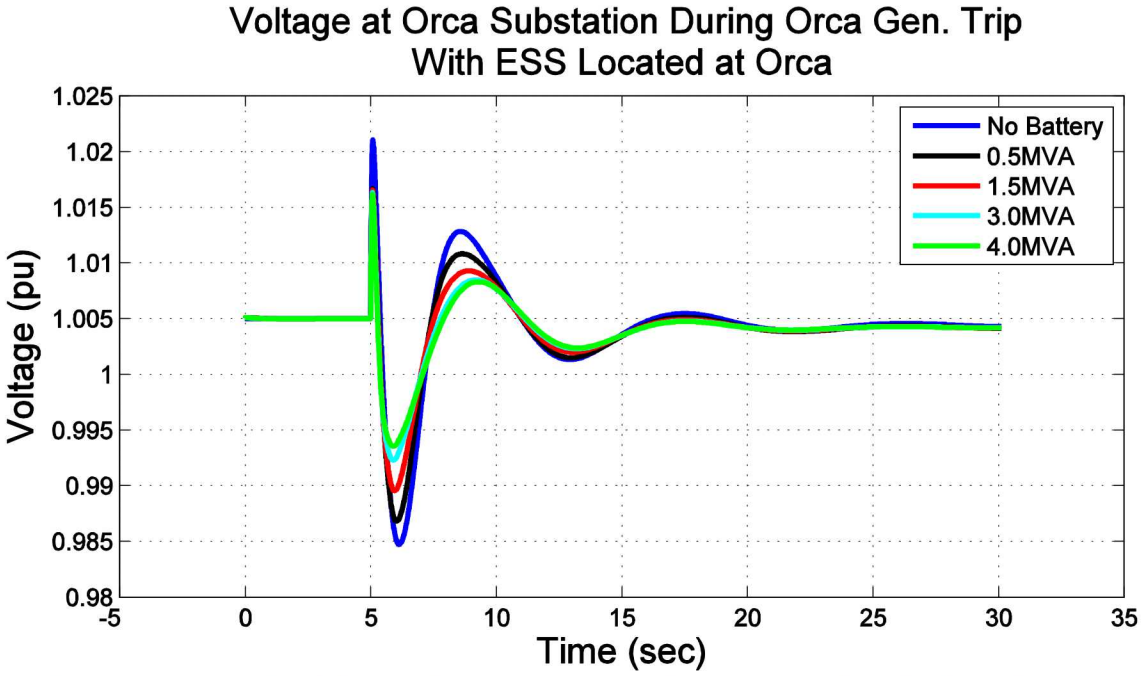

Figure 44 - Voltage at Orca Substation during generator trip, with energy storage located at Orca Substation

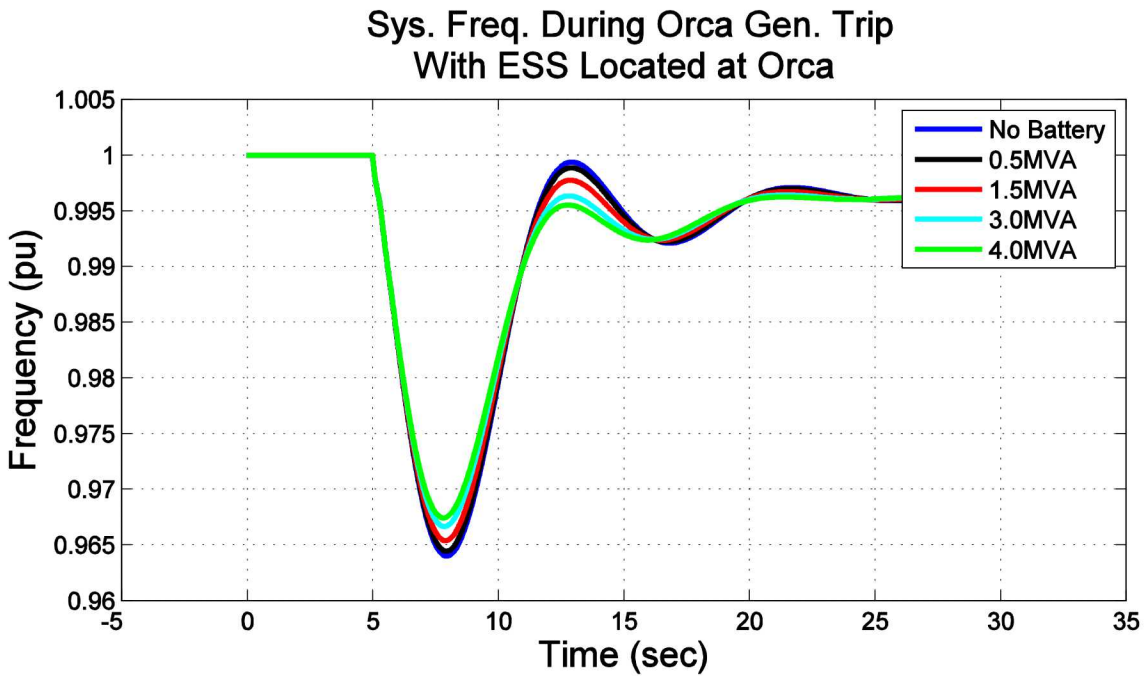

Figure 45 - System Frequency at Orca Substation during generator trip, with energy storage located at Orca Substation

The Orca 5 generator trip removes 1.406MVA of generation from the CEC electrical grid. Since the ESS's main control objective is to provide reactive power which maintains the voltage at the bus it is regulating, the voltage at the Orca Substation is dampened compared to the case where no ESS is used. As the ESS rating is increased so is the dampening of the voltage oscillation at the Orca Substation. System frequency is dampened slightly when the ESS is 1.5MVA or greater but not enough to make a significant difference when compared to the base case with no ESS.

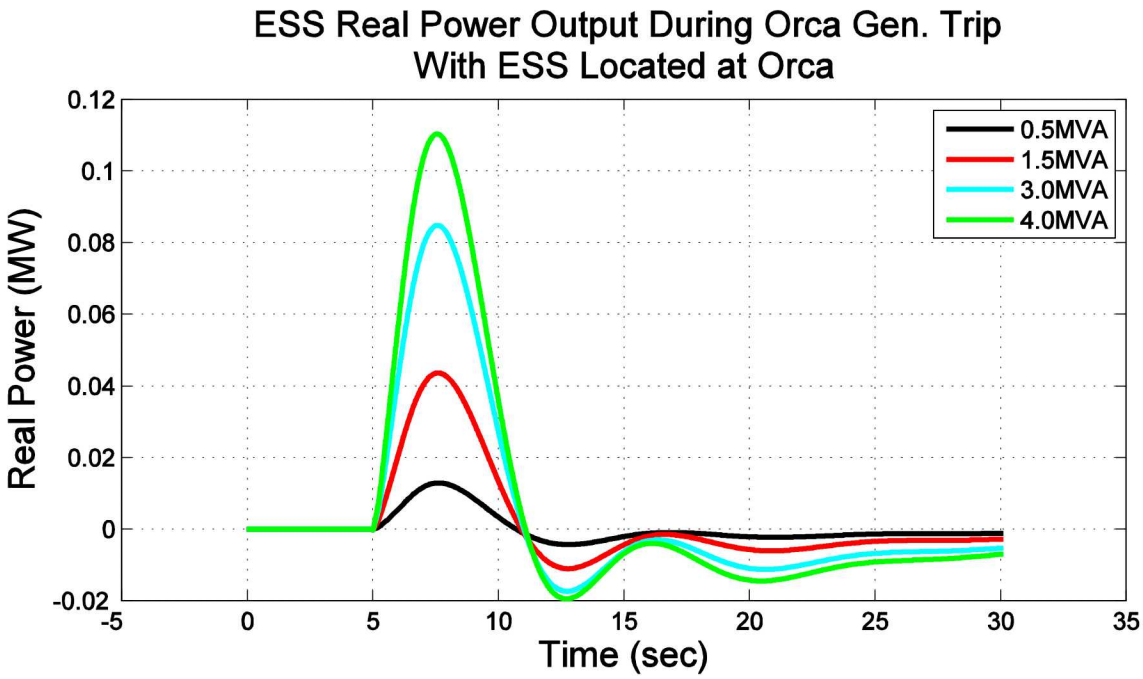

Figure 46 - Real Power Output of energy storage system located at the Orca Substation during generator trip

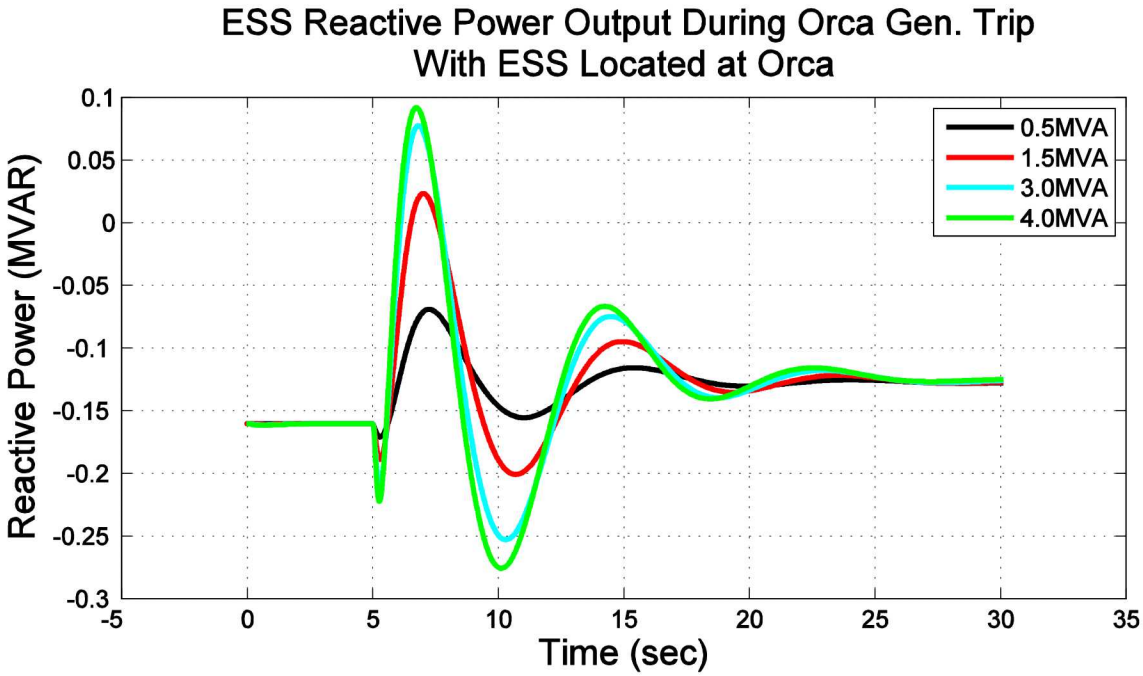

Figure 47 - Reactive Power Output of energy storage system located at the Orca Substation during generator trip

In Figure 46 and Figure 47, the reactive and real power of the ESS at different ratings is shown. Larger ESS ratings allow for more real and reactive power output to be injected and/or absorbed from the CEC electrical grid. The output from the ESS during the generator trip is not very large when compared to its rating. The 4MVA ESS only outputs approximately an absolute max of

0.15MW and 0.275MVAR. This output of the energy storage is only about 4%-7% of the rating. Low power output from the ESS can be due to the fact that the starting voltage at the Orca Substation was at 1.005 pu and the bus at which the ESS was located is next to the Orca Substation. The ESS was scheduled to maintain the voltage at its bus to 1.0 pu which approximately 0.16MVAR had to be absorbed by the ESS to achieve this. Another factor is that the Power Creek hydro-electric units are providing only 2.7MW each of their 3MW rating. With enough spinning capacity online from Orca 6 1.406MVA diesel generator and the 2 Power Creek hydro-electric units, the loss of the Orca 5 generator is covered.

From the results above, ESS provides an insignificant dampening effect on the voltage at the Orca Substation and the system frequency when the MW rating of the ESS was varied and located at the Orca Substation. Results for the dampening effect is similar when the ESS is placed at the Eyak Substation, main hospital and airport. One thing to note is that the ESS dampening effect was insignificant but at the same time it did not make the CEC electrical transient stability inferior to that without the ESS.

The MW rating of the ESS was shown that as it increases in a certain location within the CEC electrical grid, the electrical transient dampening is slightly increased but not enough to make a large impact on the CEC electrical stability. Knowing that the MW rating of the ESS did not provide significant dampening, the location where the ESS was placed was compared between one another holding the MW rating constant. This comparison was performed to determine if one location provided more transient stability than another. In the following section, a constant MW rating of 2MW was used. This value was chosen sine it is the closes to the mean of the ESS ratings, Simulations in the sections below hold the rating of the ESS at 2MVA while varying the location for different electrical disturbances. Results with all the ESS sizes is provided in Appendix G.

10.3.5. System Frequency with 2MVA ESS Varying Location

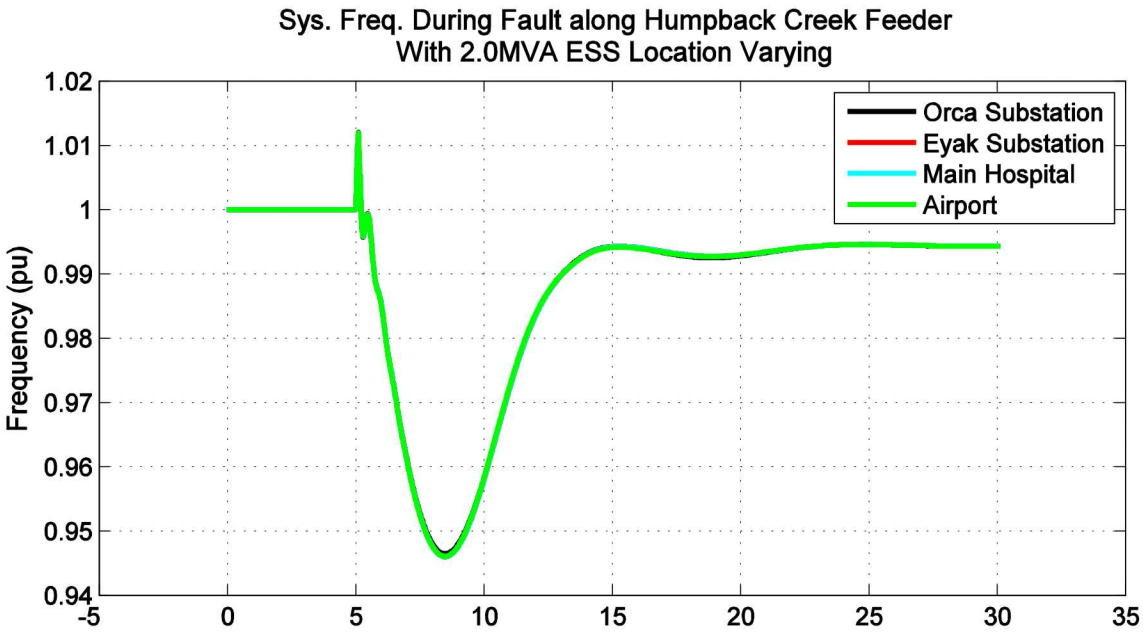

Figure 48 – System frequency with a 2MVA ESS at multiple locations during a Humpback Creek feeder fault

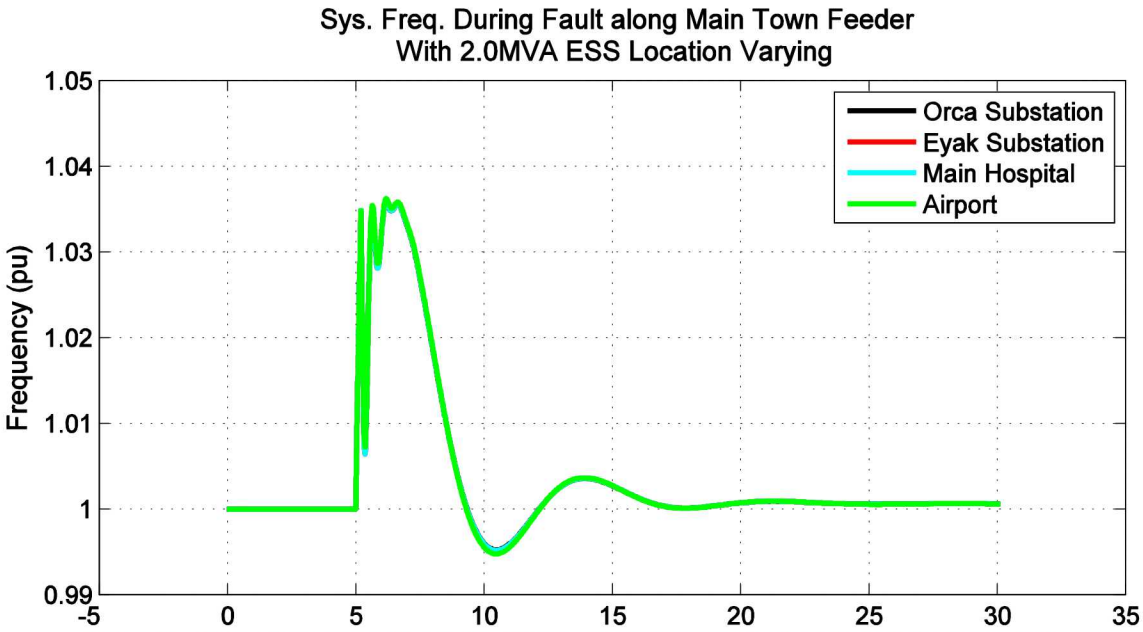

Figure 49 - System frequency with a 2MVA ESS at multiple locations during a Main Town feeder fault

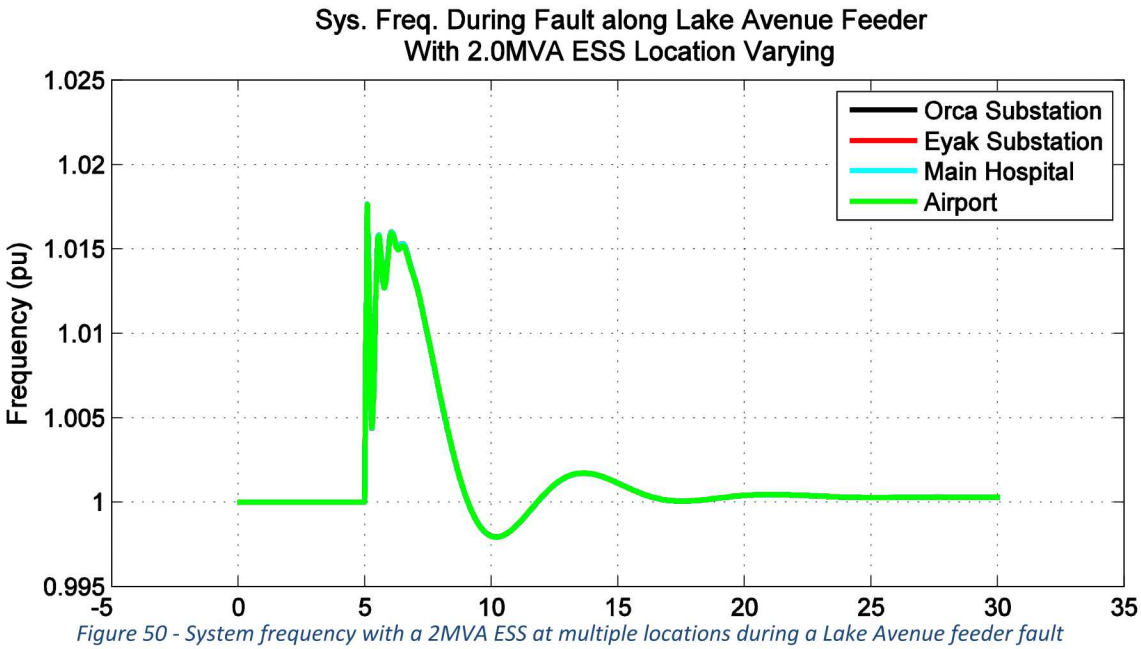

Figure 50 - System frequency with a 2MVA ESS at multiple locations during a Lake Avenue feeder fault

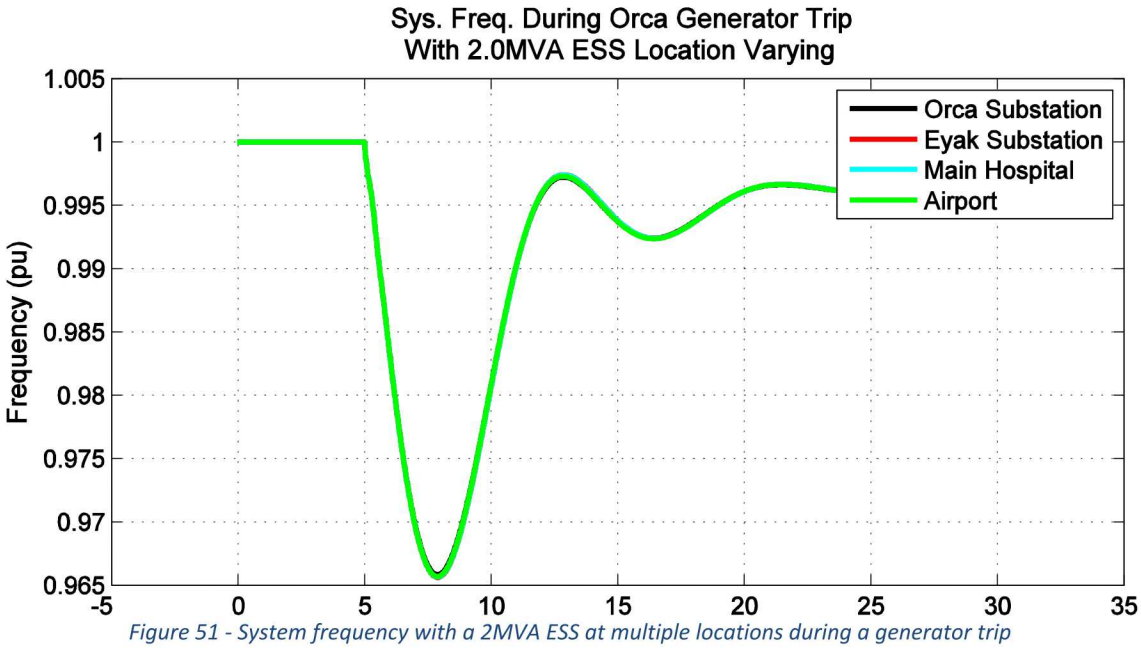

Figure 51 - System frequency with a 2MVA ESS at multiple locations during a generator trip

In Figure 48 through Figure 51, the 2MVA ESS was placed at the locations Orca Substation, Eyak Substation, main hospital and airport during a certain electrical disturbance. All the figures above suggest that the location of the ESS does not have any significant effect on the system frequency.

10.3.6. Voltage at Orca Substation with 2MVA ESS Varying Location

Figure 52 through Figure 55 show the voltage at the Orca Substation with a 2MVA ESS installed at various locations. The voltage response is similar for all the locations and electrical disturbances except that when the ESS is located at the Airport during a generator trip. Voltage at the Orca Substation is higher due to the ESS maintaining the Airport bus voltage which is at the end of a radial feeder from Eyak Substation. By the ESS maintaining the voltage at the end of the feeder, the Orca generators did not have to supply as much reactive power during steady state conditions allowing more reactive power from the Orca generators to be available during the transients. Overall, the location of the ESS has little effect on the Orca Substation voltage.

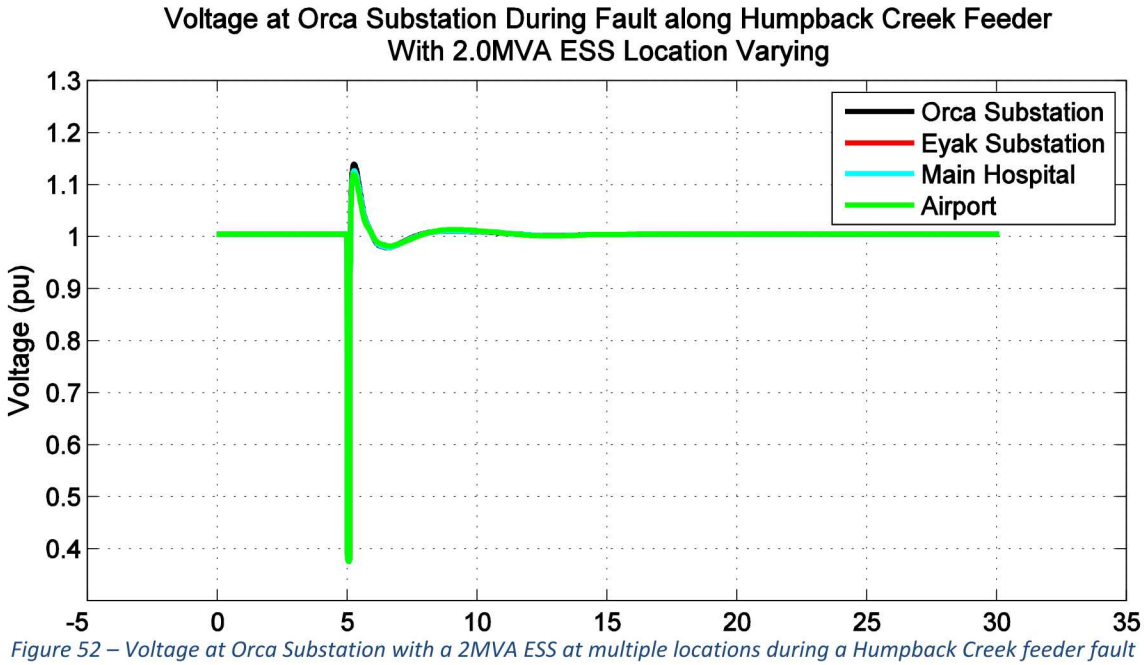

Figure 52 – Voltage at Orca Substation with a 2MVA ESS at multiple locations during a Humpback Creek feeder fault

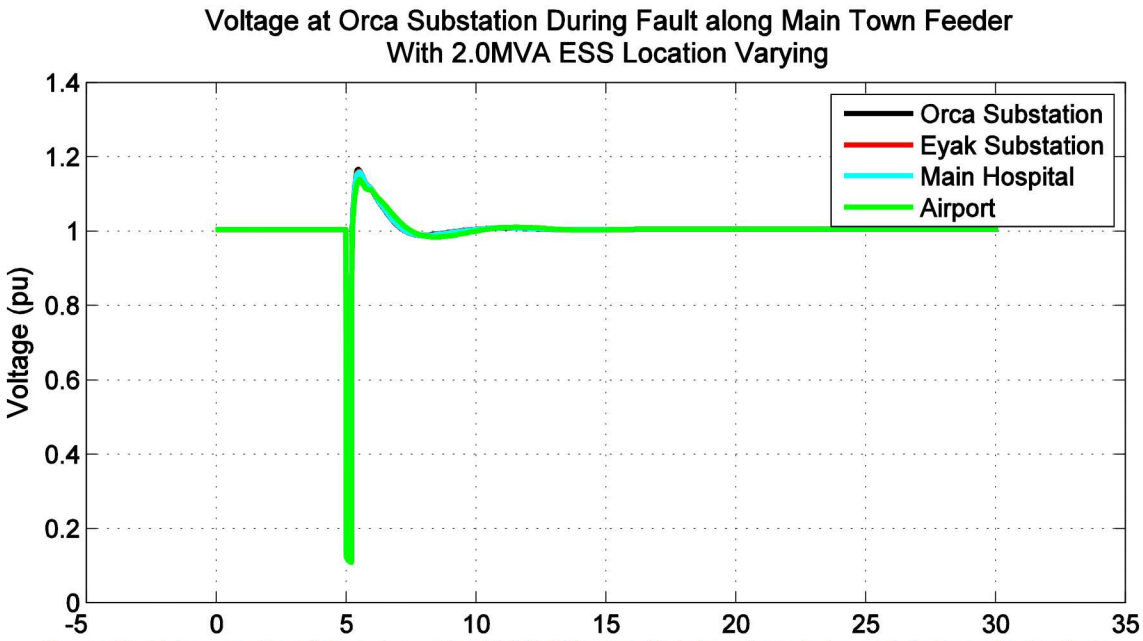

Figure 53 - Voltage at Orca Substation with a 2MVA ESS at multiple locations during a Main Town feeder fault

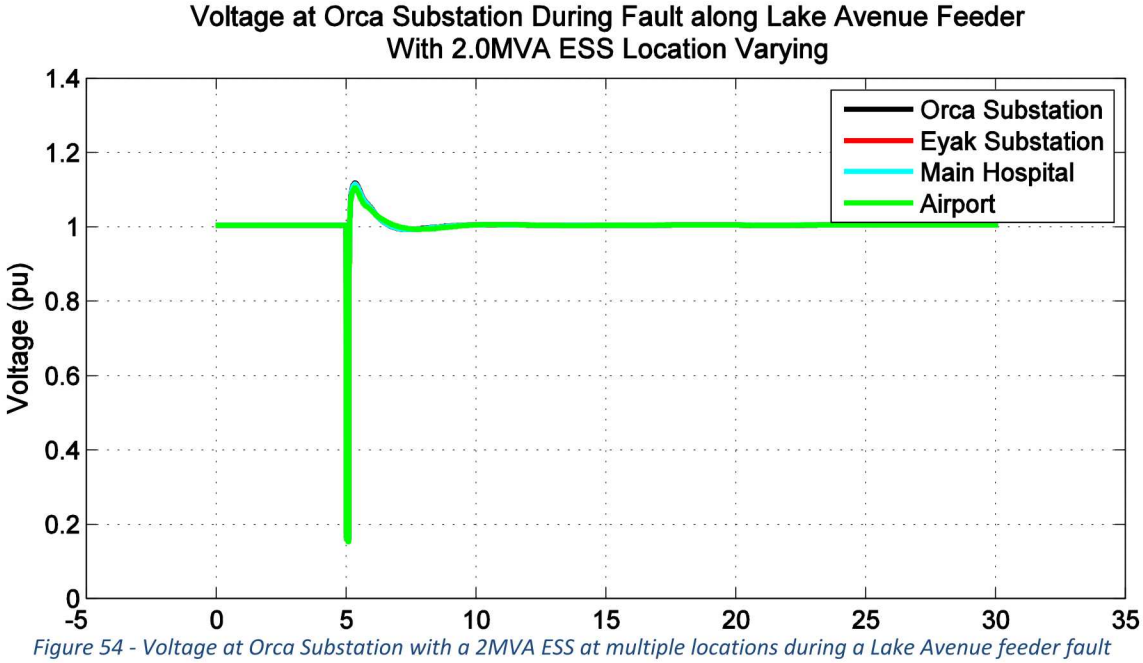

Figure 54 - Voltage at Orca Substation with a 2MVA ESS at multiple locations during a Lake Avenue feeder fault

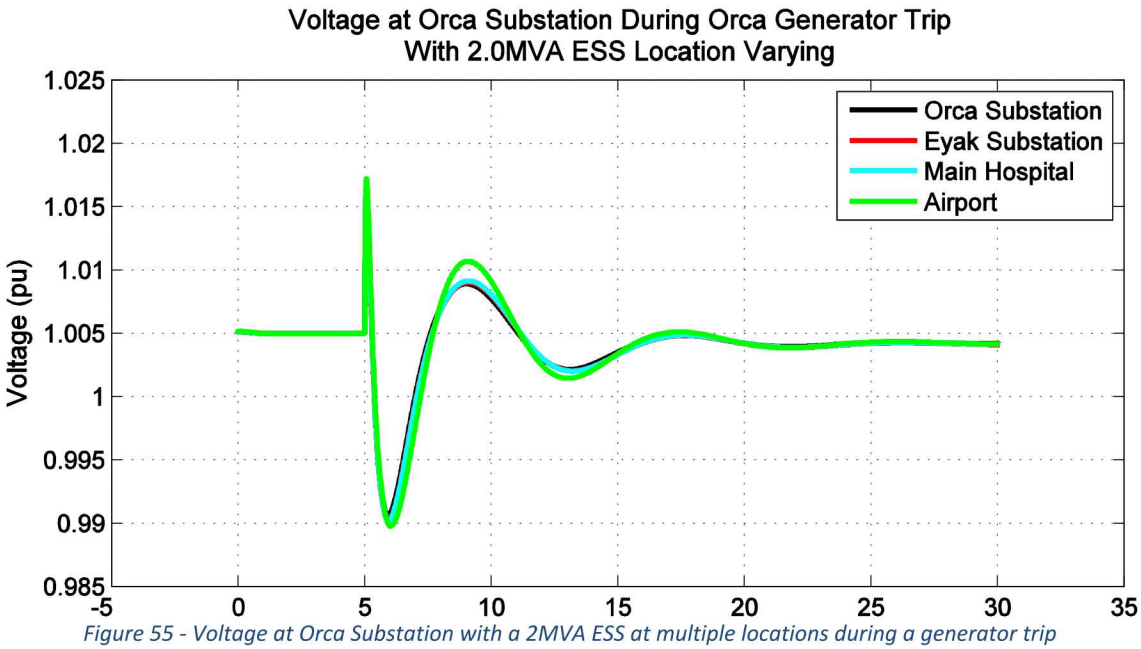

Figure 55 - Voltage at Orca Substation with a 2MVA ESS at multiple locations during a generator trip

10.3.7. ESS real power output of 2MVA ESS varying location

Real power output from the 2MVA ESS at all 4 locations and during any of the 4 electrical transients is minimal. The largest power output is during the Main Town feeder fault which the 2MVA ESS injected approximately 0.2MW (10% of ESS rating) into the CEC grid shown in Figure 57. Minimal amount of real power is due to the fact that the ESS control had priority to inject or absorb reactive power. From the figures below, the location of the ESS did not play a large role on how the ESS injected real power into the CEC grid.

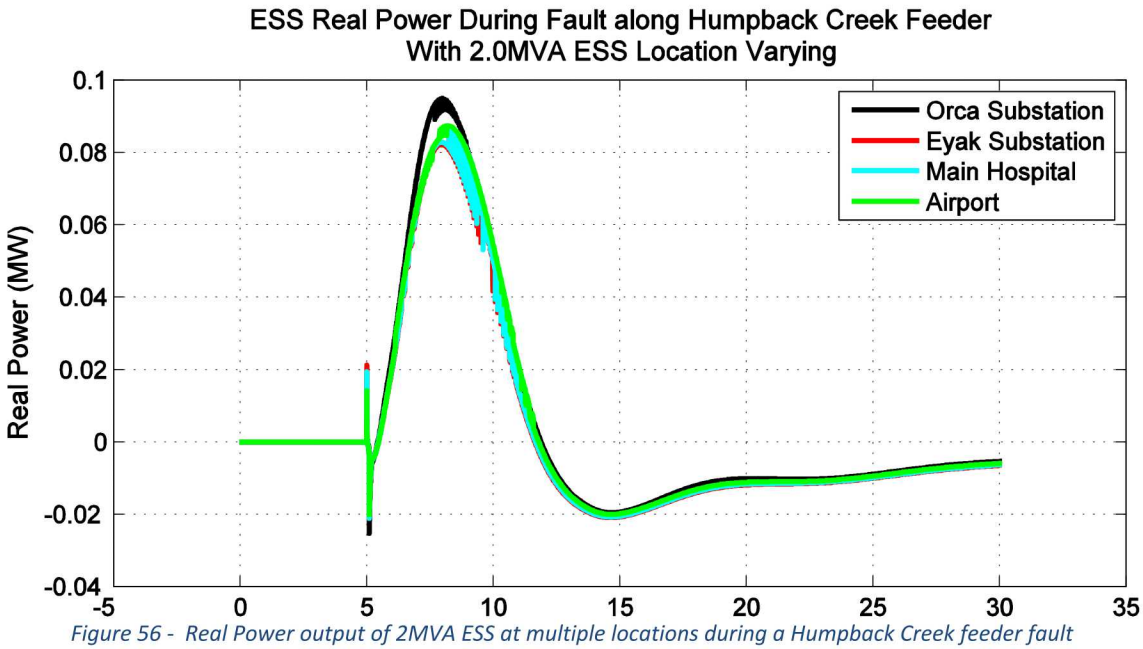

Figure 56 - Real Power output of 2MVA ESS at multiple locations during a Humpback Creek feeder fault

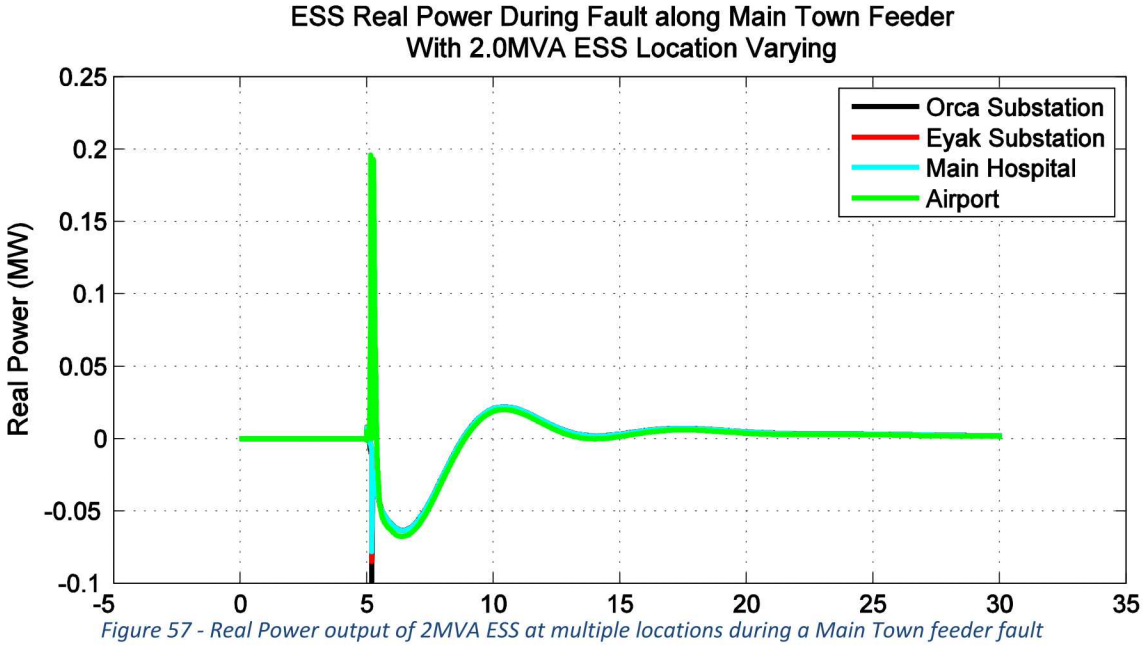

Figure 57 - Real Power output of 2MVA ESS at multiple locations during a Main Town feeder fault

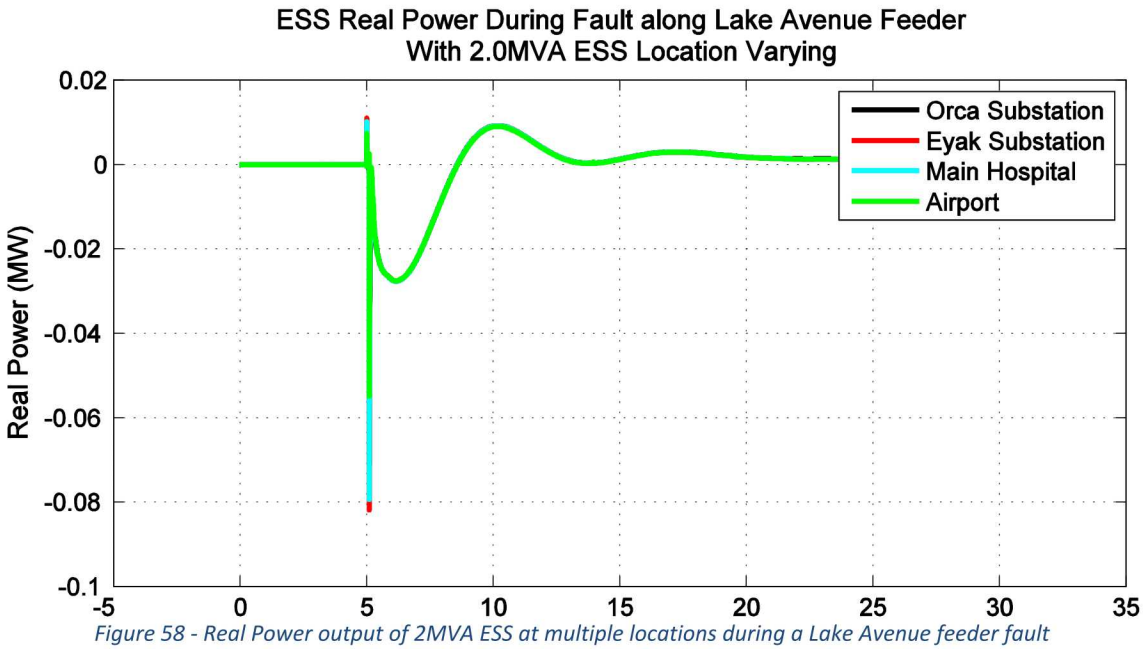

Figure 58 - Real Power output of 2MVA ESS at multiple locations during a Lake Avenue feeder fault

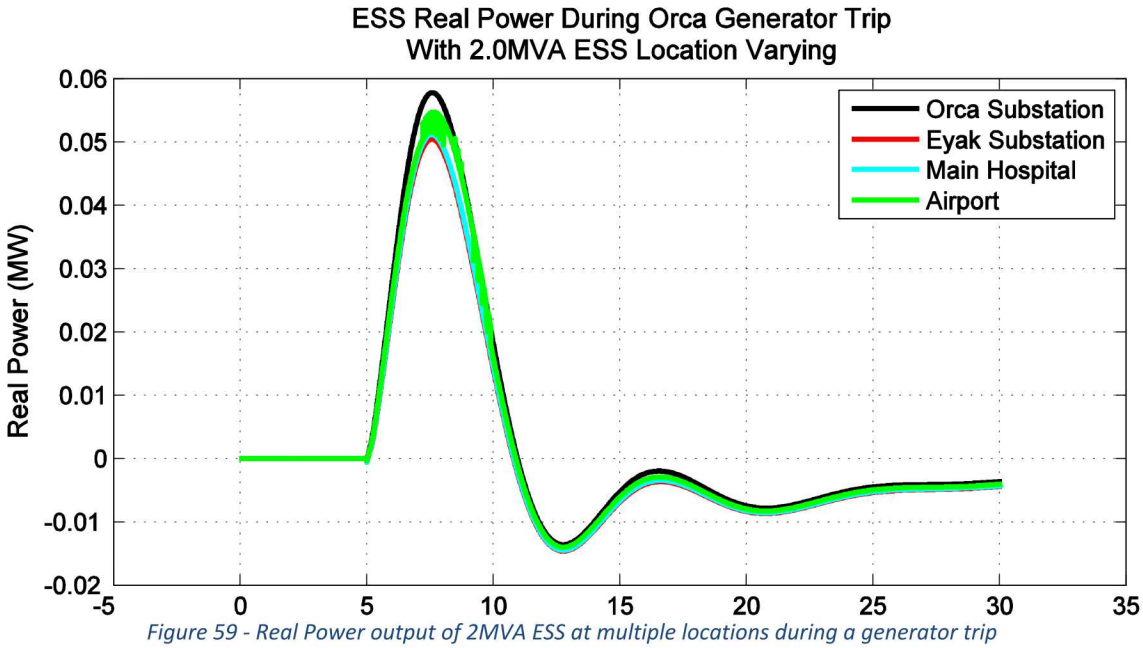

Figure 59 - Real Power output of 2MVA ESS at multiple locations during a generator trip

10.3.8. ESS reactive power output of 2MVA ESS varying location

Reactive power output magnitude is dependent on the location of the ESS. Figure 60 shows the ESS reactive power output during the fault along Humpback Creek feeder. This feeder is connected between the Orca Substation and the Humpback Creek Substation which the ESS closes to the fault is when it is in the location labeled Orca Substation. During the fault, the largest change in voltage occurs closes to the fault which in this case is the Orca Substation and

the Humpback Creek Substation. Since the ESS reactive power output magnitude is based on the error between the measured voltage at the bus it is regulating and its reference voltage of 1.0 pu, the larger voltage error occurs at the location closes to the fault. In the case with the ESS located at the Orca Substation with the fault occurring along Humpback Creek feeder, the reactive power output reaches a value of approximately 1.33 MVAR. The other locations during the Humpback Creek feeder fault reach a slightly less reactive power output of approximately 1.0MVA.

Initial reactive power output for the ESS varies depending on where in the CEC grid it is located. Higher the initial reactive power being absorbed by the ESS, the higher the voltage at the bus it is regulating is over 1.0 pu. This can be seen in all the figures below between time t=0s and t=5s with each location of the 2MVA ESS. The highest initial bus voltage is at the Eyak Substation followed by the Main Hospital, Airport and Orca Substation. This voltage magnitude at each location can be seen throughout the figures below.

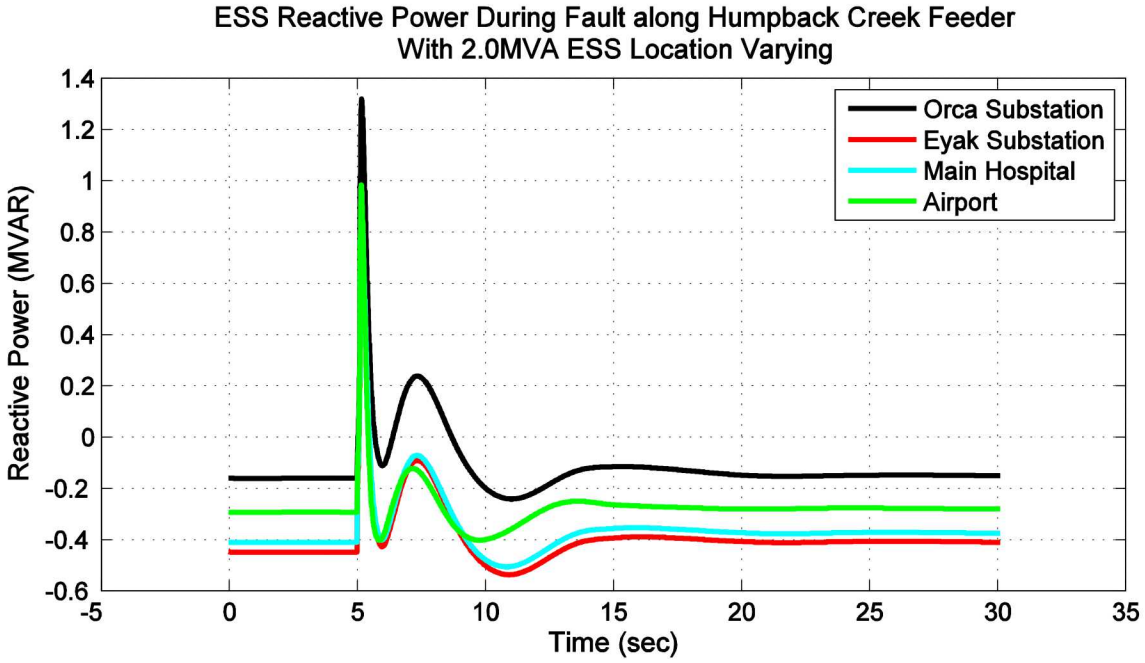

Figure 60 - Reactive Power output of 2MVA ESS at multiple locations during a Humpback Creek feeder fault

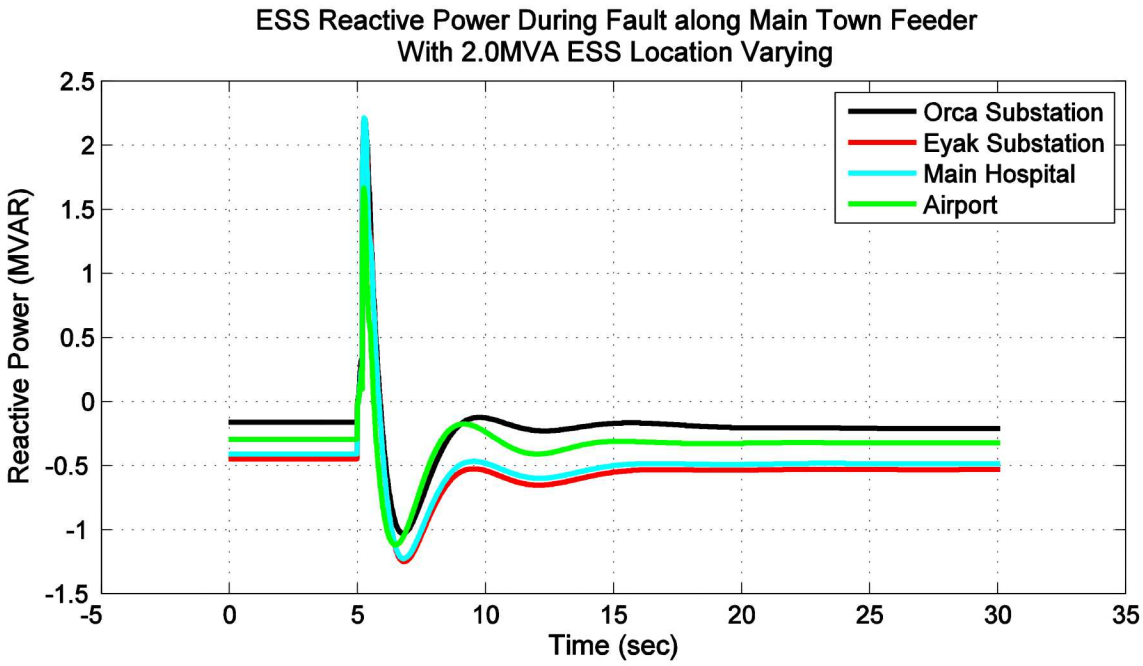

Figure 61 - Reactive Power output of 2MVA ESS at multiple locations during a Main Town feeder fault

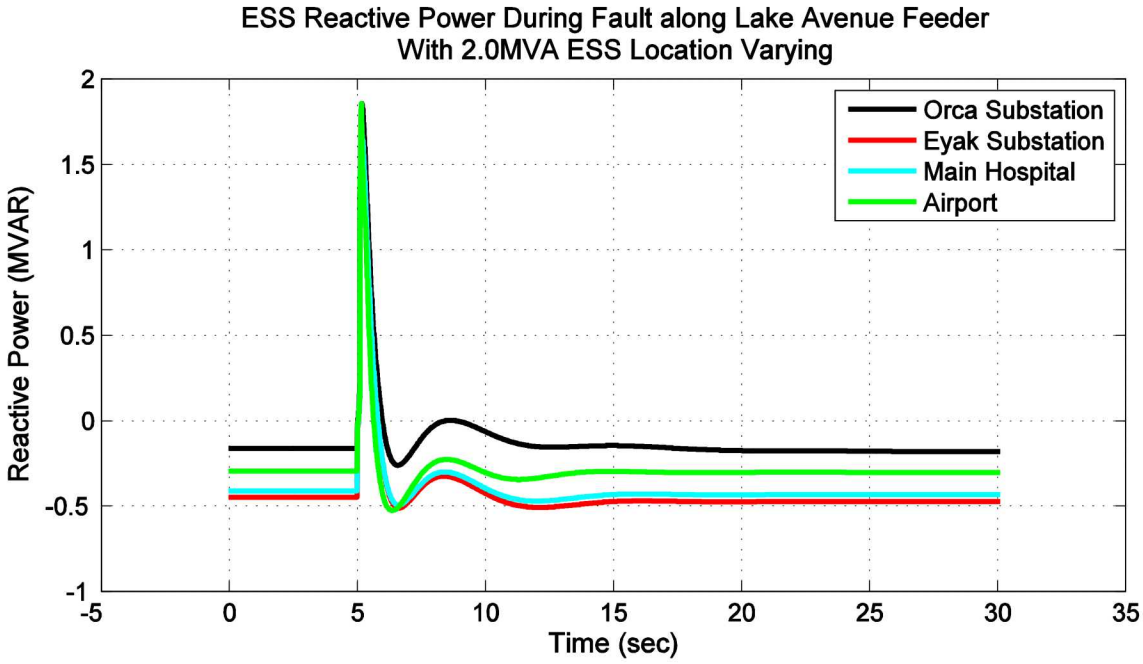

Figure 62 - Reactive Power output of 2MVA ESS at multiple locations during a Lake Avenue feeder fault

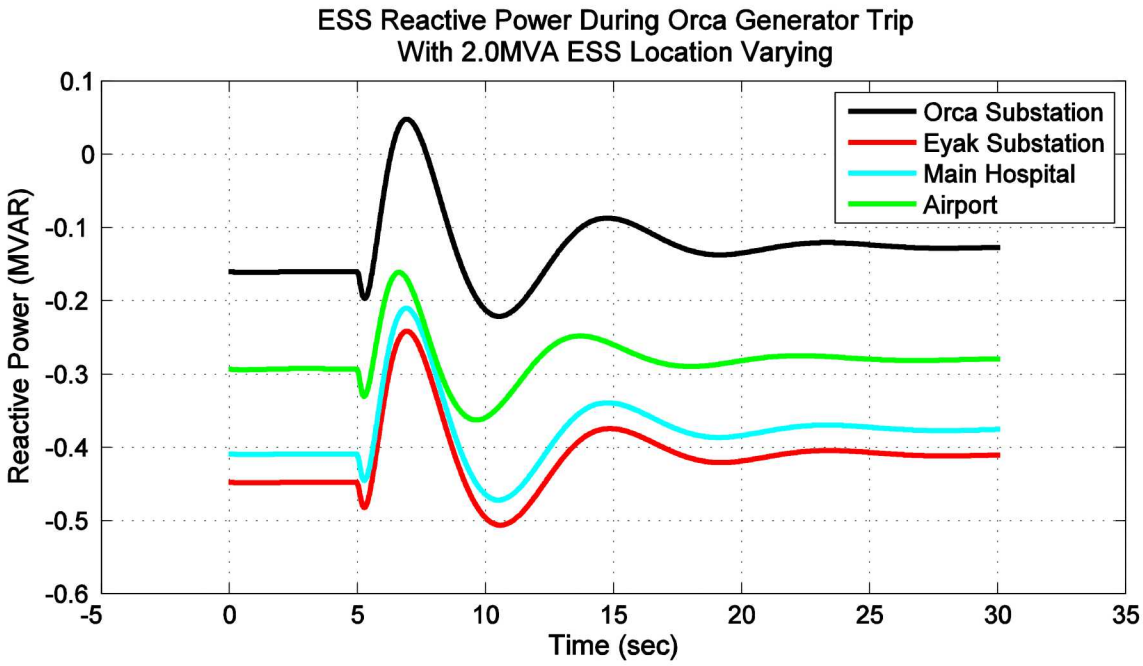

Figure 63 - Reactive Power output of 2MVA ESS at multiple locations during a generator trip

10.3.9. Summary

The dynamic analysis performed in PSLF varied the MVA rating of the ESS from 0.5MVA to 4.0MVA, placed the ESS at 4 locations within the CEC grid and simulated 3 faults and 1 generator trip. In each simulation the pertinent data was collected such as bus voltage, generator speeds and power output to name a few. ESS was modeled using standard library blocks which were the ESTOR2 and REGC_A and set to have the reactive power output be the priority over real power output.

From the results, it was concluded that the ESS did not have a significant dampening impact on the CEC electrical transients as the MVA rating of the ESS was increased. Location of the ESS did make a slight difference in the initial reactive power output of the ESS before the transients occurred. Reactive power output from the ESS is based on the difference between the actual voltage at the bus the ESS is electrically connected too and the voltage reference of 1.0 pu. As the actual voltage is increased above 1.0 pu, the ESS increases the reactive power it absorbs and vice versa. When the ESS was placed at a location such as the Eyak Substation with a high voltage, the ESS absorbed more reactive power than when placed at a place with lower voltage such as the Orca Substation. During the electrical transients, the ESS that was located closes to the location that the electrical disturbance occurred, the greater the magnitude of reactive power output was supplied or absorbed by the ESS. CEC electrical grid is small when compared to a medium or large city in the lower 48 states. Since this electrical grid is small, any electrical disturbance is seen throughout the entire grid which can be the reason why at any location the ESS was placed it provided reactive power to dampen the transient. The dampening effect by the ESS on the electrical transient based on its location was minimum therefore no location was better than another.

11. CONCLUSION AND FUTURE WORK

The energy balance model simulations which allowed the diesel generators to charge the ESS resulted in less diesel run time, higher loading on the diesels, and reduction of fossil fuel consumption by the diesel generators. However, the simulation resulted in more diesel switching and a higher utilization of the ESS. On the other hand, simulations where only hydro charged the ESS diesel run time was increased and lower loading on the diesel was seen. Even with the diesels running at lower loads and for longer durations, the diesel switching was reduced as well as the utilization of the ESS.

There were simulations where less than 10% of the total diesel savings is contributed by the ESS. In other words, only 10% of the diesel savings was discharged by the ESS. The rest of the savings resulted from the ESS supplying spinning reserve and allowing a smaller or no diesel generator to run online and more hydro to be imported. By using the ESS as a spinning reserve a relatively low utilization of the ESS is seen for the saved diesel prolonging the life of the ESS.

Significant diesel savings of 0.5 GWh (around 50% the savings of a 1.5 MW / 1 MWh ESS) were shown in simulations by only changing the diesel dispatch controls and not adding any ESS. It requires deflecting a minimum of hydro at the turbine generators to minimally load the diesel generators and maximize the hydro utilization. The addition of the ESS may be required to allow this control scheme to be possible by adding spinning reserve availability and reliability as well as additional savings.

The dynamic simulation results for the various fault and loss of generation test cases examined for summer peak conditions with an ESS did not significantly improve system stability for faults and loss of generation events. The location of the ESS within the CEC system did not result in a significant performance difference. Based on this result, the ESS can provide additional societal benefit by being placed at the Main Hospital. At this location, the ESS can provide the benefit of being an uninterruptible power supply (UPS) for the Hospital during a power outage.

In September 2017, the Cordova City Council approved funding to pursue the installation of an ESS. Sandia will work with CEC and ACEP in developing a request for proposal (RFP) for procuring, installing and commission an ESS within the CEC electrical system.

Future work needs to be done within the Energy Balance and PSLF dynamic models which include:

- Optimizing diesel dispatch schedule to reduce diesel switching and fossil fuel consumption
- Improve calculated spilled hydro by measuring the forebay water speed and dam height as well as test the calculated deflected power at the turbine generator in Cordova
- Further refine PSLF dynamic models of the generation assets and loads through recorded transient data
- Utilize newly developed PSLF standard library energy storage model with vendor specific parameters

- Perform sensitivity analysis for energy storage initial state of charge and operation state (discharge, idle, or charging) in PSLF to determine transient stability envelope

Develop a more detailed model of a specific ESS technology in PSLF and determine if a real power or reactive power priority controller provides greater transient stability.
Other future research will be to understand the controls, software and hardware required to utilize a grid tied ESS performing spinning reserve and UPS functions simultaneously. The research would be on the transition period between the ESS going from a current source to a voltage source within 10ms during a power outage and avoiding nuisance tripping during voltage sags and swells during normal operation. Hardware and prediction methods will have to be developed to accomplish this task.

REFERENCES

[1] A. Nuhic, T. Terzimehic, T. Soczka-Guth, M. Buchholz and K. Dietmayer, "Health Diagnosis and Remaining Useful Life Prognostics of Lithium-Ion Batteries Using Data-driven methods," *Power Sources,* vol. 239, 2013.

[2] R. Dufo-Lopez, J. M. Lujano-Rojas and J. L. Bernal-Agustin, "Comparison of Different Lead-acid Battery Lifetime Prediction Models for use in Simulation of Stand-alone Photovoltaic Systems," *Appl. Energy,* no. 115, 2014.

[3] H. Schaede, M. Mueller-Stoffels and C. Koplin, "Reducing Diesel Use And Maximizing Hydro Utilization in Cordova - Demand Managed Loads," Alaska Center for Energy and Power, Fairbanks Alaska, 2015.

[4] A. A. N. Alhamati, T. A. Mohammed, A. H. Ghazali, J. Norzaie and K. K. Al-Jumaily, "Determination of Coefficient of Discharge for Air-Inflated Dam Using Physical Model," *Sci. Technol,* vol. 12 No. 1, January - March 2005.

[THIS PAGE LEFT INTENTIONALLY BLANK]

APPENDIX A: ESTIMATING AVAILABLE HYDRO POWER

The total available hydro power available in Power Creek is not known. An estimate for the hydro power being spilled over the dam and deflected at the turbine generator is needed to get an idea of how much hydro is not being used. Cordova already has an estimate for the hydro being deflected at the turbine generator.

In order to estimate the water being spilled over the dam, a physical model was developed for the dam. A test was run where the spilled power was measured and relationships were developed to predict the spilled power from the measured values of dam pressure and forebay water height. The dam dynamics were modelled to determine their impact on the spilled hydro and to develop the relationship between spilled hydro, dam pressure and forebay water height.

Dam Model

This section describes the physical model developed for the Power Creek dam.

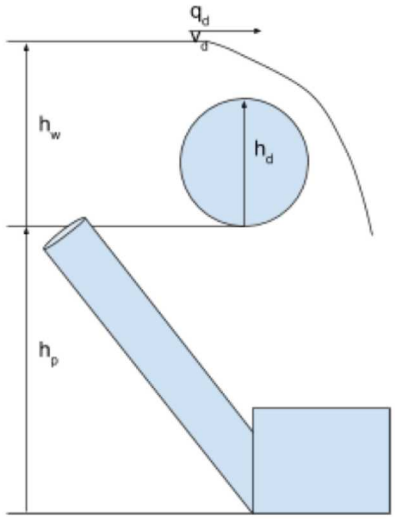

Figure 64 - Physical representation of a dam

Parameters:

h_w	Height of the water in the reservoir (m)
h_p	Height of the penstock (Google Earth show it to be 88m)
h_d	Height of the inflatable dam (m)
q_d	Mass flow of water over the dam (m^3/s)
v_d	Water speed over the dam (m/s)
v_0	Initial water speed of the river (m/s)

Schaede [1] states the power conversion of the turbine generator as 18.75 kW/cfs or 643 $kW/m^3/s$. This would indicate an efficiency of 73% using Equation 7. This is slightly lower than the efficiency of the turbine generators at rated conditions which is 77% (3125 kW at 300 ft head and 160 cfs)

Equation 7

$$643kW = 1000\frac{kg}{m^3} * 1\frac{m^3}{s} * 9.81\frac{m}{s^2} * h * \mu$$

The potential energy of a column of water above the dam is conserved as kinetic energy after flowing over the dam. The velocity of water flowing from height *h* above the dam can be calculated as shown in the following equations.

Equation 8

$$KE_1 = \frac{1}{2} * m * {v_d}^2$$

Equation 9

$$h_{diff} = h_w - h_d$$

Equation 10

$$PE_0 = m * g * h_{diff}$$

Equation 11

$$KE_0 + PE_0 = KE_1$$

Equation 12

$$v_1 = \sqrt{2 * g * h_{diff} + v_0}$$

Where:

KE_1	Kinetic energy of the water after going over the dam (J)
PE_0	Potential energy of the column of water above the dam (J)
KE_0	Kinetic energy of the water before going over the dam (J)
m	Mass of the water (kg)
g	Gravitational constant ($9.81 m/s^2$)
v_0	Initial velocity of the water before going over the dam (m/s)
v_1	Velocity of the water after going over the dam (m/s)

The average speed of water flowing over the dam is estimated with Equation 13.

Equation 13

$$v_d = \frac{\sqrt{2g}}{h_{diff}} \int_0^{h_{diff}} \sqrt{2gh_{diff}} * \frac{2}{3} + v_0$$

The volumetric flow of water over the dam can be calculated with Equation 14.

Equation 14

$$q = w * c_d * h_{diff} * v_d = w * c_d * \left(\frac{2}{3} * \sqrt{2g} * {h_{diff}}^{\frac{3}{2}} + v_0 * h_{diff}\right)$$

Where:

w	Width of the dam
c_d	Discharge coefficient for an inflatable dam

The water does not maintain the same cross section area when traveling over the dam. This is accounted for by c_d which is determined empirically and depends on dam geometry and can depend on h_{diff} and v_0. Experimental results from [2] found the best fit for c_d for dams with an h_{diff}/h_d ratio from 0.04 to 0.3 to be given by Equation 15. The average calculated values for h_{diff}/h_d and c_d when water was higher than the dam in 2011 were 0.15 and 0.32 respectively

Equation 15

$$c_d = 0.5066 * \left(\frac{h_{diff}}{h_d}\right)^{0.2447}$$

The power spilled over the dam is given by Equation 16.

Equation 16

$$P_{spill} = pg * (h_w + h_p) * q = pg * (h_w + h_p) * w * c_d * (\frac{2}{3} * \sqrt{2g} * {h_{diff}}^{\frac{3}{2}} + v_0 * h_{diff})$$

The height of the dam can be solved for with Equation 17.

Equation 17

$$\frac{2}{3} * \sqrt{2g} * {h_{diff}}^{\frac{3}{2}} + v_0 * h_{diff} = \frac{P_{spill}}{pg * (h_w + h_p) * w * c_d}$$

Solving for Coefficients

In the previous section a calculation of the spilled power was derived based on the variable h_{diff} which is the difference between the height of water in the reservoir and the height of the dam. The height of the water in the reservoir is known. A relationship must be found to calculate the height of the dam. A 2.5 hour test was run where P_{spill} was measured. From P_{spill} the height of the dam was calculated. Those values indicated a relationship between the pressure in the dam and the height of the water in the reservoir shown be Equation 18 and solved to have the coefficients shown in Equation 19.

Equation 18

$$h_d = c_1 {p_d}^3 + c_2 {p_d}^2 + c_3 p_d + c_4 {h_w}^2 + c_5 h_w + c_6 p_d h_w + c_7$$

Equation 19

$$h_d = 0.256 * {p_d}^3 - 2.500 * {p_d}^2 + 3.748 * p_d - 1.955 * {h_w}^2 + 3.460 * h_w + 1.939 * p_d h_w - 4.353$$

In order to calculate the dam height, the initial water speed of the river is needed. It was initially assumed to be constant at 0.7 m/s. After solving for dam height, it was solved for using Equation 20. It did not vary significantly with water height and so it was considered constant at it mean value of 0.7 m/s.

Equation 20

$$v_0 = P_{spill}(pg * (h_w + h_p) * w_d * (h_w - h_d) * c_d - \sqrt{2g * h_{diff}} * \frac{2}{3}$$

From the values calculated for the height of the dam (h_d) and the discharge constant, the speed, flow rate and spilled power can be calculated. Figure 65 compares the calculated spilled power with the measured spilled power. The blue line shows spilled hydro power. The orange line show the spilled hydro calculated with Equation 16. It has a standard deviation from the measured spilled hydro of 99 kW.

There are different dynamics around switching with the orange line than the blue line. This is because the blue line does not take into account the dam dynamics. The dam dynamics are analyzed in Appendix B. Figure 66 shows comparison of the calculated and measured spilled hydro after updating the measured spilled hydro with the dam dynamics. The new standard deviation is 87 kW.

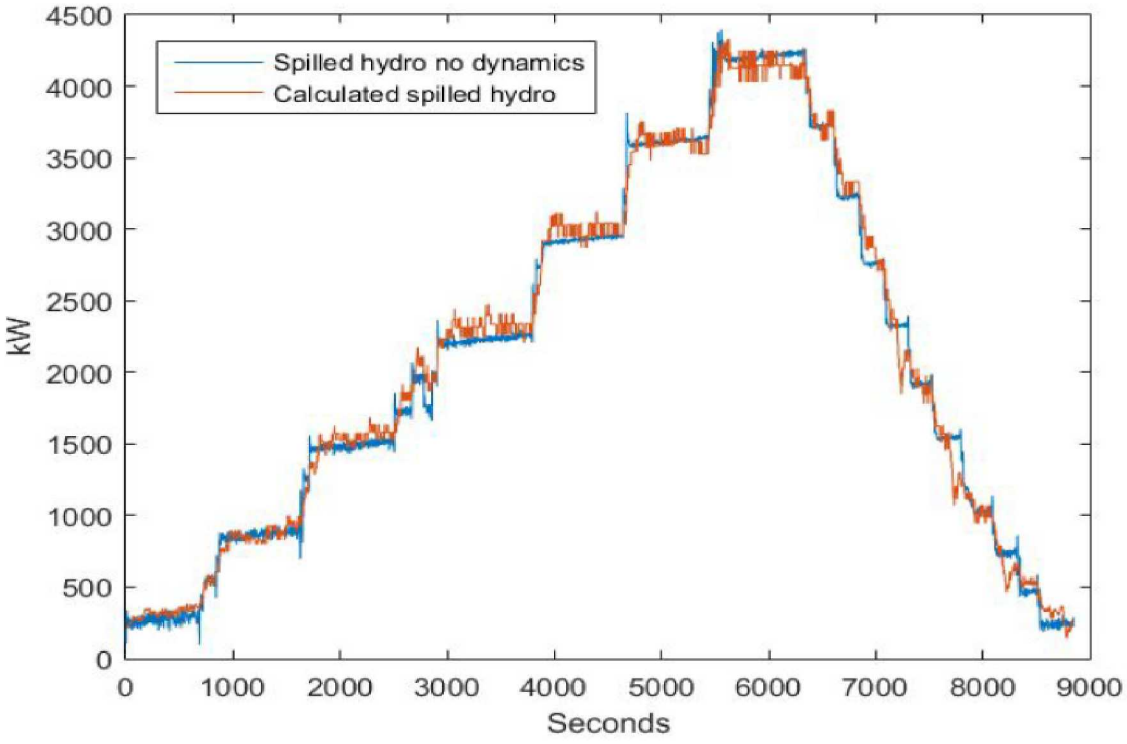

Figure 65 - Comparison of calculated and measured spilled hydro from the test

Measured spilled hydro was determined by subtracting the turbine generator output from the total available hydro. The measure spilled hydro does not take into account dam dynamics.

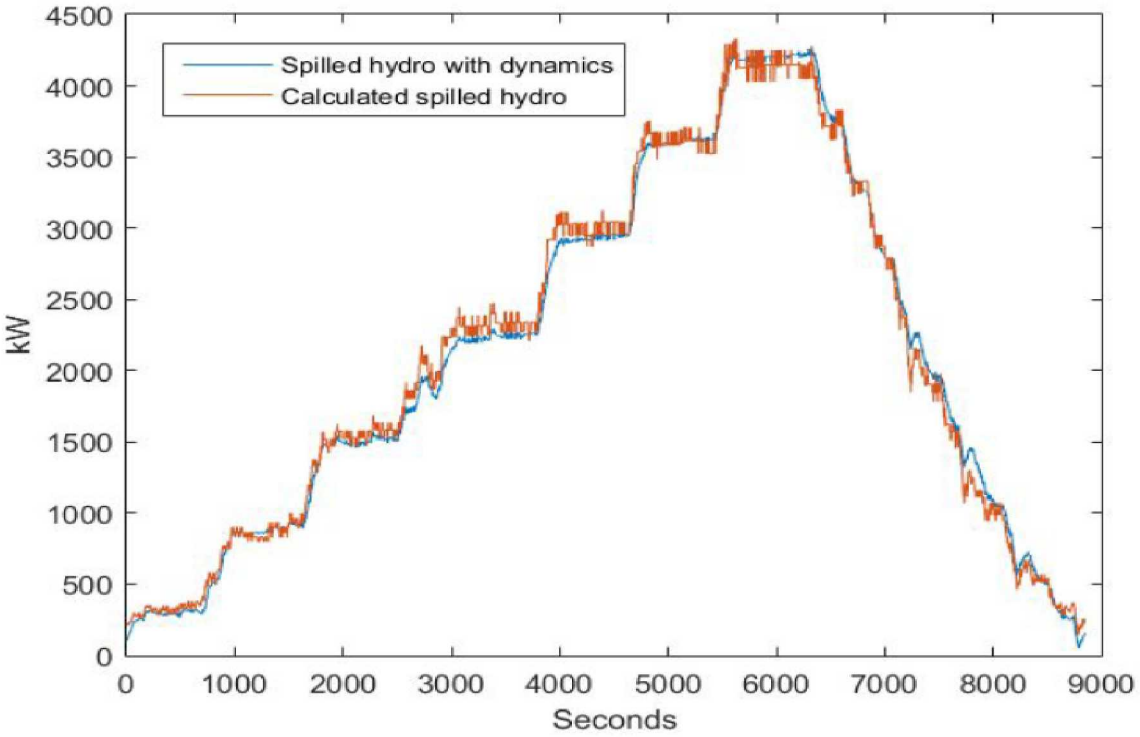

Figure 66 - Comparison of calculated and measured spilled hydro from the test after revision

Measured spilled hydro was determined by subtracting the turbine generator output form the total available hydro and updated with the dam dynamics calculated in Appendix B.

[PAGE LEFT INTENTIONALLY BLANK]

APPENDIX B: DAM DYNAMICS

The power of a hydro turbine generator is given by:
Equation 21

$$P_{hydro} = \rho q g h \mu$$

Where,

ρ	Density of water, around 1000 kg/m3
q	Flow rate of water in m3/sec
g	Gravitational constant 9.81 m/s2
h	Height of the dam above the turbine generator in m
μ	Efficiency of the turbine generator

Using the analogy of an electrical circuit, flow rate (m3/s) is analogous to current and pressure
(Pa) to voltage.

q≃current
ρgh≃voltage

The equivalent electrical circuit of the hydro dam is shown Figure 68. Qcreek is the flow of water coming down the creek in m3/s. Qt, qd and qr are the water flows into the turbine generator, over the dam and into the reservoir in m3/s. Pp is the pressure at the head of the penstock, or at the reservoir, in Pa. Pd is the pressure of the water on top of the penstock due to the height of the dam. Rd is the 'resistance' of the water flowing over the dam resulting in the height or pressure difference between the level of the dam and the level of the water in the reservoir. Resistance is calculated by p/q, or pressure/flow with units Pa/(m3/s). Cr is the 'capacitance' of the reservoir. The multiplication of capacitance and resistance should result in seconds. The unit of capacitance is m3/Pa.

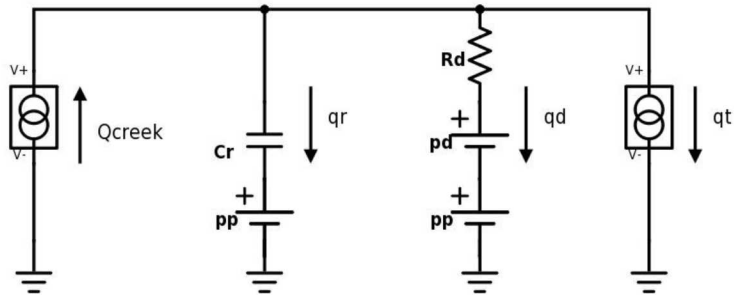

Figure 67 - Electrical circuit equivalent of the dam.

Using Thevenin equivalent circuits, this circuit can be simplified to the one shown in Figure 68

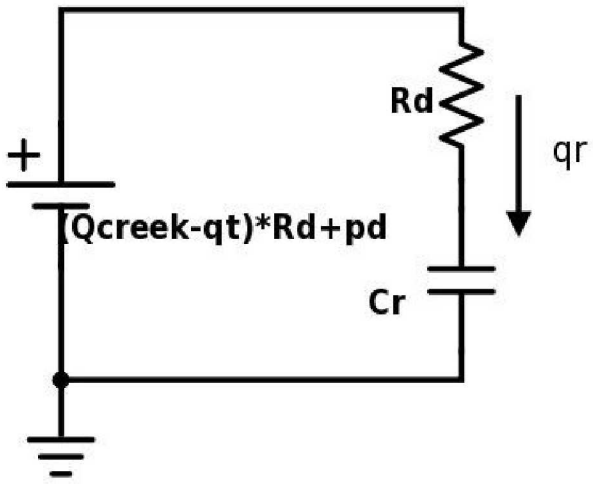

Figure 68 - Thevenin equivalent of the electrical circuit equivalent of the dam.

The change in qr is given by

Equation 22

$$(Q_{creek} - q_t) * R_d + p_d = q_t p_d + \frac{1}{C_r}\int_{t_0}^{t} q_r(\tau)dt$$

Equation 23

$$\frac{d}{dt}((Q_{creek} - q) * R_d + p_d) = \frac{dq_r}{dt}R_d + \frac{q_r}{C_r}$$

Equation 24

$$\frac{dq_r}{dt} = \frac{d}{dt}(Q_{creek} - q_t) + \frac{d}{dt}(q_d) * \frac{1}{R_d} - \frac{q_r}{C_r R_d}$$

The resistance R_d is calculated as follows:

Equation 25

$$P_d = \frac{(p_r - p_d)^2}{R_d} + q_d(p_d + p_p)$$

Equation 26

$$R_d = \frac{(p_r - p_d)(p_r + p_r)}{p_d}$$

Table 17 outlines the experimental calculation of R_D and C_R from the data. Step changes in P_D and P_T resulting from changes in power output of the turbine generator or starting the compressor for the dam resulted in dynamic behavior in between steady states of operation. Steady state measurements were made of the reservoir pressure before and after the step (p_{r0}

and p_{r1}). From these values the $p_r(\tau)$ was calculated. The time at which $p_r(\tau)$ occurred was located from the data to obtain τ . R_{D1} was calculated and R_D was used to calculated C_R. Using $RC = \tau$. ,C_R should be a constant value. The average values of C_R = 50.6 and R_D = 1.3 are used.

Table 17: Derivation of the dam resistance and reservoir capacitance

p_{r0} [kPa]	p_{r1} [kPa]	$p_r(\tau)$ [kPa]	p_{d1} [kPa]	τ [sec]	P_{T1} [kW]	P_{D1} [kW]	R_d $\frac{Pa \cdot s}{}$	C_R $\frac{}{m^3}$
23.79	24.03	23.94	21.14	43	5001	1879	1.36	31.56
23.88	24.21	24.09	20.09	67	3262	3655	1.00	67.08
24.06	24.30	24.21	19.72	36	2418	4488	0.90	39.79
24.21	23.94	24.04	19.38	100	2438	4070	0.99	100.85
23.70	23.46	23.55	19.59	30	3819	1558	2.20	13.64

Using R_D and C_R the value of the current entering the reservoir as opposed to going over the dam or penstock can be calculated based on the differential of turbine generator power and dam height.

Equation 27

$$\frac{dq_r}{dt} = \frac{d(Q_c - q_t)}{dt} + \frac{dp_d}{dt} * \frac{1}{R_d} - \frac{q_r}{R_d C_r}$$

Where

Q_c River currents

q_t Turbine generator currents

Equation 28

$$q_t = \frac{P_{turbine}}{p_w + p_p}$$

Equation 29

$$Q_c = \frac{P_{creek}}{p_w + p_p}$$

Where

p_w	Water pressure in the reservoir
p_p	Water pressure in the penstock

The resulting dynamic current into the reservoir can be used to update the static model of P_{spill}. It can be calculated using total creek current known for this test period as in Equation 29 or the current over the dam calculated using dam height and water height as in Equation 31.

Equation 30

$$P_{spill} = (Q_c - q_t - q_r) * (p_w + p_p)$$

Equation 31

$$P_{spill} = q_d * (p_w + p_p)$$

The dynamic power entering the reservoir is shown in Figure 69. The resulting calculated spilled power incorporating reservoir dynamics from Equation 24 and the spilled power calculated using dam height and water height from Equation 31 are shown in Figure 70. Incorporating dam dynamics significantly improved the fit around switching. The standard deviation decreases from 99 kW to 87 kW.

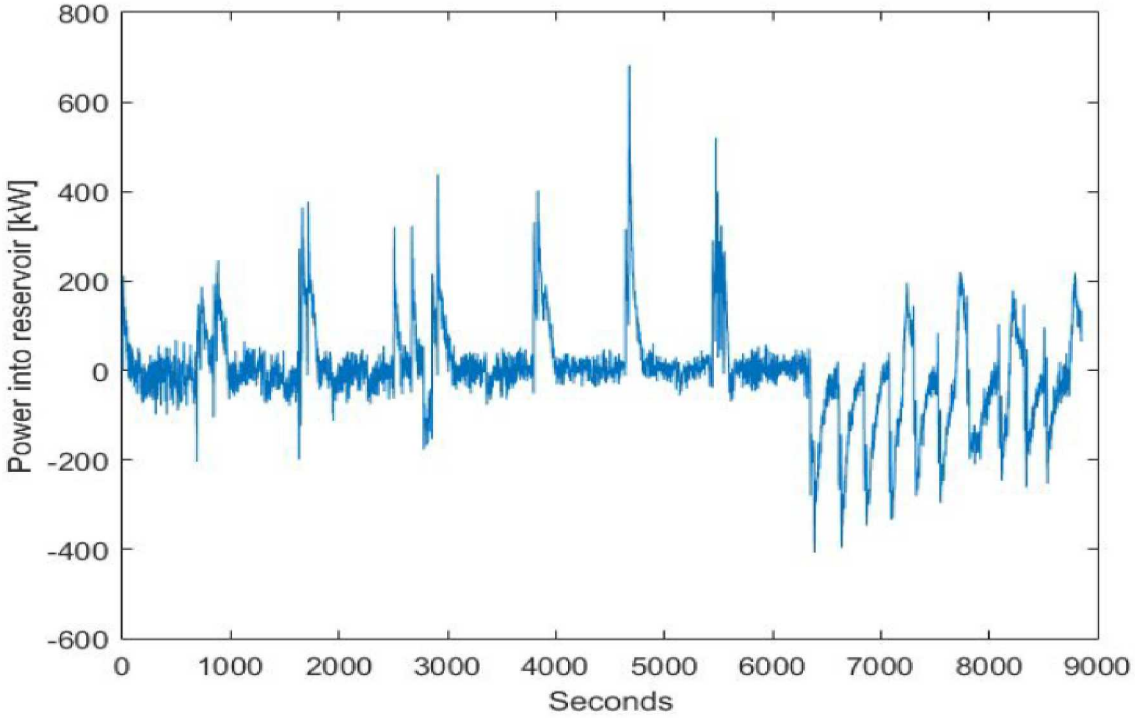

Figure 69 - Power flowing into the reservoir as opposed to flowing over the dam or down the penstock as a results of the dam dynamics

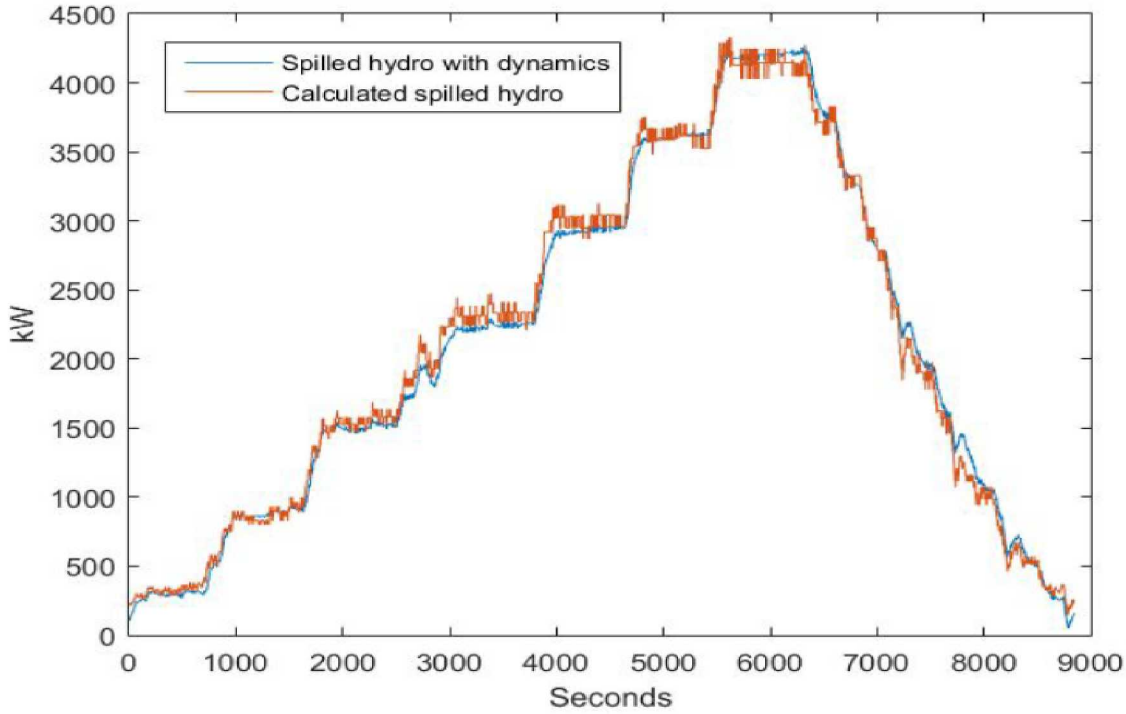

Figure 70 - Comparison of calculated and measured spilled hydro from the test

[PAGE LEFT INTENTIONALLY BLANK]

APPENDIX C: COMPARE DAM TEST RANGE WITH ACTUAL OPERATING RANGE

There are two places where water can bypass the hydro turbines: it can be spilled over the dam, or diverted just before the turbines (referred to as the reserve). CEC records an estimate for the reserve. This estimate has not been fully verified and is considered to be conservative, based on conversations with dam operators and engineers. CEC does not have an estimate for the amount of water being spilled over the dam.

In order to come up with an estimate, as test was performed as described in Section 2 The amount of water being spilled over the dam was varied, while the pressure of the air inside the dam and the height of the water behind the dam where recorded. A linear regression was formed between the power of the water being spilled over the dam, the height of the dam and the pressure of the air inside the dam. It had a very good fit, with a standard error of just 87 kW (under 2% of the nameplate capacity of the turbines).

However, when the spilled hydropower was calculated for the rest of the year using the regression, it did not appear to match the recorded value for the water being diverted just before the turbine. For example, before switching to diesel-off, the power of the water being diverted before the turbine will increase till around 1,100 kW. After switching, the power of the water being diverted before the turbine drops to 500 kW, the loading on the turbine increases by whatever the diesel loading was before switching (between 400 and 700 kW) and the remaining water is spilled over the dam. The total available power in the water (turbine power + diverted + spilled) should remain roughly the same. However, the calculated value for the spilled hydropower shows a sudden increase in total available hydropower after switching to diesel-off.

Figure 74 shows a period where the calculated spill has been applied to the data. The blue line is the turbine electrical output. The red line shows the turbine output plus the recorded reserve (water deflected just before the turbine). The yellow line shows the turbine output, reserve and the calculated spilled hydropower over the dam. Whenever there was significant spill (yellow line significantly greater than red line) the grid was operating in diesel-off. The sudden jump in total available hydropower (yellow line) can be seen when the grid is in diesel-off.

There are several possible causes. The first is that the calculated spilled hydropower is too high. The second is that the recorded diverted hydropower is too low (which is based on an estimate, not a measurement). The more conservative option is to assume the spilled hydropower is too high. Scaling the spilled hydropower by 0.5 resulted in a more constant total available hydropower during transitions between diesel-on and diesel-off states. This is shown in Figure 75.

Figure 71 to Figure 73 compare the values of air pressure inside the dam and forebay water height observed in the test (black circles) with the normal operating values during diesel-off (red box and asterisk), when essentially all spill occurs. The contour lines show the calculated spilled hydropower (in kW) based on measurements made during the test at the points indicated by the black circles. Most test values fall outside the normal operating values. This indicates that the linear regression used to calculate spilled hydropower will not be as accurate when applied to normal operating values.

It has been recommended to CEC to begin to measure and record the total unused hydropower. The measured values can be used to validate the calculations used for hydropower spilled over the dam and diverted before the turbine (reserve).

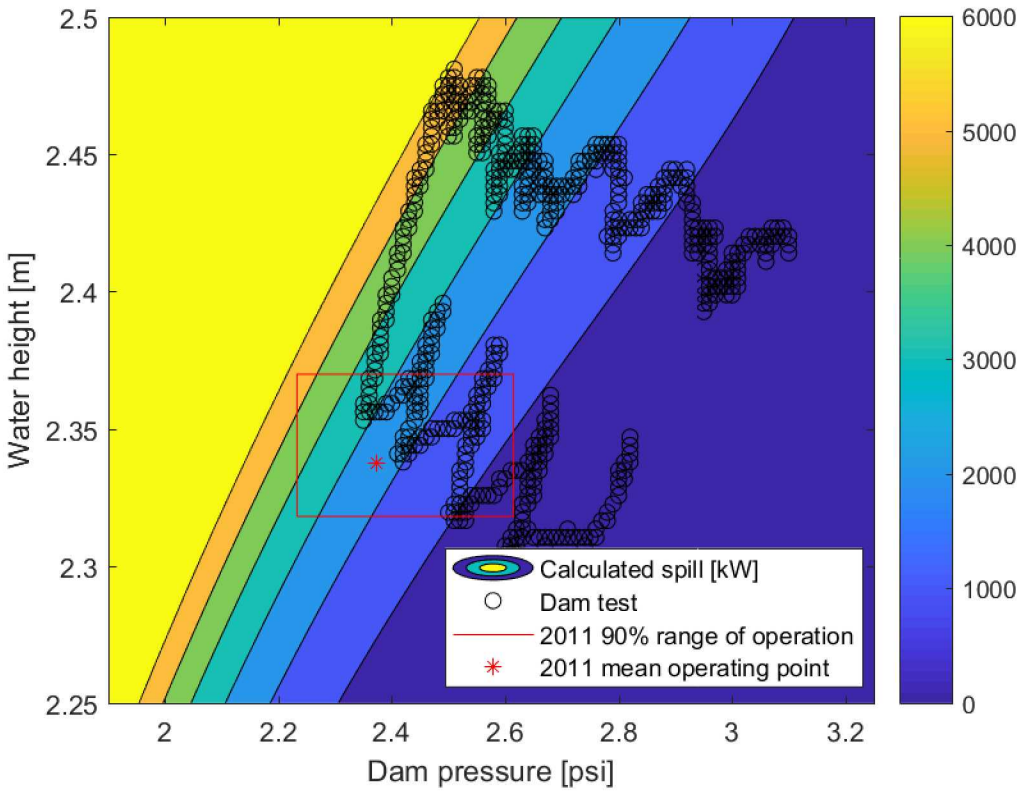

Figure 71 - Operating region of the dam test compared to normal operation in 2011

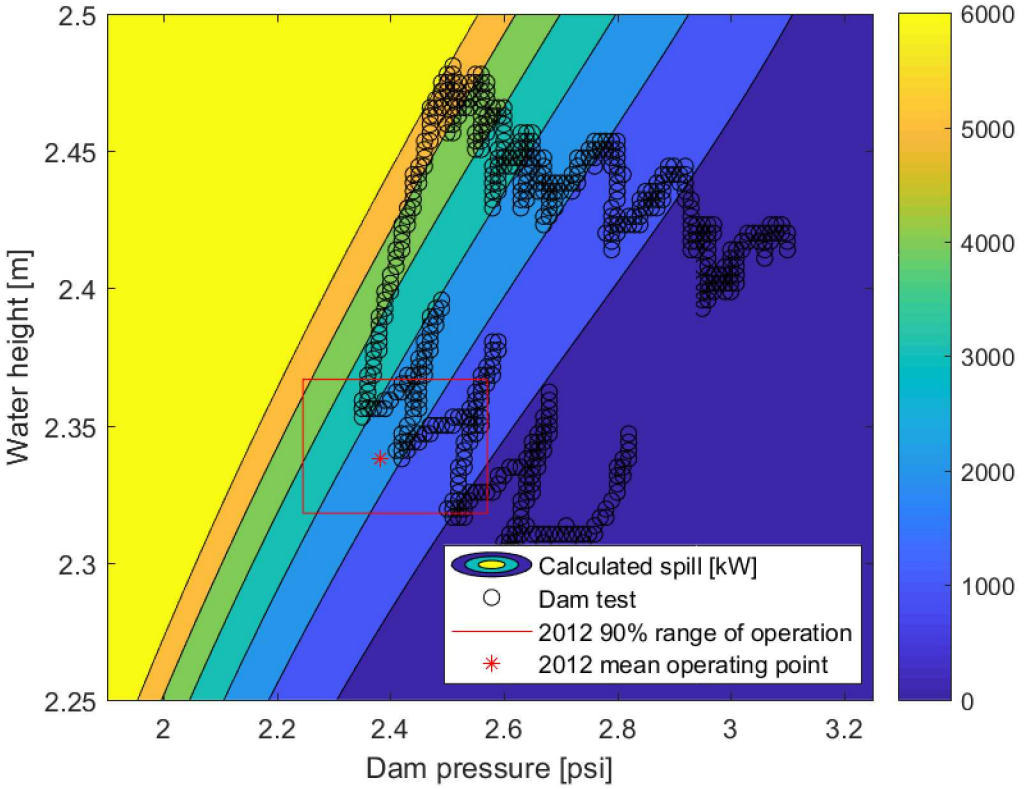

Figure 72 - Operating region of the dam test compared to normal operation in 2012

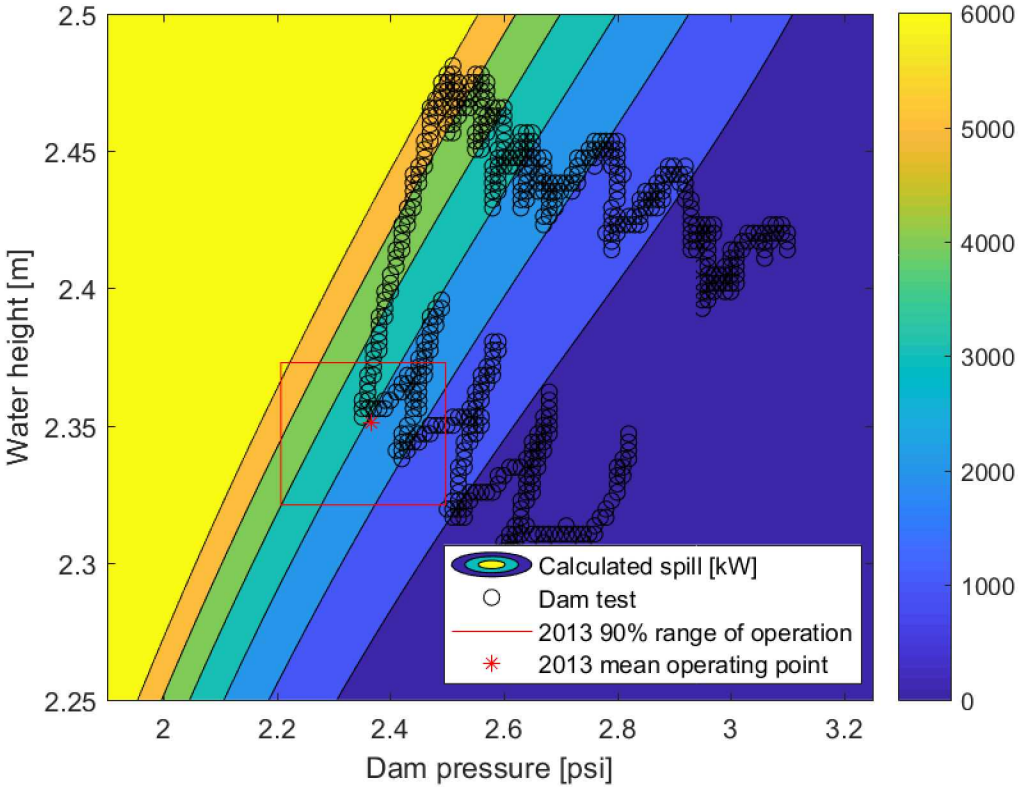

Figure 73 - Operating region of the dam test compared to normal operation 2013

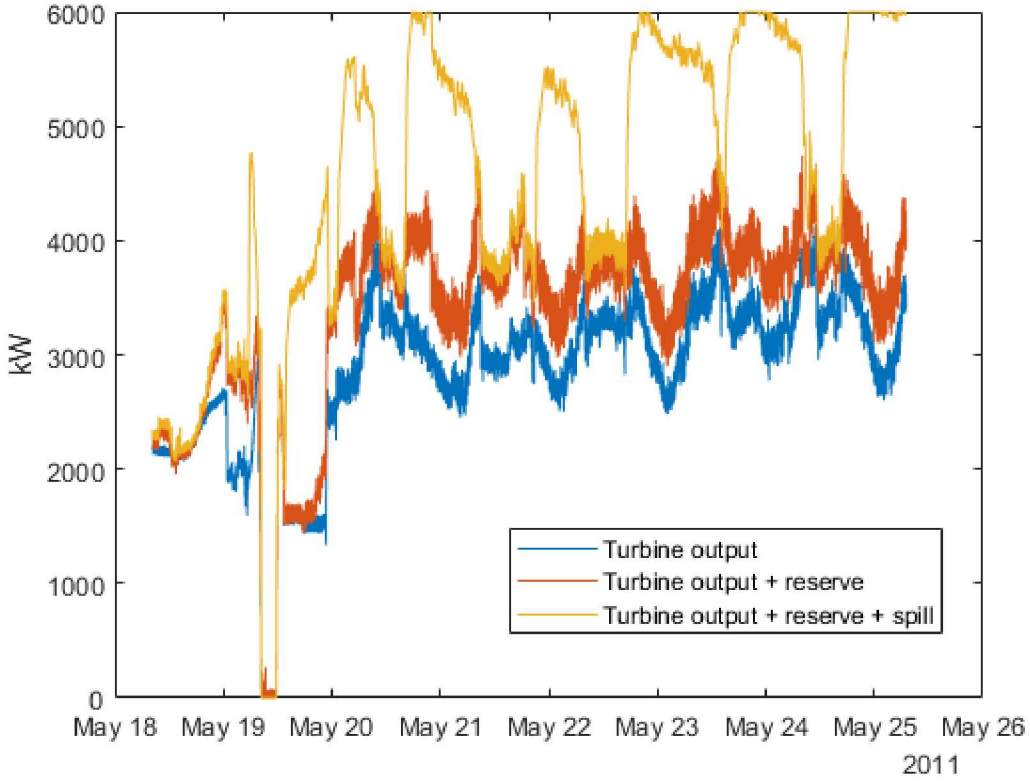

Figure 74 - Calculated total available hydro

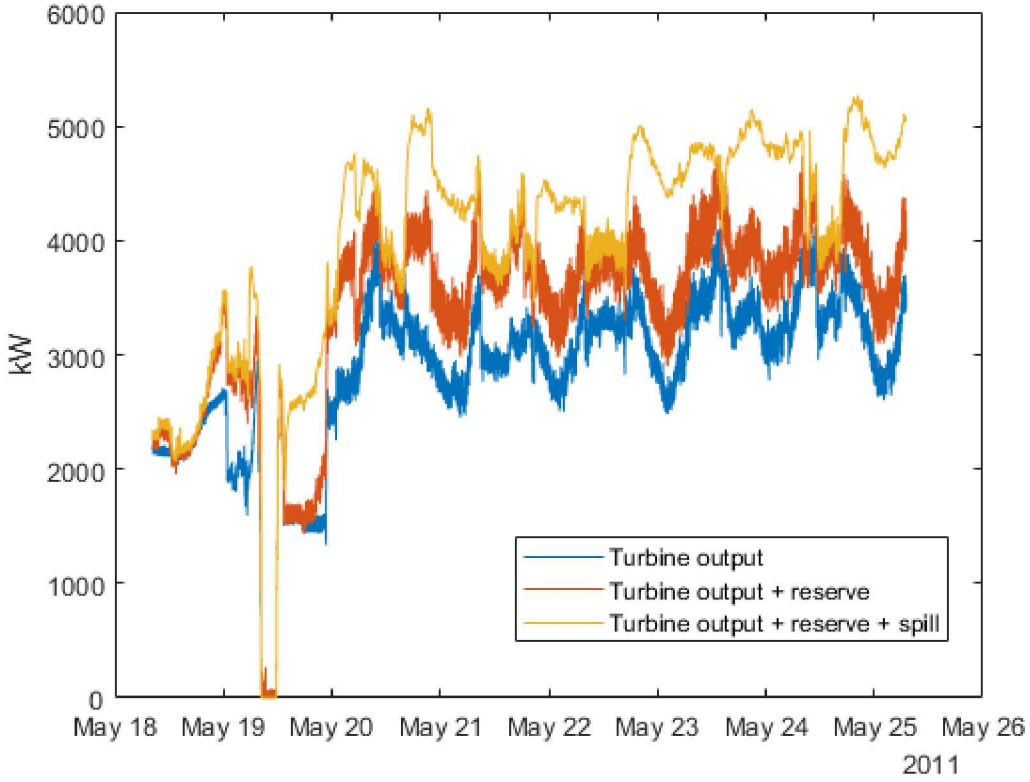

Figure 75 - Calculate hydro with spilled hydro scaled by half

APPENDIX D: CALCULATING THE LOAD

The load was calculated as the sum of all generation. Figure 76 shows the probability distribution of discrete ramp rates between 1 second time steps for each generator. There are some very high ramp rates, up to 1500 kW/s. Figure 77 shows the probability distribution of ramp rates in the load which is calculated as the sum of all generation. Table 18 shows the total number of absolute discreet ramp rates over 500 kW/s for each generator and for the sum of all generators, which is the total load.

There were some load steps in the data that were very large (500 to over 1500 kW/sec) and seemed to result from oscillations in the measurement, outages or bringing the hydro off and online to clear the rack, as shown in Figure 78 and Figure 79. These events can cause grid blackouts in the simulation since there is only 500 kW of spinning reserve required.

Ramp rates over 500 kW/s were filtered out in the load. The resulting probability distribution of ramp rates for the load can be seen in Figure 80 The improved oscillations and drops in the load can be seen in Figure 81 and Figure 82. There are still very high ramp rates in the load which can cause problems with the diesel dispatch.

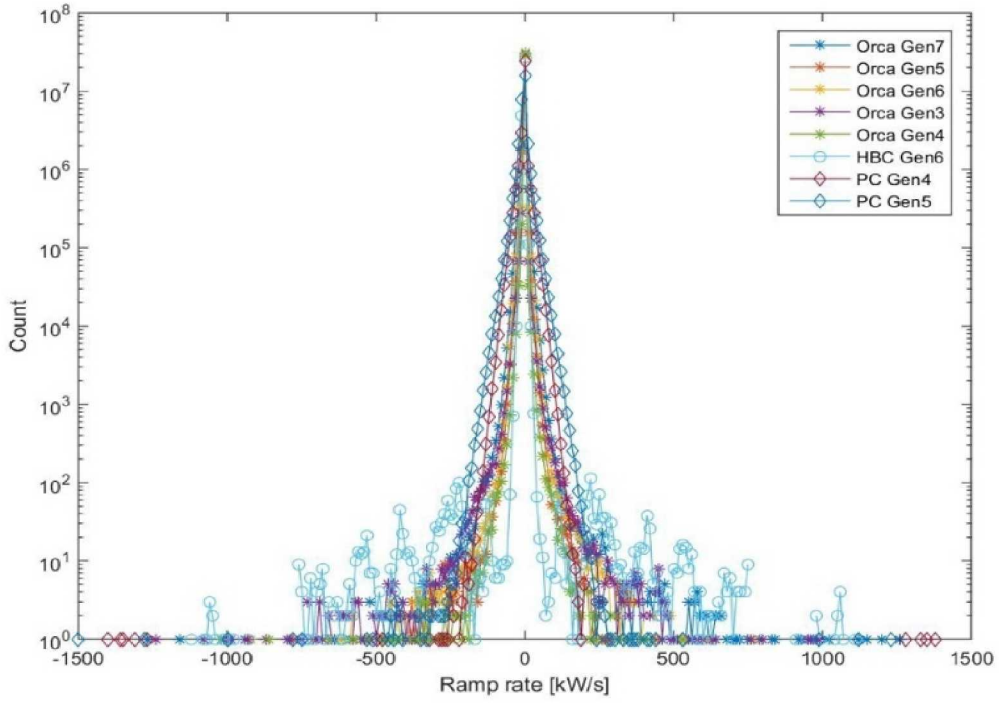

Figure 76 - Probability distribution of ramp rates from the different generators

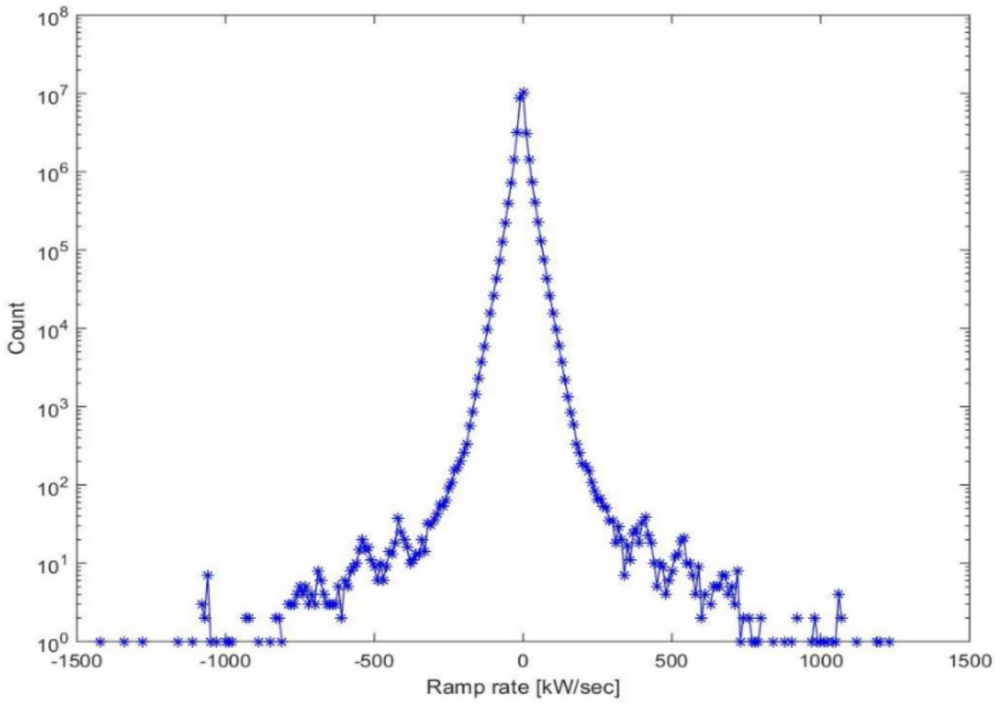

Figure 77 - Probability distribution of ramp rates from in the calculated load.

Table 18: Total number of absolute discreet ramp rates over 500 kW/s for each generator and for the sum of all generators

Generator	Orca Gen 7	Orca Gen5	Orca Gen6	Orca Gen3	Orca Gen4	HBC Gen6	PC Gen4	PC Gen5	Sum Gens
Count of Absolute Ramp Rates	76	5	14	54	10	307	13	28	434

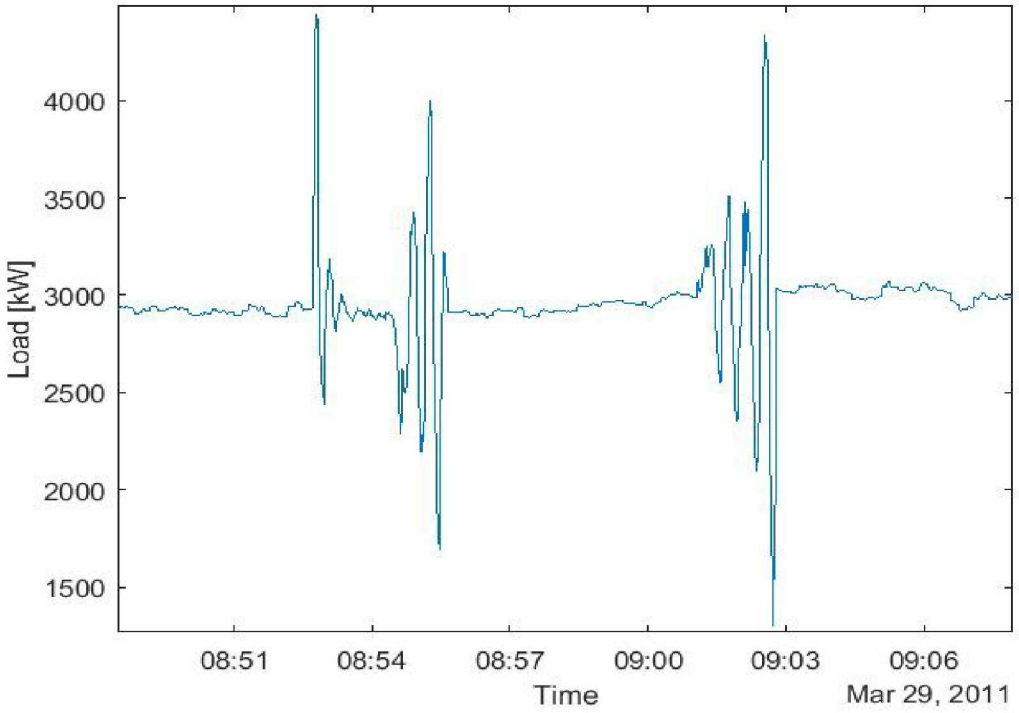

Figure 78 - High oscillations in the calculated load. This seems to be the result of a measurement sensor.

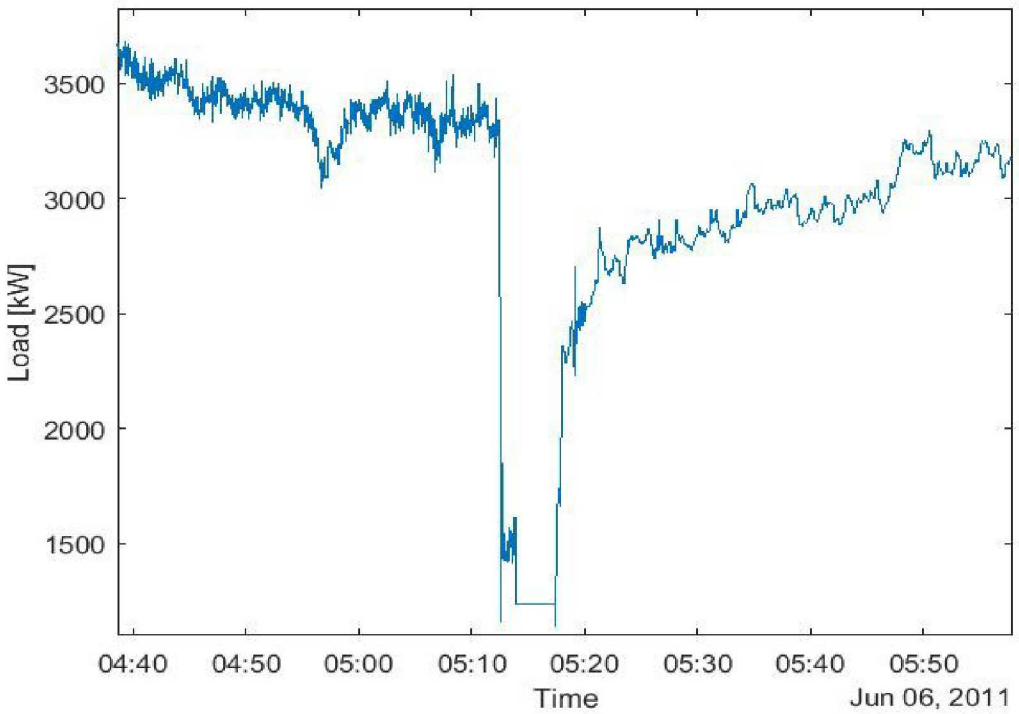

Figure 79 - The abrupt in the load was limited to a minimum of 1 MW, otherwise the drop would be to zero. This could be the result of a blackout.

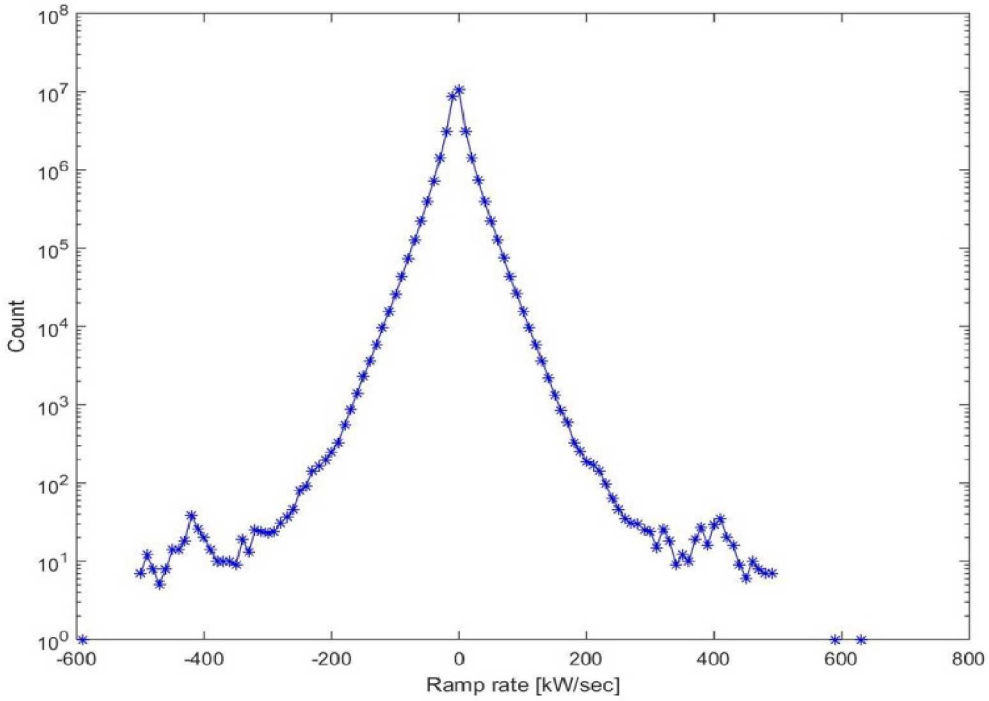

Figure 80 - Probability distribution of load steps after reducing ramp rates over 500 kW/s/

The following figures show the original load (blue) and after load steps greater than 500 kW/s have been reduced (orange) for oscillations and drops.

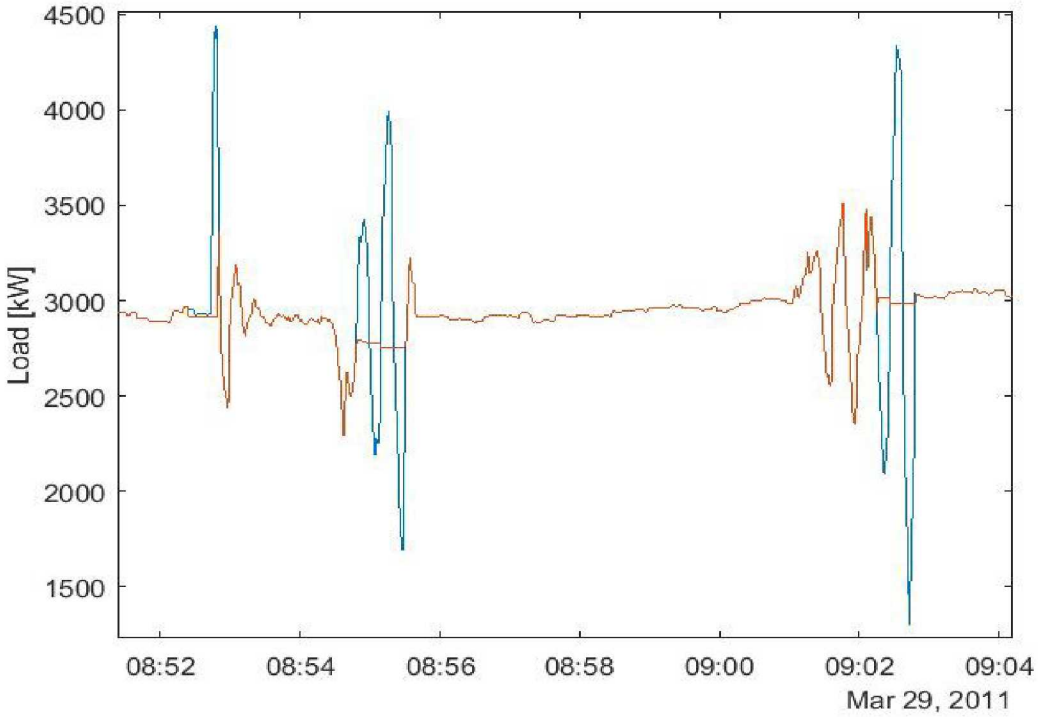

Figure 81 - Oscillations in the load (blue) and after eliminating load ramp rates over 500 kW/s (red). There are still high ramp rates which can cause a problem with the dispatch.

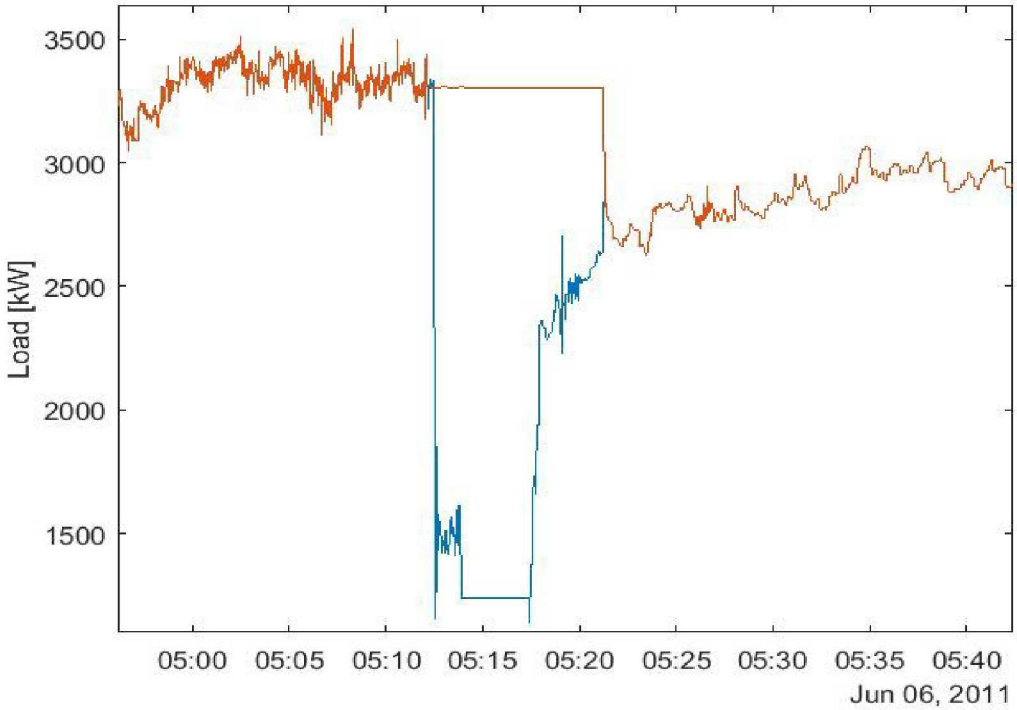

Figure 82 - Drop in load (blue) and after eliminating load ramp rates over 500 kW/s (red)

[PAGE LEFT INTENTIONALLY BLANK]

APPENDIX E: DISPATCH RULES

Table 19: Dispatch rules when operating in hydro only mode

System States	Action	Conditions
Demand is less than hydro available	Charge ESS	up to maximum charging power of ESS
The hydro is unable to supply required SRC	Supply SRC with ESS	up to maximum discharging power of ESS
		The ESS charge must be able to sustain the SRC power while discharging for the time required to turn on diesels times a safety factor.
		If ESS is unable to supply SRC initiate the diesel schedule
Demand exceeds hydro available (maximum available minus some safety)	Discharge ESS	Up to maximum discharging power of ESS, minus required SRC
		The SOC of the ESS must be able to sustain the current discharge plus the SRC for the timer required to turn on diesels
		If the SOC of the ESS is not high enough, initiate the diesel schedule
Frequency support (fast load following)	ESS charges and discharges to absorb fast fluctuations in load	FIR filter implemented with different numbers of taps
		Up to a certain fraction of the maximum charge and discharge powers
Var support	ESS supplies reactive power	up to a certain fraction of the maximum discharge reactive power
		If the ESS is unable to supply all VARS, the hydro begins to supply.

Table 20: Dispatch rules when operating in hydro-diesel mode.

System States	Action	Conditions
Available hydro	Use hydro to supply some of the load	Diesel must be run above their MOL
		Available hydro power greater than the difference of the load minus the diesel MOL (Pload-MOL) is excess.
Excess hydro	Charge ESS	up to maximum charging power of ESS (Pch_max)
		If over the past 5 min dumped hydro exceeds 25 kW, intitiate diesel schedule
The diesel and hydro are unable to supply SRC	Supply SRC with ESS	up to maximum discharging power of ESS (Pdis_max)
		The ESS charge must be able to sustain the SRC power (Psrc) while discharging for the time required to turn on diesels times a safety factor (tsw_on*1.5)
		If over past 1 minute a total of 3 kW of SRC has not been supplied, initiate the diesel schedule
Demand exceeds hydro and diesel available (a fraction of the maximum hydro available plus a fraction of the max diesel capacity)	Discharge ESS	The maximum discharge power of ESS must be greater than the required discharge plus SRC (Pch_max >Pdis+Psrc)
		The SOC of the ESS must be able to sustain the current discharge plus the SRC (Pdis + Psrc) for the time required to turn on diesels times a safety factor (tsw_on*1.5)
		If over past 1 minute a total of 3 kW of SRC has not been supplied, initiate the diesel schedule
		If the diesels are operating above their maximum loading times a safety factor (90%*full capacity), initiate diesel schedule
Diesels operating below MOL	Charge ESS	up to maximum charge power of ESS (Pch_max)
		If over the past 1 minute the load has been over 3 kW below MOL, initiate the diesel schedule
Frequency support (fast load following)	ESS charges and discharges to absorb fast fluctuations in load	FIR filter implemented with different numbers of taps
		Up to a certain fraction of the maximum charge and discharge powers
Var support	ESS supplies reactive power	up to a certain fraction of the maximum discharge reactive power If the ESS is unable to supply all VARS, the diesel or hydro begins to supply.

Table 21: Dispatch rules when operating in diesel only mode.

System States	Action	Conditions
There is available hydro	Bring hydro turbine geneartors online	Over the past 5 min dumped hydro exceeds 25 kW
		There is adequate load for diesels to run above MOL with hydro
Diesel operating below MOL	Charge ESS	up to maximum charge power of ESS (Pch_max)
		If over the past 1 minute the load has been over 3 kW below MOL, initiate the diesel schedule
Demand exceeds online diesel capacity	Discharge ESS	The maximum discharge power of ESS must be greater than the required discharge plus SRC (Pch_max >Pdis+Psrc)
		The SOC of the ESS must be able to sustain the current discharge plus the SRC (Pdis + Psrc) for the time required to turn on diesels times a safety factor (tsw_on*1.5)
		If over past 1 minute a total of 3 kW of SRC has not been supplied, initiate the diesel schedule
		If the diesels are operating above their maximum loading times a safety factor (90%*full capacity), initiate diesel schedule
Frequency support (fast load following)	ESS charges and discharges to absorb fast fluctuations in load	FIR filter implemented with different numbers of taps
		Up to a certain fraction of the maximum charge and discharge powers
Var support	ESS supplies reactive power	up to a certain fraction of the maximum discharge reactive power
		If the ESS is unable to supply all VARS, the diesel begins to supply.

[PAGE LEFT INTENTIONALLY BLANK]

APPENDIX F: ENERGY BALANCE MODEL RESULTS

Simulation with Smoothing and Diesel Charging

The set of simulation in this section allowed the diesels to charge the ESS up to 75% and smoothed the loading on the diesel and hydro generators. Charging the ESS with diesel generators results in an ESS that is maintained at a higher SOC. This allows the ESS to supply spinning reserve capacity which allows a smaller capacity of diesel generators to run online allowing more hydro to be delivered to the grid.

Allowing the diesel generators to charge the ESS resulted in lower diesel output, lower fuel consumption, and higher diesel loading compared to simulations where the ESS was charged only with hydro. Smoothing the loading on the diesel and hydro generators resulted in higher diesel fuel consumption and lower diesel generator loading compared to the simulations in the sections above, where there was no smoothing or diesel charging.

There are two main disadvantages to these simulations with smoothing and diesel charging. They have the highest utilization of the ESS and the highest level of diesel switching compared to any of the other simulations. This is a result of charging the ESS with diesel generators and smoothing the loading on the diesels and hydro generators. Charging the ESS with diesel may have additional costs if the ESS is provided as a service from a third party. When charging the ESS with diesel, the utility would likely sell electrical energy to the ESS provider at the hydro cost (around 7 cents/kWh) and buy it back at the cost of generating diesel (around 35 cents/kWh). Thus, the utility would have to pay nearly twice as much for the diesel generation that is used to charge the ESS.

Diesel Output

Figure 83 shows the diesel output for each generator in each of the simulations. Gen7, Gen5 and Gen6 are the most commonly used. Figure 11 and Figure 85 show the effect of ESS capacity and power rating on diesel output. Increasing the ESS capacity and power rating results in more significant reduction in diesel output.

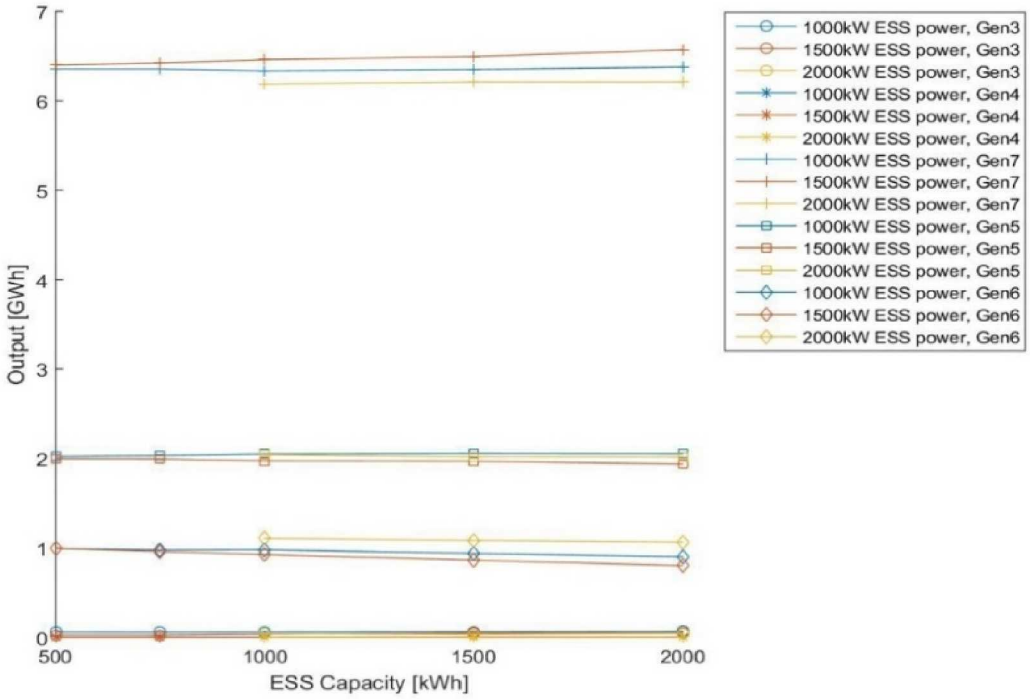

Figure 83 - The output of each diesel generator for different ESS capacities and powers.

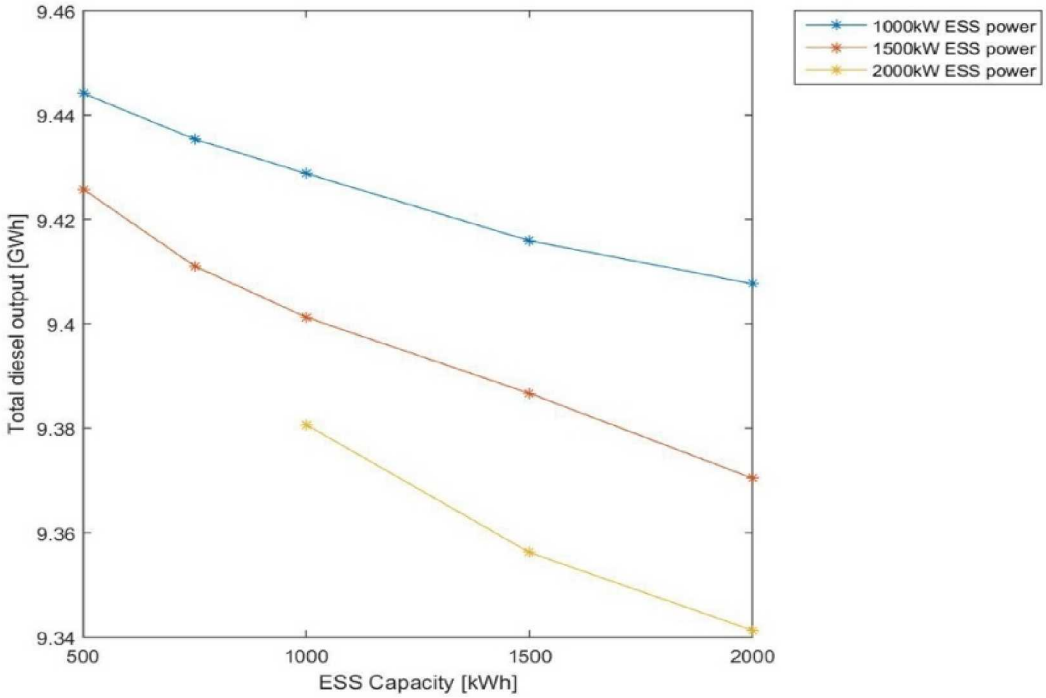

Figure 84 - The total diesel output for different ESS capacities and powers

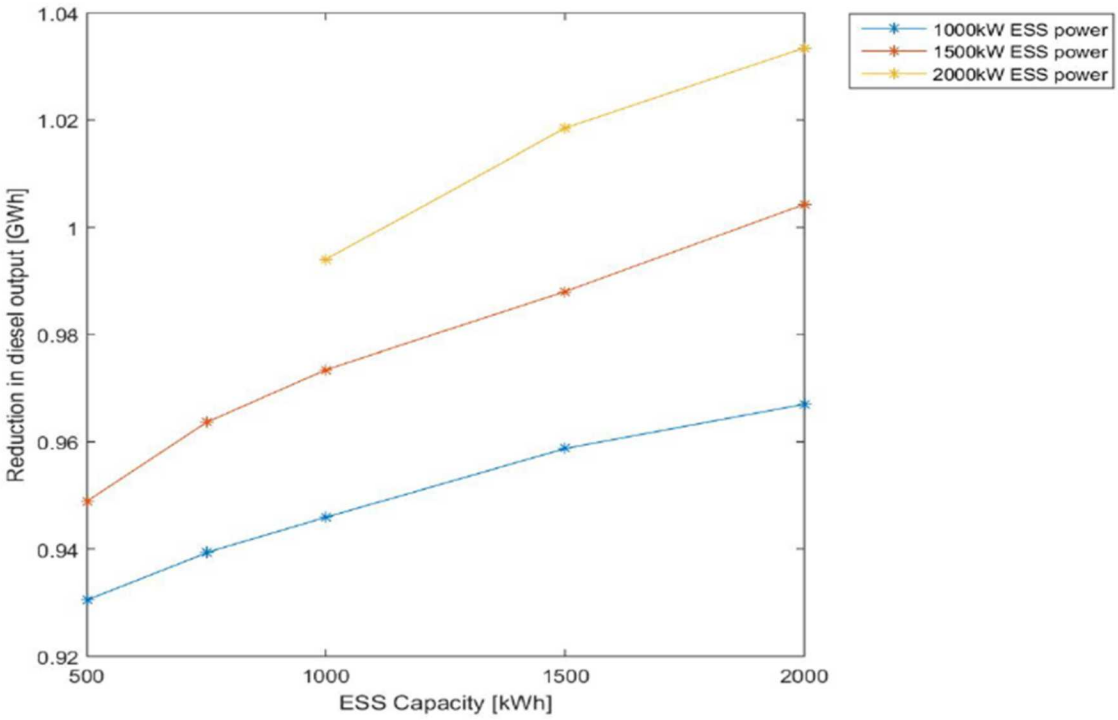

Figure 85 - Reduction in total diesel output for different ESS capacities and powers

Diesel Consumption

Figure 86 shows the diesel consumption for each generator in each simulation. Figure 87 and Figure 88 show the total consumption and reduction in total consumption. The reduction in consumption is a result of the reduction in diesel output as well as running the diesel generators at a higher and more efficient loading.

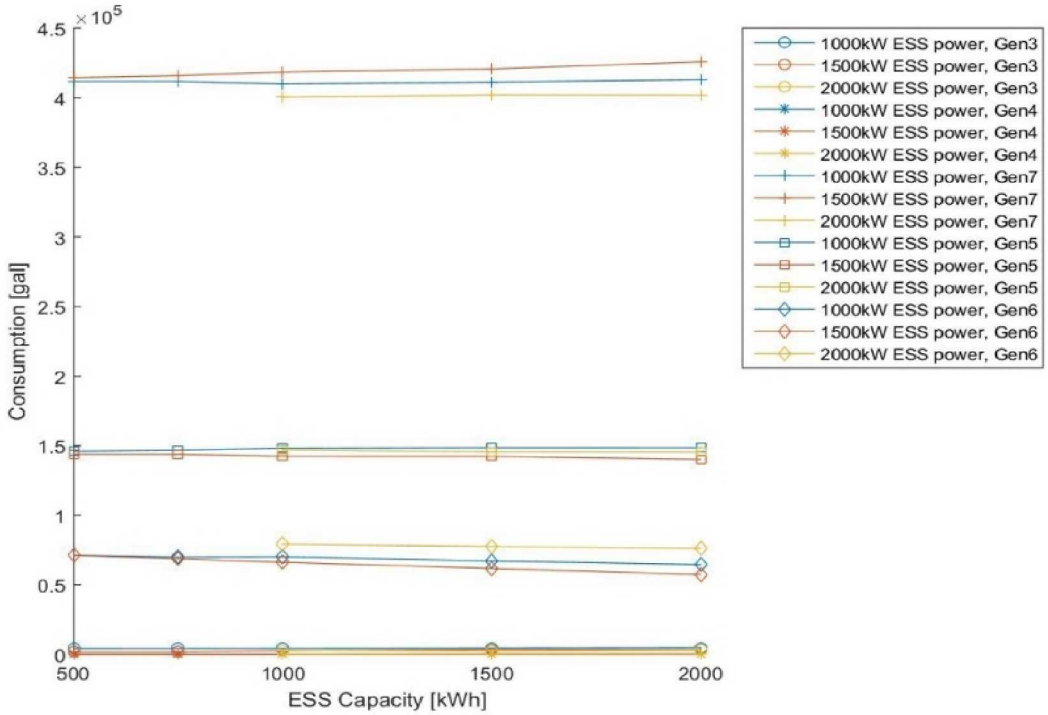

Figure 86 - The diesel consumption of each diesel generator for different ESS capacities and powers.

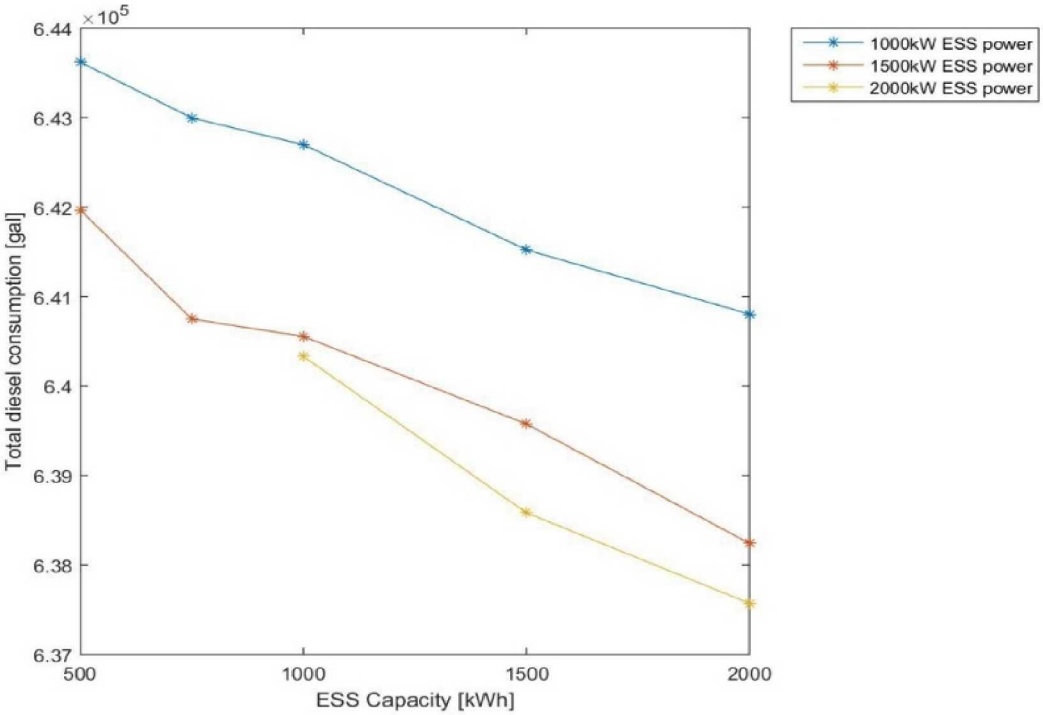

Figure 87 - The total diesel consumption for different ESS capacities and powers.

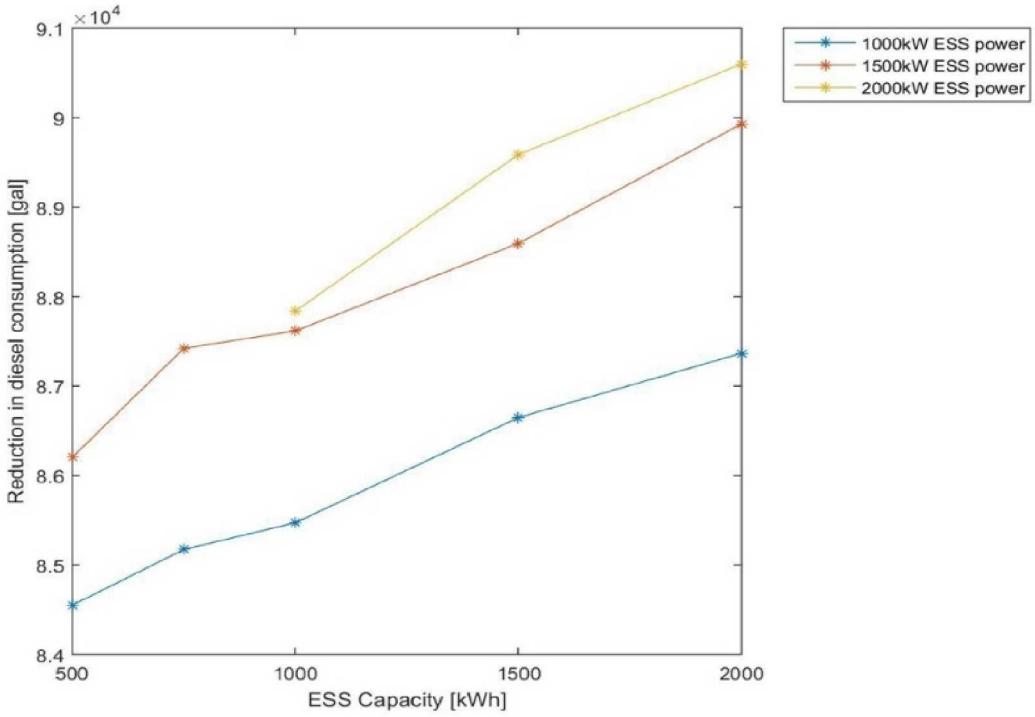

Figure 88 - The reduction in diesel consumption for different ESS capacities and powers.

Diesel off time

Figure 89 shows the time spent in diesel off in 2011. Figure 90 shows the increase in time spent in diesel off. Increasing ESS capacity and power increases the time spent in diesel off.

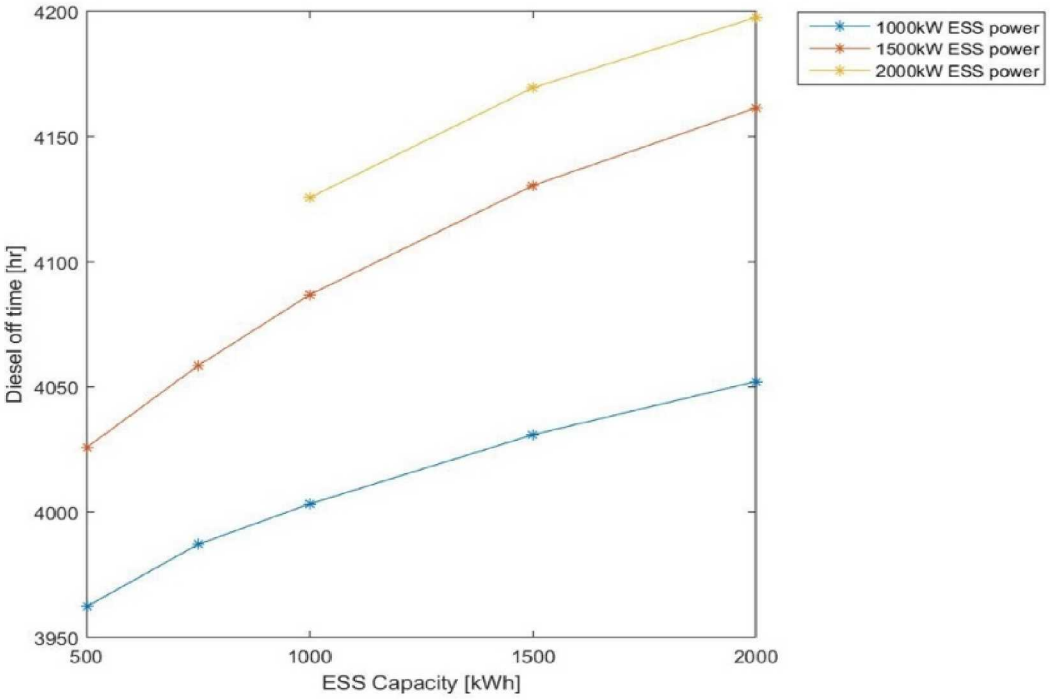

Figure 89 - Time spent in diesel off mode in 2011 for different capacities and powers.

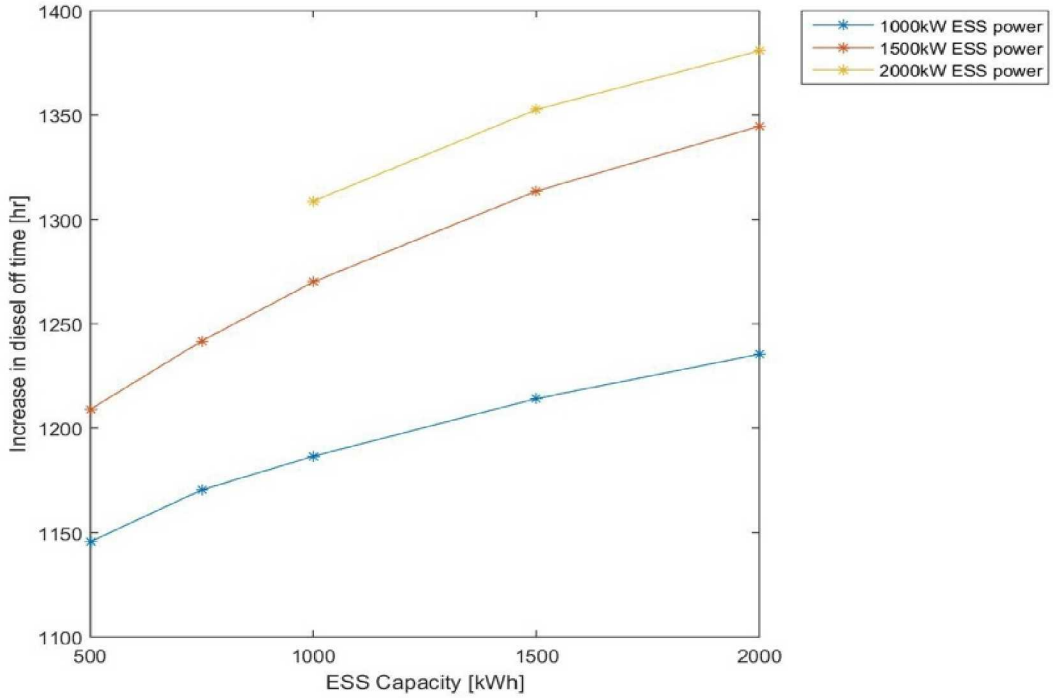

Figure 90 - Increase in time spent in diesel-off mode in 2011 for different ESS capacities and powers.

Diesel run time

Figure 91 shows the run time for each diesel generator for different ESS capacities and power ratings. Figure 92 shows the total diesel run time and Figure 93 shows the decrease in diesel run time. Increasing the ESS capacity reduces diesel run-time which results from multiple diesel generators being run online together. So, increasing the ESS power from 1.5 MW to 2 MW increases diesel-off time but also increases diesel run time. This is because two generators are run online more often with a 2 MW ESS than with a 1.5 MW in these simulations.

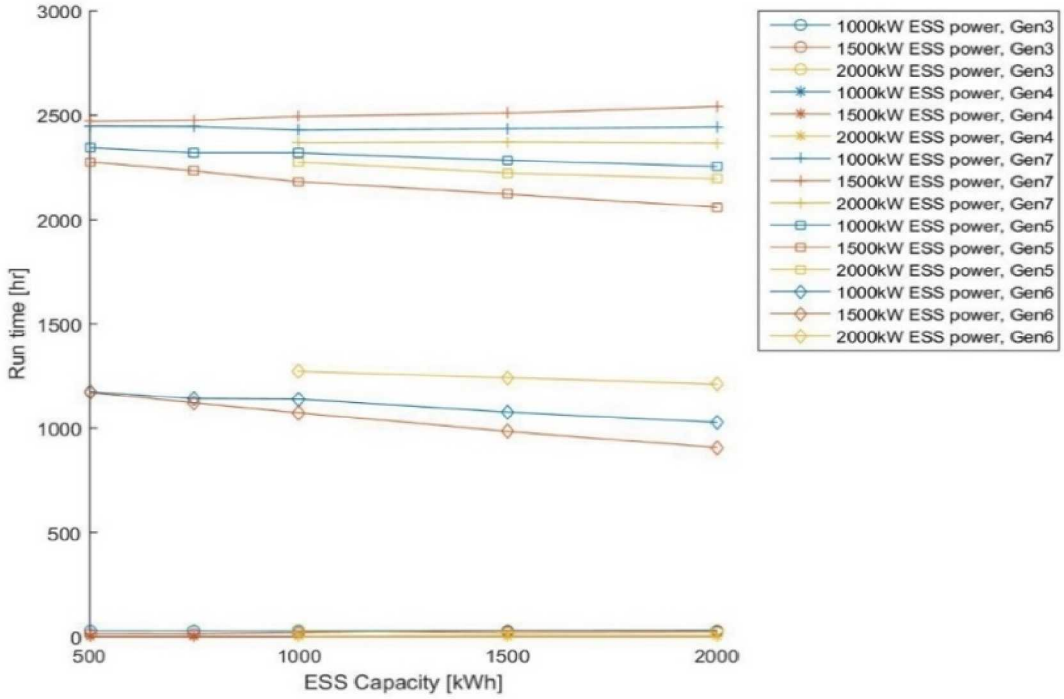

Figure 91 - The run time for each diesel generator for different ESS capacities and powers

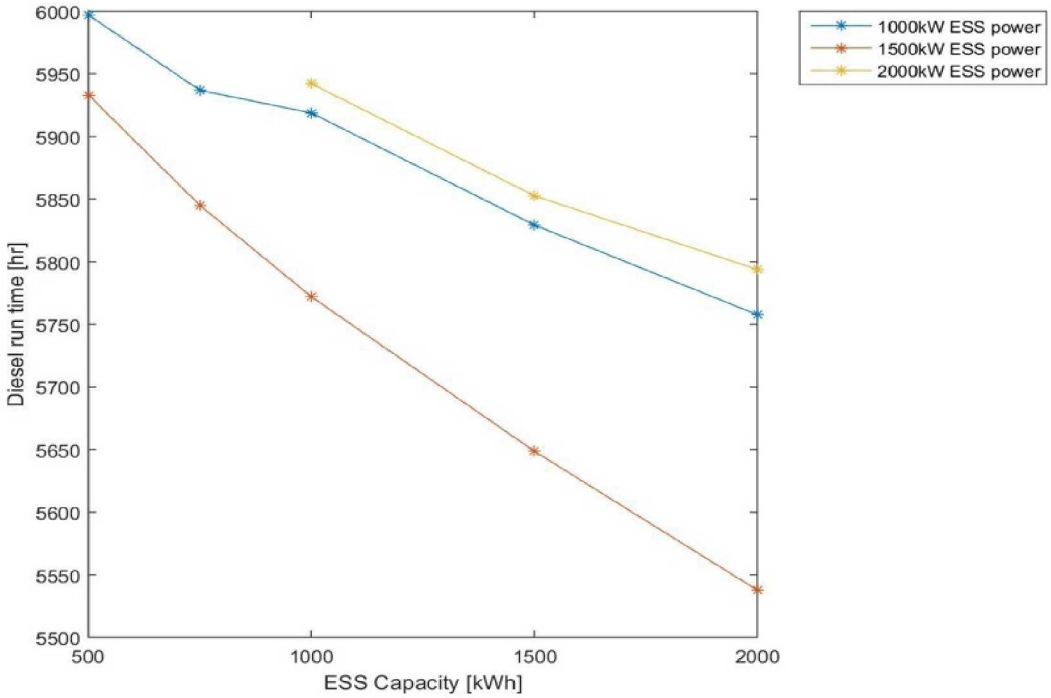

Figure 92 - The total diesel run time for different ESS capacities and powers.

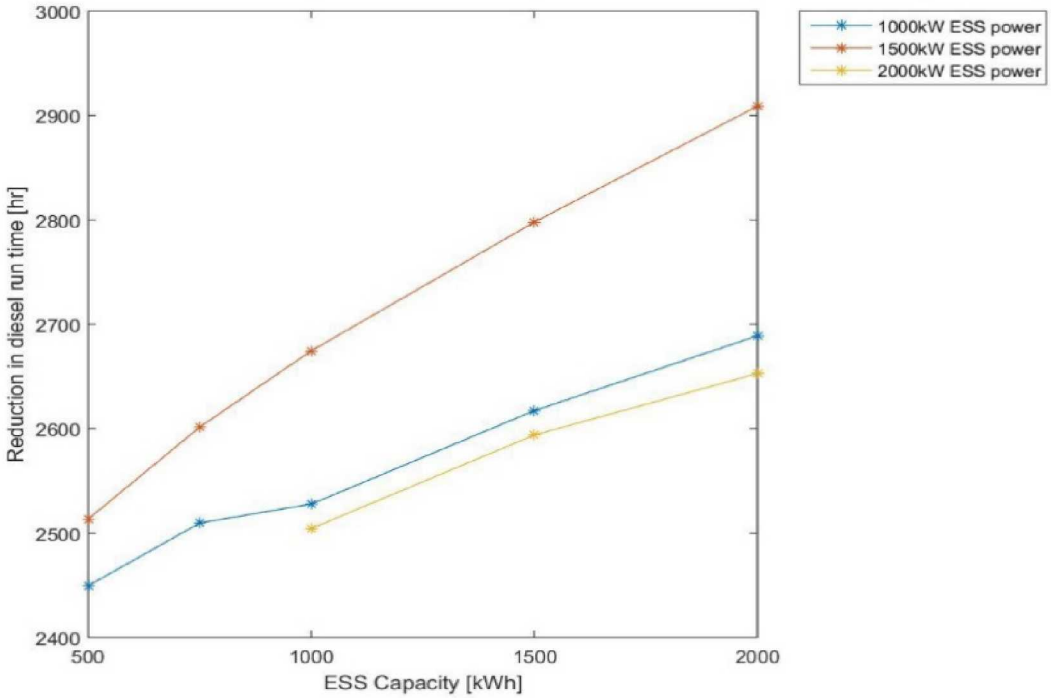

Figure 93 - The reduction in diesel run time for different ESS capacities and powers.

Diesel Capacity Factor

Figure 94 and Figure 95 show the diesel capacity factor for each diesel generator and the total diesel capacity factor for different ESS capacities and powers. A higher ESS capacity and power resulted in a higher diesel capacity factor. These simulations show a significant increase in diesel capacity factor from the 61% measured value for 2011.

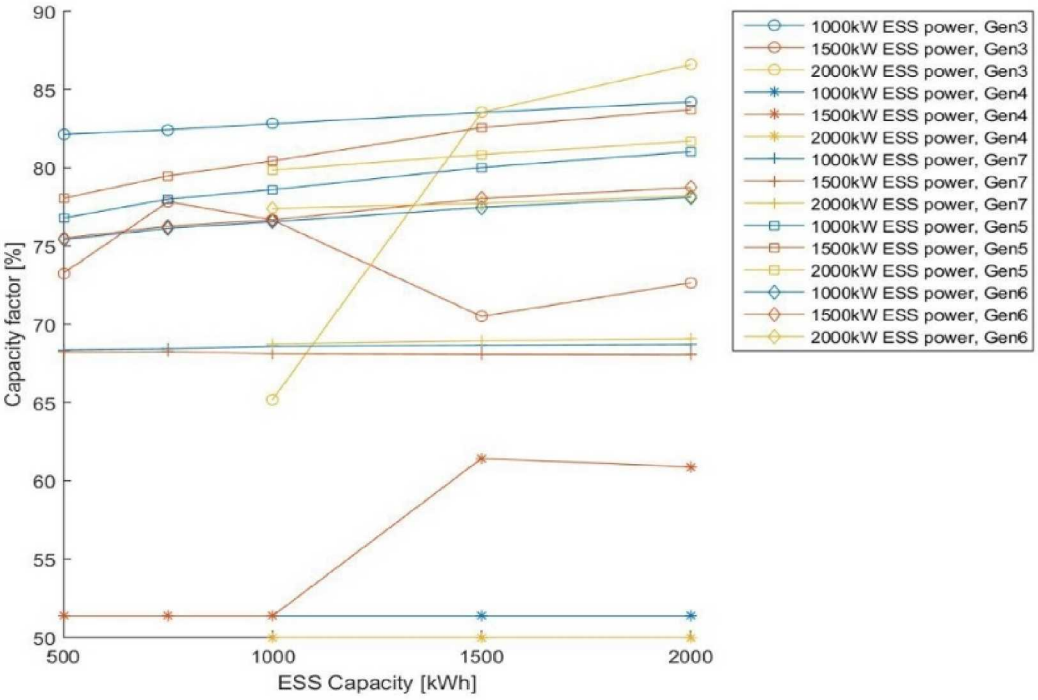

Figure 94 - Capacity factor for each generator for different ESS capacities and powers.

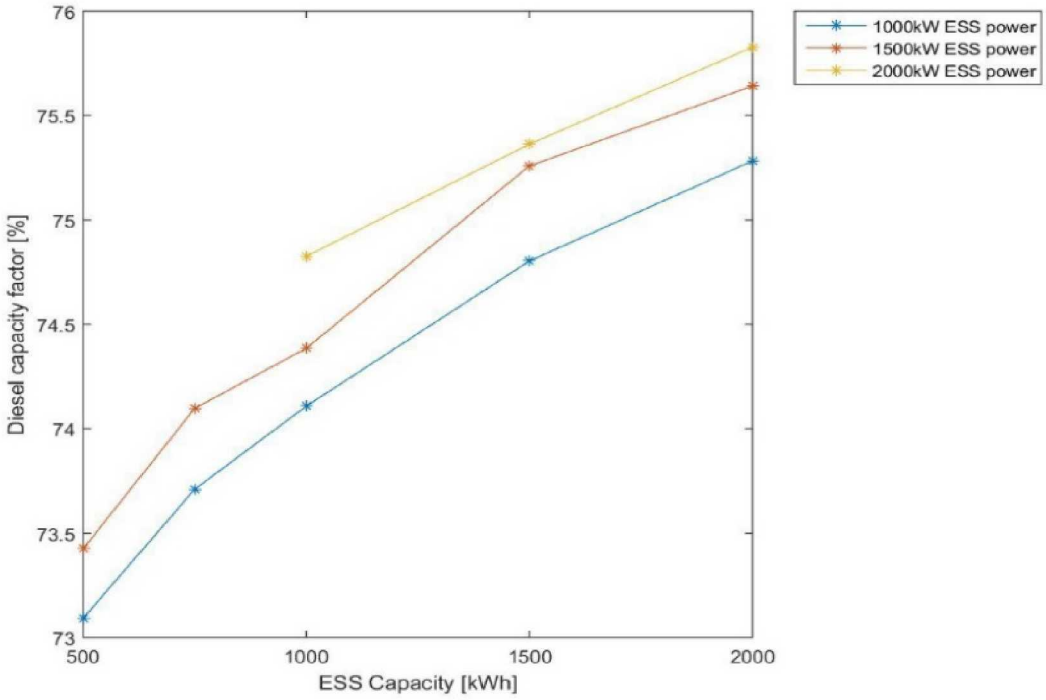

Figure 95 - The number of times each diesel generator is switched online for different ESS capacities and powers.

Diesel Switching

Figure 96 and Figure 97 show the number of times each diesel generator and all diesel generators are switched online for different ESS capacities and powers. Simulations show a significant increase in diesel switching compared to the measured value of 1001 times for 2011.

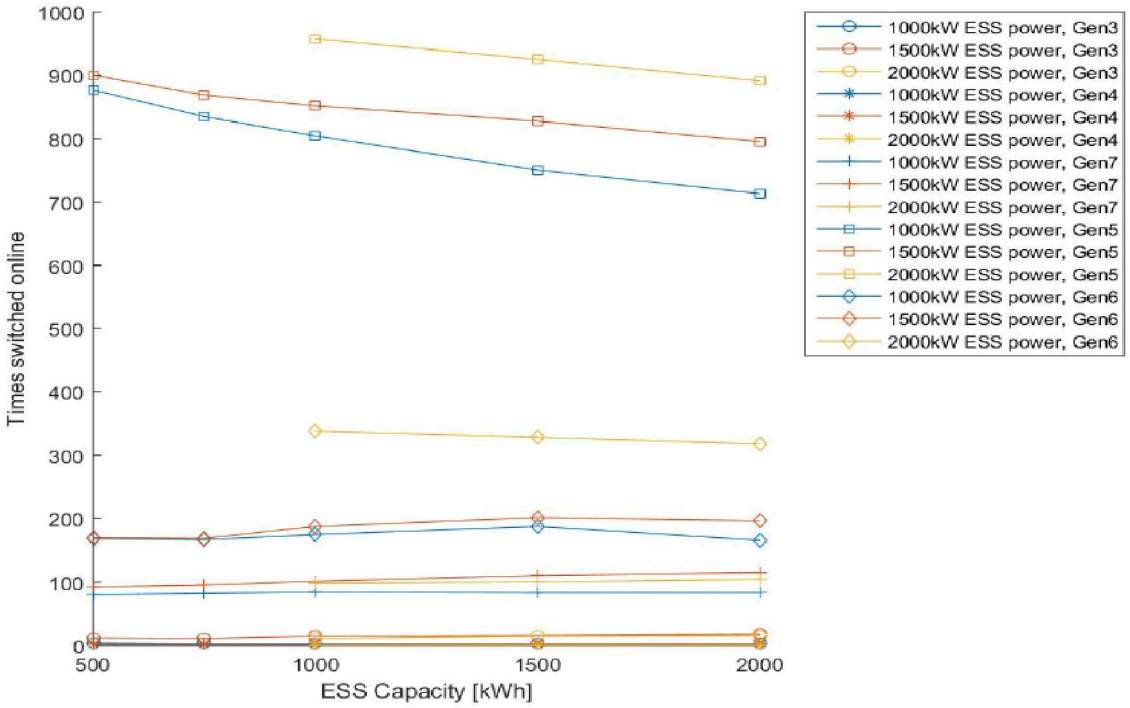

Figure 96 - Number of times each diesel generator is switched online for different ESS capacities

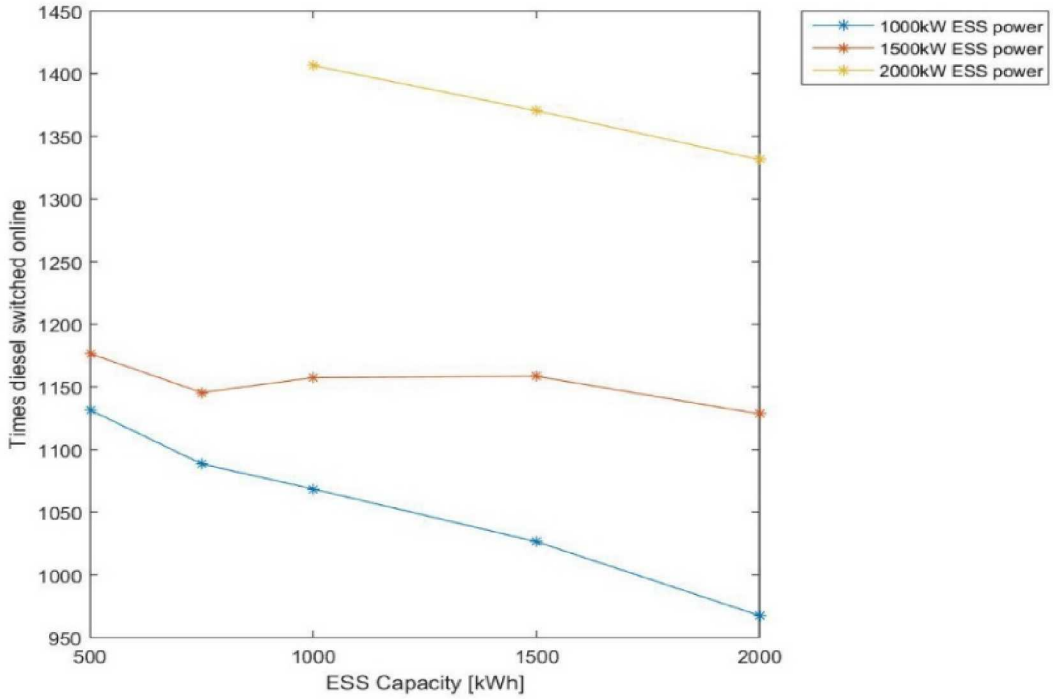

Figure 97 - The total number of times diesel generators are switched online for different ESS capacities and powers.

Diesel Ramp Rate

Figure 98 shows the probability distribution of diesel ramp rates for different ESS capacities and powers. There is not much difference between the different ESS capacities and powers. They have a mean value of around 0.31 kW/s which is a significant improvement over the average measured value of 3.13 kW/s for 2011.

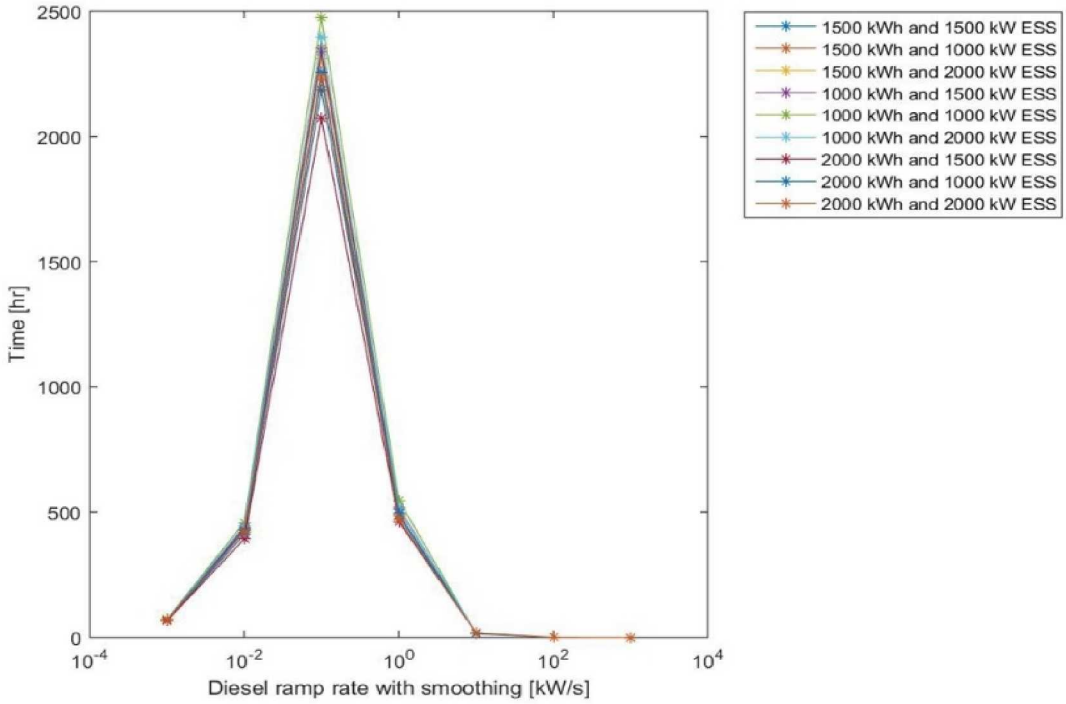

Figure 98 - Probability distribution of diesel ramp rates on the diesel generators for different ESS capacities and powers.

ESS Equivalent Cycles

Figure 99 shows the number of equivalent full ESS cycles. Multiple ESS cycles that add up to the full ESS capacity are considered to be one equivalent ESS cycle. These simulations have very high ESS cycling which negatively affect the life of most ESS technologies.

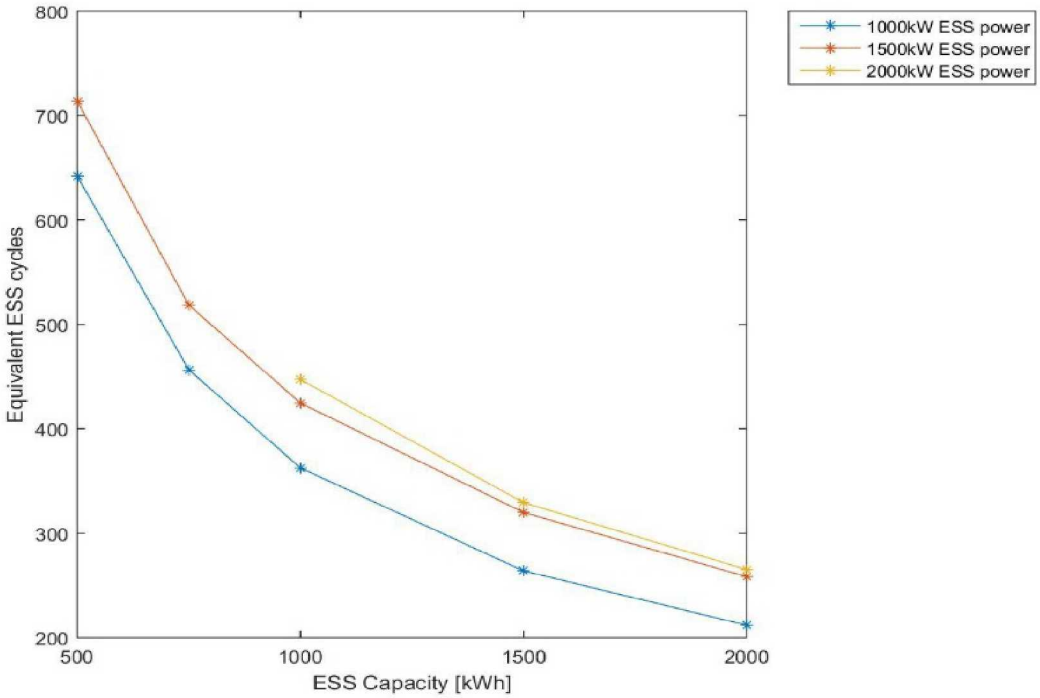

Figure 99 - The number of equivalent full ESS cycles for different ESS capacities and powers.

Number of ESS Cycles

Rainflow counting was used to calculate the number of ESS cycles of varying amplitude experienced by the ESS. Figure 100 shows the number of ESS cycles for each cycle amplitude for different ESS capacities and powers. The number of cycles decrease with increasing amplitude. Smoothing the load on the diesel and hydro generators results in more low amplitude cycles, which contributes to increased equivalent full ESS cycles.

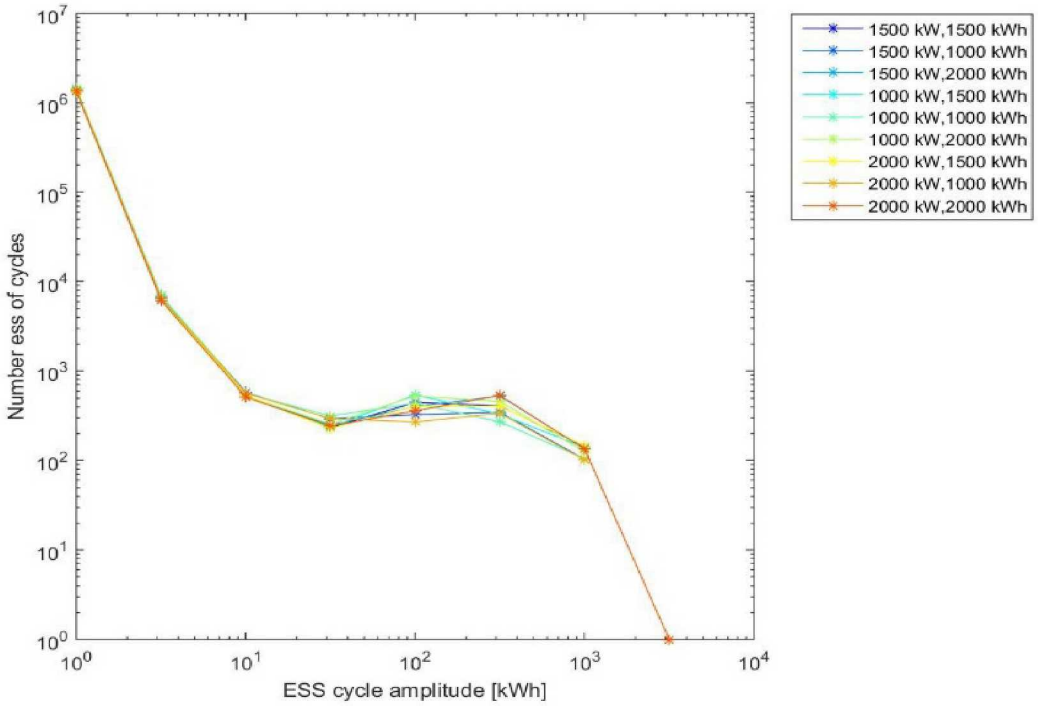

Figure 100 - The number of ESS cycles at different cycle amplitudes for different ESS capacities and powers.

ESS Power Levels

The amount of time the energy storage system spends charging and discharging at different power levels, measured in kW, is shown in Figure 101.

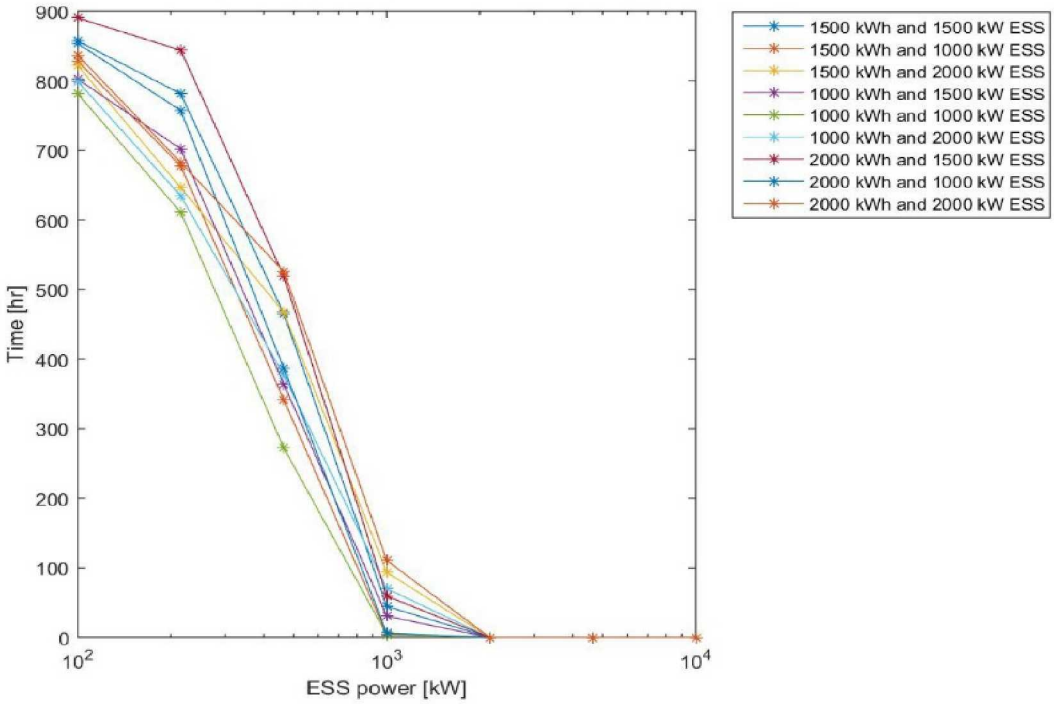

Figure 101 - The time the ESS spend charging or discharging at different power levels.

ESS Ramp Rate

Figure 102 shows the probability distribution of ESS ramp rates for different ESS capacities and powers. The mean ramp rate is 12 kW/sec, which is the same as the mean ramp rate of the load.

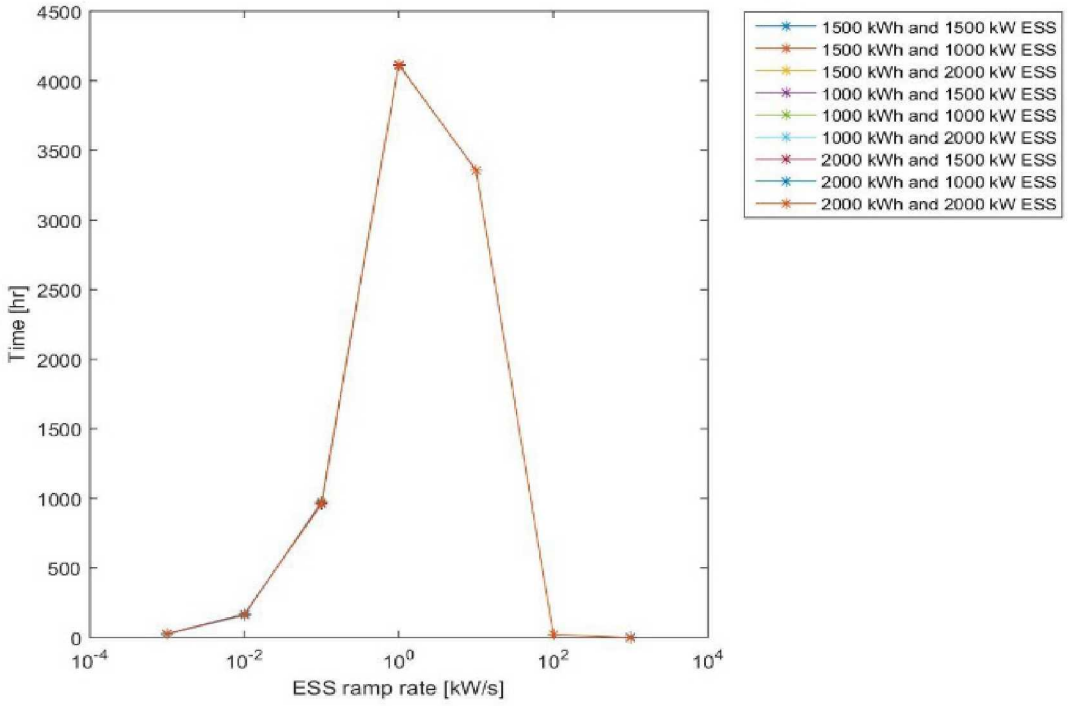

Figure 102 - Probability distribution of ESS ramp rates for different ESS capacities and powers.

ESS Throughput

Figure 103 shows the total ESS throughput for different ESS capacities and powers. With increasing capacity and power, throughput increases.

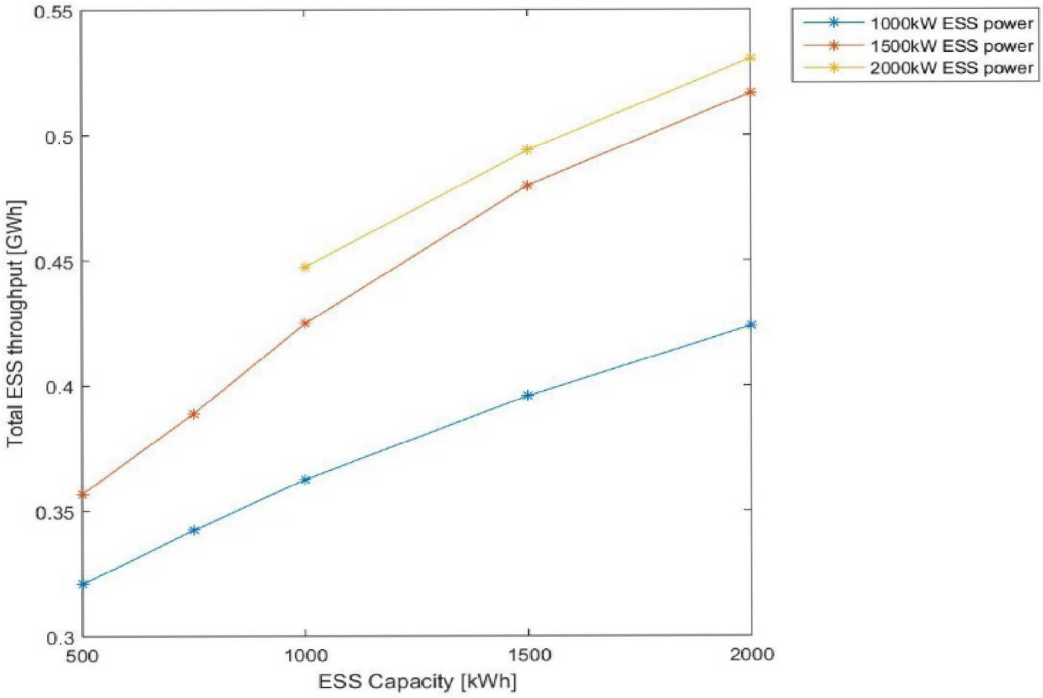

Figure 103 - ESS throughput for different ESS capacities and powers.

ESS Direct Contribution to Diesel Reduction

Figure 104 shows the ESS direct contribution to diesel reduction for different ESS capacities and powers. It is calculated as the total reduction in diesel output that did not go through the ESS. In other words, the ESS enabled the reduction of diesel without actually having to charge and discharge.

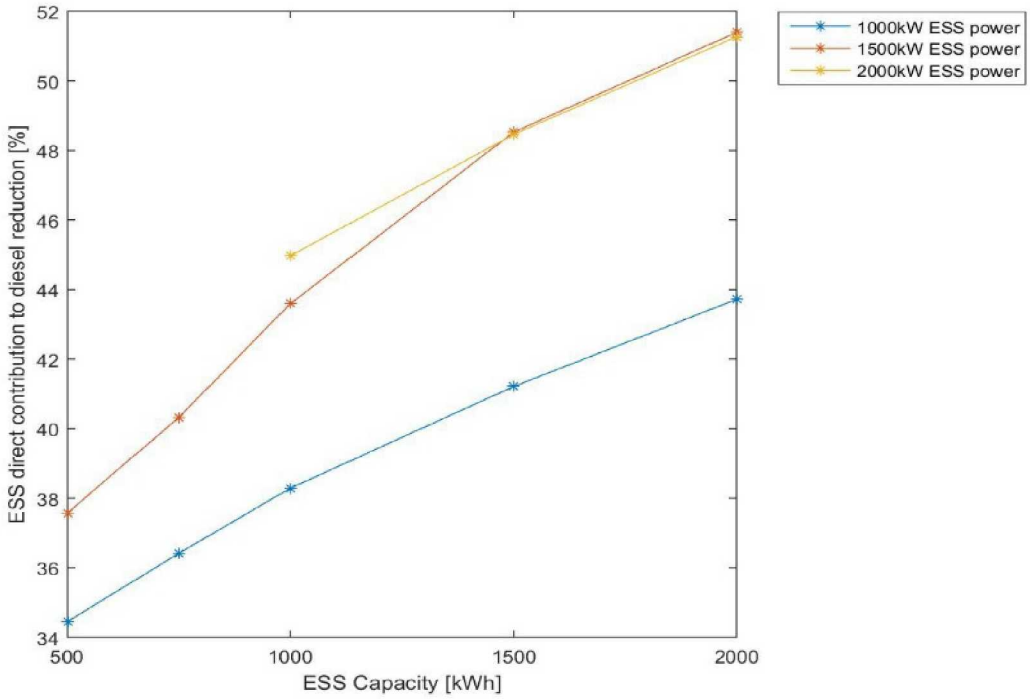

Figure 104 - ESS direct contribution to diesel reduction for different ESS capacities and powers.

ESS Charging from Diesel

Figure 105 shows the percent of total ESS charging that was from diesel generators. These simulations have high percentages, as a result of charging the ESS with diesel generators and smoothing the loading on the diesels.

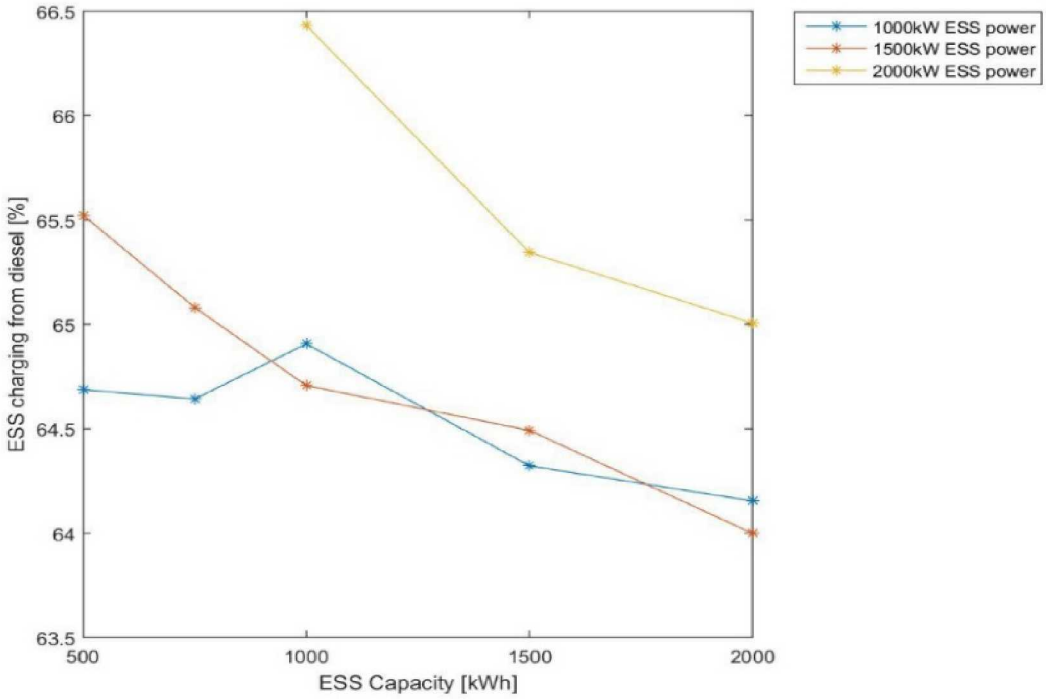

Figure 105 - The percent of total ESS charging that was from diesel generators for different ESS capacities and powers.

Simulation with No Smoothing and Diesel Charging

In this set of simulations the lowest diesel consumption, highest diesel off time and diesel loading is seen. Diesel switching is reduced as well as the ESS utilization when compared to the simulations that had no ESS but are higher than the simulations that in the previous section.

Diesel Output

Figure 106 shows the diesel output for each generator in each of the simulations. Gen7, Gen5 and Gen6 are the most commonly used diesel generators. Figure 107 shows the total diesel output for each simulation and Figure 108 shows the reduction in diesel output. Increasing the ESS capacity and power result in increasing reduction in diesel output.

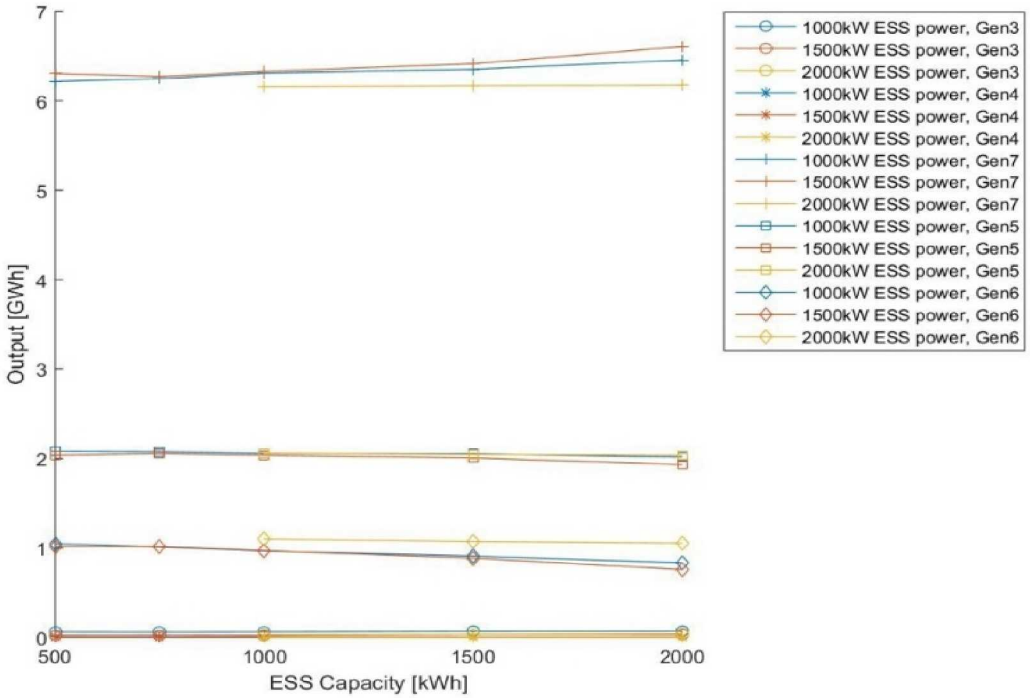

Figure 106 - The output of each diesel generator for different ESS capacities and powers.

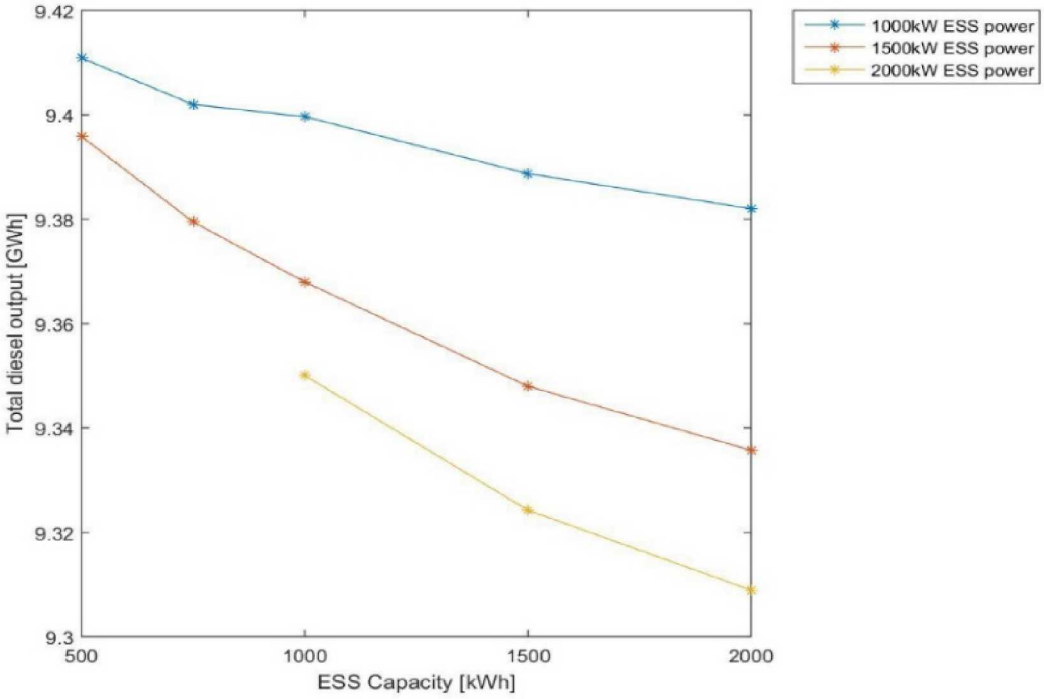

Figure 107 - The total diesel output for different ESS capacities and powers.

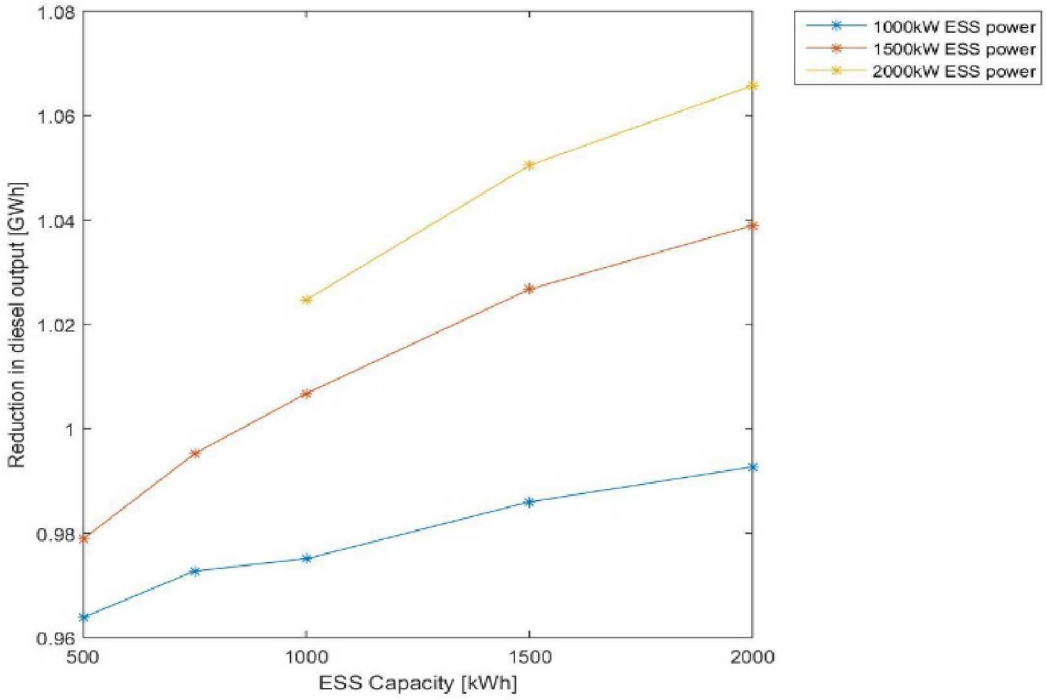

Figure 108 - Reduction in total diesel output for different ESS capacities and powers.

Diesel Consumption

Figure 109 shows the diesel consumption for each generator in each simulation. Figure 110 and Figure 111 show the total consumption and reduction in total consumption. Increasing ESS capacity and power reduces diesel consumption. The reduction in consumption is a result of the reduction in diesel output as well as running the diesel generators at a higher and more efficiency loading.

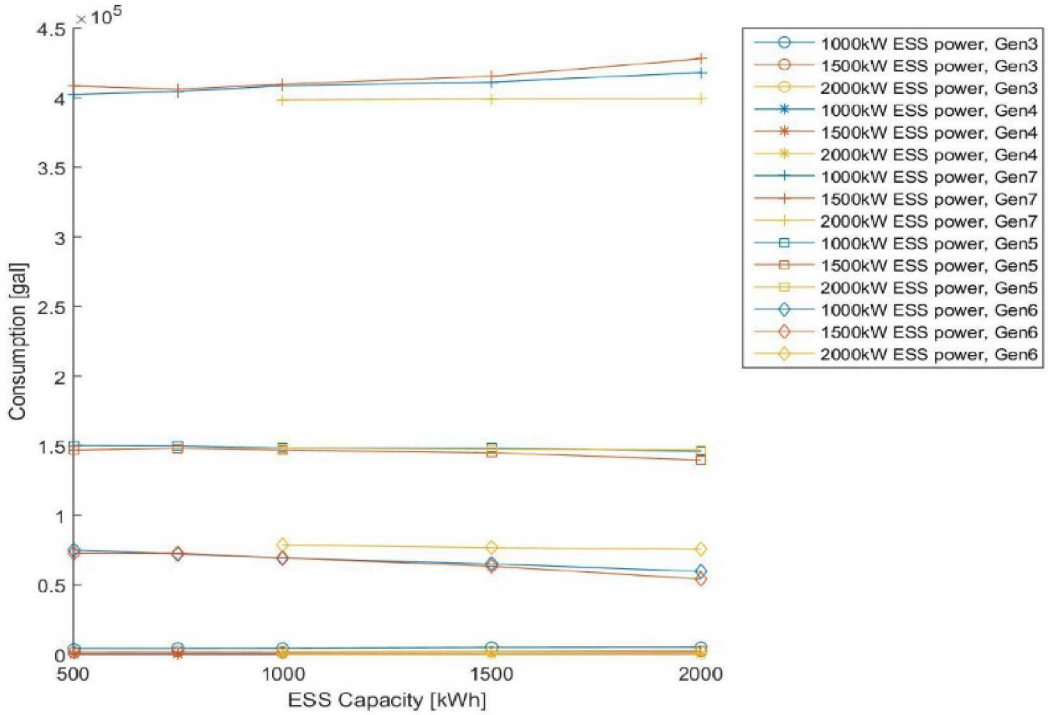

Figure 109 - The diesel consumption of each diesel generator for different ESS capacities and powers

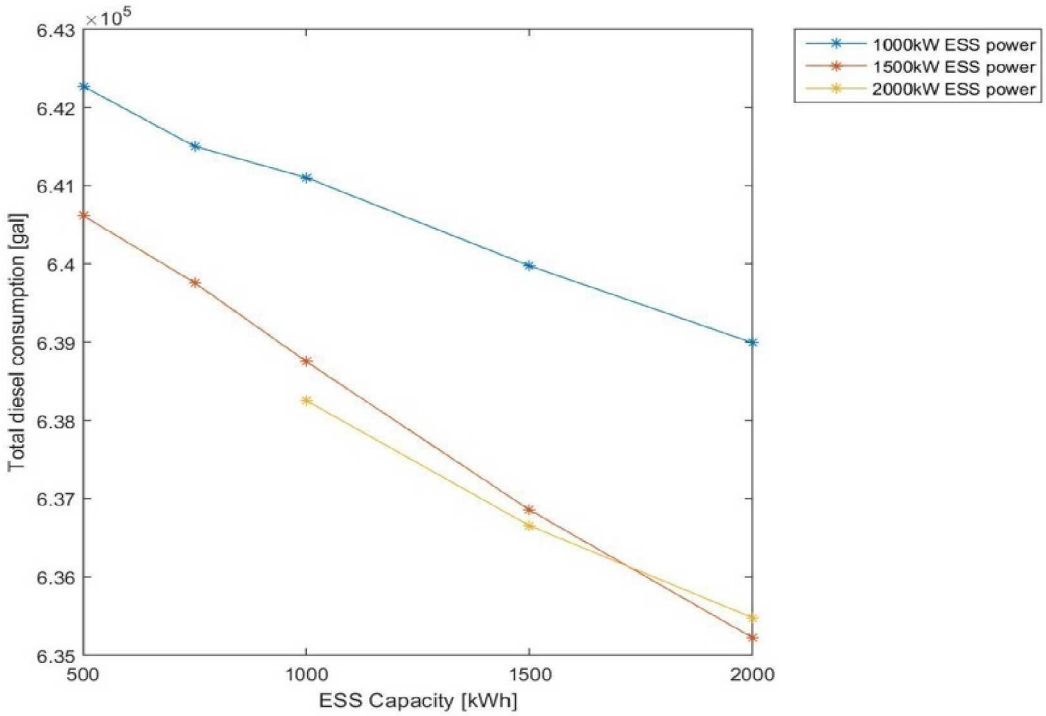

Figure 110 - The total diesel consumption for different ESS capacities and powers

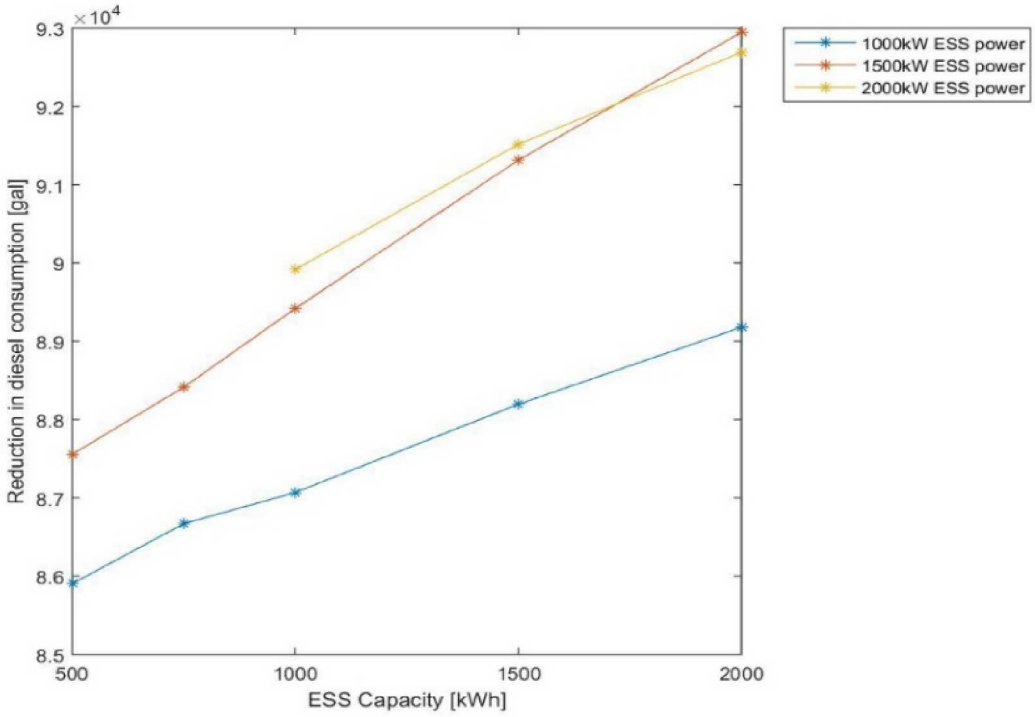

Figure 111 - The reduction in diesel consumption for different ESS capacities and powers.

Diesel Off Time

Figure 112 shows the time spent in diesel off in 2011. Figure 113 shows the increase in time spent in diesel off. Increasing ESS capacity and power increases the time spent in diesel off.

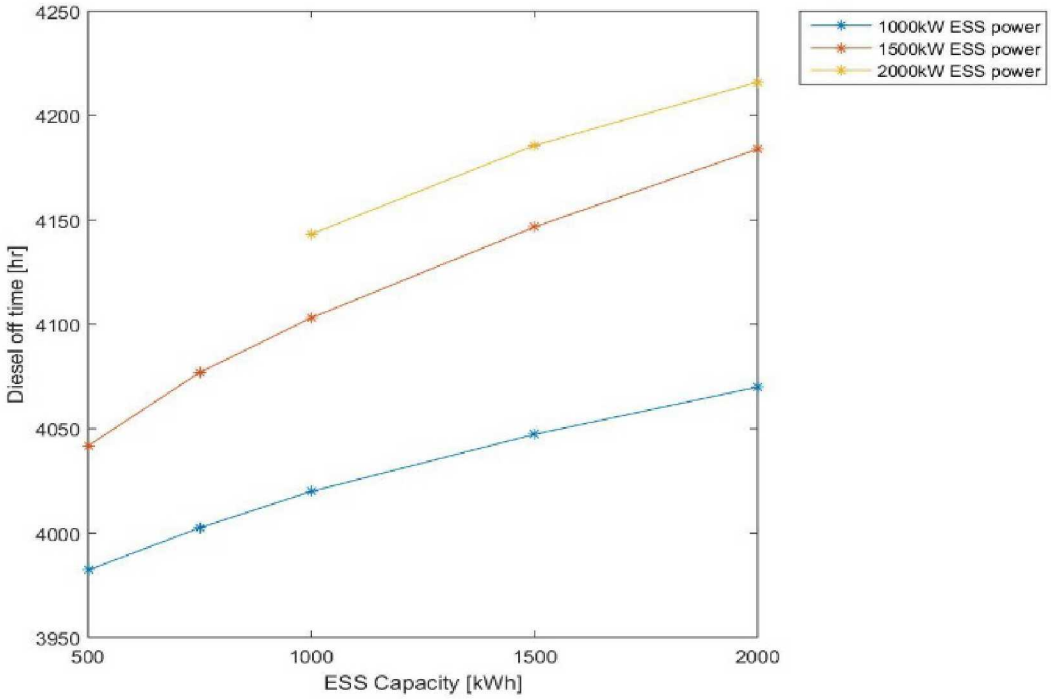

Figure 112 - Time spent in diesel off mode in 2011 for different ESS capacities and powers

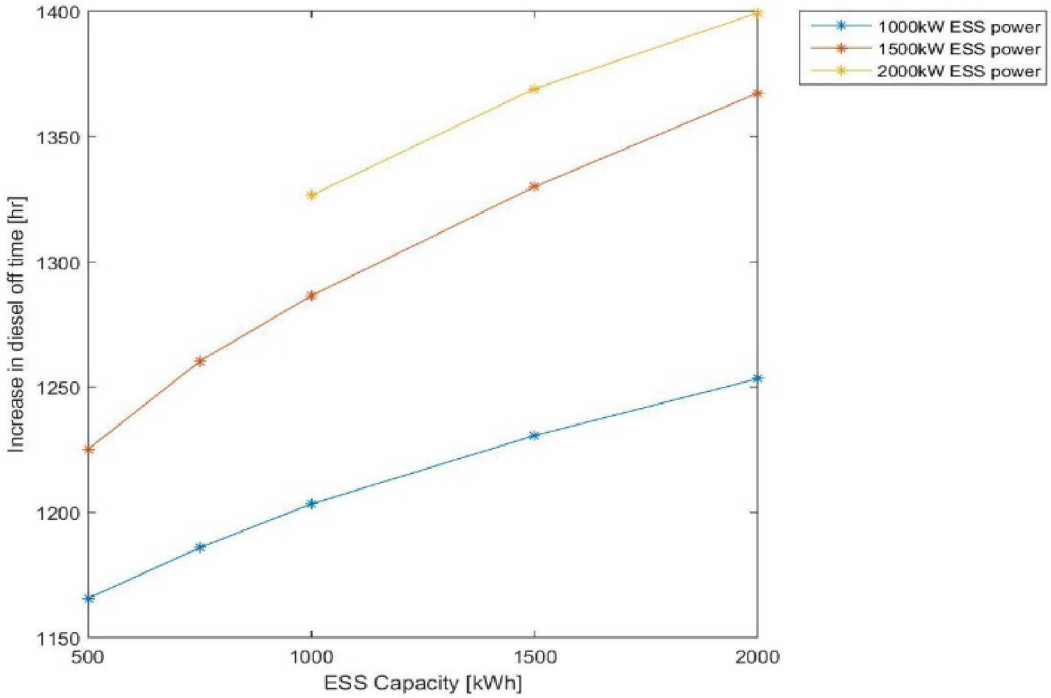

Figure 113 - Increase in time spent in diesel off mode in 2011 for different ESS capacities and powers.

Diesel Run Time

Figure 114 shows the run time for each diesel generator for different ESS capacities and powers. Figure 115 shows the total diesel run time. Figure 116 shows the decrease in diesel run time. Increasing the ESS capacity reduces diesel run time but does not necessarily reduce the ESS run time. This results from multiple diesel generators being run online together. So increasing the ESS power from 1.5 MW to 2 MW increases diesel-off time but also increases diesel run time.

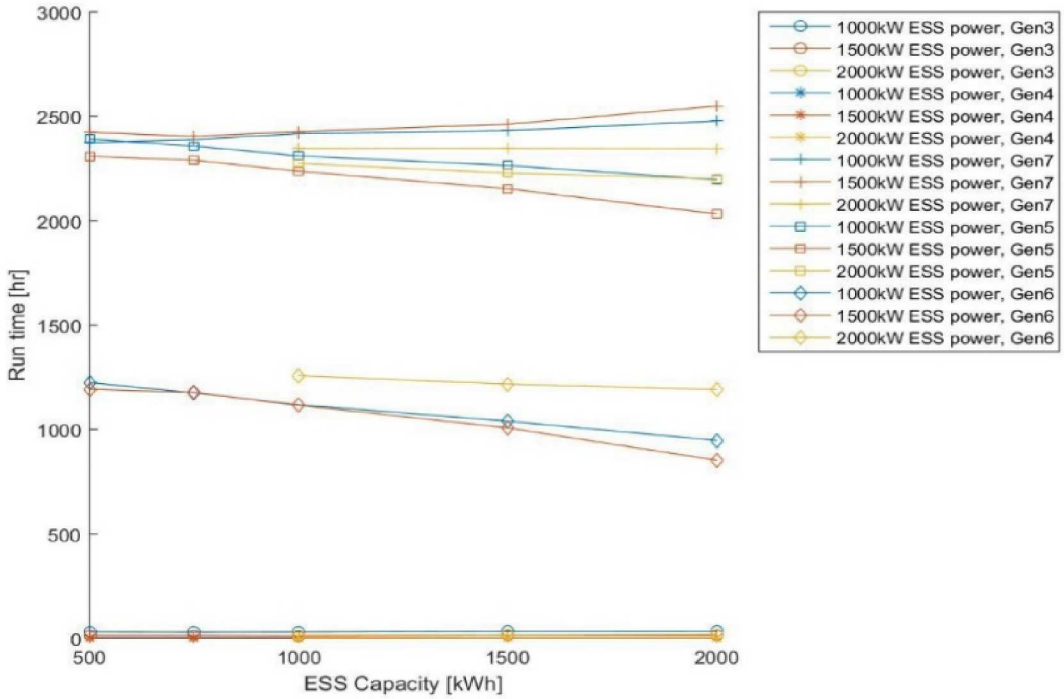

Figure 114 - The run time for each diesel generator for different ESS capacities and powers

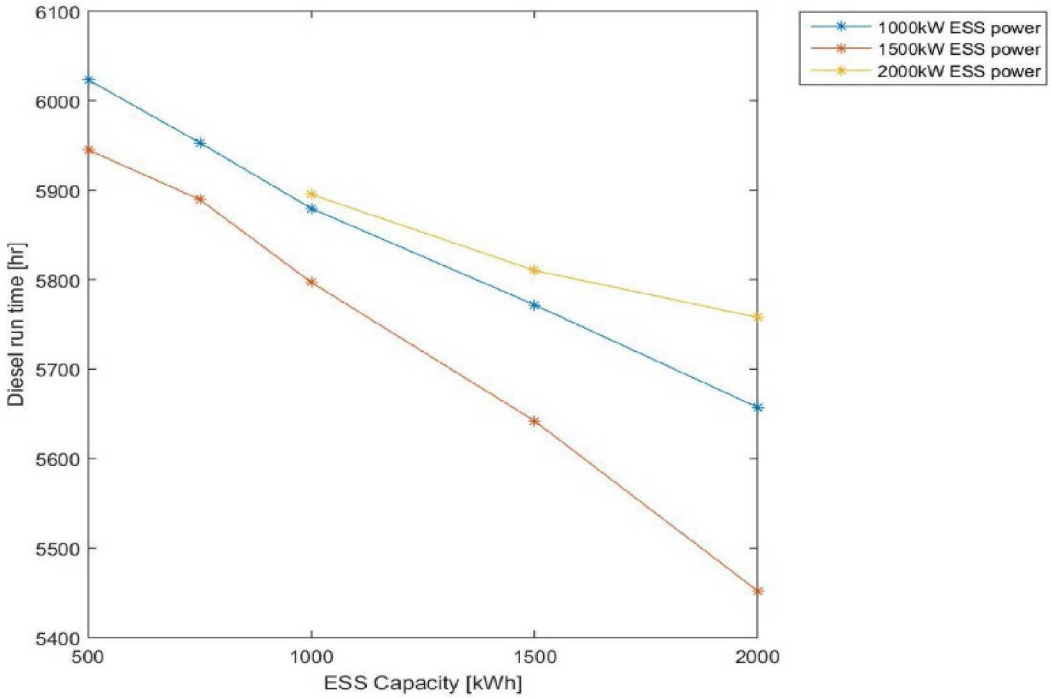

Figure 115 - The total diesel run time for different ESS capacities and powers

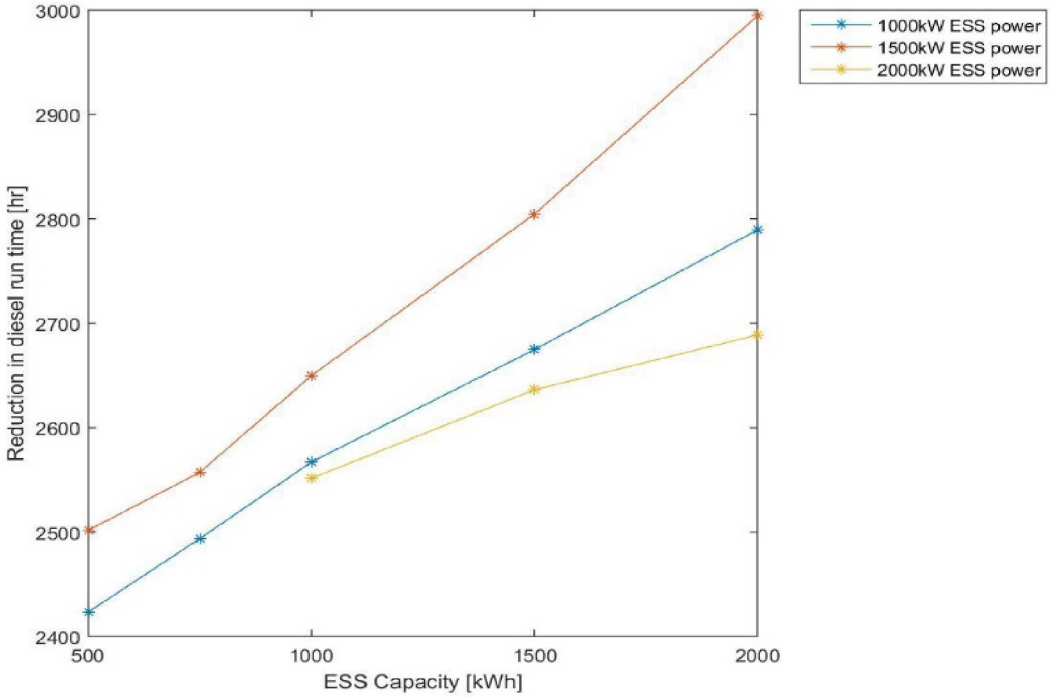

Figure 116 - The reduction is diesel run time for different ESS capacities and powers.

Diesel Capacity Factor

Figure 117 and Figure 118 show the diesel capacity factor for each diesel generator and the total diesel capacity factor for different ESS capacities and powers. A higher ESS capacity and power resulted in a higher diesel capacity factor. These simulations show a significant increase in diesel capacity factor from the measured value for 2011 or 61%.

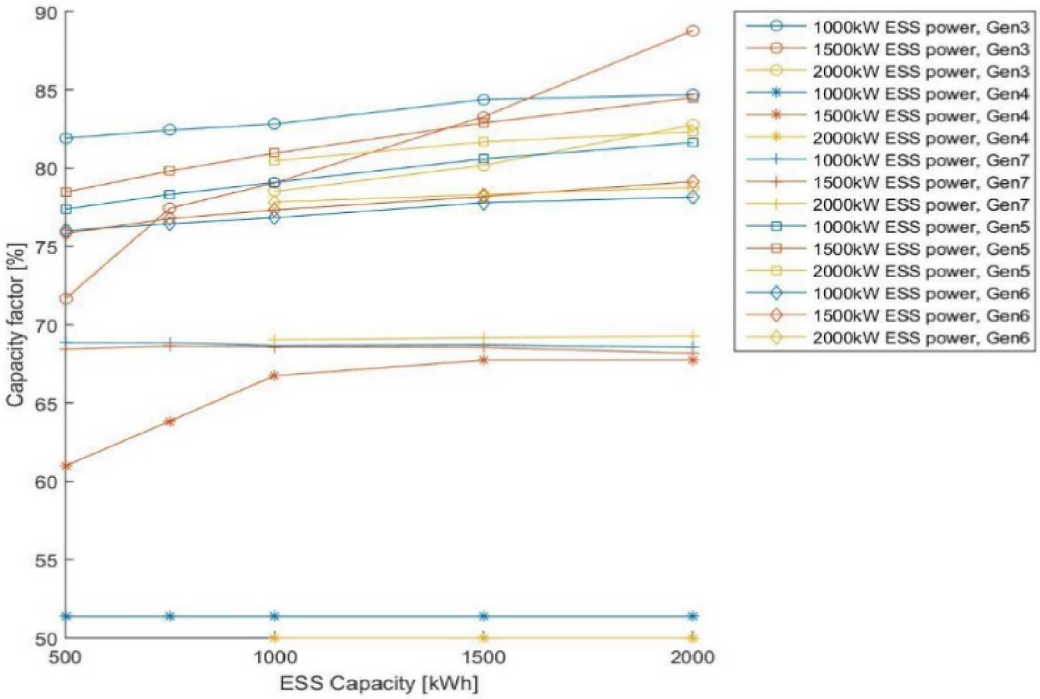

Figure 117 - Capacity factor for each diesel generator for different ESS capacities and powers.

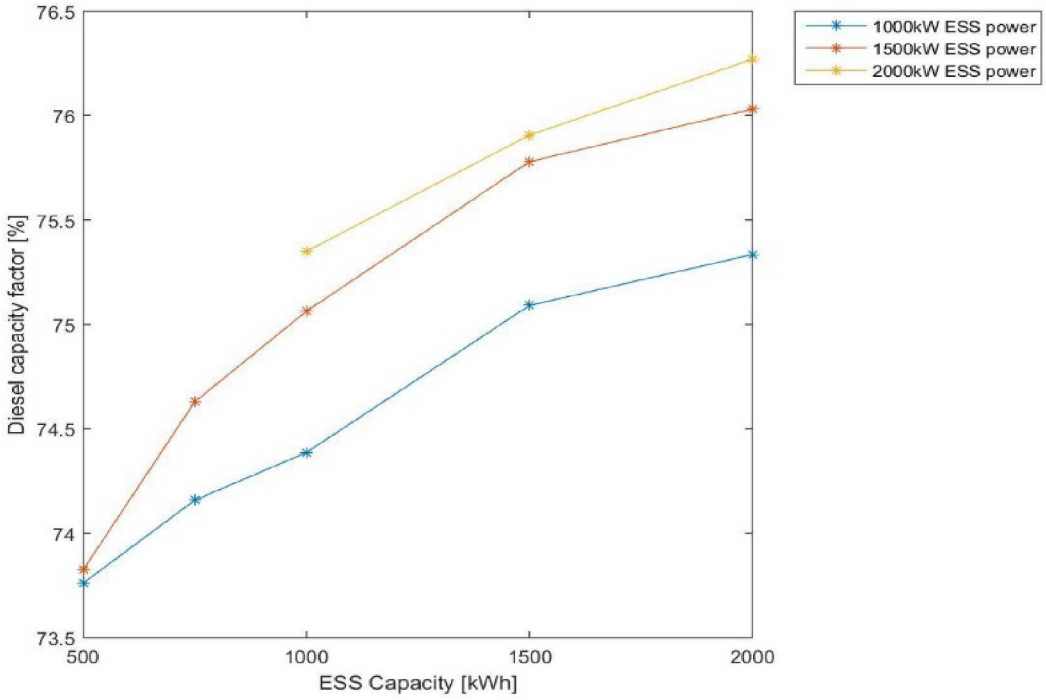

Figure 118 - Overall diesel capacity factor for different ESS capacities and powers.

Diesel Switching

Figure 119 and Figure 120 show the number of times each diesel generator and all diesel generators are switched online for different ESS capacities and powers. They show an increase in diesel switching compared to the measured value of 1001 times for 2011.

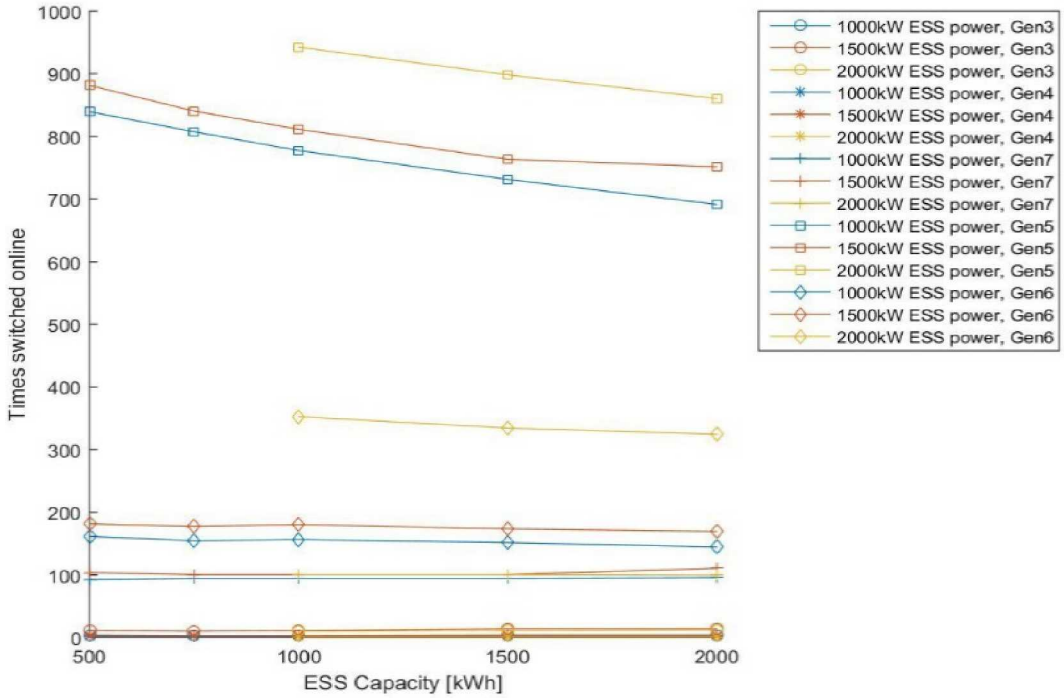

Figure 119 - The number of times each diesel generator is switched online for different ESS capacities and powers.

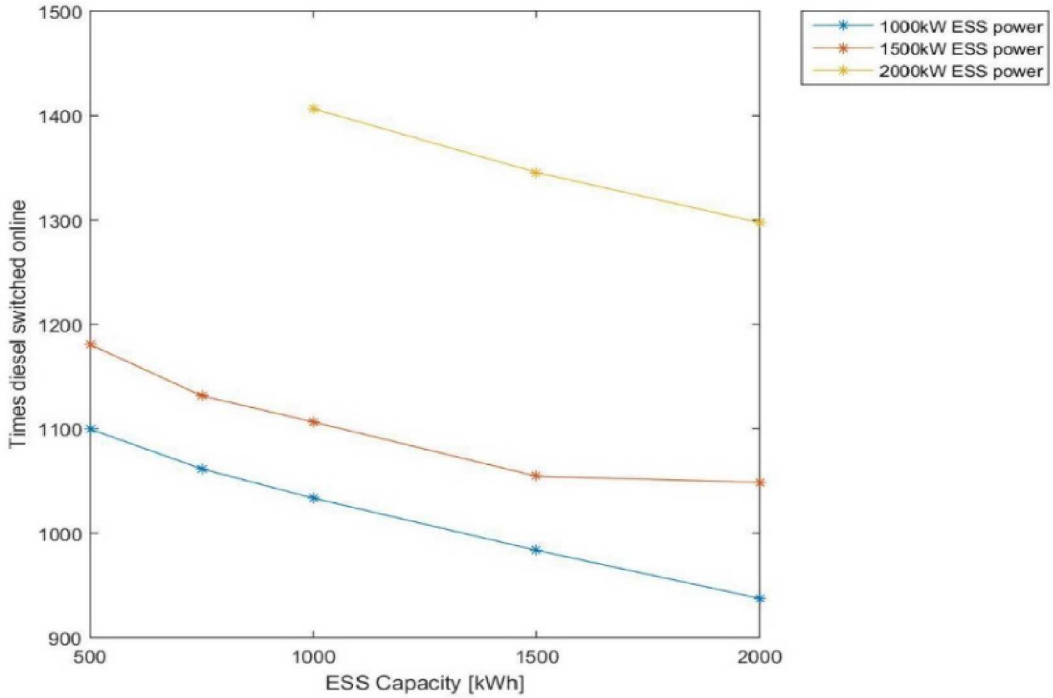

Figure 120 - The total number of times diesel generators are switched online for different ESS capacities and powers.

Diesel Ramp Rate

Figure 121 shows the probability distribution of diesel ramp rates for different ESS capacities and powers. There is not much difference between the different ESS capacities and powers. They have a mean value of around 3.9 kW/s which is higher than the average measured value of 3.1 kW/s for 2011.

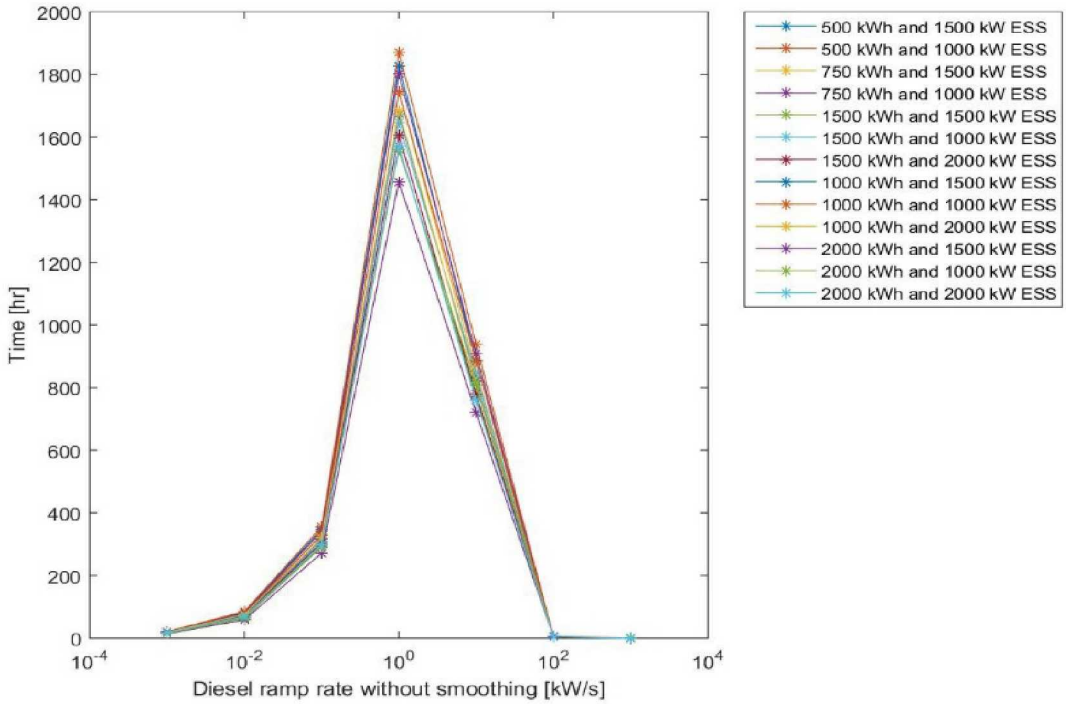

Figure 121 - A probability distribution of the ramp rates on the diesel generators for different ESS capacities and powers.

ESS Equivalent Cycles

Figure 122 shows the number of equivalent full ESS cycles. Multiple ESS cycles that add up to the full ESS capacity are considered to be one equivalent ESS cycle. These simulations have high ESS cycling which negatively affect the life of most ESS technologies.

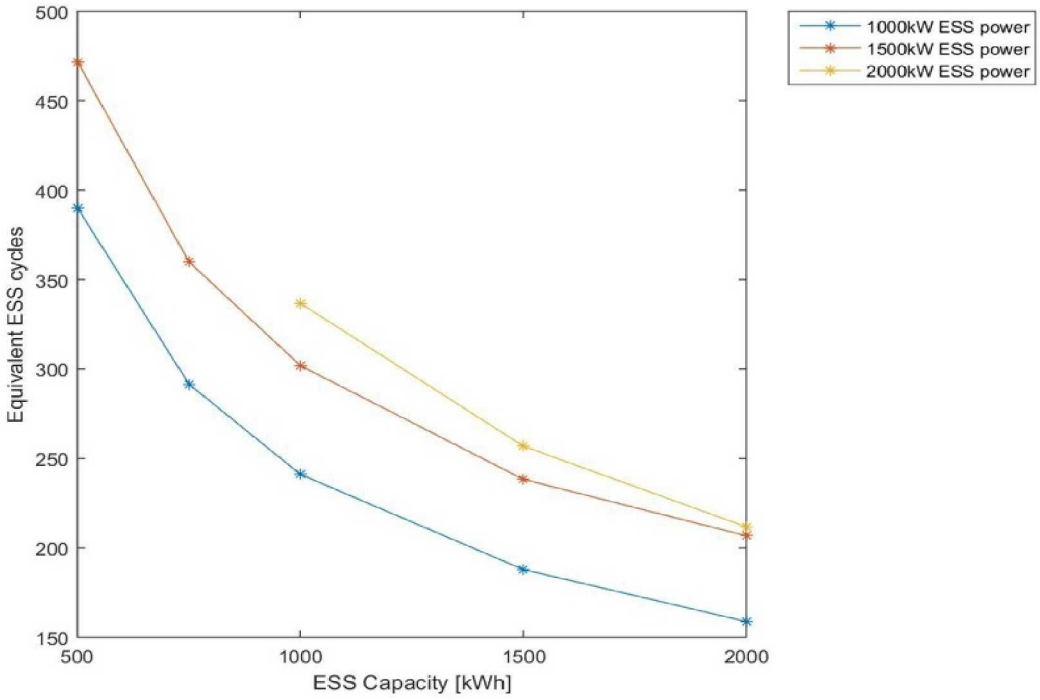

Figure 122 - The number of equivalent full ESS cycles for different ESS capacities and powers.

Number of ESS Cycles

Rainflow counting was used to calculate the number of ESS cycles of varying amplitude experienced by the ESS. Figure 123 shows the number of ESS cycles for each cycle amplitude for different ESS capacities and powers. The number of cycles decrease with increasing amplitude.

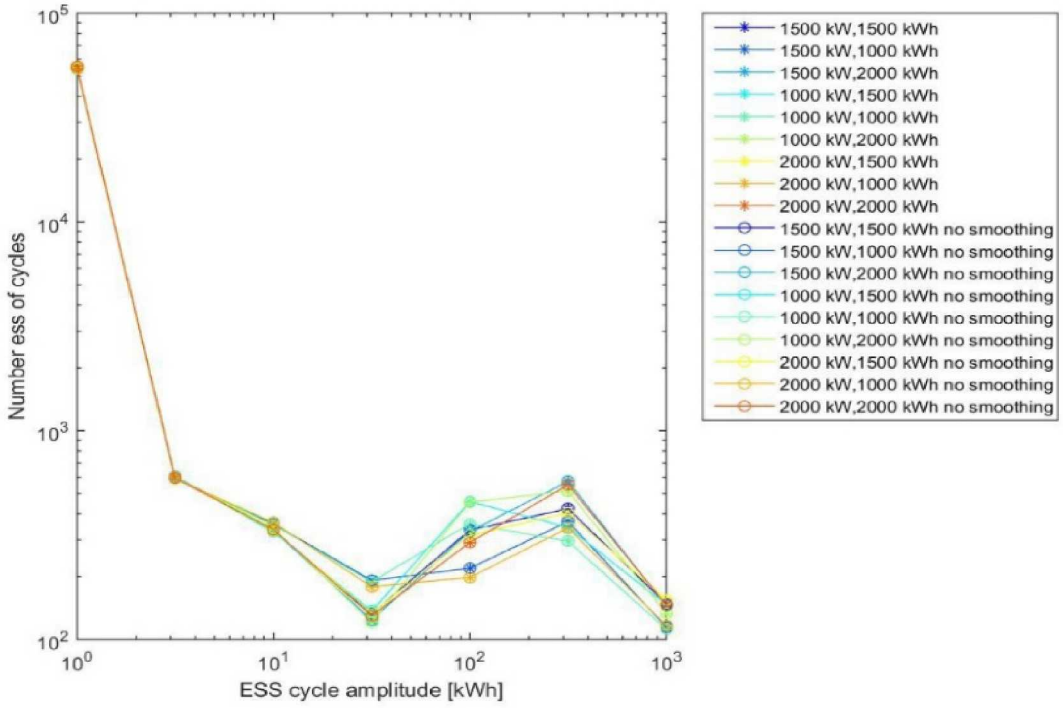

Figure 123 - The number of ESS cycles at different cycles amplitudes for different ESS capacities and powers.

ESS Power Levels

Figure 124 shows the time the ESS spends charging or discharging at different power levels. The ESS has majority of charge and discharge cycles at 100 kW – 200 kW.

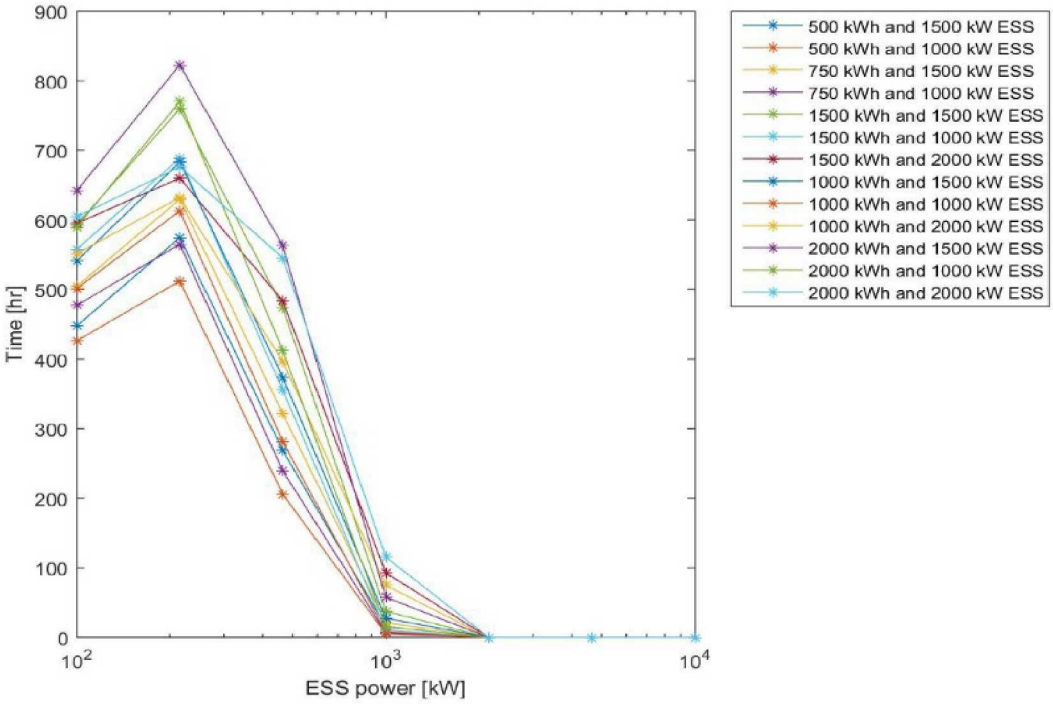

Figure 124 - The time the ESS spends charging or discharging at different power levels.

ESS Ramp Rate

Figure 125 shows the probability distribution of ESS ramp rates for different ESS capacities and powers. The mean ramp rate is 3 kW/sec, which is significantly lower than the ramp rates of simulations that smooth the diesel and hydro generators.

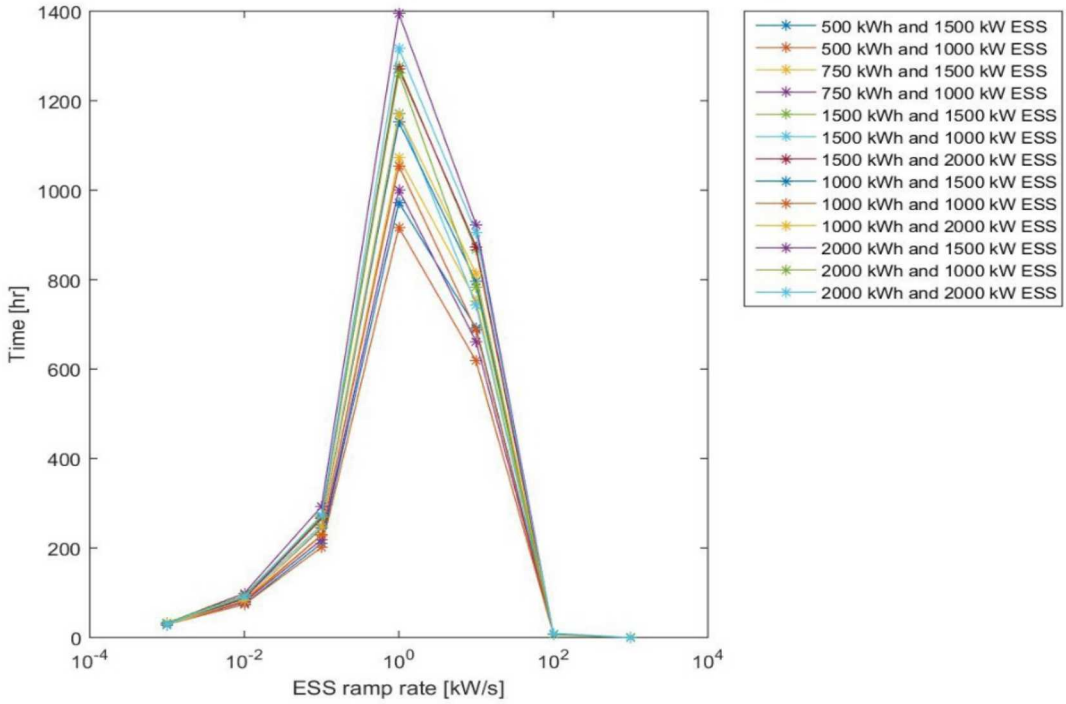

Figure 125 - Probability distribution of ESS ramp rates for different ESS capacities and powers.

ESS Throughput

Figure 126 shows the total ESS throughput for different ESS capacities and powers. With increasing capacity and power, throughput increases.

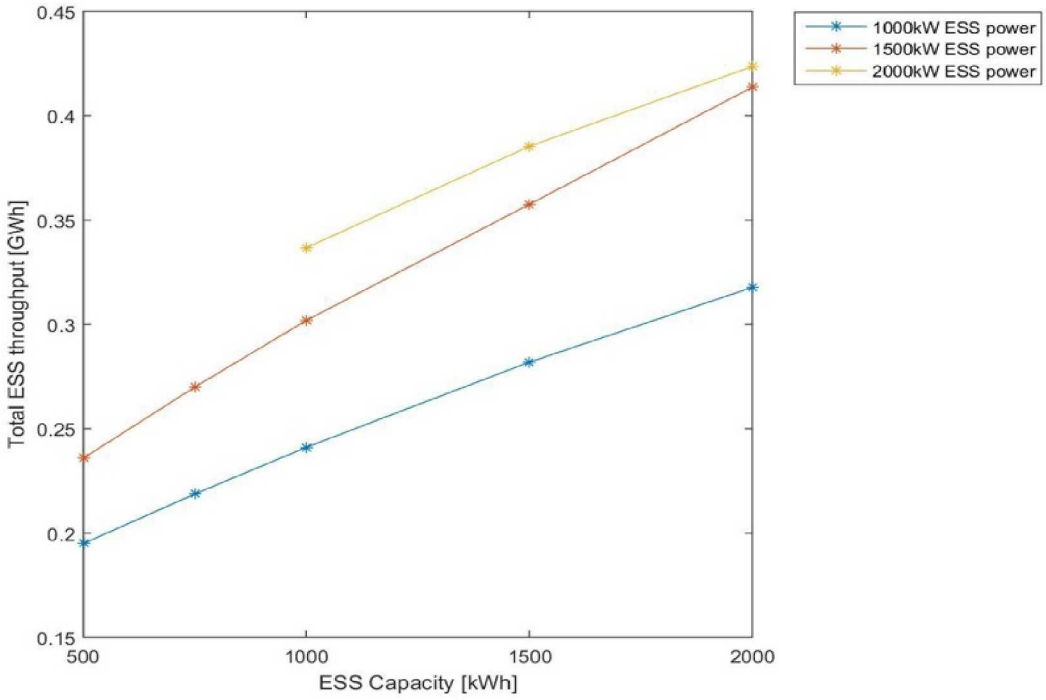

Figure 126 - ESS throughput for different ESS capacities and powers.

ESS Contribution to Diesel Reduction

Figure 127 shows the ESS direct contribution to diesel reduction for different ESS capacities and powers. It is calculated as the total reduction in diesel output that did not go through the ESS. In other words, the ESS enabled the reduction of diesel without actually having to charge and discharge.

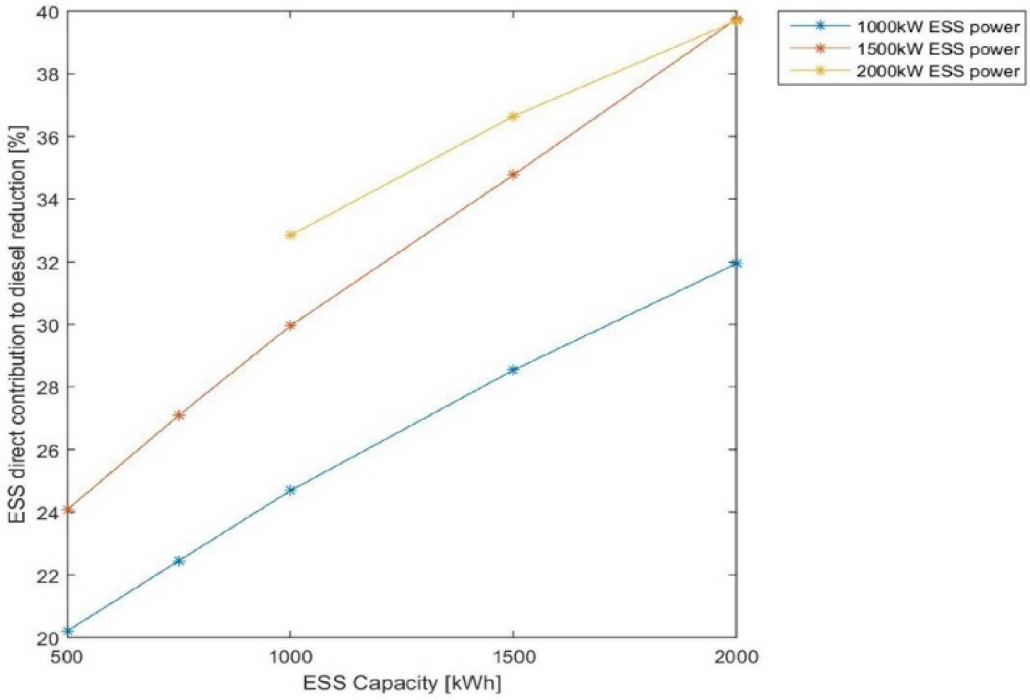

Figure 127 - ESS direct contribution to diesel reduction for different for different ESS capacities and powers.

ESS Charging from Diesel

Figure 128 shows the percent of total ESS charging that was from diesel generators. These simulations have the highest percentages.

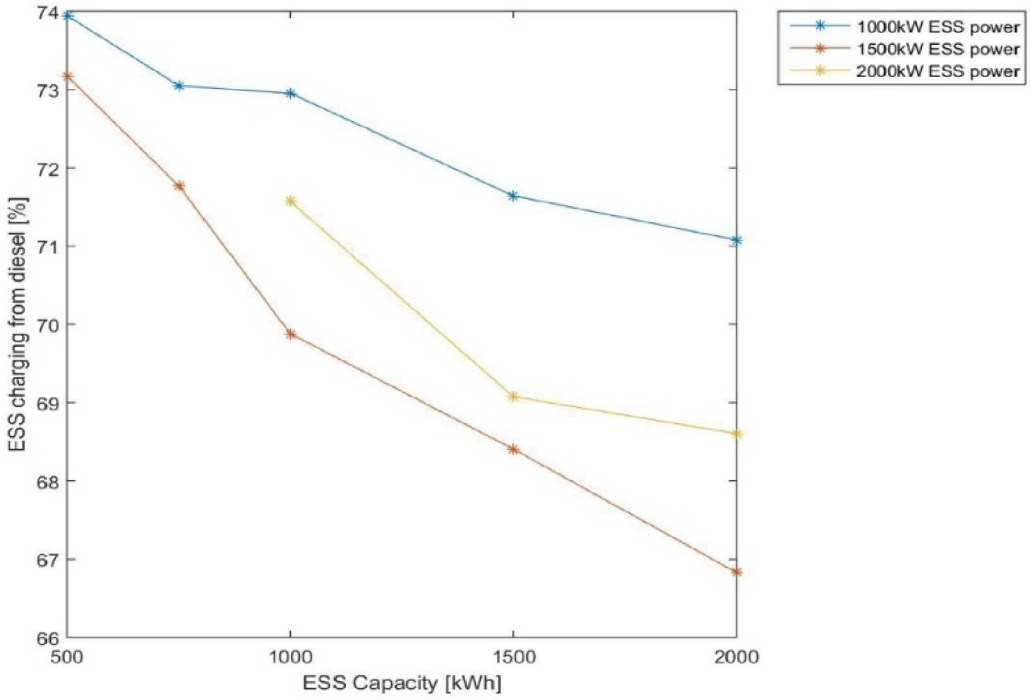

Figure 128 - The percent of total ESS charging that was from diesel generators for different ESS capacities and powers.

2011: Simulation with Smoothing and No Diesel Charging

This set of simulations did not allow the diesel to charge the ESS but smoothed the loading on the diesel and hydro generators. These simulations have the lowest diesel capacity factor of 62% which result in the highest (by a small margin) diesel consumption. The diesel switching and the ESS utilization is significantly lower than in the simulations which allowed the diesel generators to charge the ESS but still higher than the simulations which did not smooth the load on the diesel and hydro generators.

Diesel Output

Figure 129 shows the diesel output for each generator in each of the simulations. Generators Gen7, Gen5 and Gen6 are the most commonly used. Figure 130 shows the total diesel output for each simulation and Figure 131 shows the reduction in diesel output. Increasing the ESS capacity and power resulting in increasing reduction in diesel output.

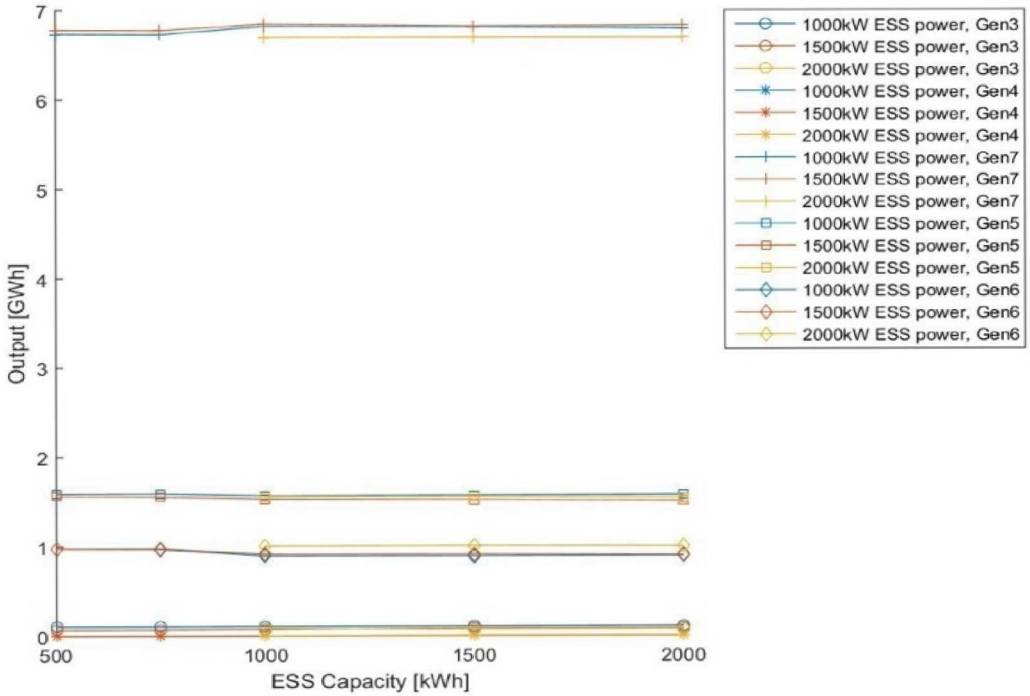

Figure 129 - The output of each diesel generator for different ESS capacities and powers.

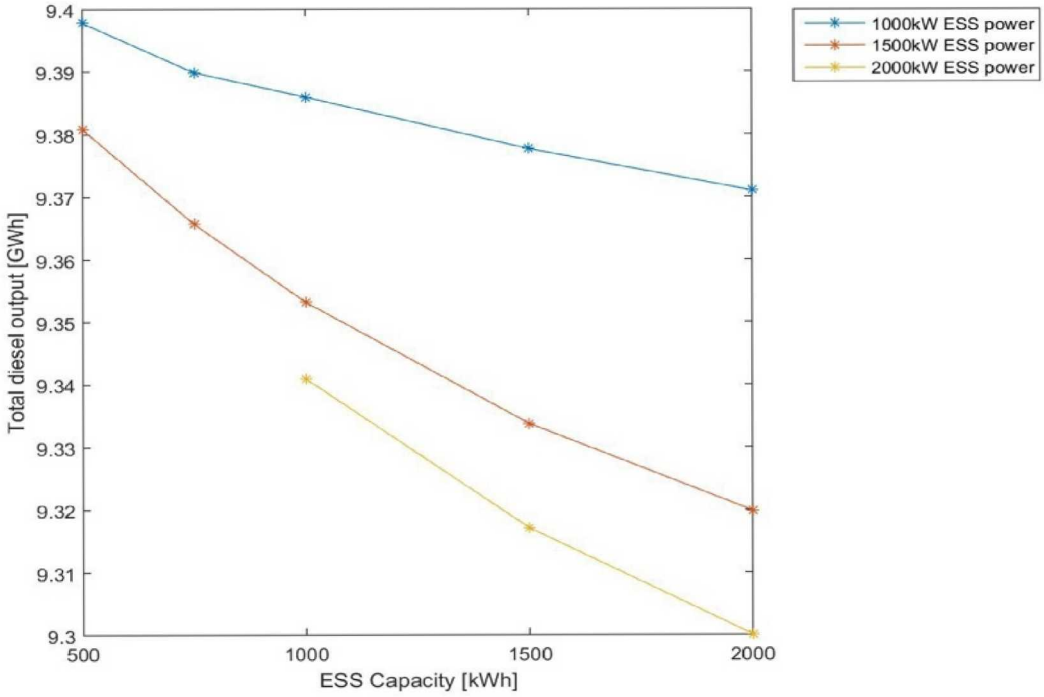

Figure 130 - The total diesel output for different ESS capacities and powers.

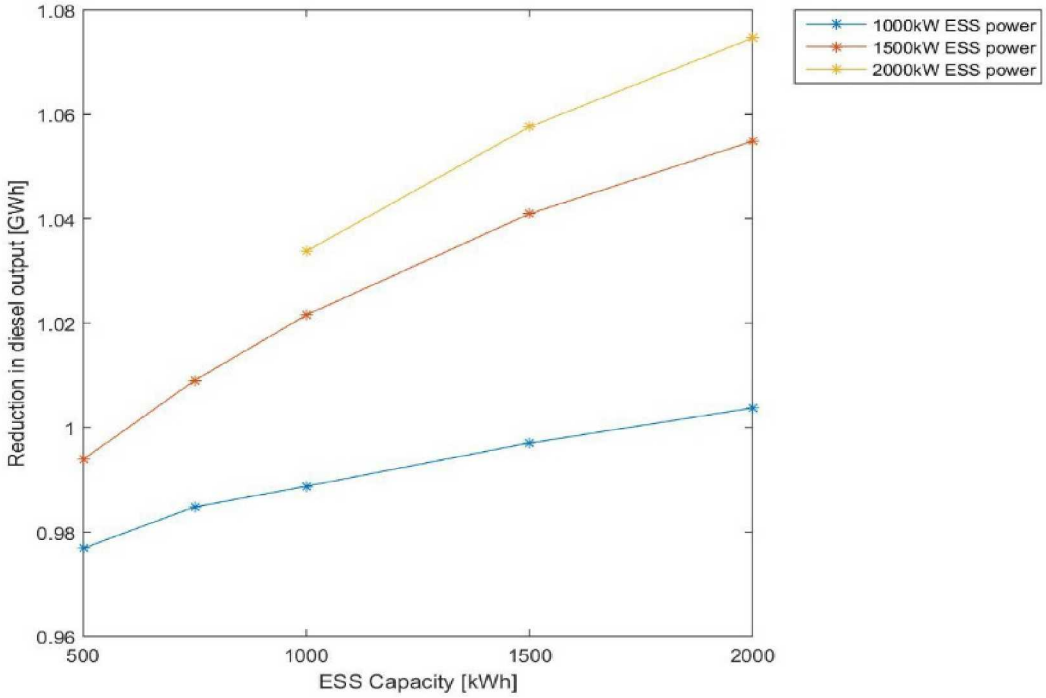

Figure 131 - The reduction in total diesel output for different ESS capacities and powers.

Diesel Consumption

Figure 132 shows the diesel consumption for each generator in each simulation. Figure 133 and Figure 134 show the total consumption and reduction in total consumption. Increasing ESS capacity and power reduces diesel consumption. The reduction in consumption is a result of the reduction in diesel output as well as running the diesel generators at a higher and more efficiency loading.

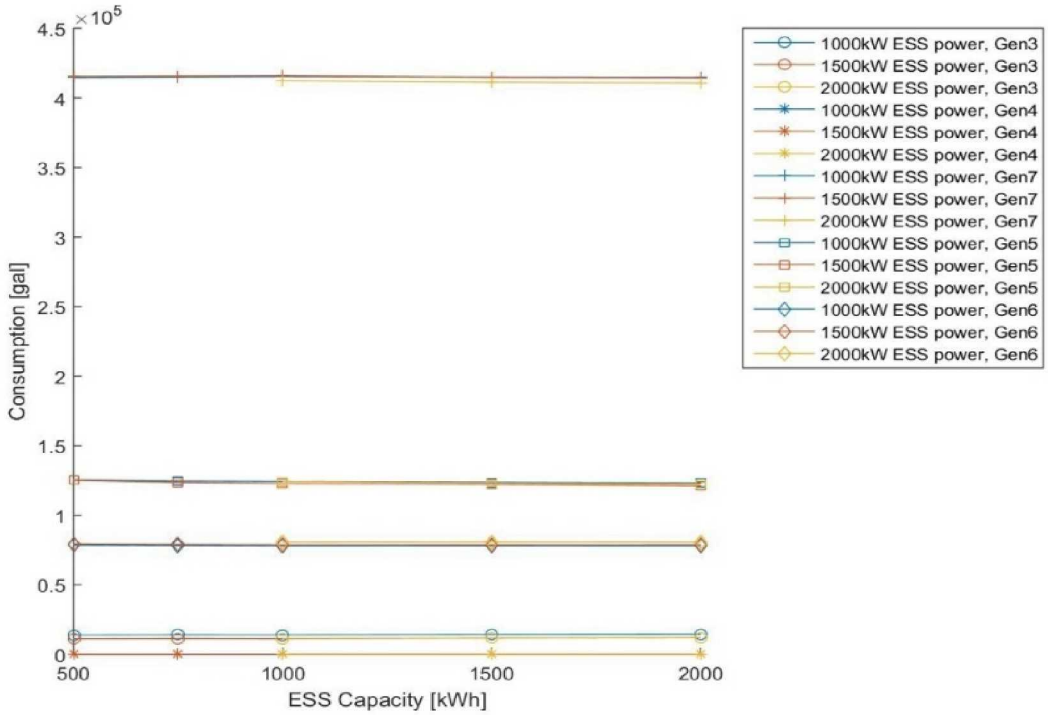

Figure 132 - The diesel consumption of each diesel generator for different ESS capacities and powers

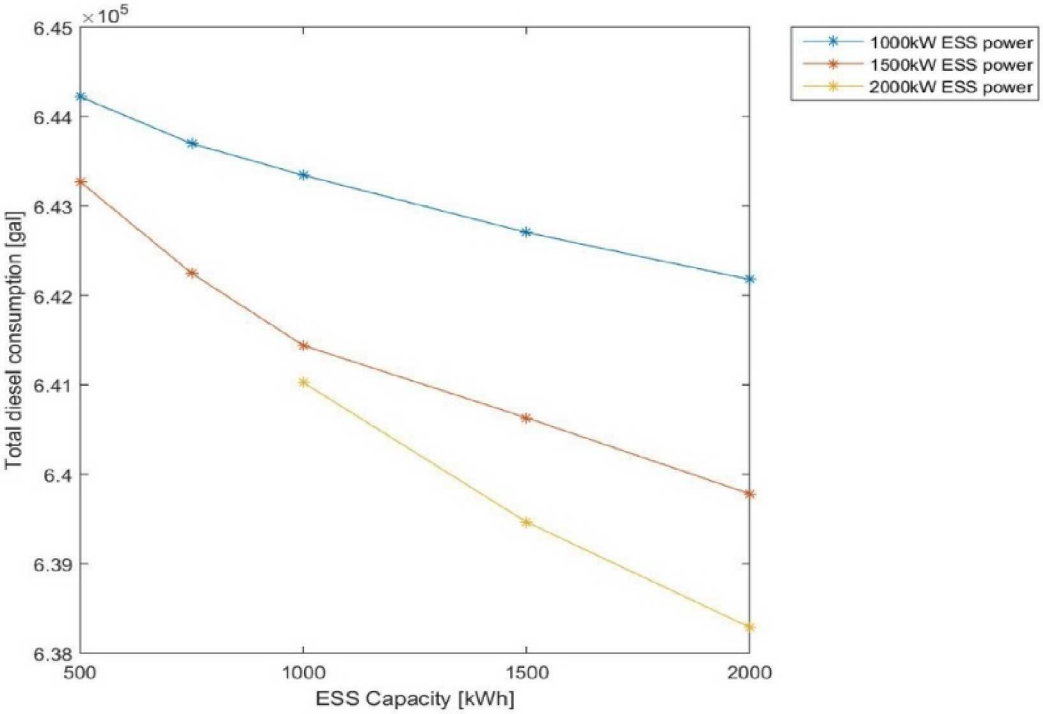

Figure 133 - The total diesel consumption for different ESS capacities and powers.

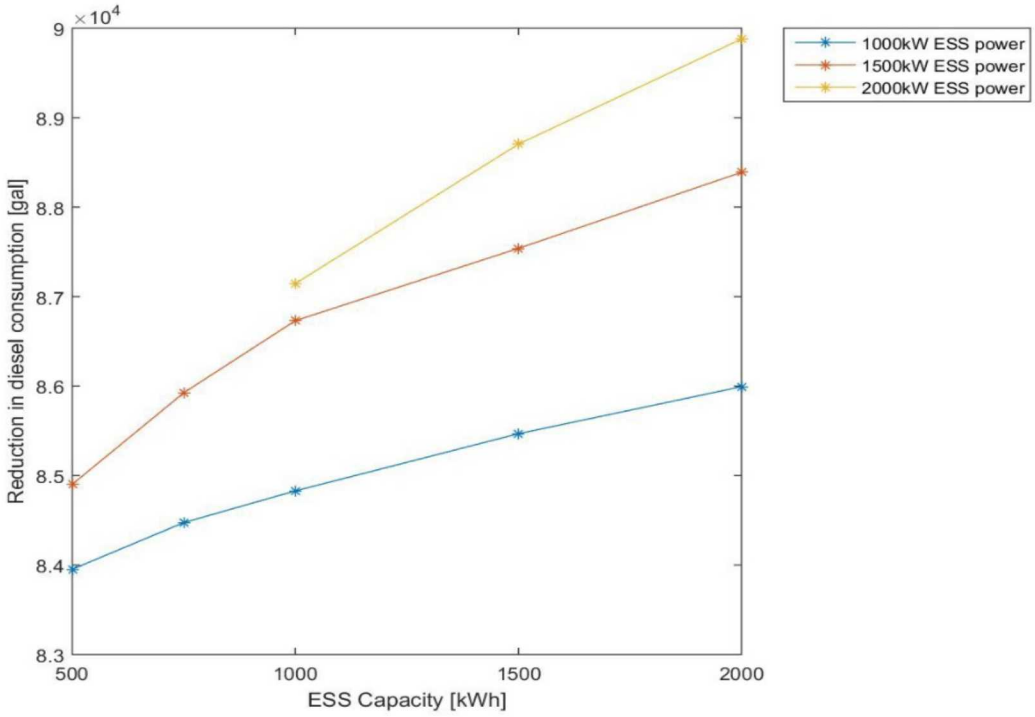

Figure 134 - The reduction in diesel consumption for different ESS capacities and powers.

Diesel Off Time

Figure 135 shows the time spent in diesel off in 2011. Figure 136 shows the increase in time spent in diesel off. Increasing ESS capacity and power increases the time spent in diesel off.

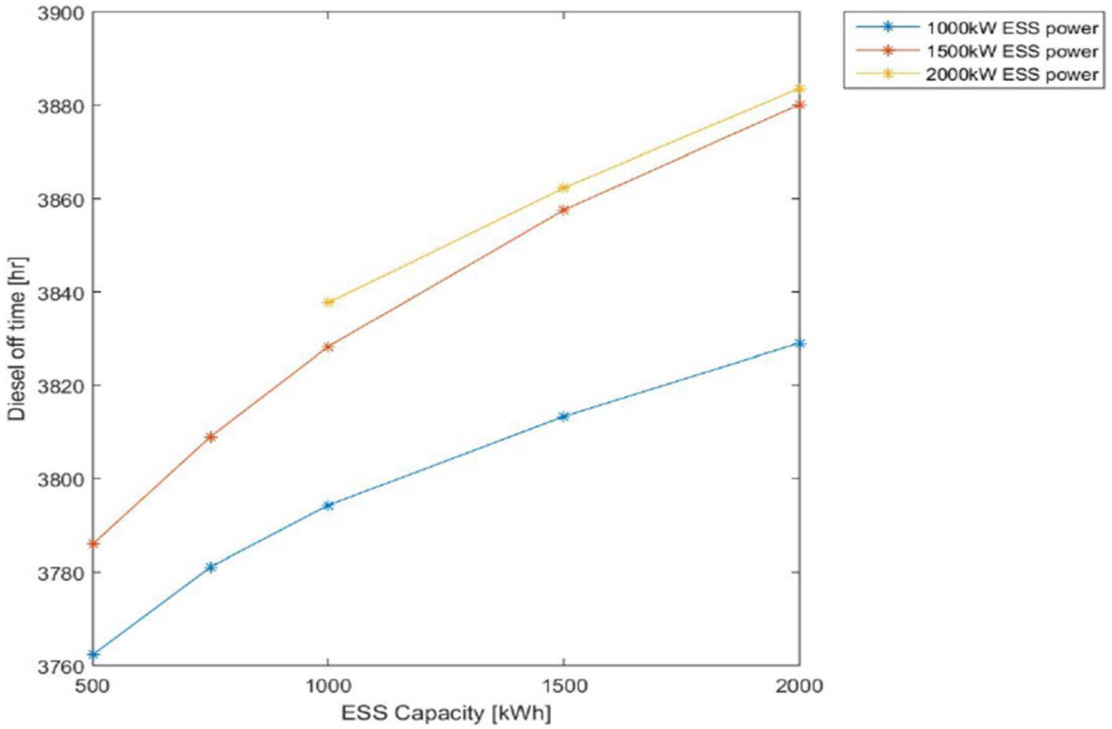

Figure 135 - The time spent in diesel off mode in 2011 for different ESS capacities and powers

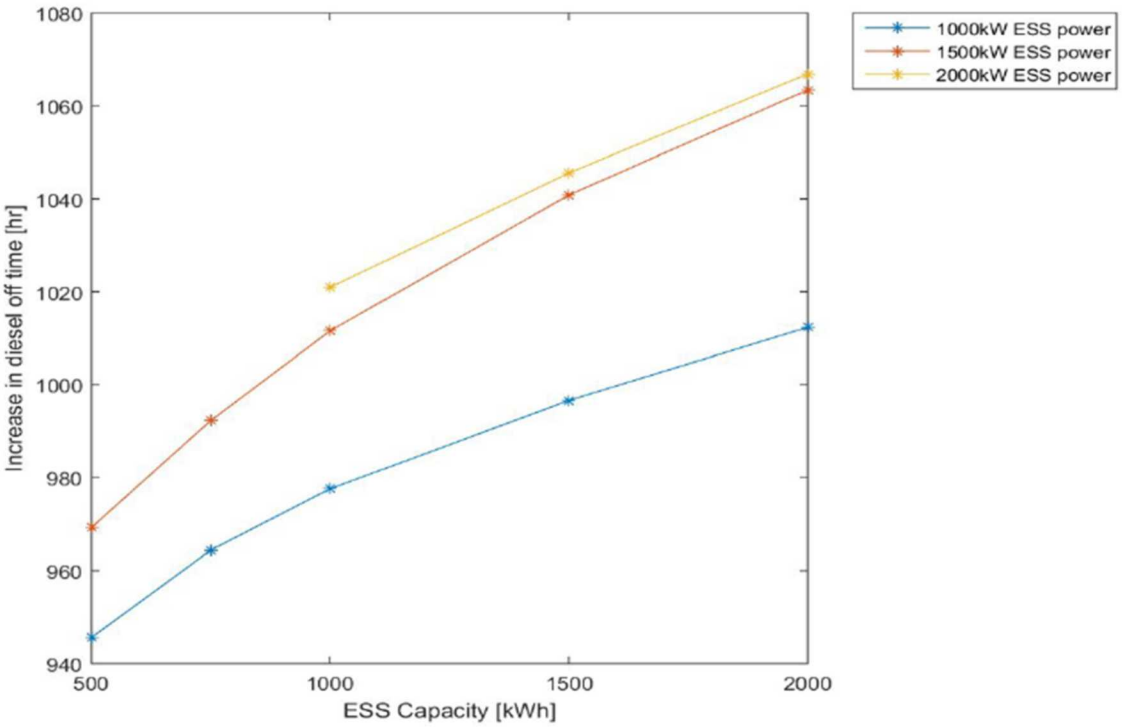

Figure 136 - The increase in time spent in diesel off mode in 2011 for different ESS capacities and powers

Diesel Run Time

Figure 137 shows the run time for each diesel generator for different ESS capacities and powers. Figure 138 shows the total diesel run time and Figure 139 show the decrease in diesel run time. Increasing the ESS capacity reduces diesel run time. Changes in diesel-off time are not directly related to changes in diesel run time, since multiple generators can be running online for different lengths of time.

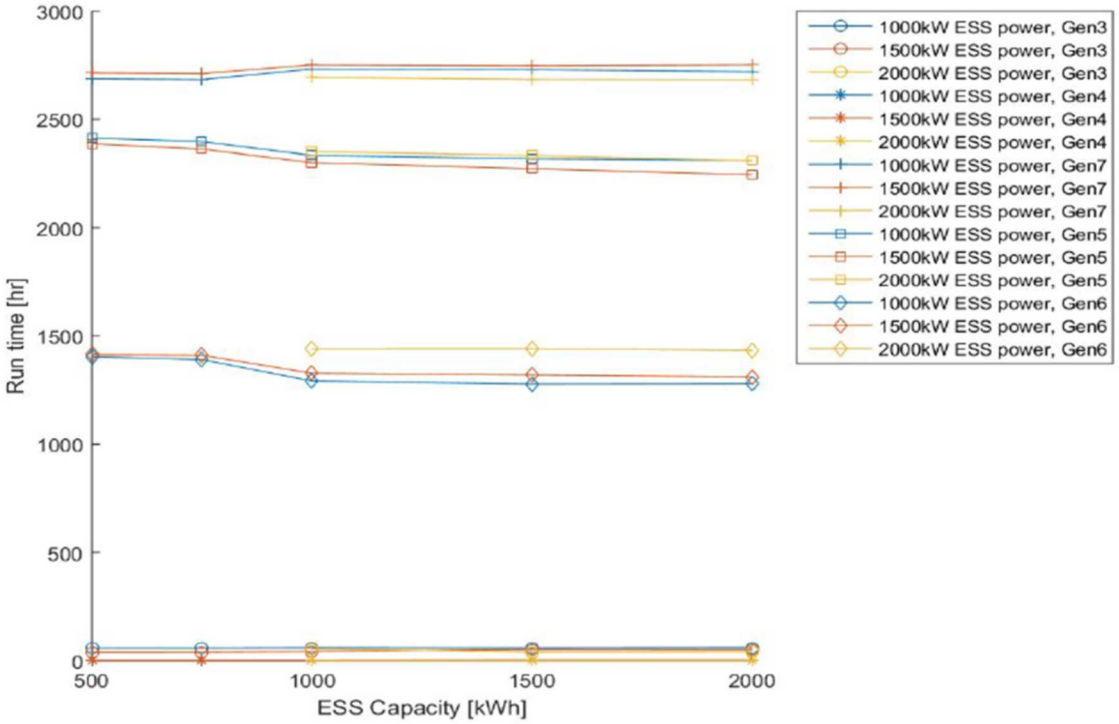

Figure 137 - The run time for each diesel generator for different ESS capacities and powers

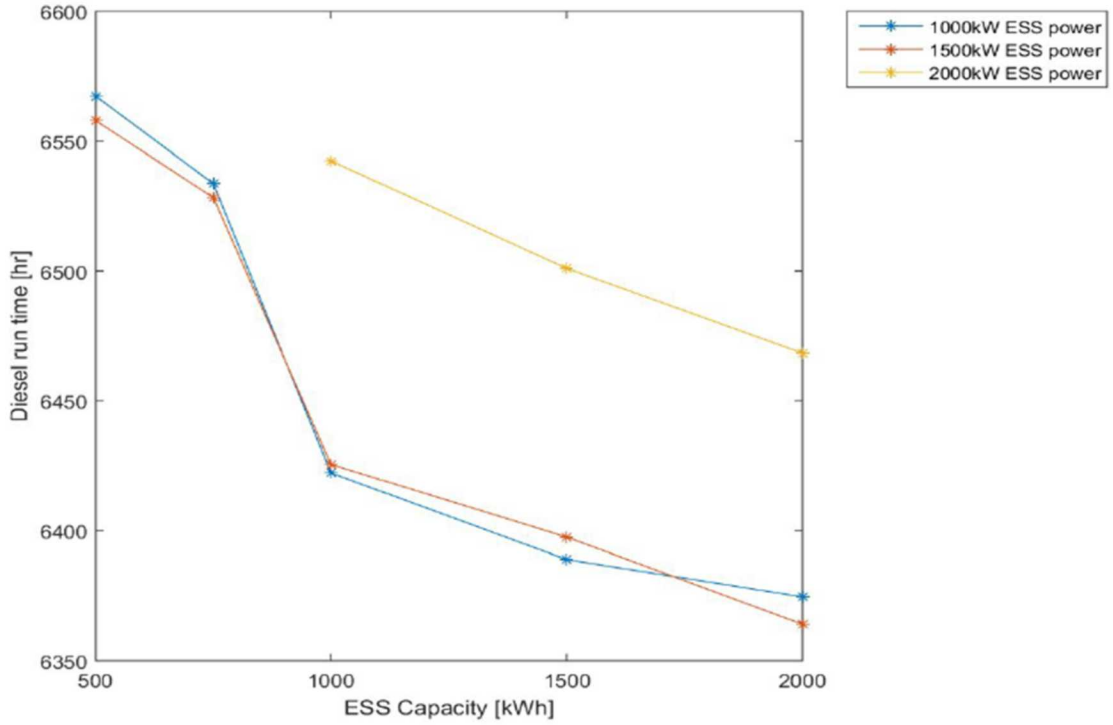

Figure 138 - The total diesel run time for different ESS capacities and powers

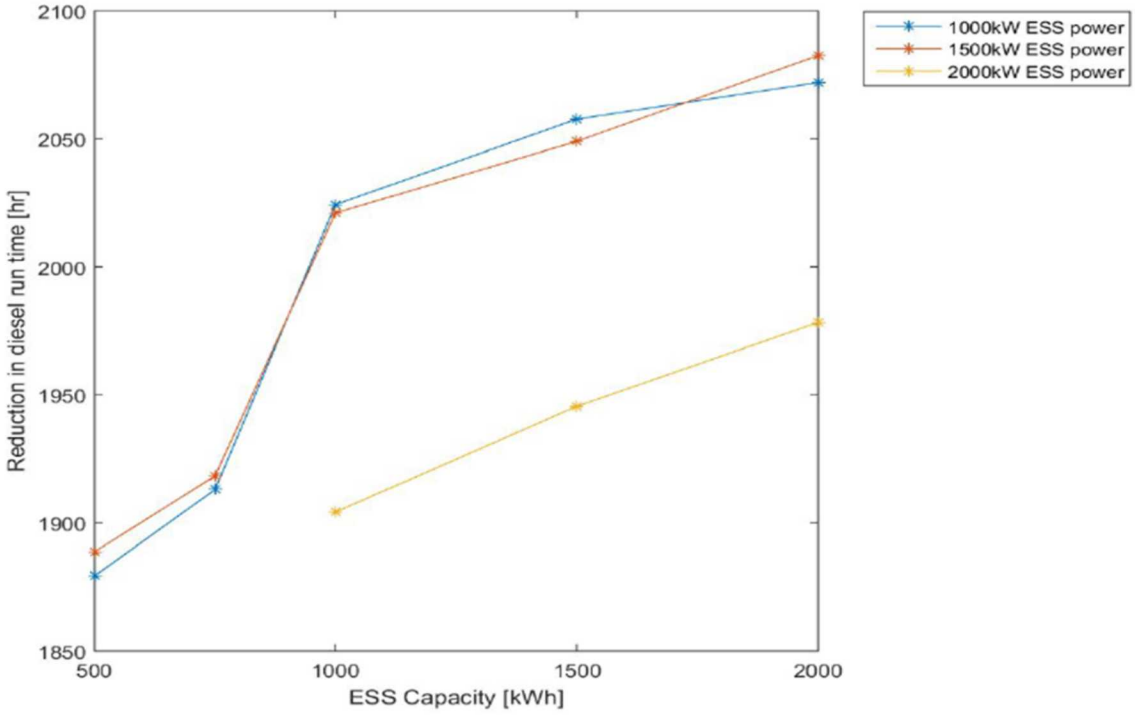

Figure 139 - The reduction in diesel run time for different ESS capacities and powers

Diesel Capacity Factor

Figure 140 and Figure 141 show the diesel capacity factor for each diesel generator and the total diesel capacity factor for different ESS capacities and powers. A higher ESS capacity and power resulted in a higher diesel capacity factor. These simulations show a marginal increase in diesel capacity factor from the measured value for 2011 or 61%.

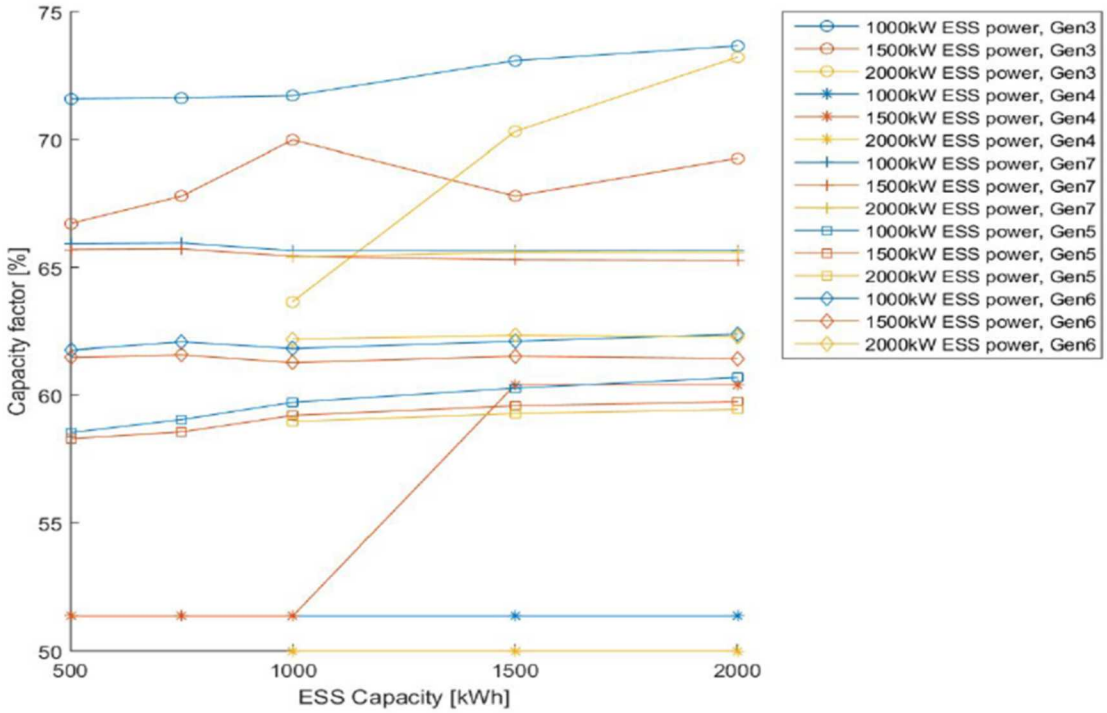

Figure 140 - Capacity factor for each diesel generator for different ESS capacities and powers

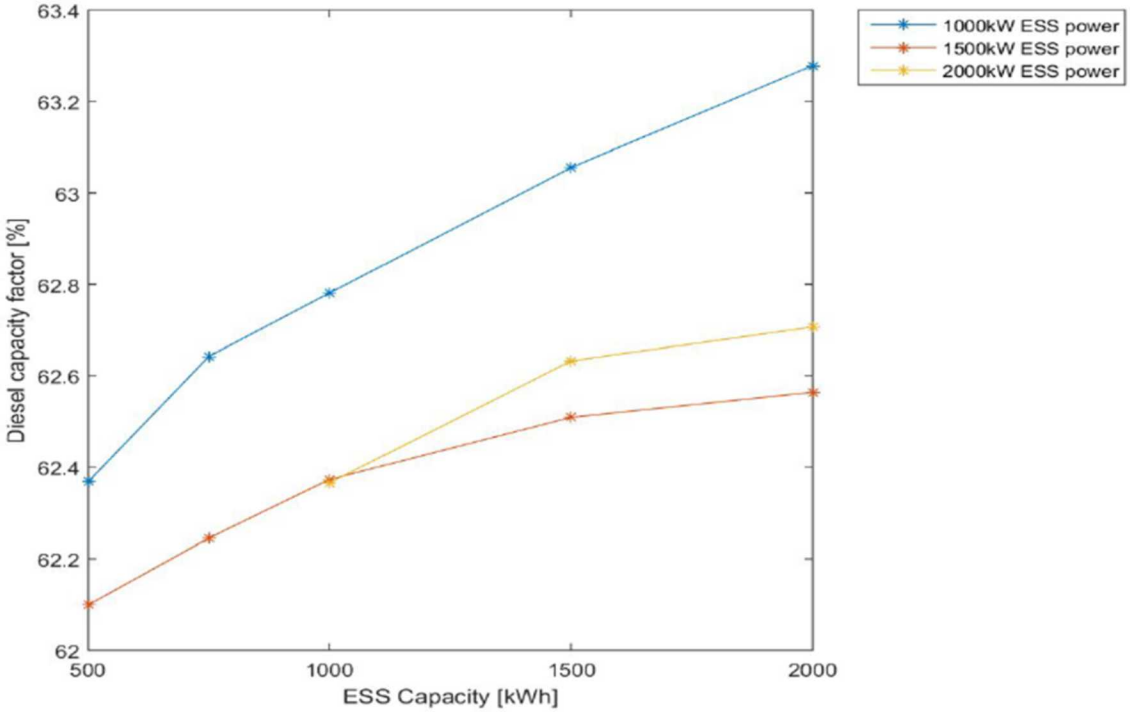

Figure 141 - Overall diesel capacity factor for different ESS capacities and powers

Diesel switching

Figure 142 and Figure 143 show the number of times each diesel generator and all diesel generators are switched online for different ESS capacities and powers. They show a decrease in diesel switching compared to the measured value of 1001 times for 2011.

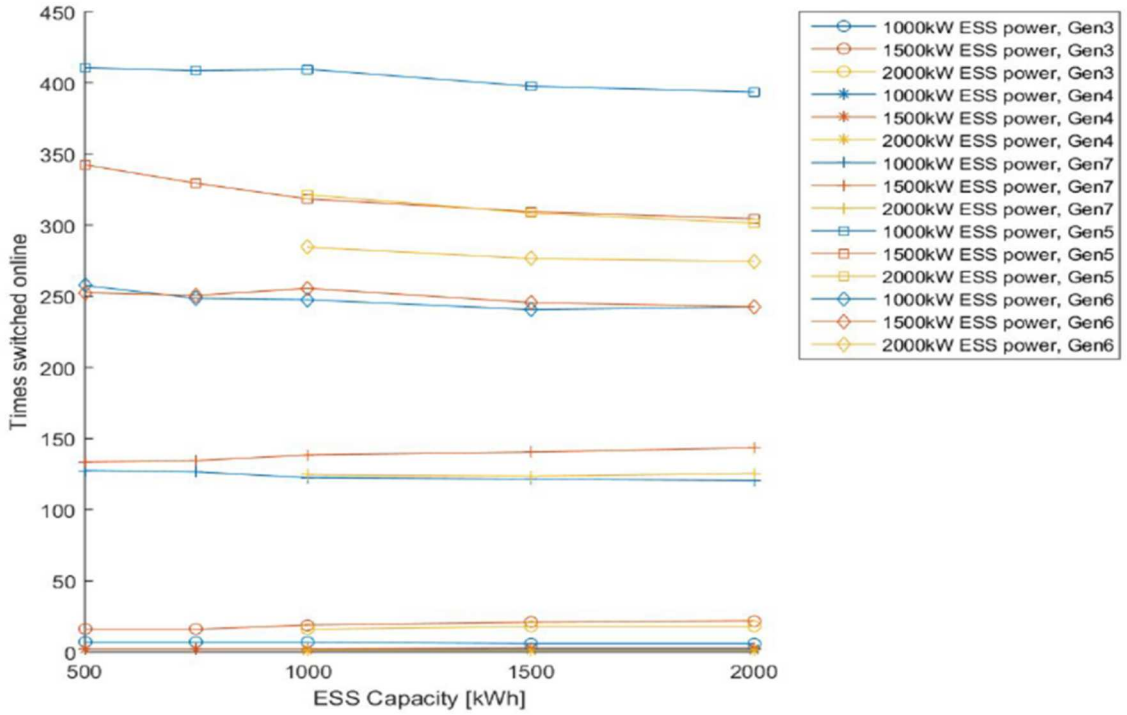

Figure 142 - The number of times each diesel generators is switched online for different ESS capacities and powers

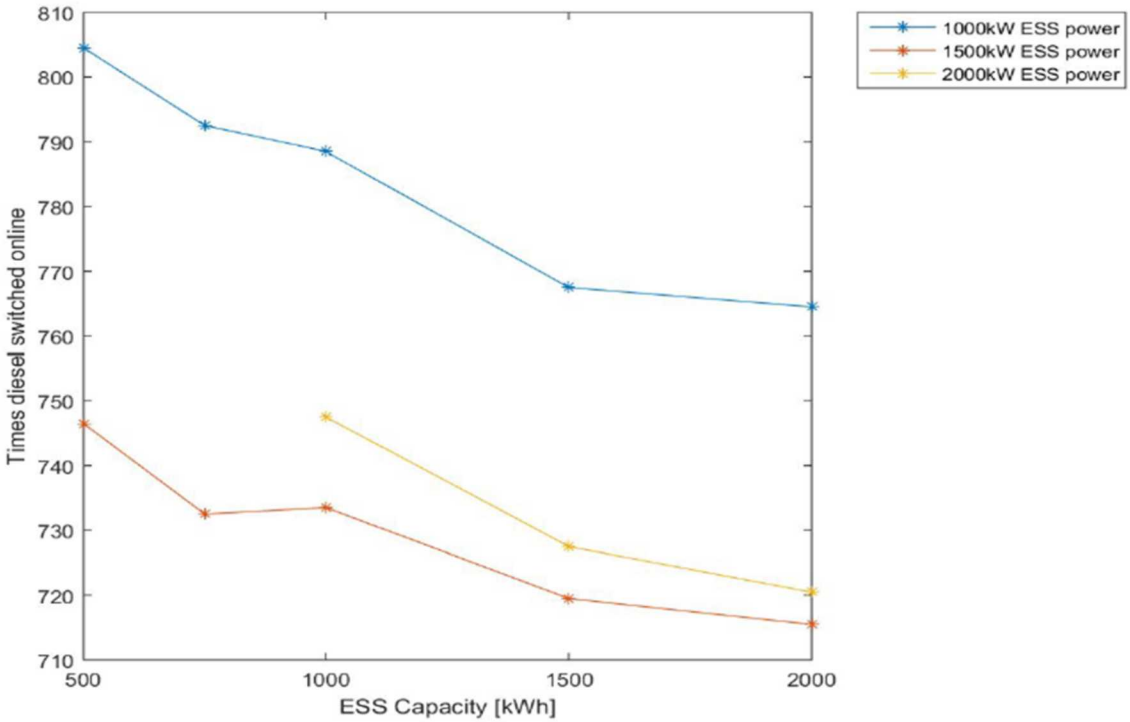

Figure 143 - The total number of times diesel generators are switched online for different ESS capacities and powers

Diesel Ramp Rate

Figure 144 shows the probability distribution of diesel ramp rates for different ESS capacities and powers. There is not much different between the different ESS capacities and powers. They have a mean value of 3.13 kW/s for 2011.

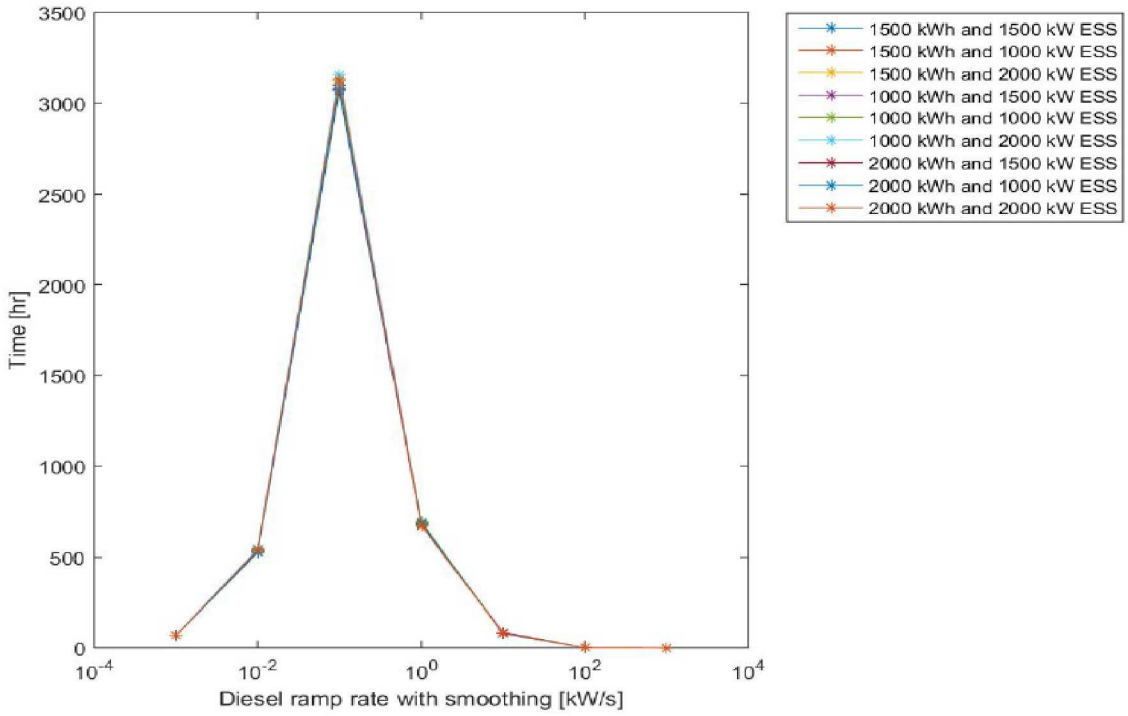

Figure 144 - Probability distribution of the ramp rates on the diesel generators for different ESS capacities and powers

ESS Equivalent Cycles

Figure 145 shows the number of equivalent full ESS cycles. Multiple ESS cycles that add up to the full ESS capacity are considered to be one equivalent ESS cycle. Cycles range from 125 – 440 cycles per year.

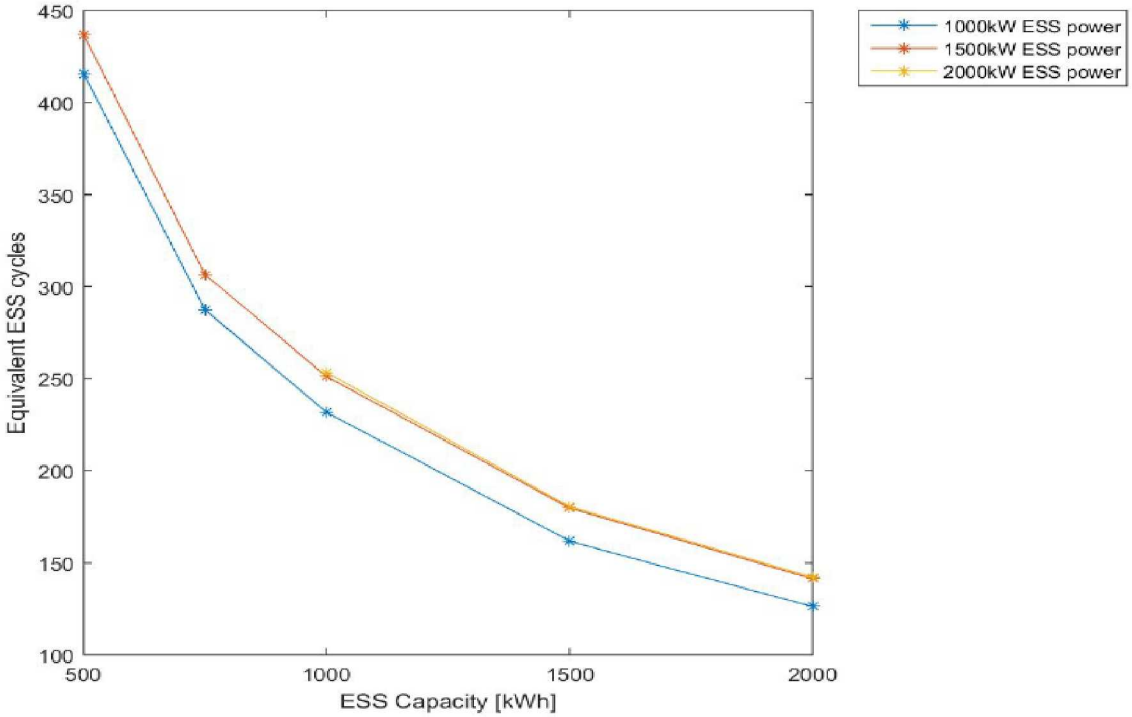

Figure 145 - Number of equivalent full ESS cycles for different ESS capacities and powers

Number of ESS Cycles

Rainflow counting was used to calculate the number of ESS cycles of varying amplitude experienced by the ESS. Figure 146 shows the number of ESS cycles for each cycle amplitude for different ESS capacities and powers. The number of cycles decrease with increasing amplitude. Smoothing the load on the diesel and hydro generators results in more low amplitude cycles which contributes to increased equivalent full ESS cycles.

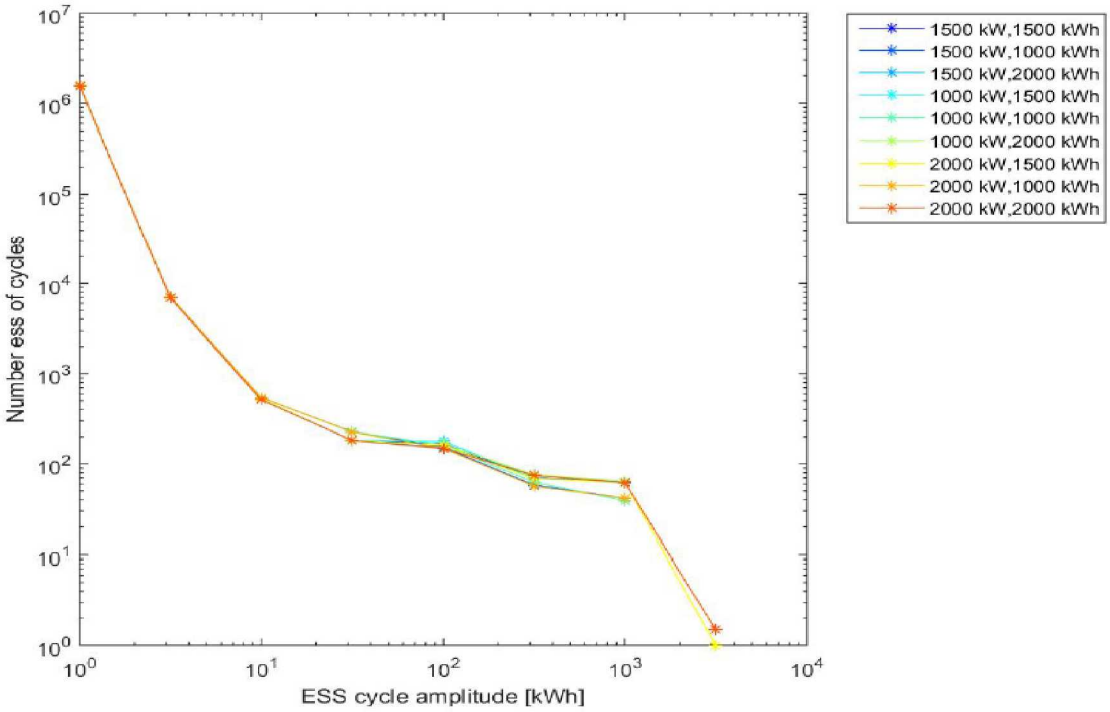

Figure 146 - Number of ESS cycles at different cycle amplitudes for different ESS capacities and powers.

Power levels

Figure 147 shows the time the ESS spends charging or discharging at different power levels.

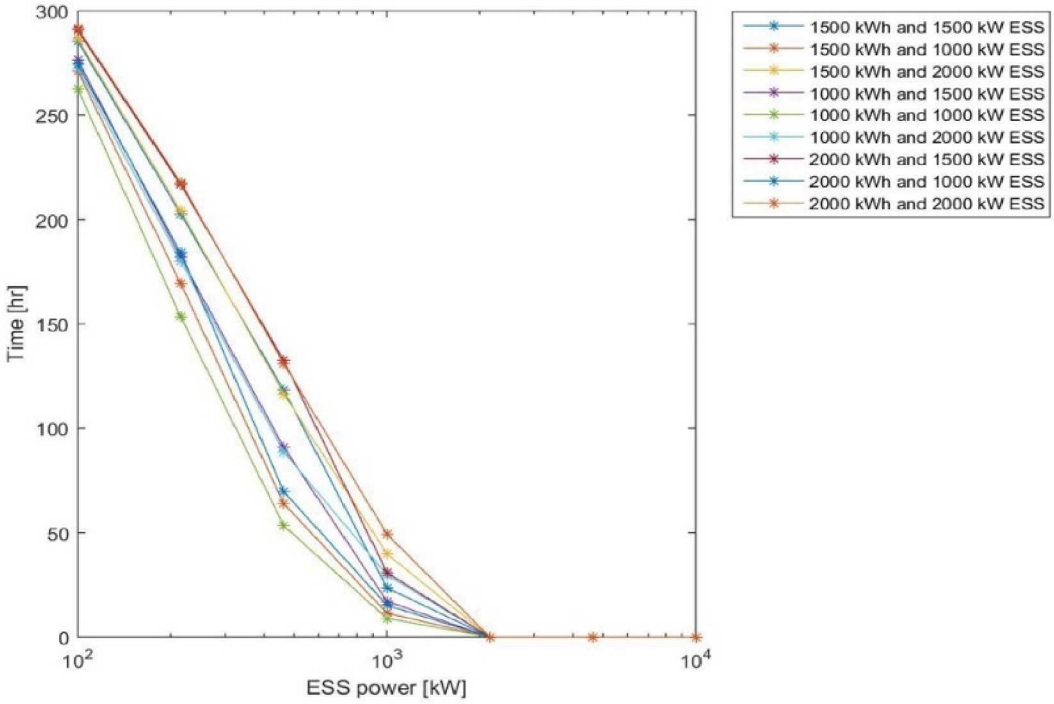

Figure 147 - The time the ESS spends charging or discharging at different power levels.

ESS Ramp Rate

Figure 148 shows the probability distribution of ESS ramp rates for different ESS capacities and powers. The mean ramp rate is 12 kW/sec, which is the same as the mean ramp rate of the load.

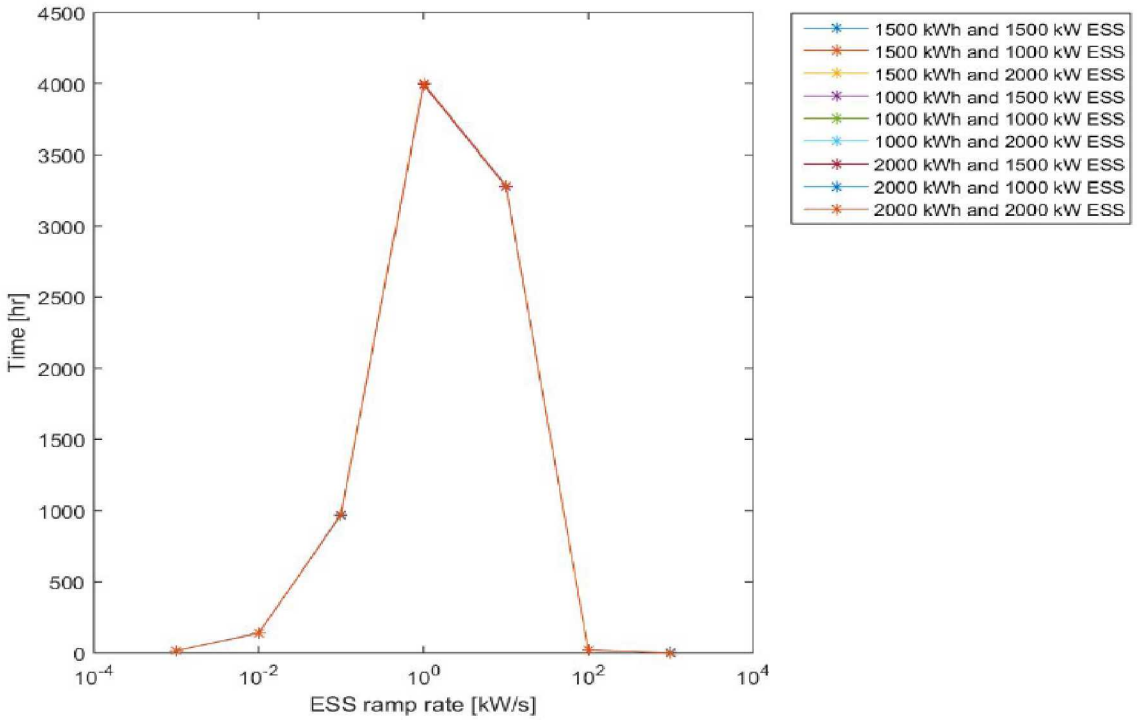

Figure 148 - Probability distribution of ESS ramp rates for different ESS capacities and powers

ESS Throughput

Figure 149 shows the total ESS throughput for different ESS capacities and powers. With increasing capacity and power, throughput increases.

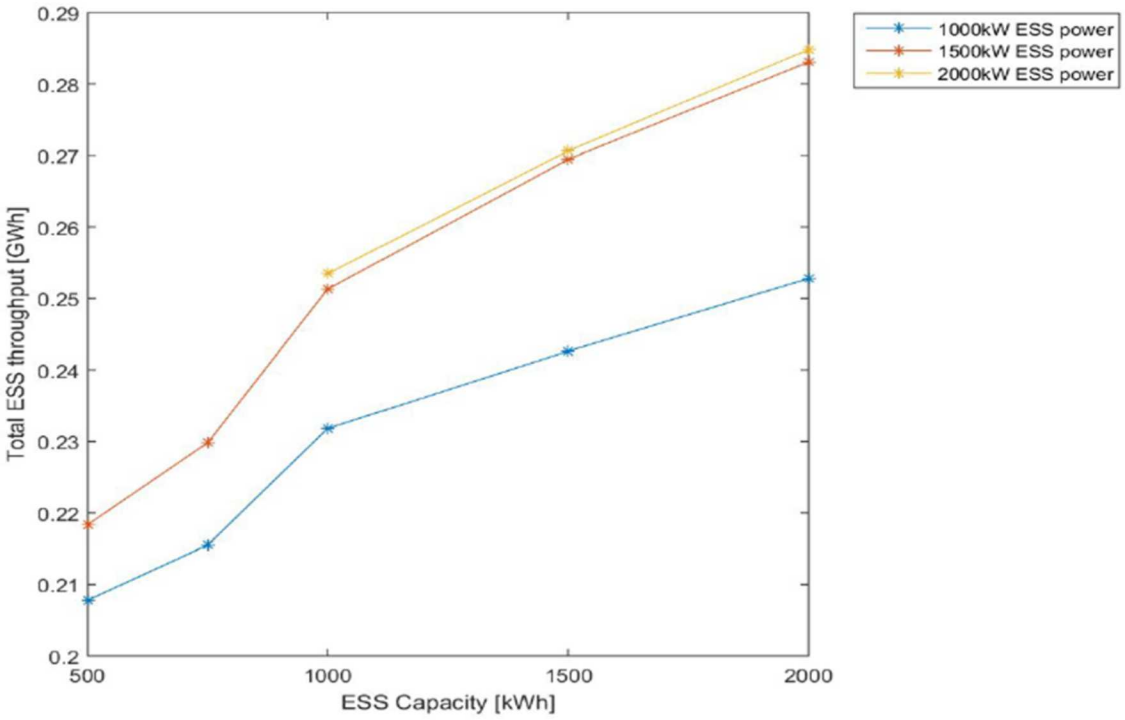

Figure 149 - ESS throughput for different and powers

ESS Contribution to Diesel Reduction

Figure 150 shows the ESS direct contribution to diesel reduction for different ESS capacities and powers. It is calculated as the total reduction in diesel output that did not go through the ESS. In other words, the ESS enabled the reduction of diesel without actually having to charge and discharge.

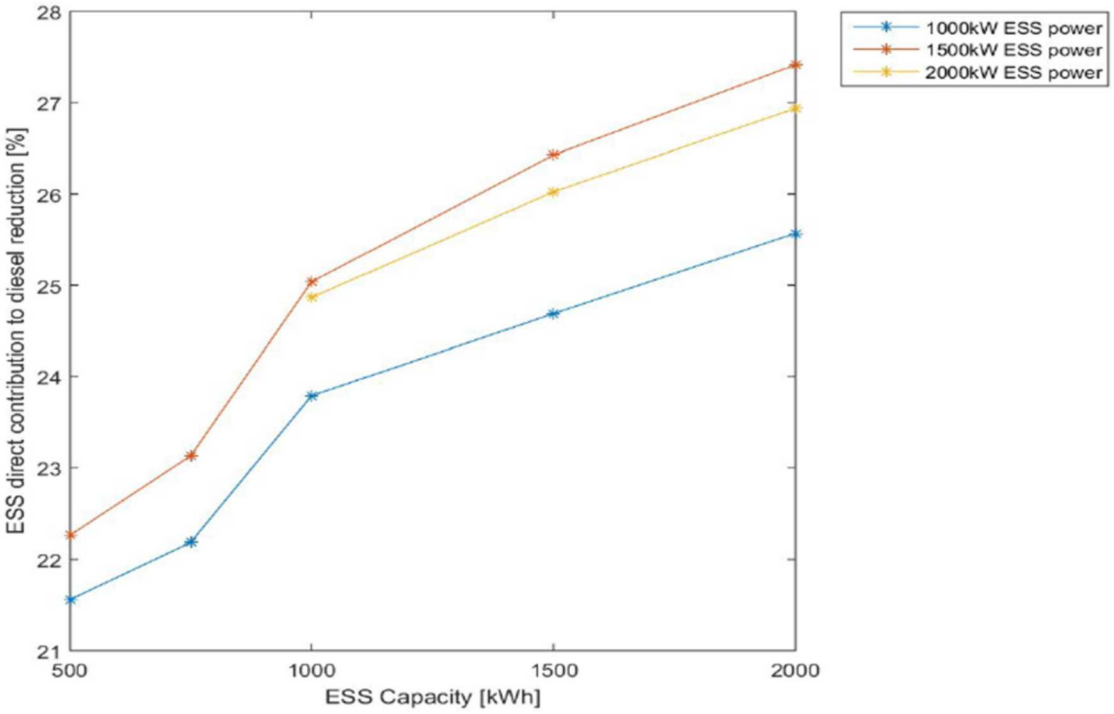

Figure 150 - The ESS direct contribution to diesel reduction for different ESS capacities and powers

ESS Charging from Diesel

Figure 151 shows the percent of total ESS charging that was from diesel generators.

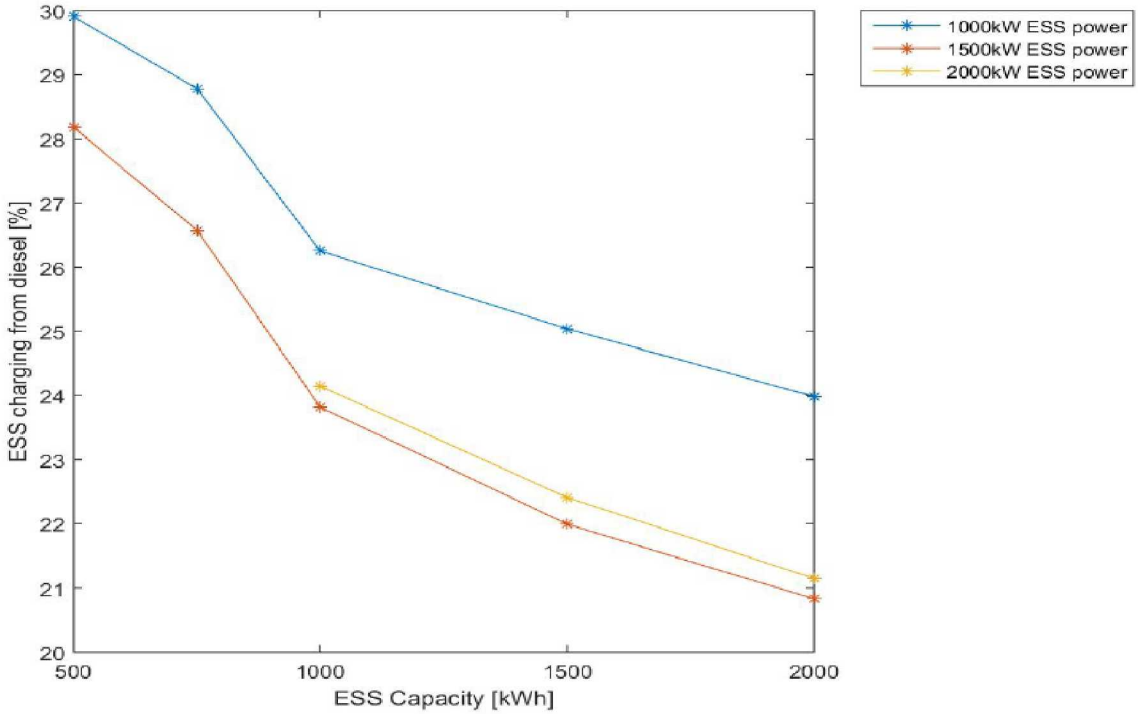

Figure 151 - Percent of total ESS charging that was from diesel generators for different ESS capacities and powers

2011: Simulation with No Smoothing and No Diesel Charging

Diesel Output

Figure 152 shows the diesel output for each generator in each of the simulation. Generators Gen7, Gen5 and Gen6 are the most commonly used. Figure 153 show the total diesel output for each simulation and Figure 154 shows the reduction in diesel output. As the ESS capacity and power increases the diesel output reduces.

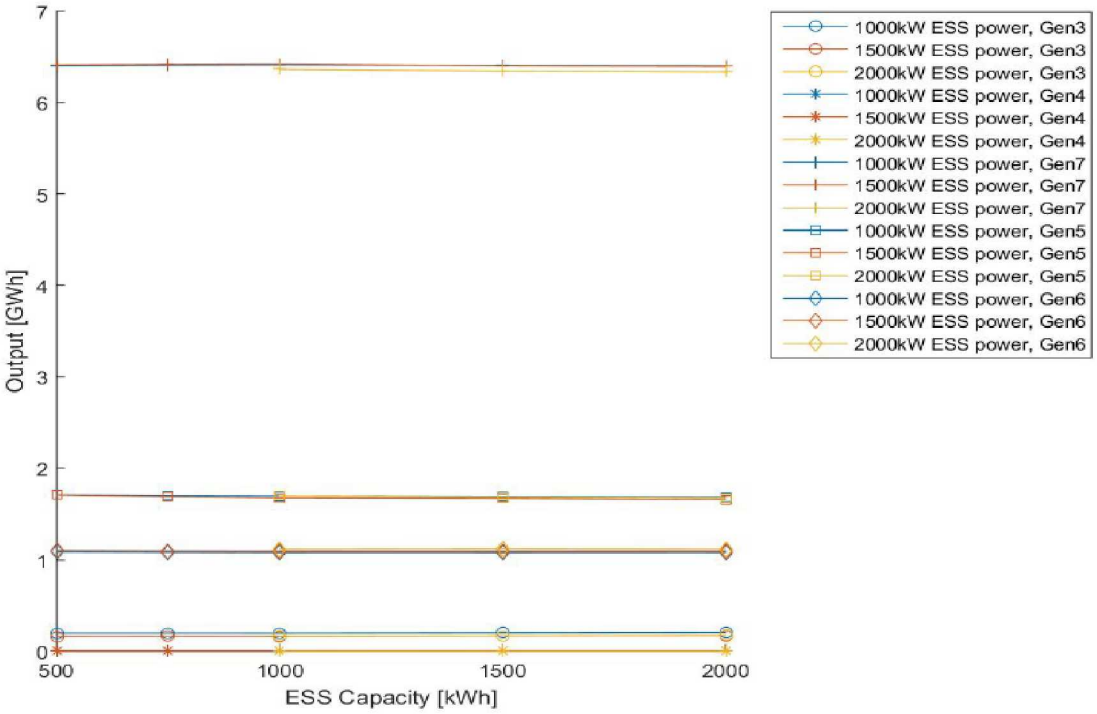

Figure 152 - The output of each diesel generator for different ESS capacities and powers

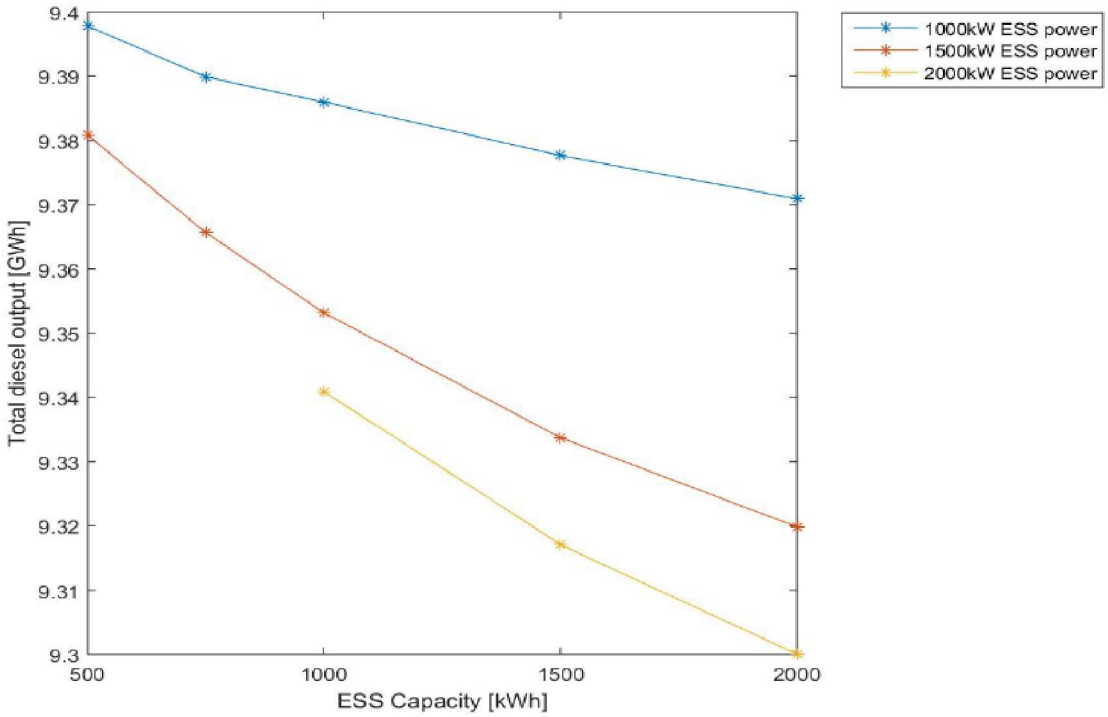

Figure 153 - The total diesel output for different ESS capacities and powers

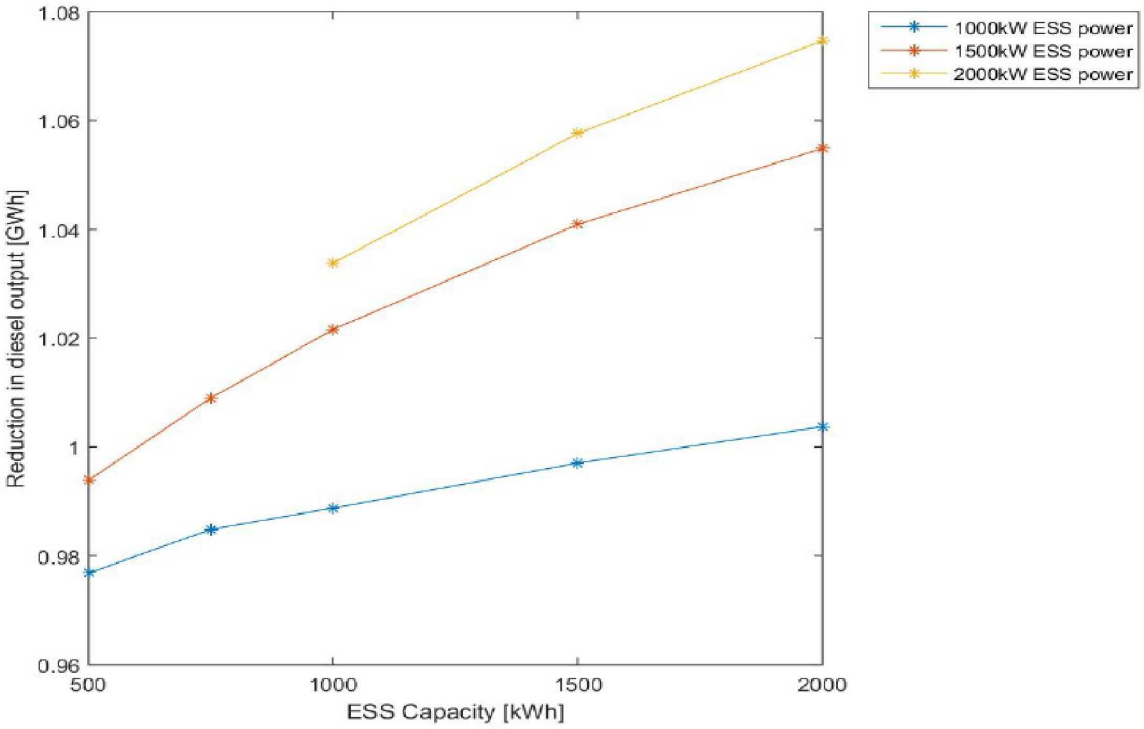

Figure 154 - Reduction in total diesel output for different ESS capacities and powers

Diesel Consumption

Figure 155 shows the diesel consumption for each generator in each simulation. Figure 156 and Figure 157 show the total consumption and reduction in total consumption. Increasing ESS capacity and power reduces diesel consumption. The reduction in consumption is a result of the reduction in diesel output as well as running the diesel generators at a higher and more efficiency loading.

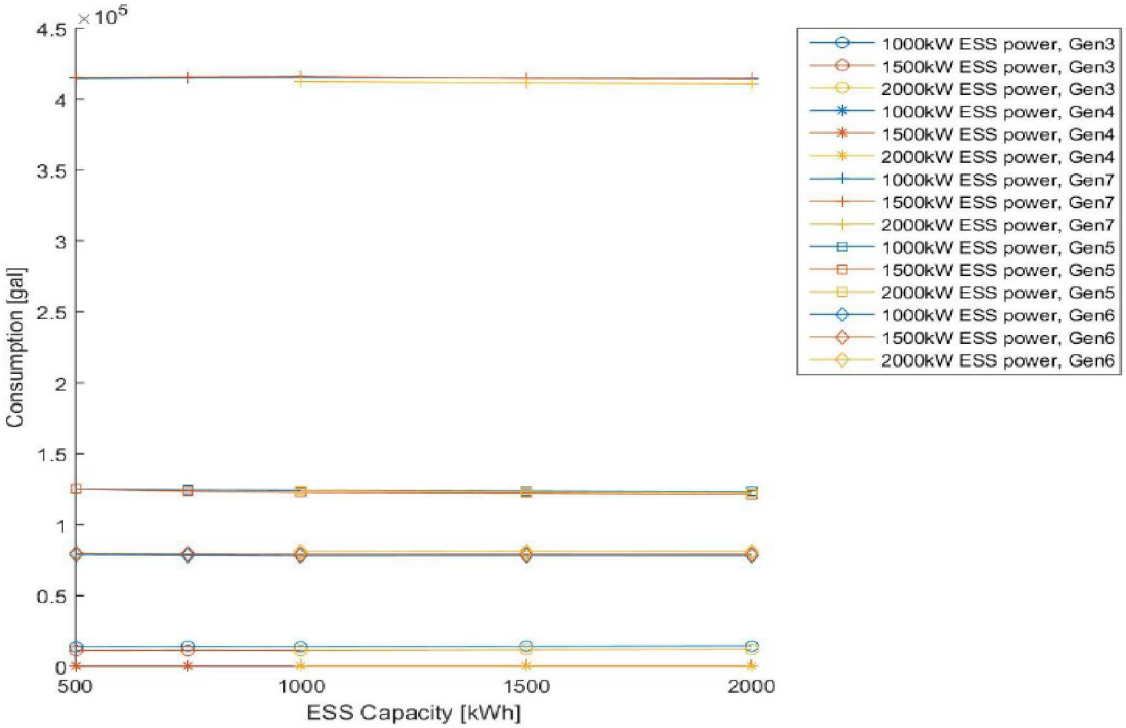

Figure 155 - Diesel consumption of each diesel generator for different ESS capacities and powers

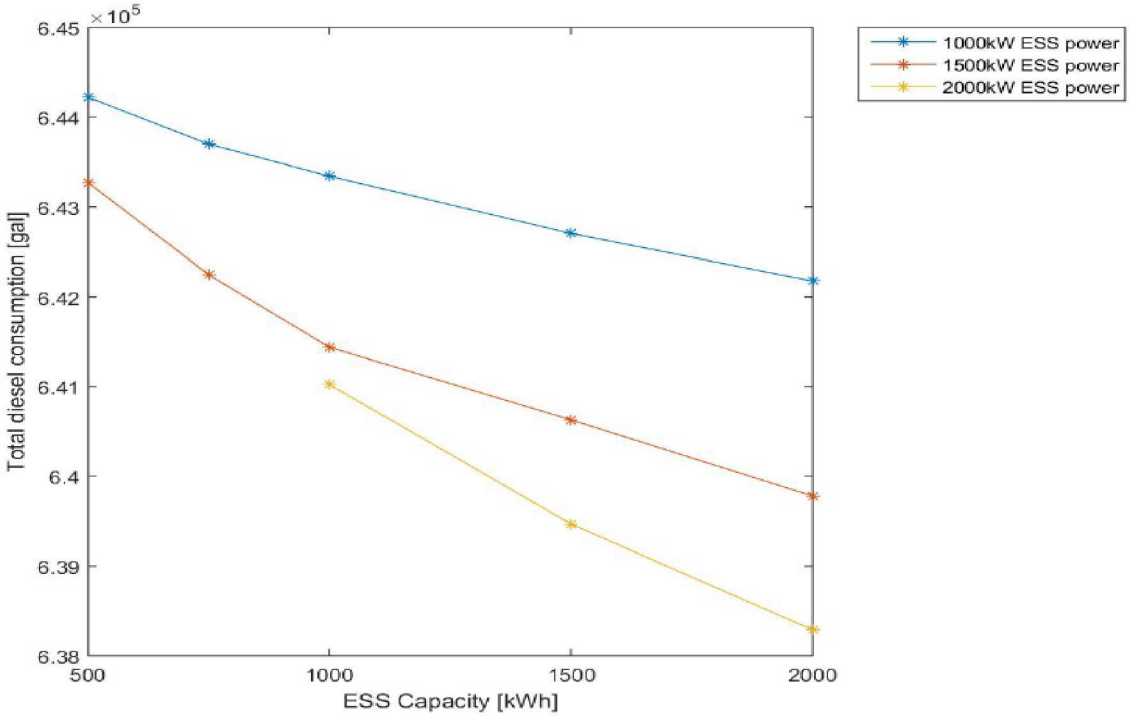

Figure 156 - Total diesel consumption for different ESS capacities and powers

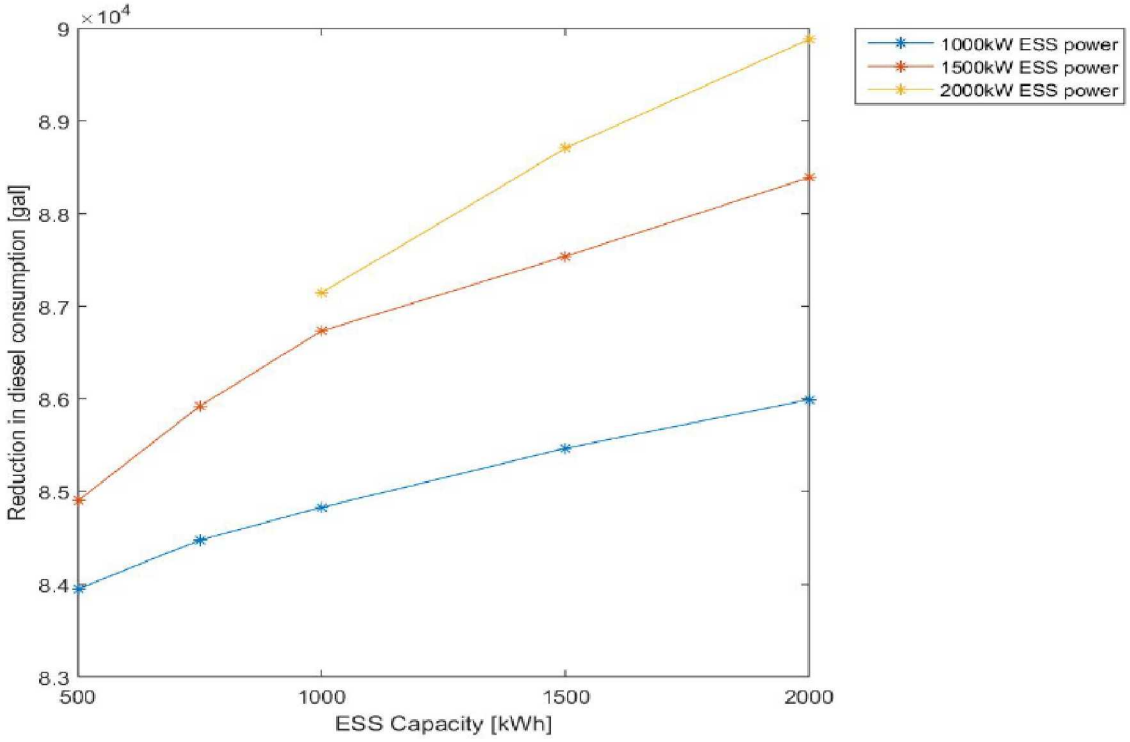

Figure 157 - Reduction in diesel consumption for different ESS capacities and powers

Diesel Off Time

Figure 158 shows the time spent in diesel off in 2011. Figure 159 shows the increase in time spent in diesel off. Increasing ESS capacity and power increases the time spent in diesel off.

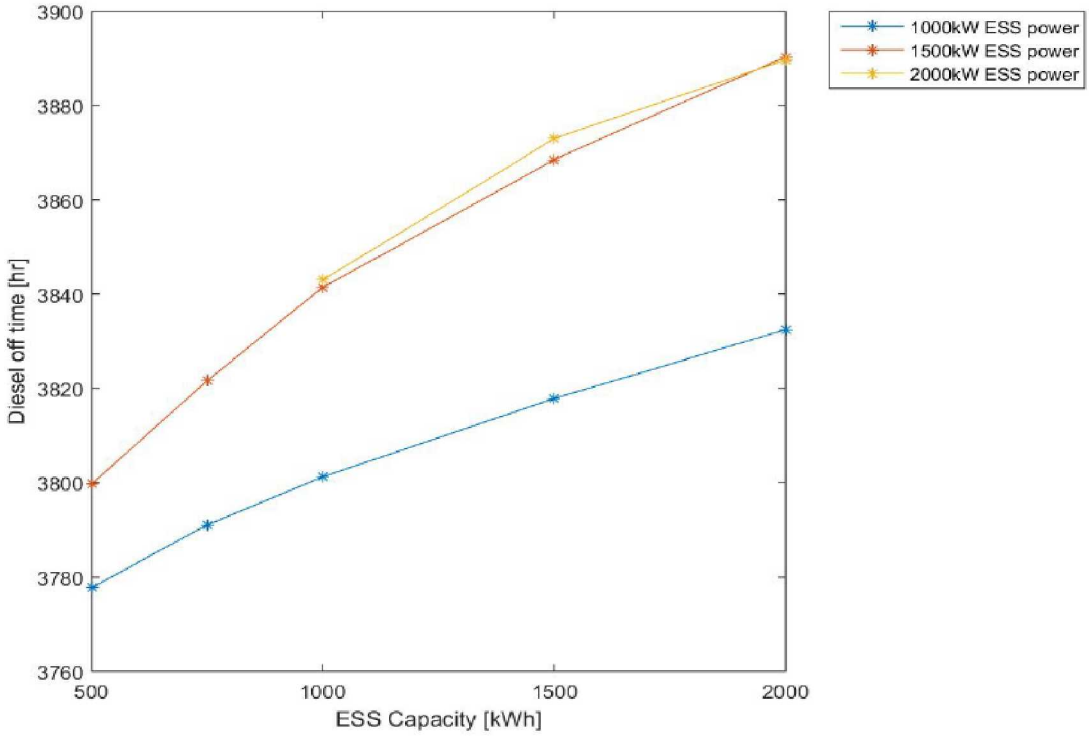

Figure 158 - Time spent in diesel off mode in 2011 for different ESS capacities and powers

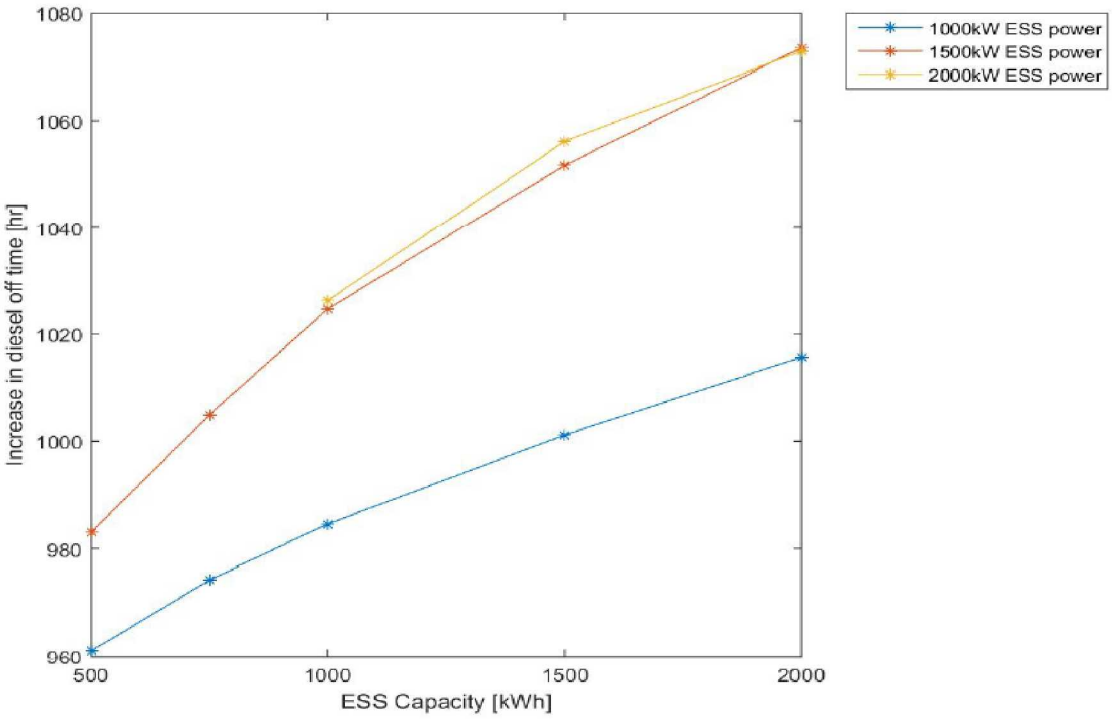

Figure 159 - Increase in time spent in diesel-off mode in 2011 for different ESS capacities and powers

Diesel Run Time

Figure 160 shows the run time for each diesel generator for different ESS capacities and powers. Figure 161 shows the total diesel run time and Figure 162 shows the decrease in diesel run time. Increasing the ESS capacity reduces diesel run time. Changes in diesel-off time are not directly related to changes in diesel run time, since multiple generators can be running online for different lengths of time.

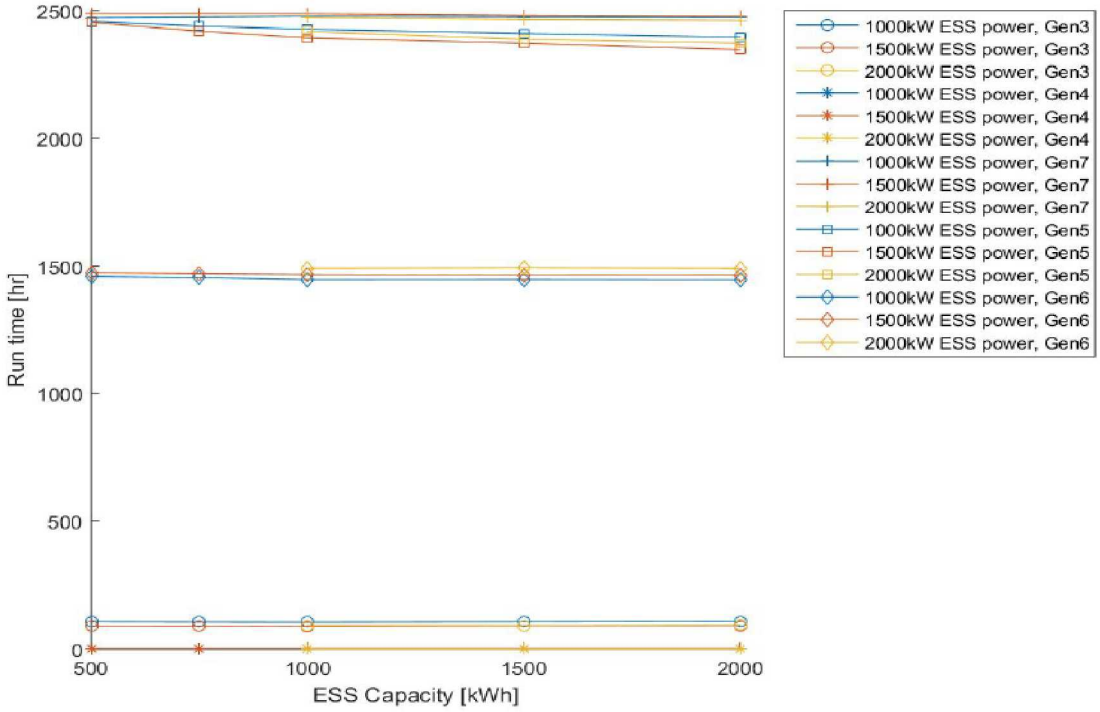

Figure 160 - Run time for each diesel generator for different ESS capacities and powers

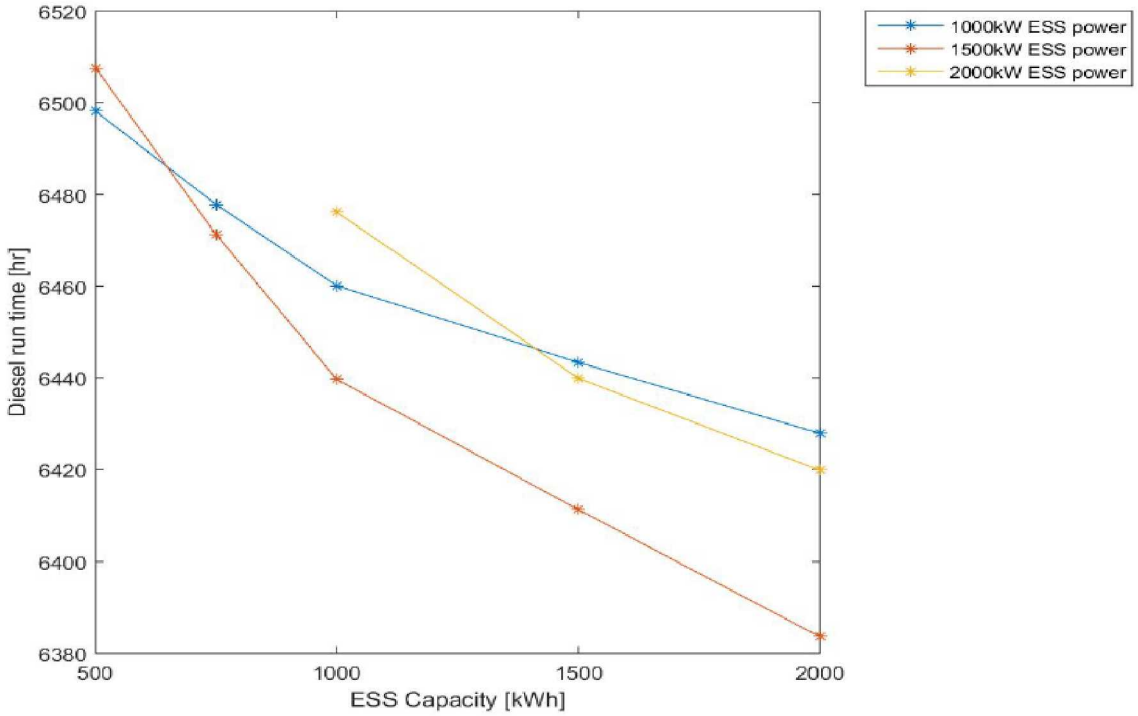

Figure 161 - Total diesel run time for different ESS capacities and powers

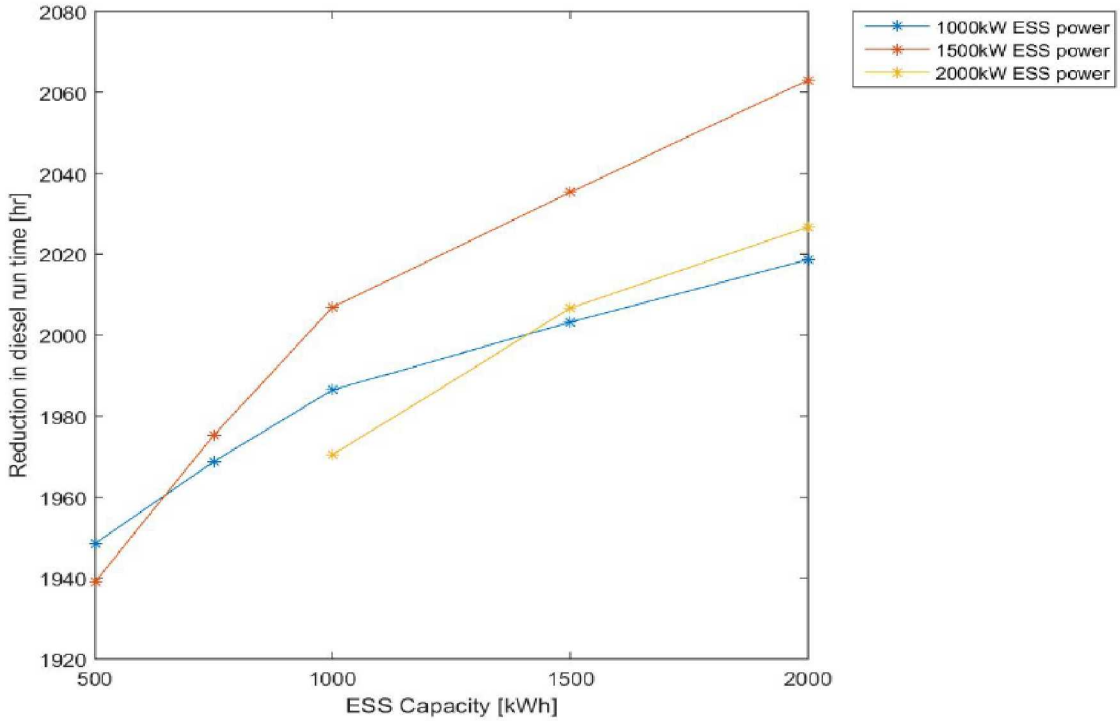

Figure 162 - Reduction in diesel run time for different ESS capacities and powers

Diesel Capacity Factor

Figure 163and Figure 164 show the diesel capacity factor for each diesel generator and the total diesel capacity factor for different ESS capacities and powers. A higher ESS capacity and power resulted in a higher diesel capacity factor. These simulations show a marginal increase in diesel capacity factor from the measured value for 2011 or 61%.

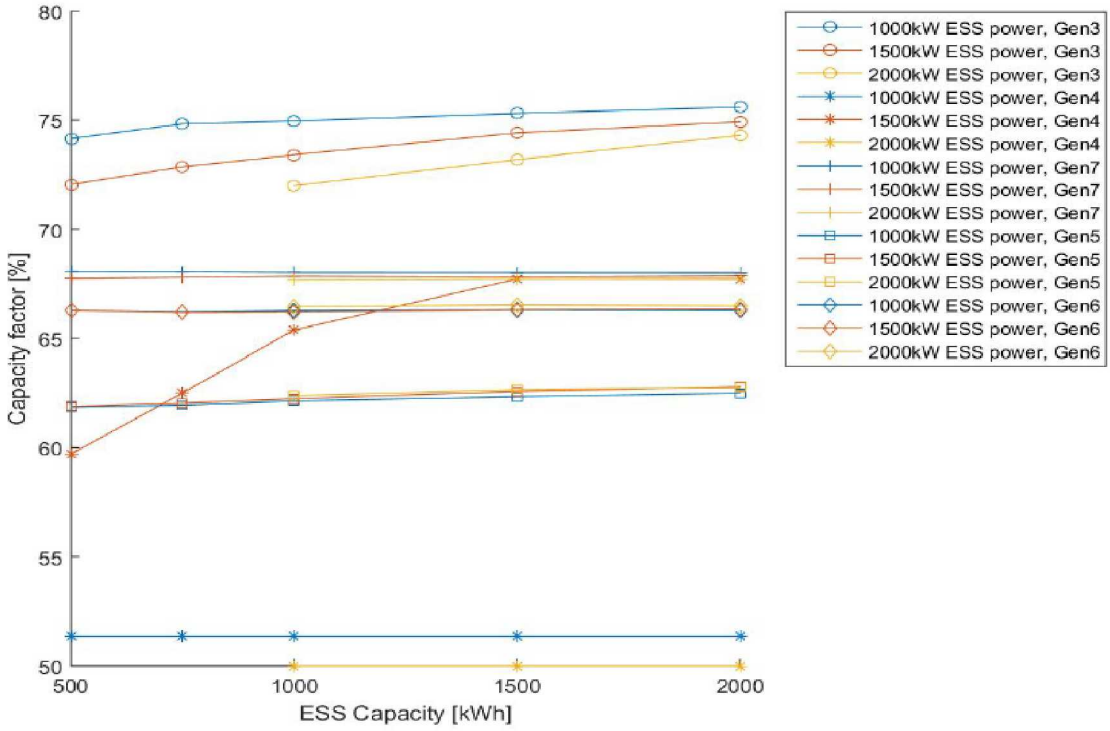

Figure 163 - Capacity factor for each diesel generator for different ESS capacities and powers

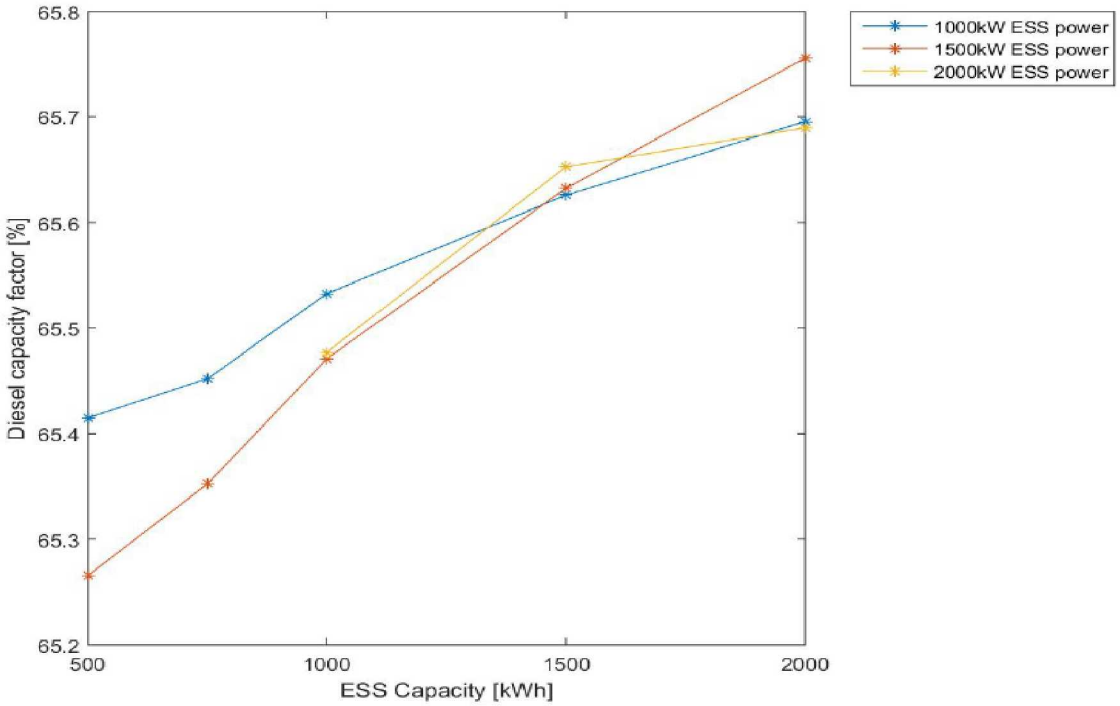

Figure 164 - Overall diesel capacity factor for different ESS capacities and powers

Diesel Switching

Figure 165 and Figure 166 show the number of times each diesel generator and all diesel generators are switched online for different ESS capacities and powers. As seen in the graphs, a decrease in diesel switching compared to the measured value of 1001 times for 2011.

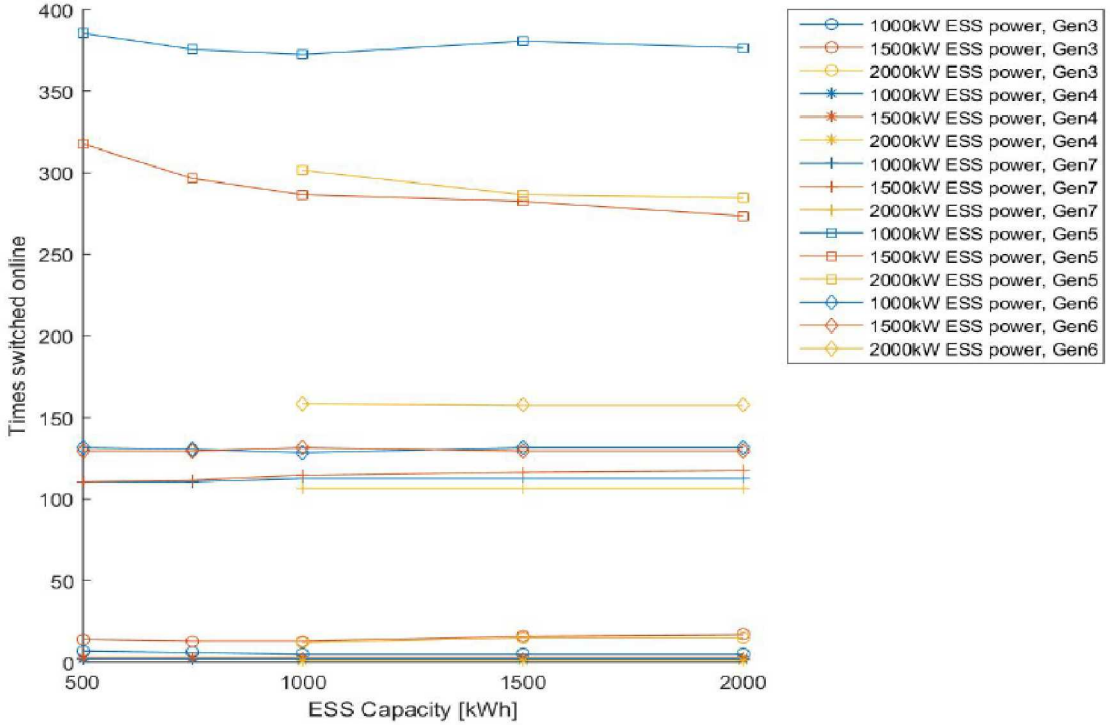

Figure 165 - Number of times each diesel generator is switched online for different ESS capacities and powers

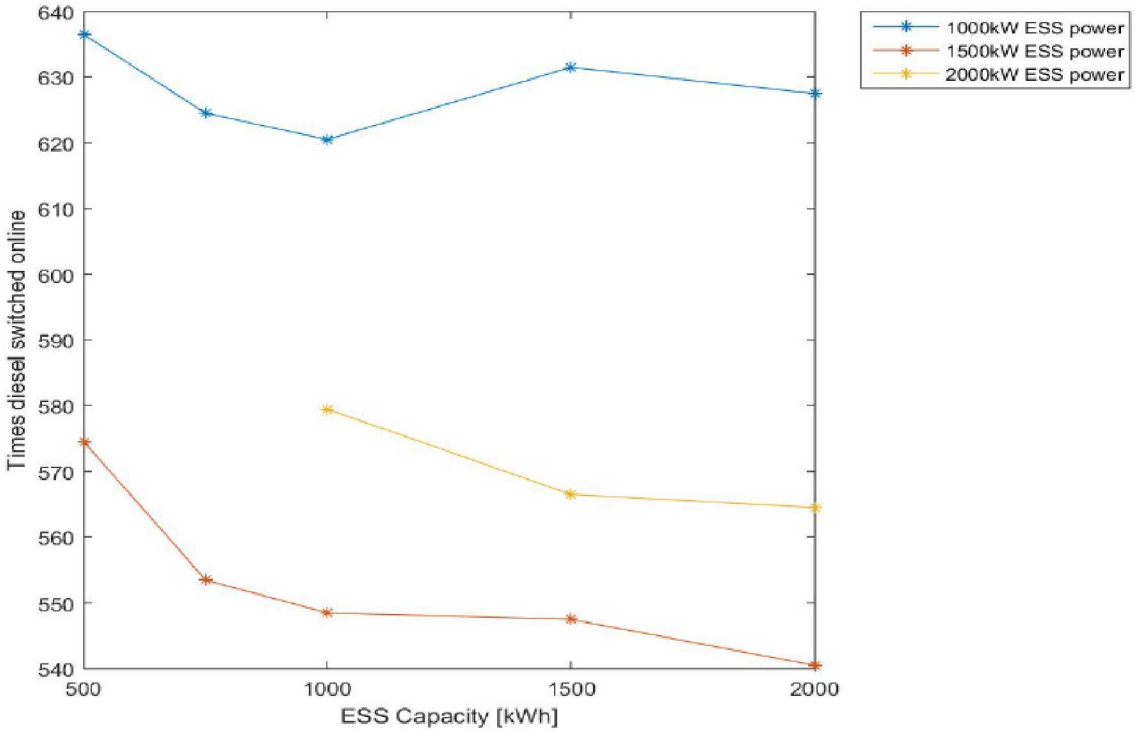

Figure 166 -Total number times diesel generators are switched online for different ESS capacities and powers

Diesel Ramp Rate

Figure 167 shows the probability distribution of diesel ramp rates for different ESS capacities and powers. There is not much difference between the different ESS capacities and powers. The combined ramp rates have a mean value of around 3.9 kW/s which is slightly higher than the average measured value of 3.13 kW/s for 2011.

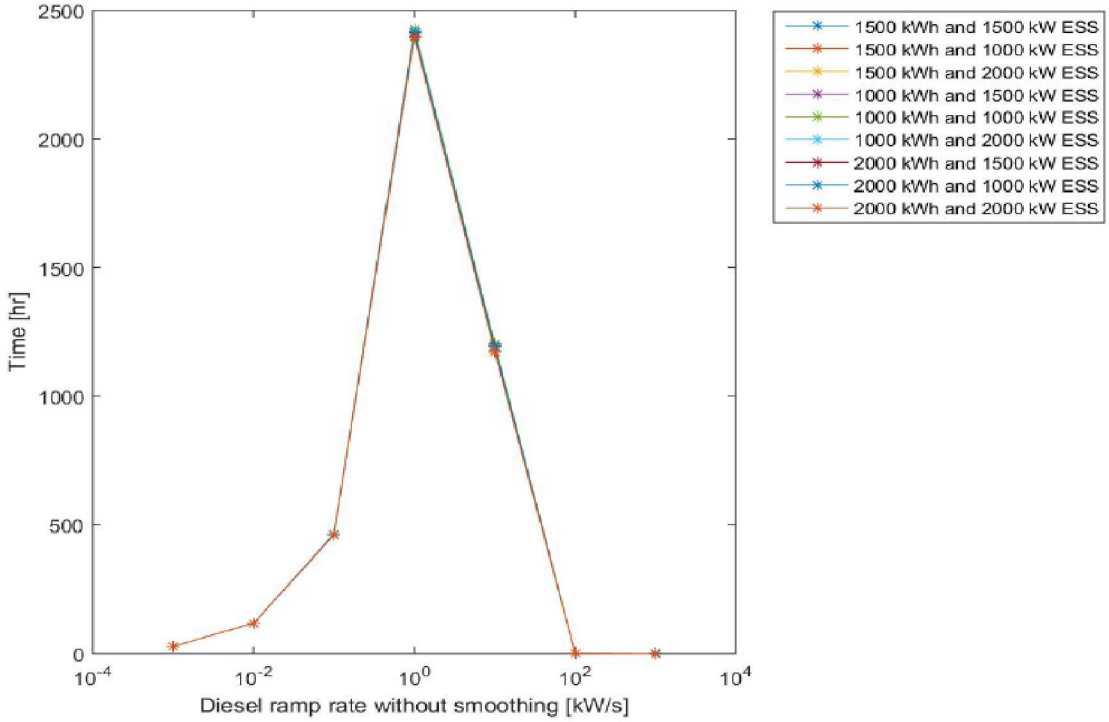

Figure 167 - Probability distribution of diesel ramp rates for different ESS capacities and powers

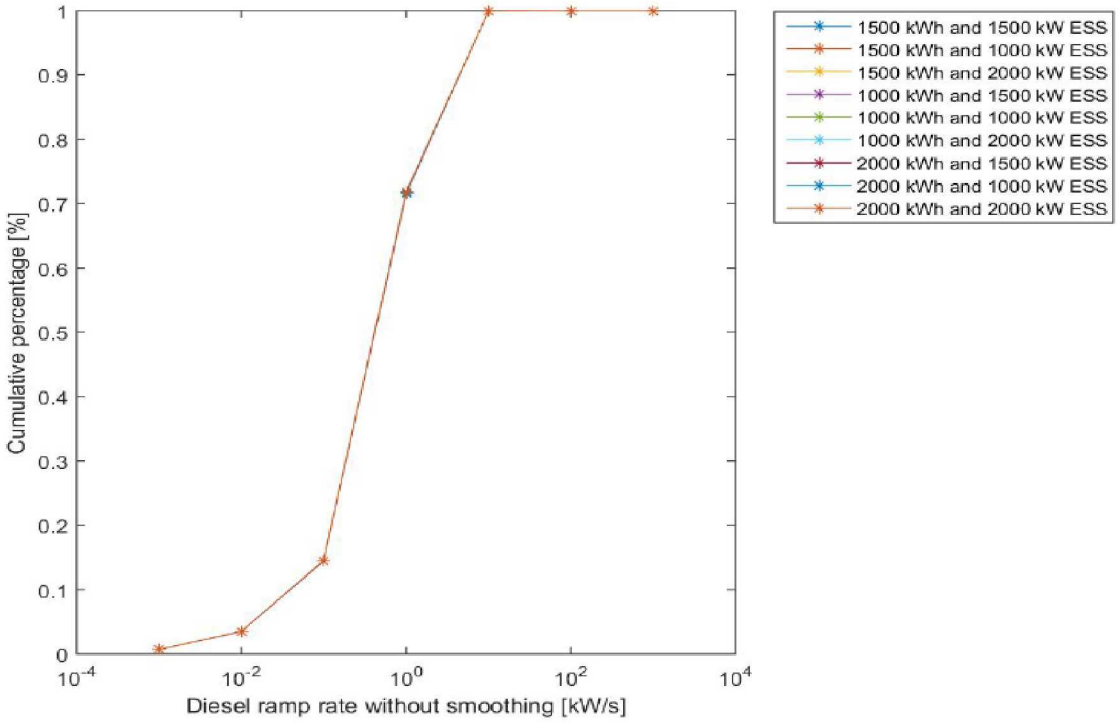

Figure 168 - Cumulative percentage of diesel ramp rate for different ESS capacities and powers

ESS Equivalent Cycles

Figure 169 shows the number of equivalent full ESS cycles. Multiple ESS cycles that add up to the full ESS capacity are considered to be on equivalent ESS cycle. These simulation have low ESS cycling which increases the life of most ESS technologies.

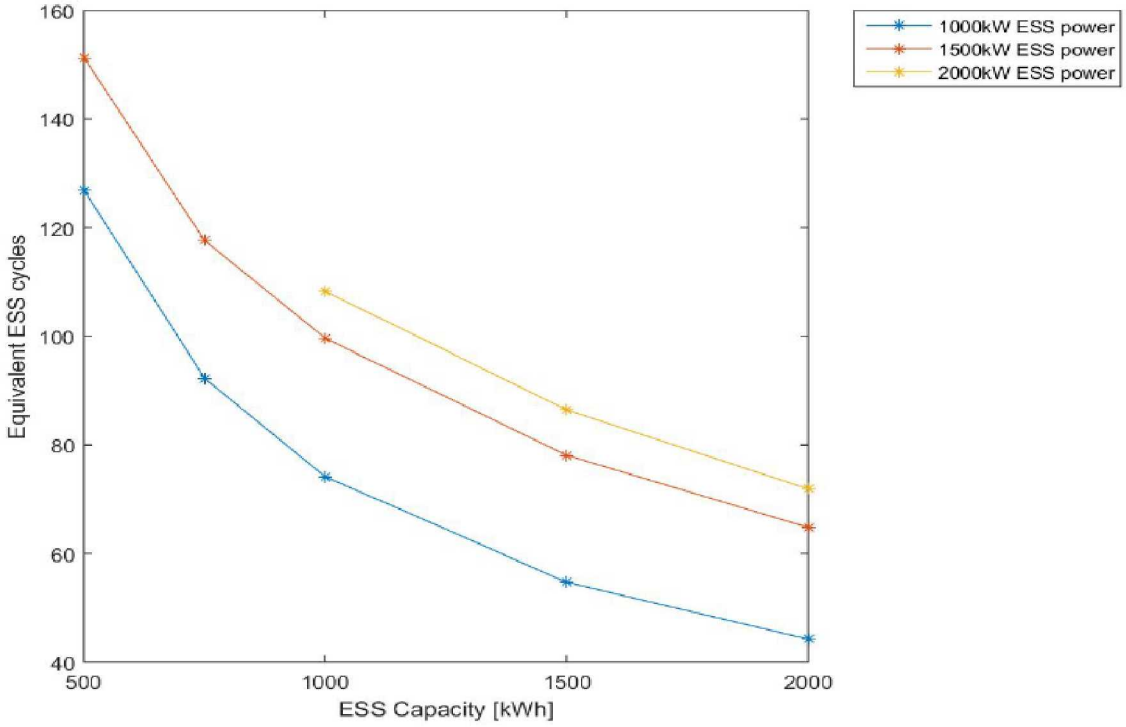

Figure 169 - Number of equivalent full ESS cycles for different ESS capacities and powers

Number of ESS Cycles

Rainflow counting was used to calculate the number of ESS cycles of varying amplitude experienced by the ESS. Figure 170 shows the number of ESS cycles for each cycle amplitude for different ESS capacities and powers. The number of cycles decreases with increasing amplitude.

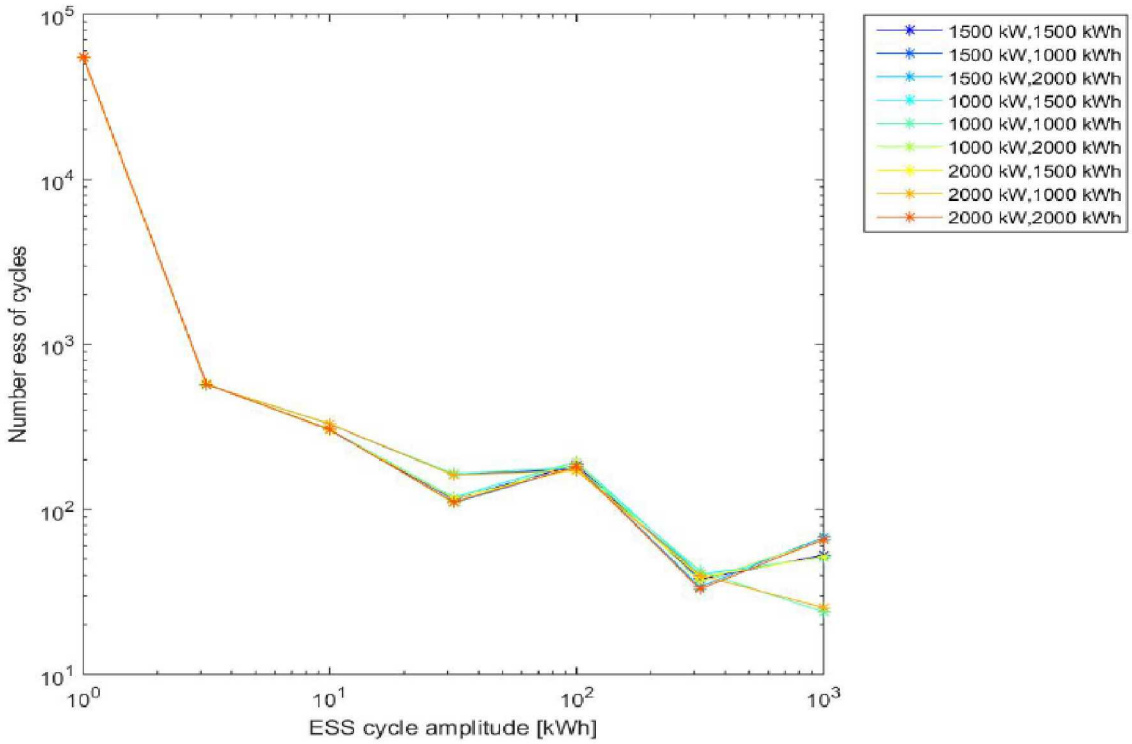

Figure 170 - Number of ESS cycles at different cycle amplitudes for different ESS capacities and powers.

ESS Power Levels

Figure 171 shows the time the ESS spends charging or discharging at different power levels. Since the ESS is being used as spinning reserve capacity and not for smoothing, majority of the ESS cycles are 100 kW or less.

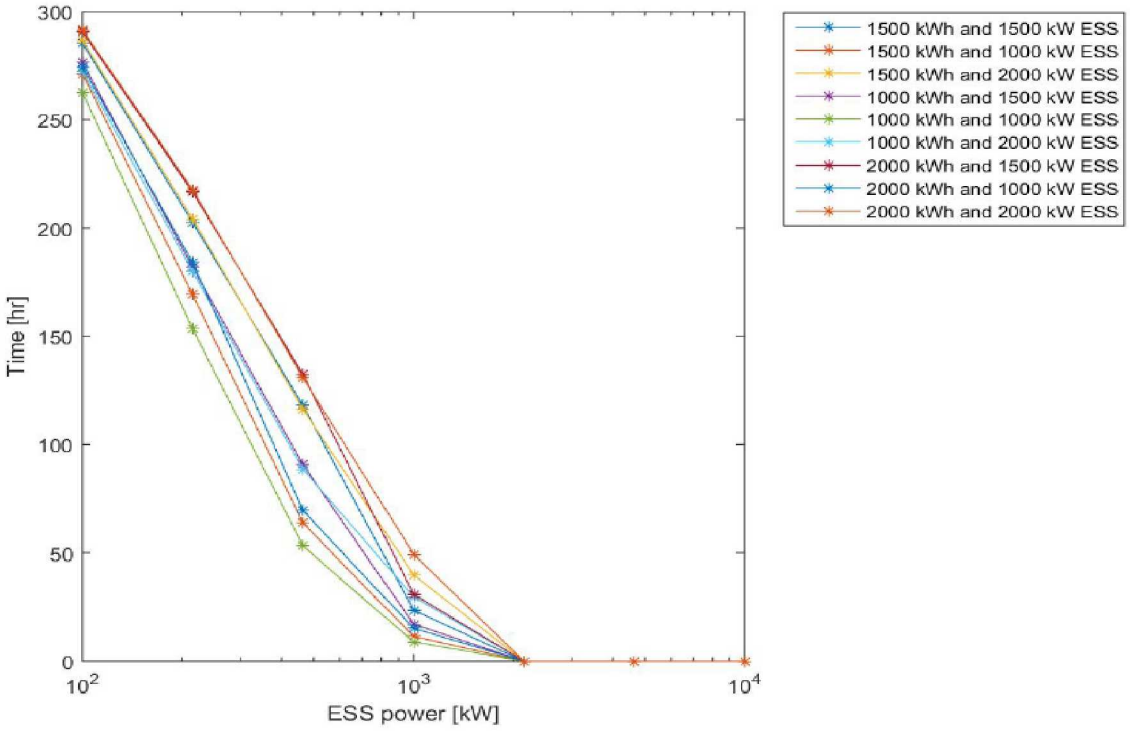

Figure 171 - Time the ESS spent charging or discharging at different power levels

ESS Ramp Rate

Figure 172 shows the probability distribution of ESS ramp rates for different ESS capacities and powers. The mean ramp rate is 1.6 kW/s, which is the lowest among the other simulations.

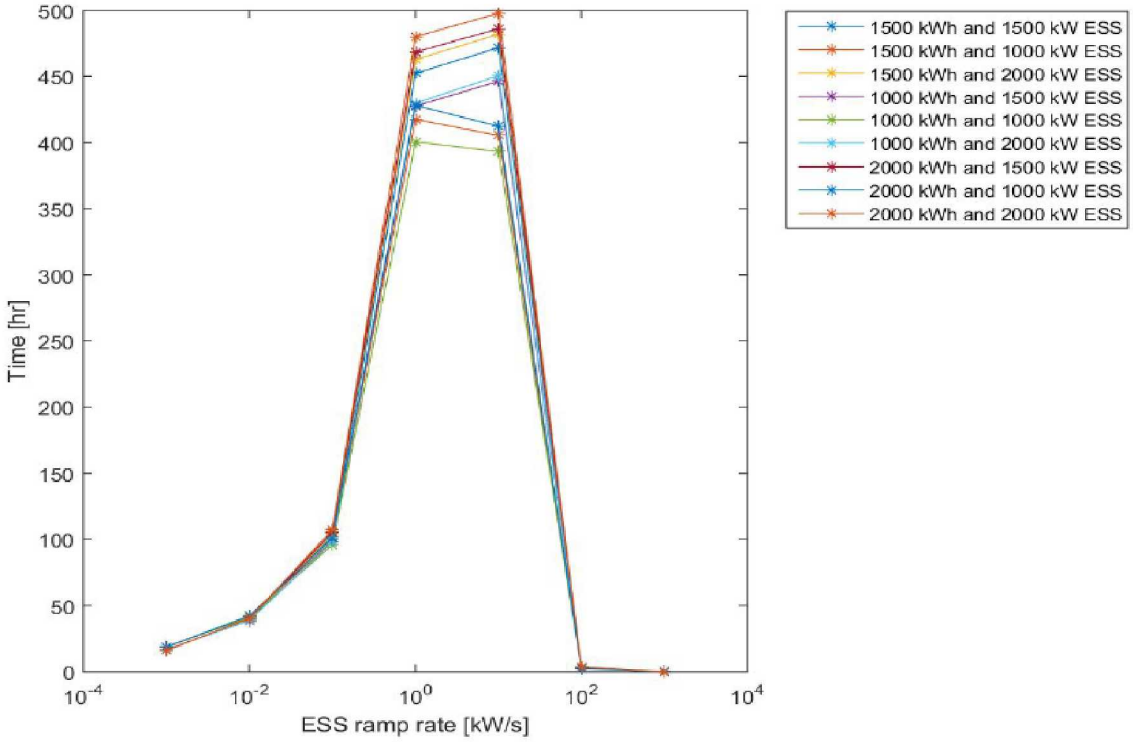

Figure 172 - Probability distribution of ESS ramp rates for different ESS capacities and powers

ESS Throughput

Figure 173 shows the total ESS throughput for different ESS capacities and powers. As the ESS capacity and power increases the throughput increases.

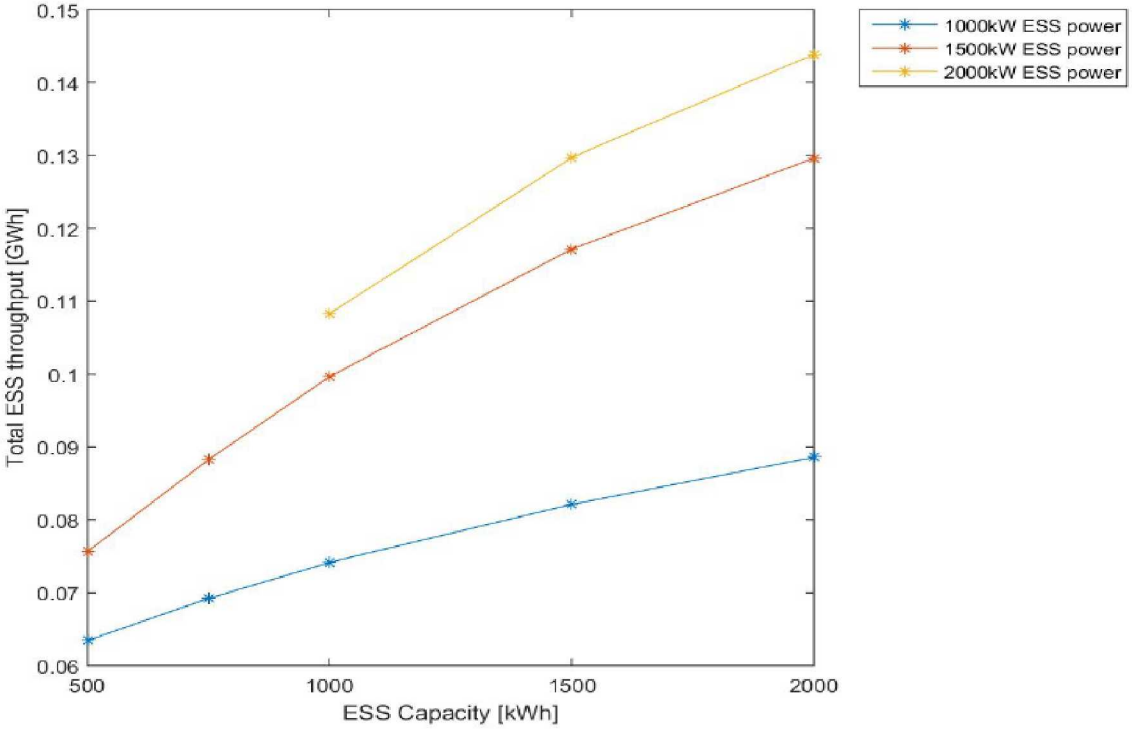

Figure 173 - ESS throughput for different ESS capacities and powers

[PAGE LEFT INTENTIONALLY BLANK]

APPENDIX G: DYNAMIC RESULTS OF ENERGY STORAGE

Sensitivity Analysis

In the PSLF ESTOR2 model there are multiple parameters that can be set to shape the output and control the energy storage system as the user needs it. Sandia has been evaluating energy storage systems for over 15 years and has experience on how energy storage responds to different control commands as well as response times.

In Figure 174, the PSLF block diagram of the model ESTOR2 is shown. The top control block diagram is commanding the real power output based on change of frequency of the energy storage system while the middle control block diagram is controlling the reactive power based on voltage. Last block diagram is based on if the energy storage system is charging or discharging and the efficiency of that operation mode.

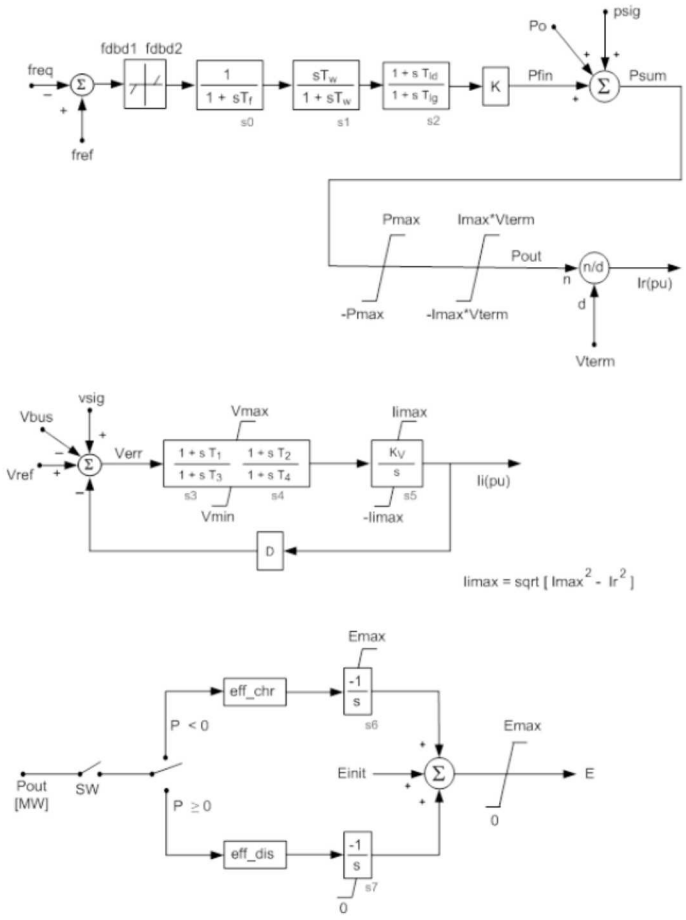

Figure 174 - PSLF block diagram of the model ESTOR2

The parameters provided below are from the GE PSLF manual as well as the default settings for the ESTOR2 model.

Variable	Default Value	Description
Tf	0.15	Time Constant, sec.
fdbd1	0.0	Deadband lower limit, p.u.
fdbd2	0.0	Deadband upper limit p.u.
Tw	10.0	Washout time constant, p.u.
Tld	0.0	Lead time constant, sec.
Tlg	0.0	Lag time constant, sec.
K	1.0	Gain, p.u.
Pmax	1.0	Power limit, p.u.
Imax	1.0	Current limit, p.u.
T1	0.0	Lead time constant, sec.
T2	0.0	Lead time constant, sec.
T3	0.0	Lag time constant, sec.
T4	0.0	Lag time constant, sec.
Vmax	0.20	Upper limit, p.u.
Vmin	-0.2	Lower limit, p.u.
Kv	10.0	Gain, p.u.
D	0.0	Droop, p.u.
eff_chr	0.0	Charging efficiency
eff_dis	0.0	Discharging efficiency
Emax	0.0	Maximum energy, MWs
Einit	0.0	Initial stored energy, MWs
Tsw	999.0	Time at which switch SW is closed, sec.

For this study, variables that were fixed constant from the default values were eff_chr from 0.0 to 0.92 and eff_dis from 0.0 to 0.92. The battery modeled in this project was a lithium-ion with a system roundtrip efficiency of 85%. To calculate the efficiency for charging and discharging, the values for each were deemed to be even. Therefore, the calculation for the energy storage efficiency for both discharging and charging was the square root of 0.85 which came to approximately 0.92. Values that were varied to determine how it affected the energy storage output were Tf, D, Kv and K. The table below state the different values that were used for the following varying parameters.

Table 22 - Dynamic sensitivity analysis values of parameters Tf, D, Kv and K

Parameter	Value 1	Value 2	Value 3
Tf	0.15	0.05	0.01
D	0	10	20
K	1	10	100
Kv	1	10	20

In the figures below, each variable was changed one at a time such that if Tf was varied from 0.01 to 0.15 the other values D, K and Kv were held at the default values from PSLF. Reasoning for this was to analyze how each parameter affected the output of the energy storage system by one variable at a time. Figures show that by adjusting the parameter Tf it did not have any significant effect on the output of the energy storage system. Tf was set to the value of 0.05. This value was chosen based on equipment process time which typically occurs in the 50ms

range which most time constants for lowpass filters are set to. Parameter D had a large effect on how the energy storage behaved in the system. When D was set to 40, figure not included, the energy storage system became unstable. The D parameter is in the voltage control loop of the model which by making this value a non-zero, the controller becomes a low pass filter. Since the model is to be in the reactive power control mode throughout the simulations, the D parameter needs to be 0 so the controller becomes an integrator over time. Due to this, the D parameter was set to 0.

As the K parameter value increased from 1 to 100, the reactive power from the energy storage response time increased and the real power output increased but had a slow settling time. Due to the settling times and the increase in real power over reactive power with an increasing K value, the K was left at the default value of 1.0. Last parameter that was varied was the Kv gain value in the voltage control mode which the default is 10.0. As the parameter Kv value increased, the output from the energy storage system initial response was greater when there is a voltage difference between the voltage at the bus being regulated and the scheduled voltage of 1.0 p.u This was expected since this parameter is a gain value that magnifies the error of the voltage difference. When Kv is set to 20, the energy storage system during the Main Town feeder fault responds by supplying reactive power equal to its rating and then in approximately 1 second absorbs the reactive power to about 90% of its rated power. This is quite a large swing for an energy storage system to accomplish meaning that the Kv value is set a little high. The default value of 10 does allows the energy storage system to supply its maximum rated value on its initial response to the voltage error. After a second, the energy storage starts absorbing power and reaches approximately half of its rated power. This is more realistic of how an energy storage behaves then when the Kv parameter was set to 20. In most cases where an energy storage system of the technology lithium ion is tracking a frequency regulation signal, the system going from discharging 100% of its rating to charging 100% of its rating sometimes can take up to 2 seconds.

Humpback Creek Fault Sensitivity Graphical Results

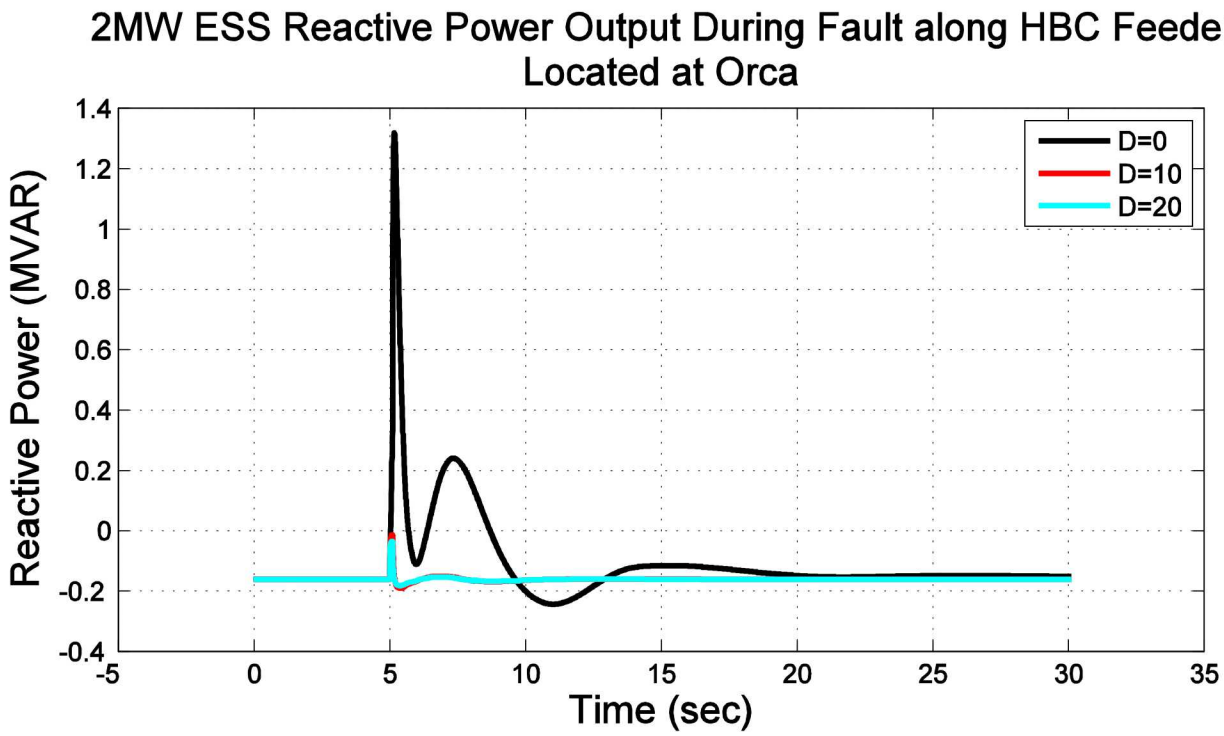

Figure 175 - 2MW ESS Reactive Power output during Humpback Creek Fault Varying D

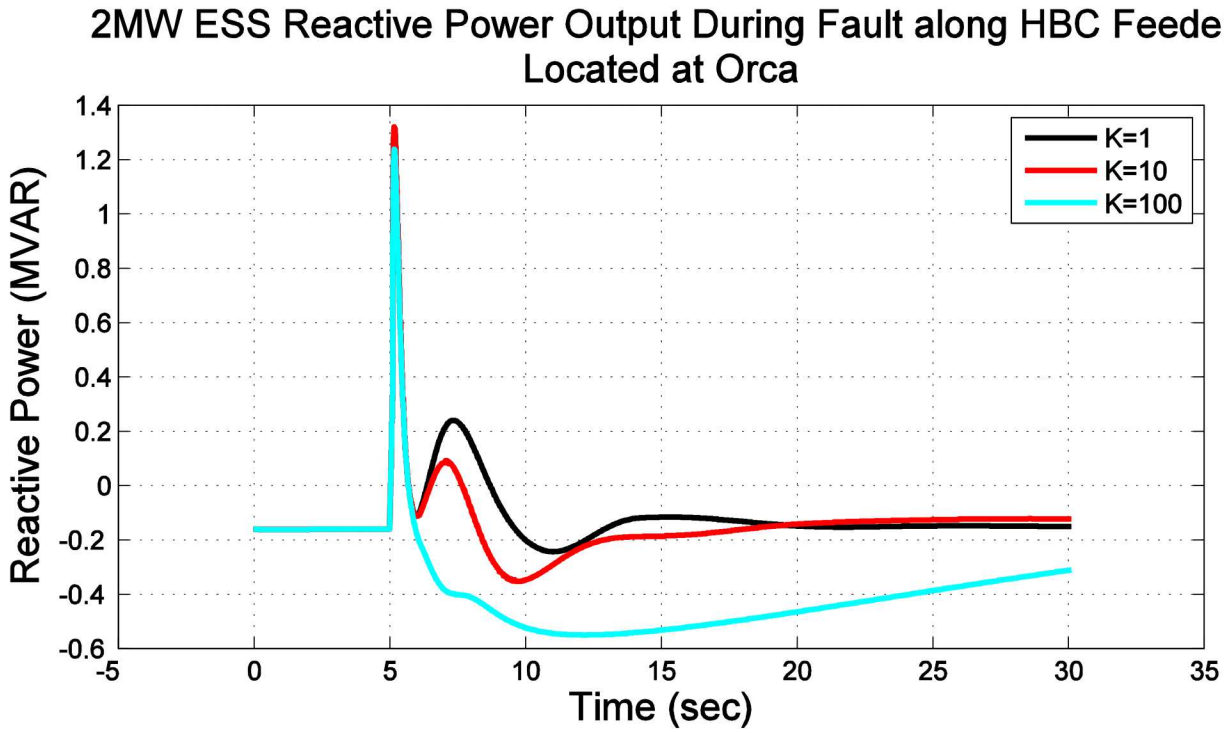

Figure 176 - Figure 134 - 2MW ESS Reactive Power output during Humpback Creek Fault Varying K

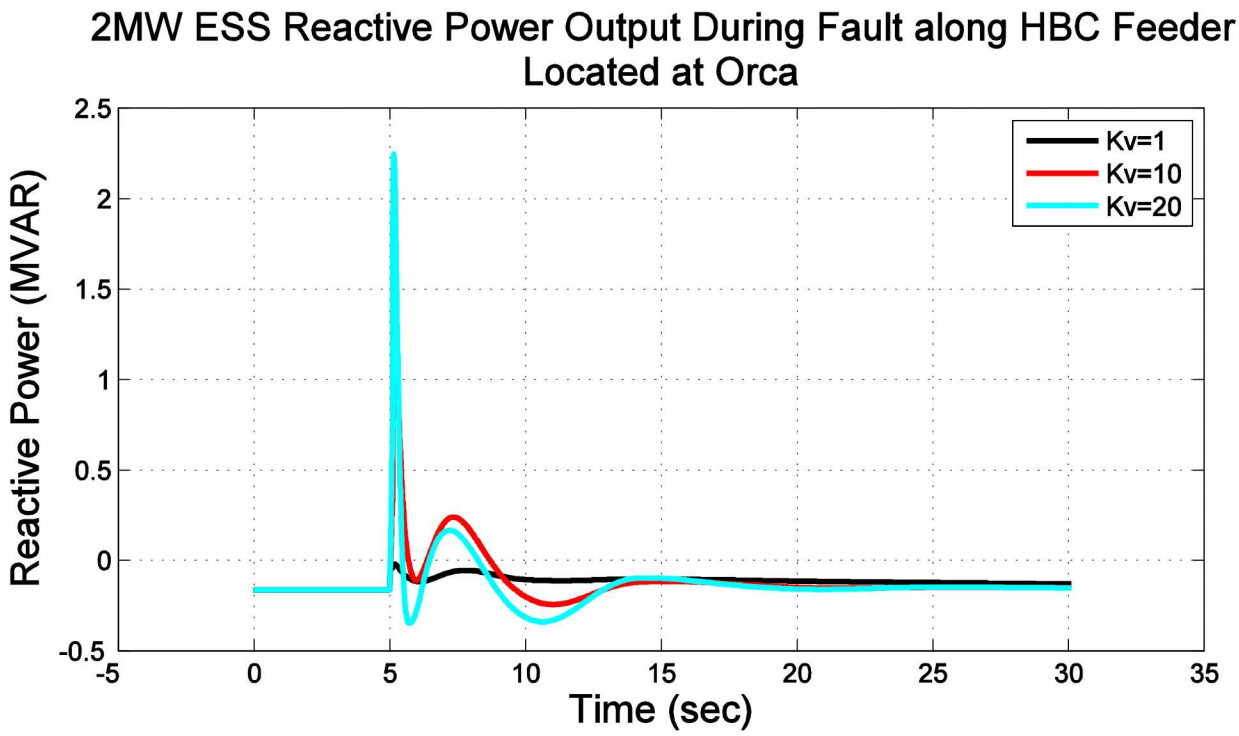

Figure 177 - Figure 134 - 2MW ESS Reactive Power output during Humpback Creek Fault Varying Kv

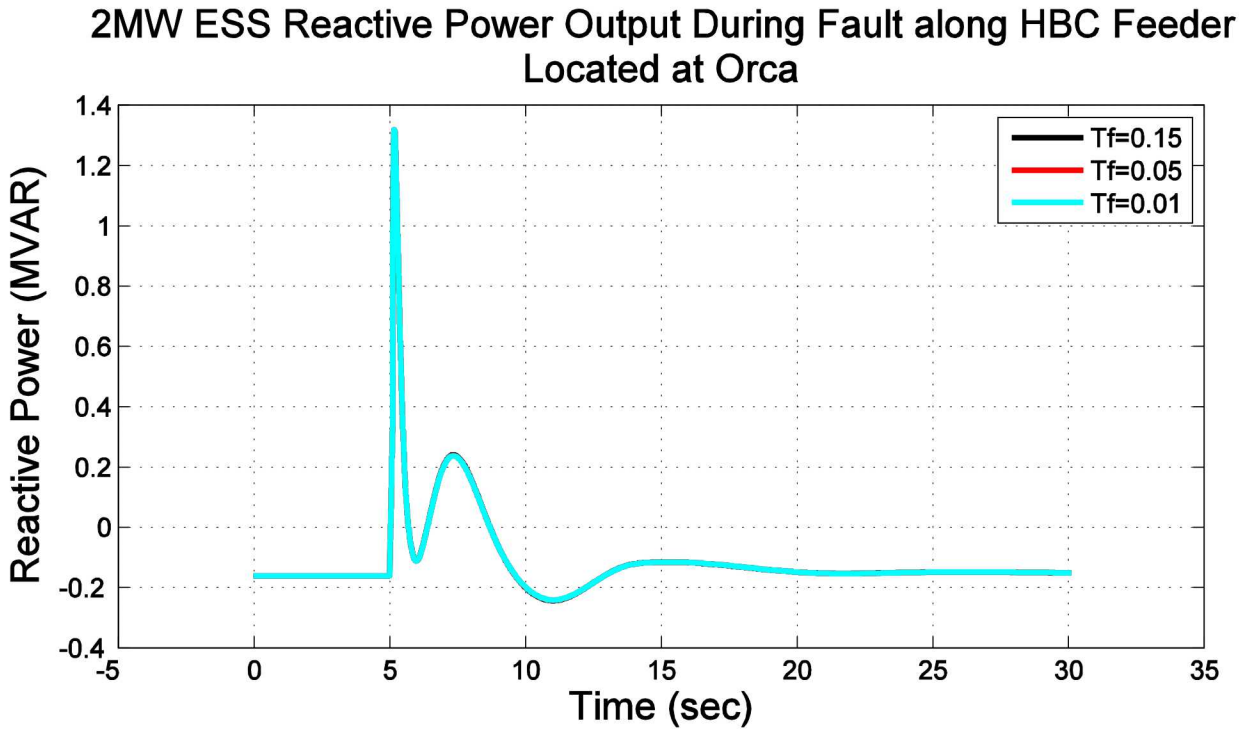

Figure 178 - Figure 134 - 2MW ESS Reactive Power output during Humpback Creek Fault Varying Tf

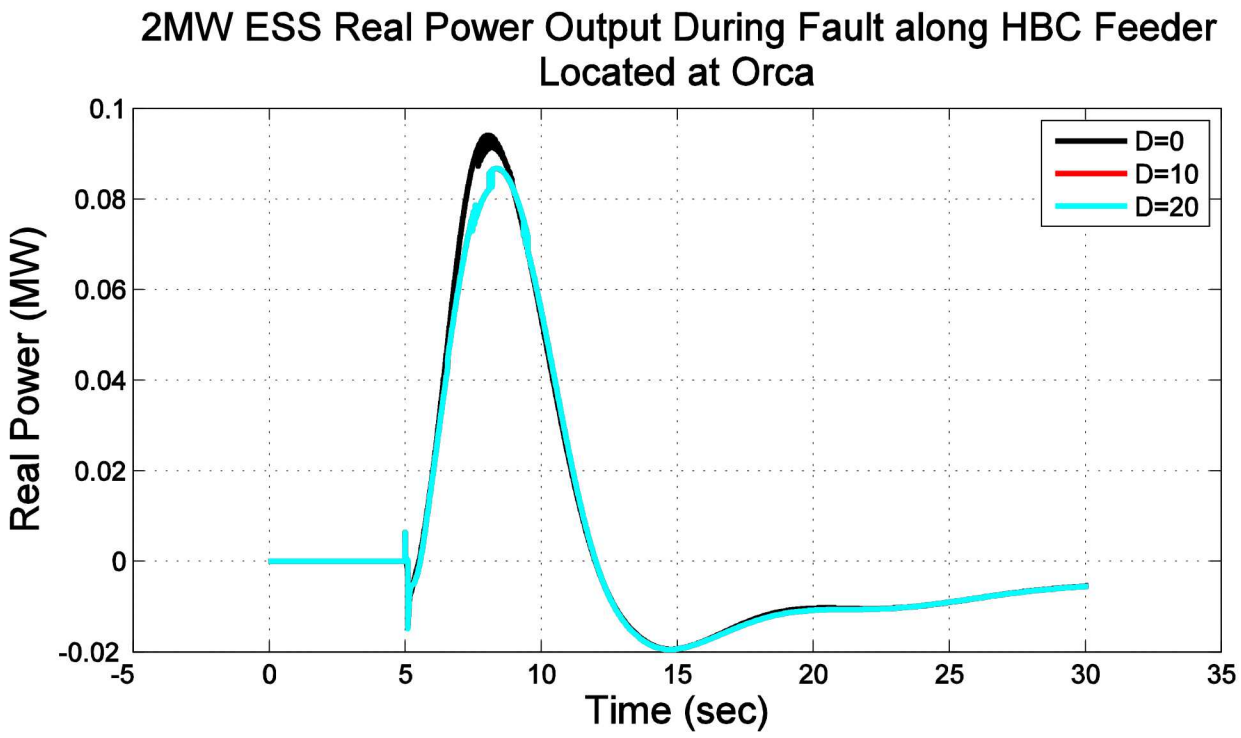

Figure 179 - 2MW ESS Real Power output during Humpback Creek Fault Varying D

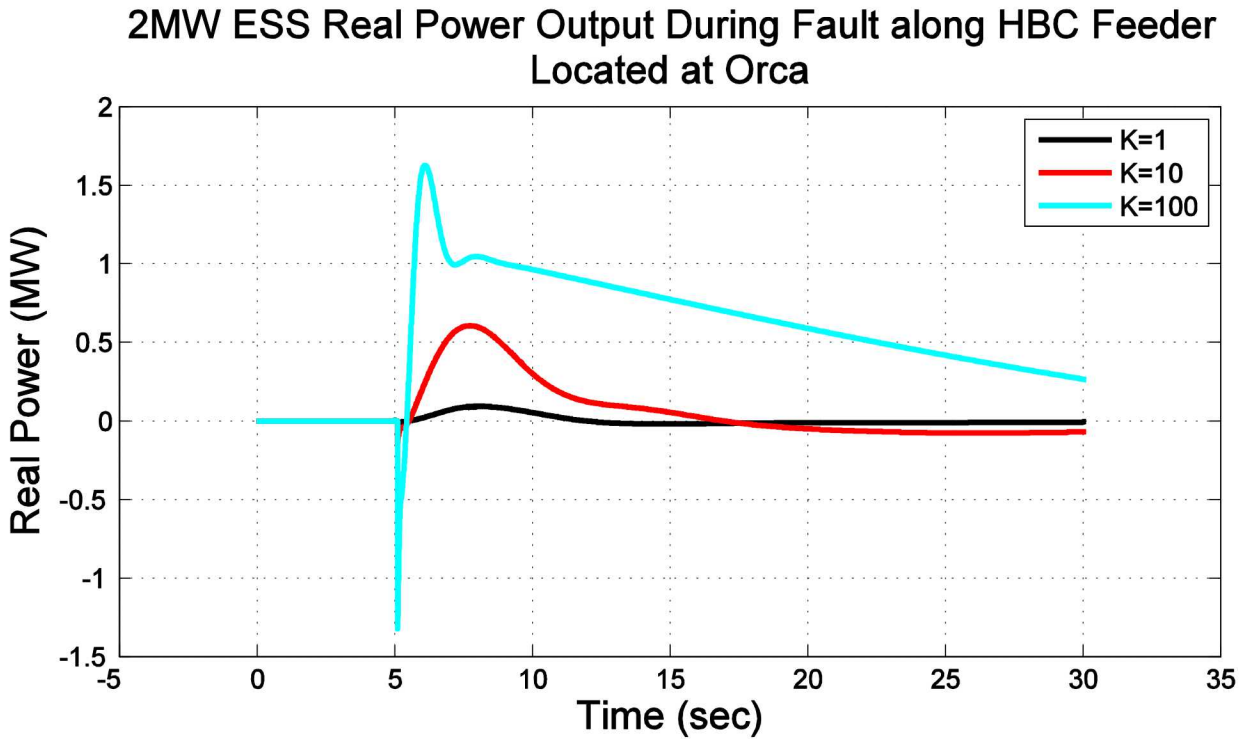

Figure 180 - 2MW ESS Real Power output during Humpback Creek Fault Varying K

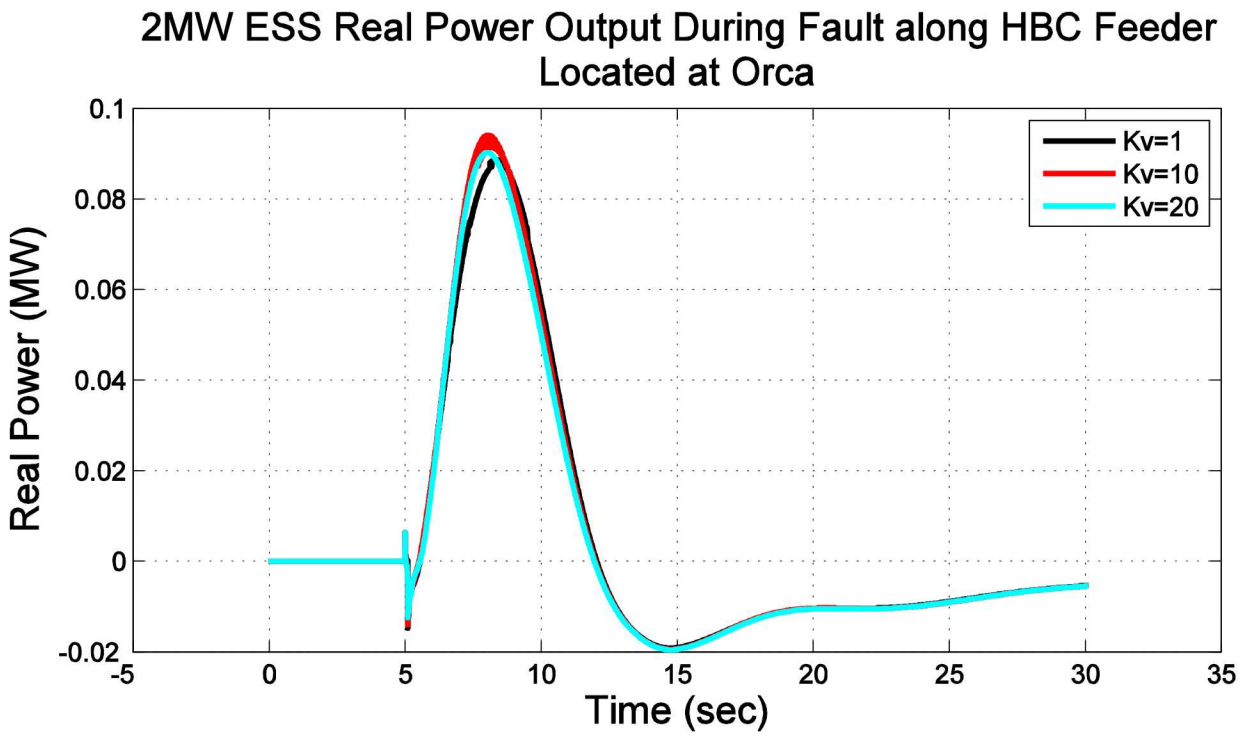

Figure 181 - 2MW ESS Real Power output during Humpback Creek Fault Varying Kv

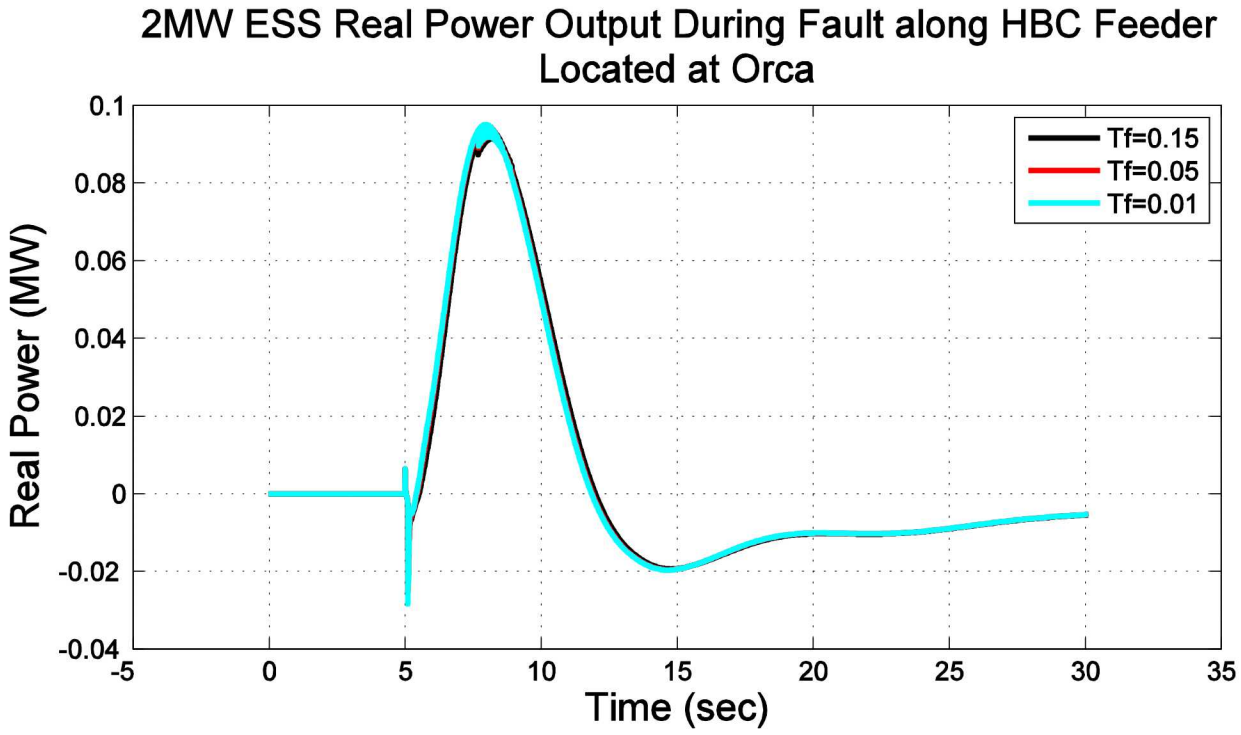

Figure 182 - 2MW ESS Real Power output during Humpback Creek Fault Varying Tf

Main Town Feeder Fault Sensitivity Graphical Results

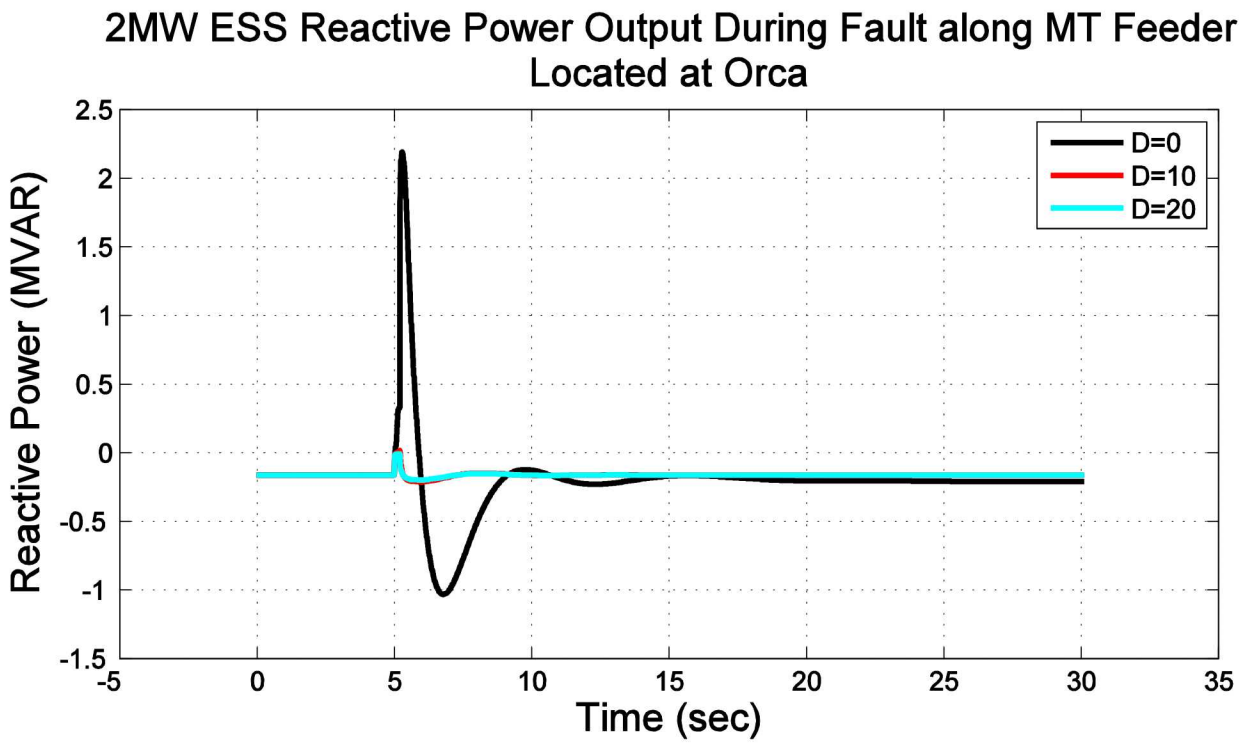

Figure 183 - 2MW ESS Reactive Power output during Main Town Feeder Fault Varying D

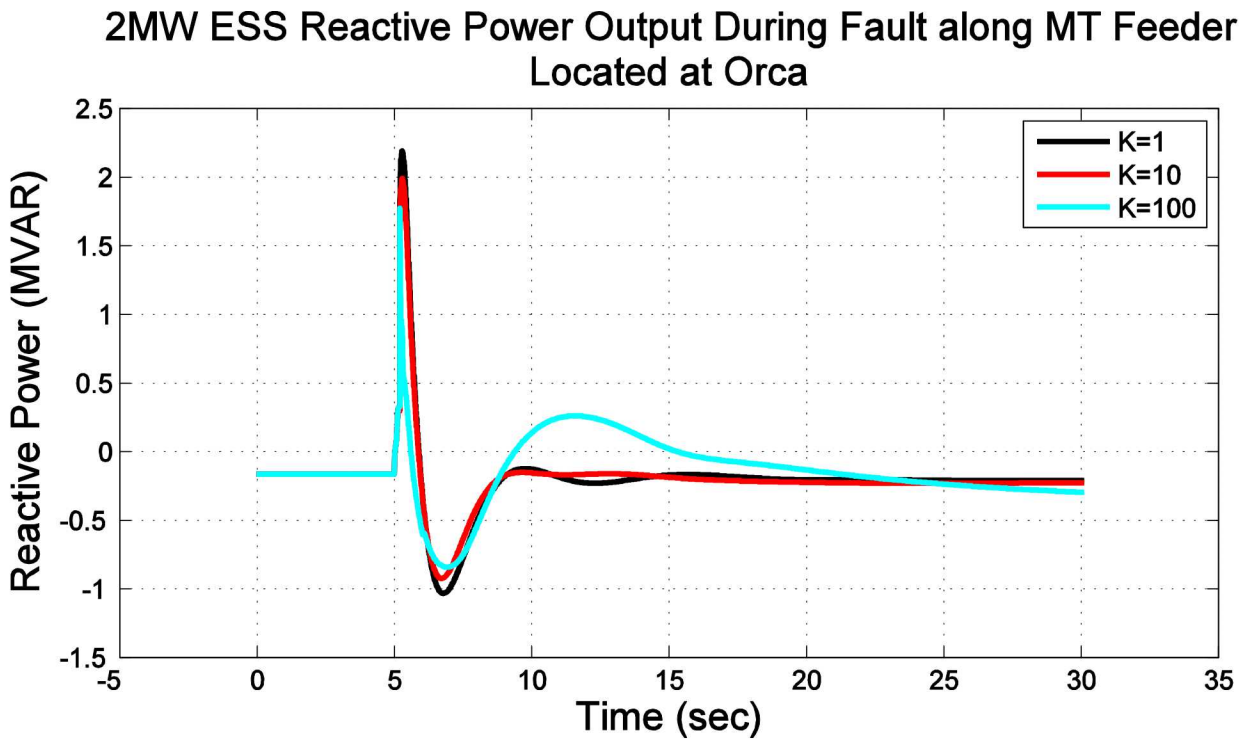

Figure 184 - 2MW ESS Reactive Power output during Main Town Feeder Fault Varying K

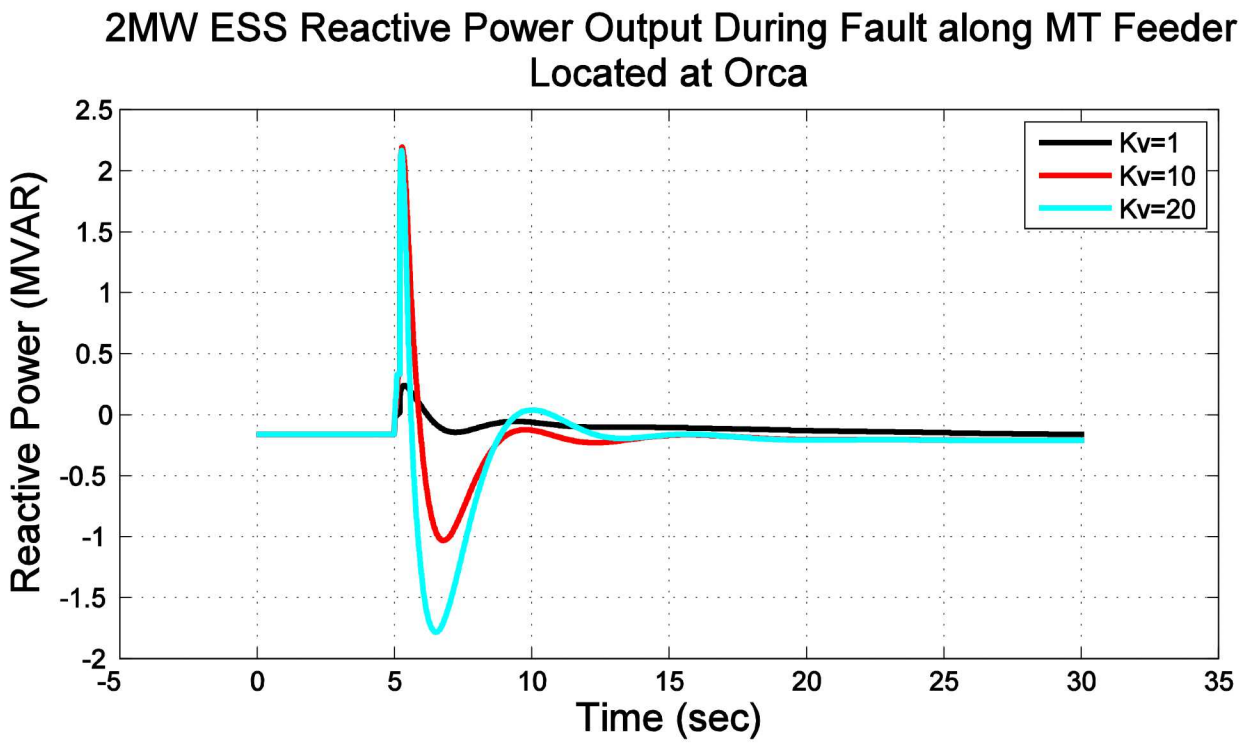

Figure 185 - 2MW ESS Reactive Power output during Main Town Feeder Fault Varying Kv

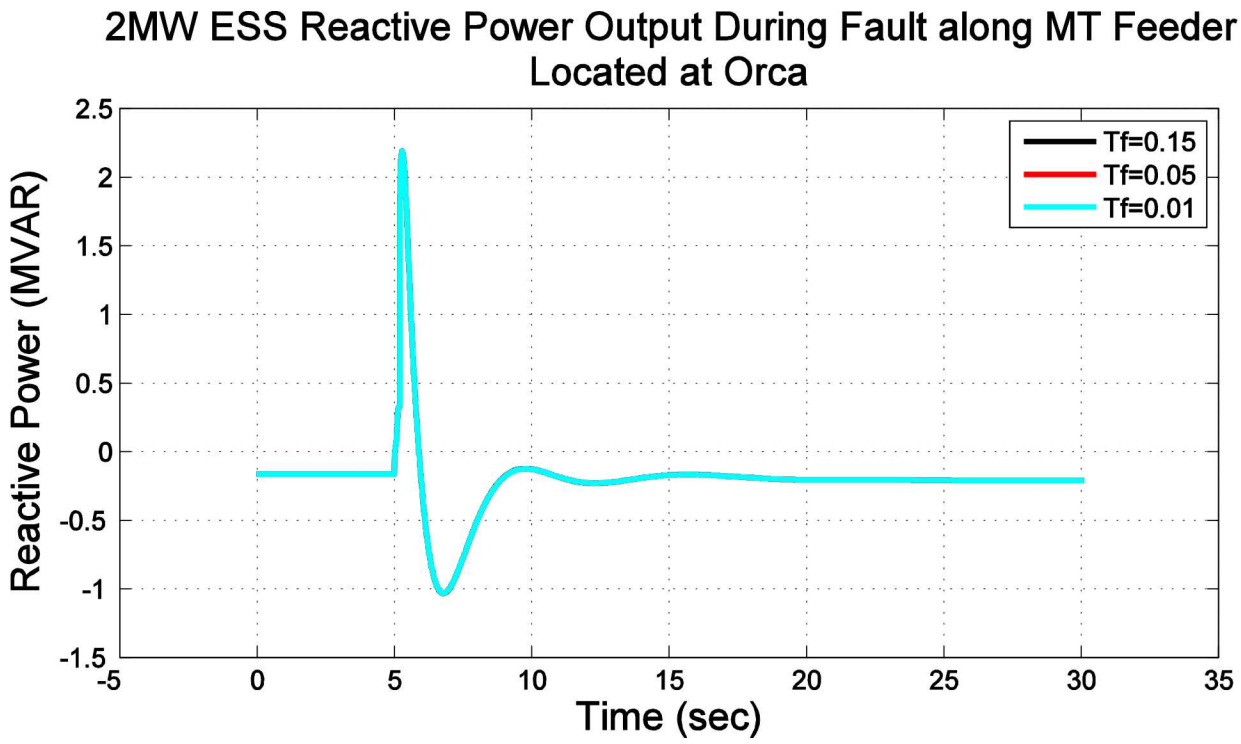

Figure 186 - 2MW ESS Reactive Power output during Main Town Feeder Fault Varying Tf

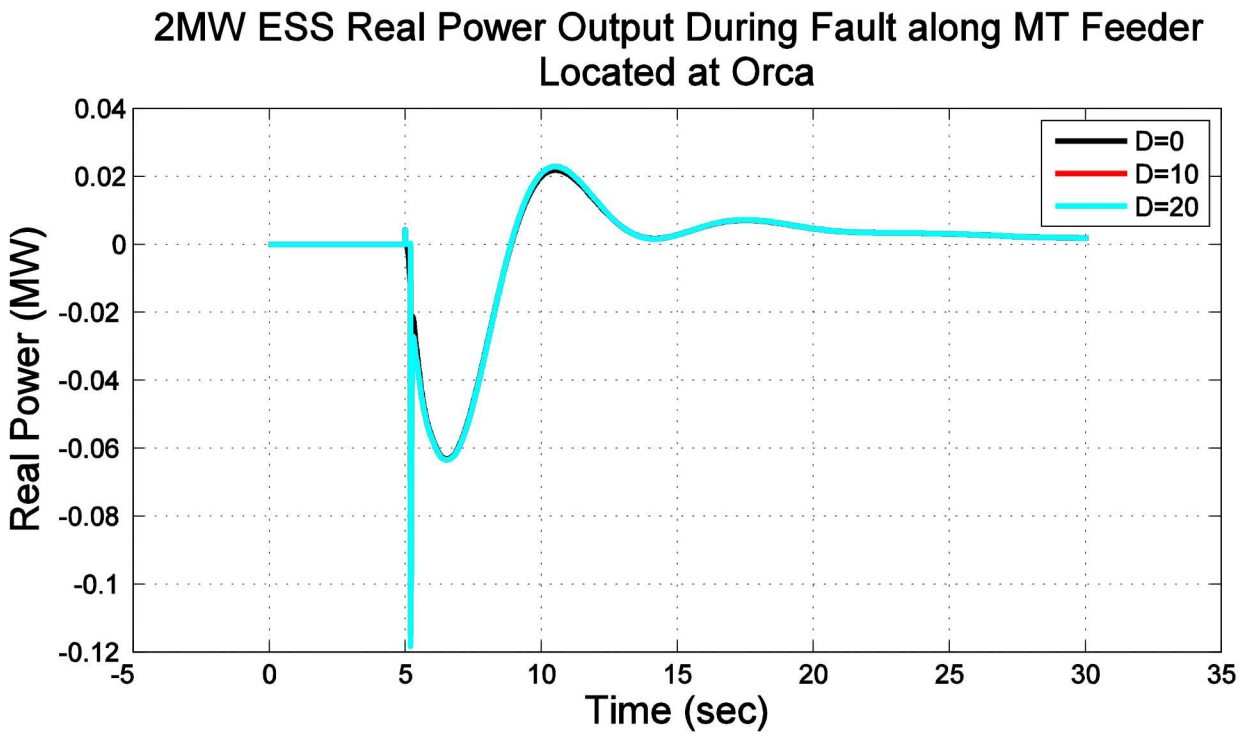

Figure 187 - 2MW ESS Real Power output during Main Town Feeder Fault Varying D

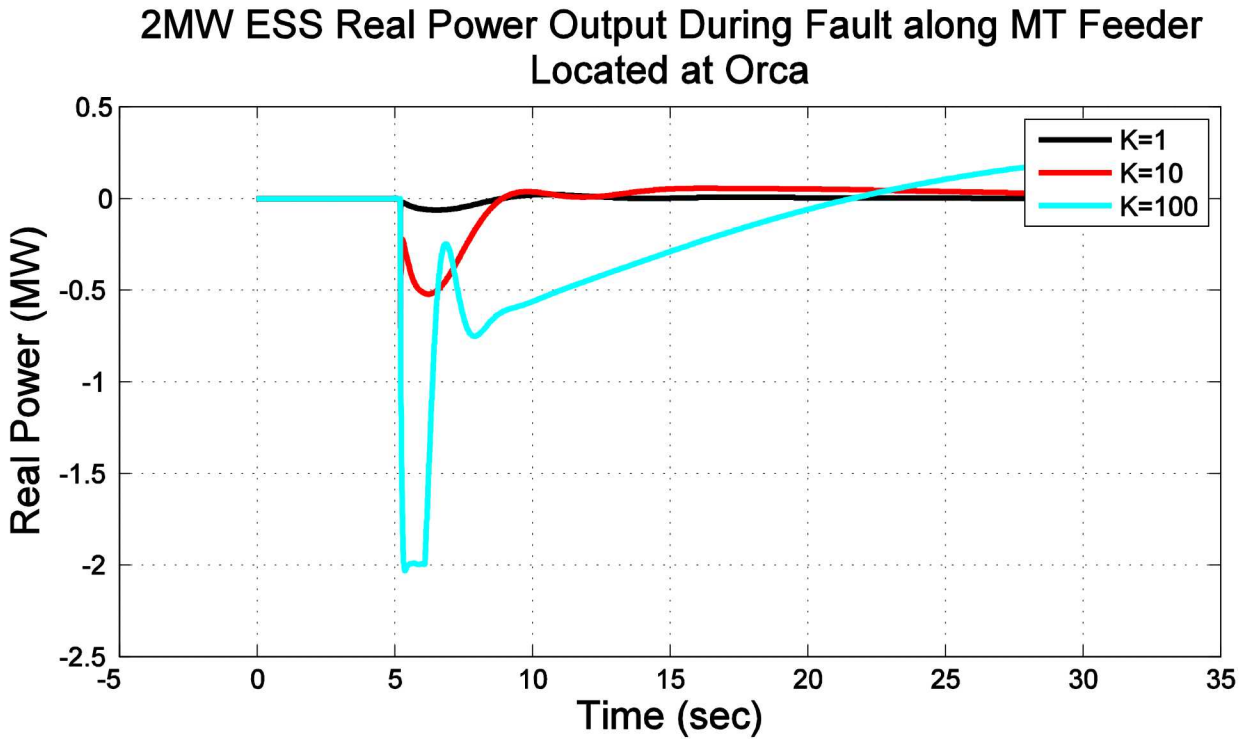

Figure 188 - 2MW ESS Real Power output during Main Town Feeder Fault Varying K

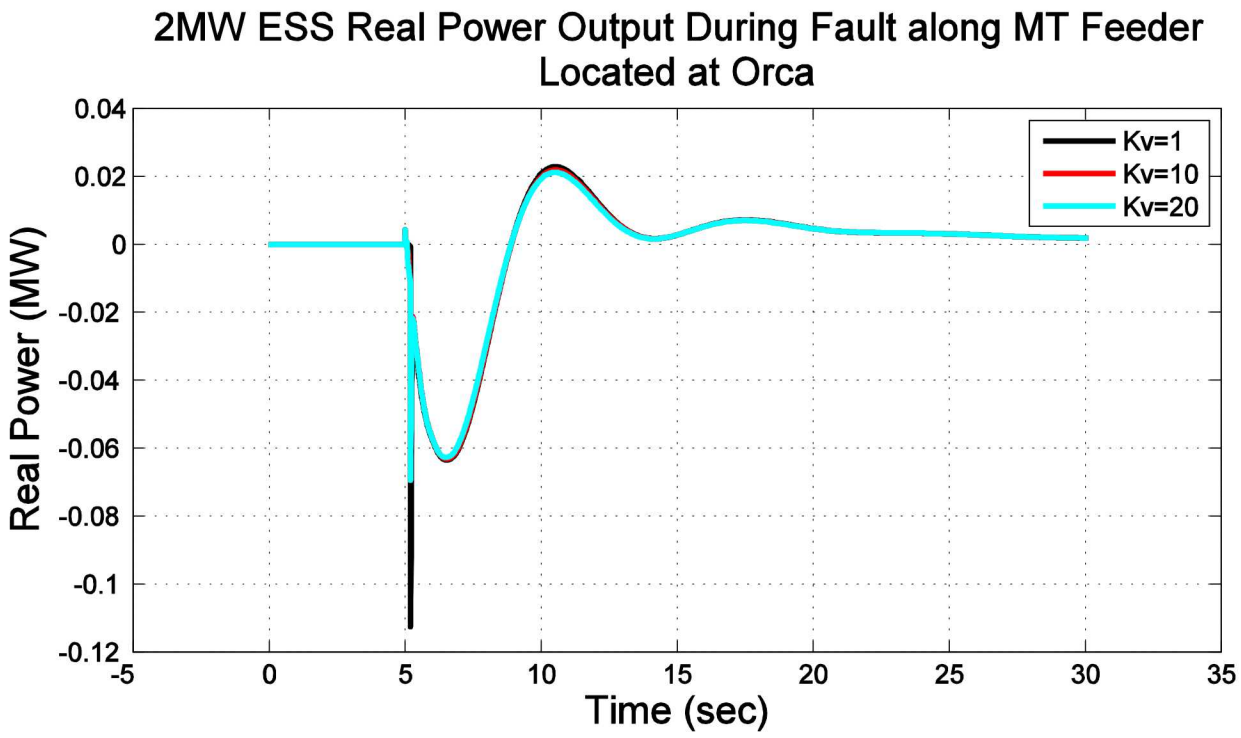

Figure 189 - 2MW ESS Real Power output during Main Town Feeder Fault Varying Kv

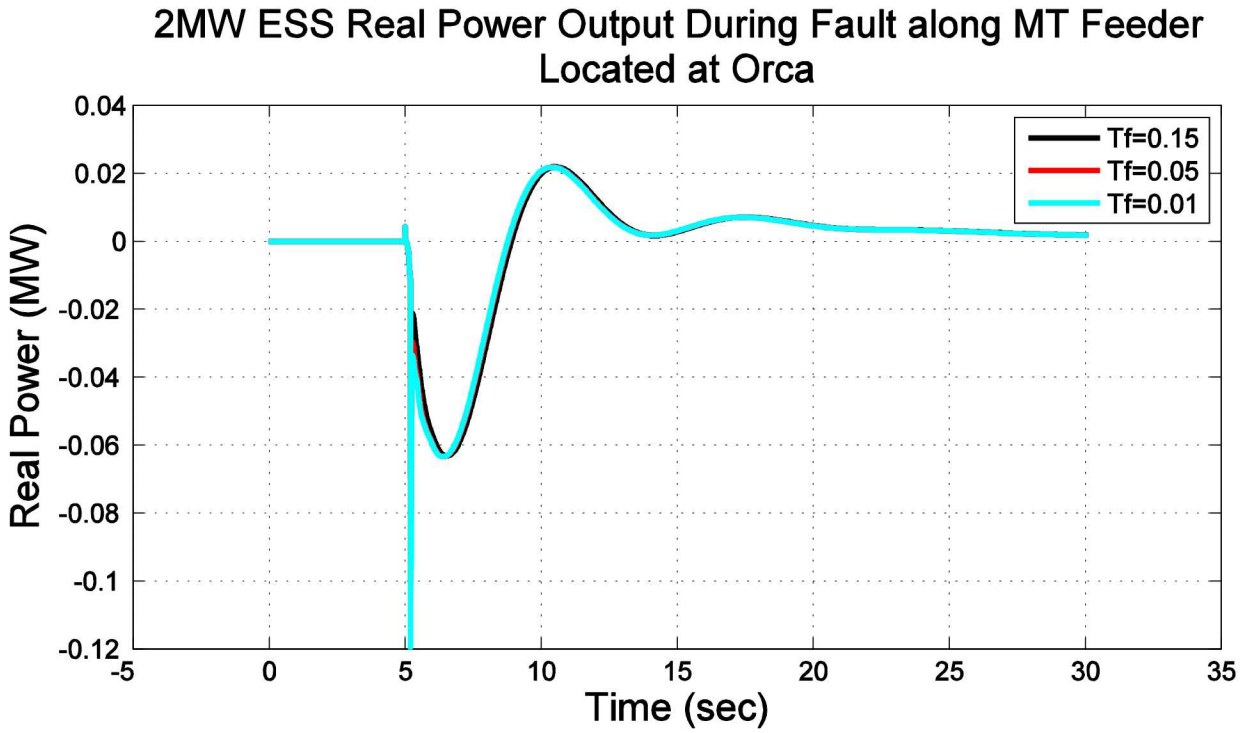

Figure 190 - 2MW ESS Real Power output during Main Town Feeder Fault Varying Tf

Comparison of Energy Storage MVA Rating Size

This section has the results from the dynamic simulation comparing various energy storage ratings at the same location during different transient conditions. Based on the results, the rating of the ESS did not have a significant dampening effect on the transients.

ESS located at Orca Substation during Humpback Creek feeder fault

Figures in this section are results from the PSLF dynamic simulation varying the ESS MVA ratings while located at the Orca substation during a fault along the Humpback Creek feeder.

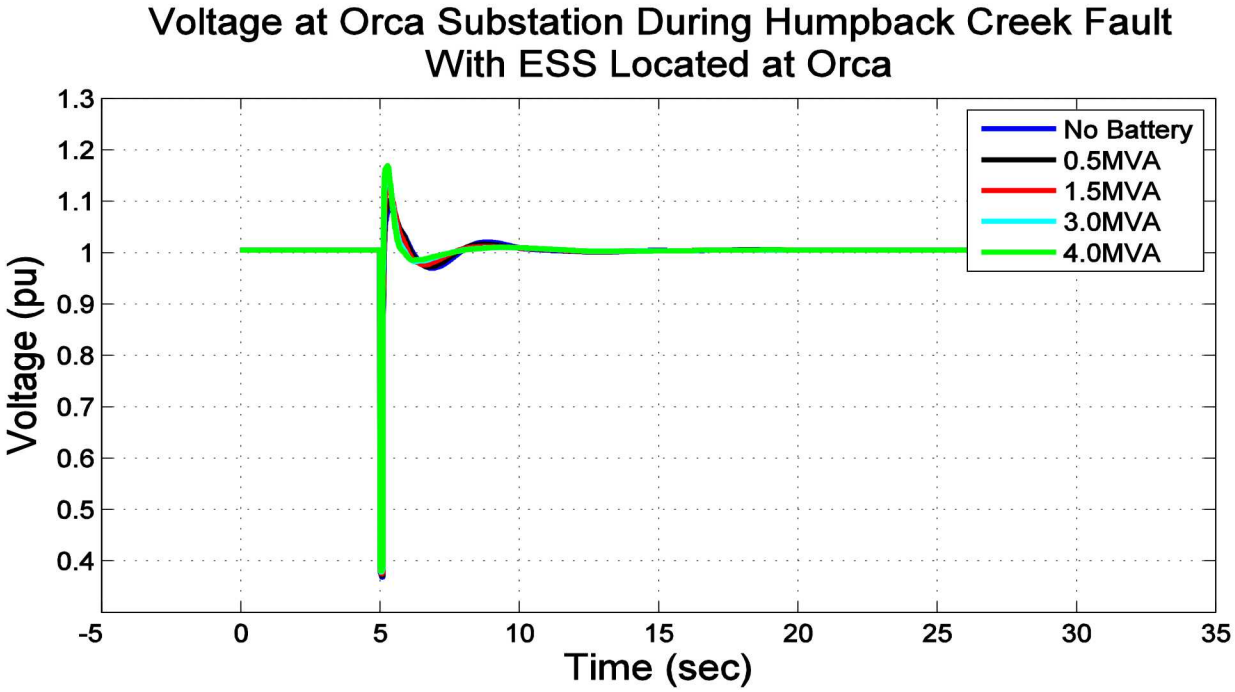

Figure 191 – Voltage at Orca Substation with varying ESS MVA ratings at Orca Substation during fault along Humpback Creek feeder

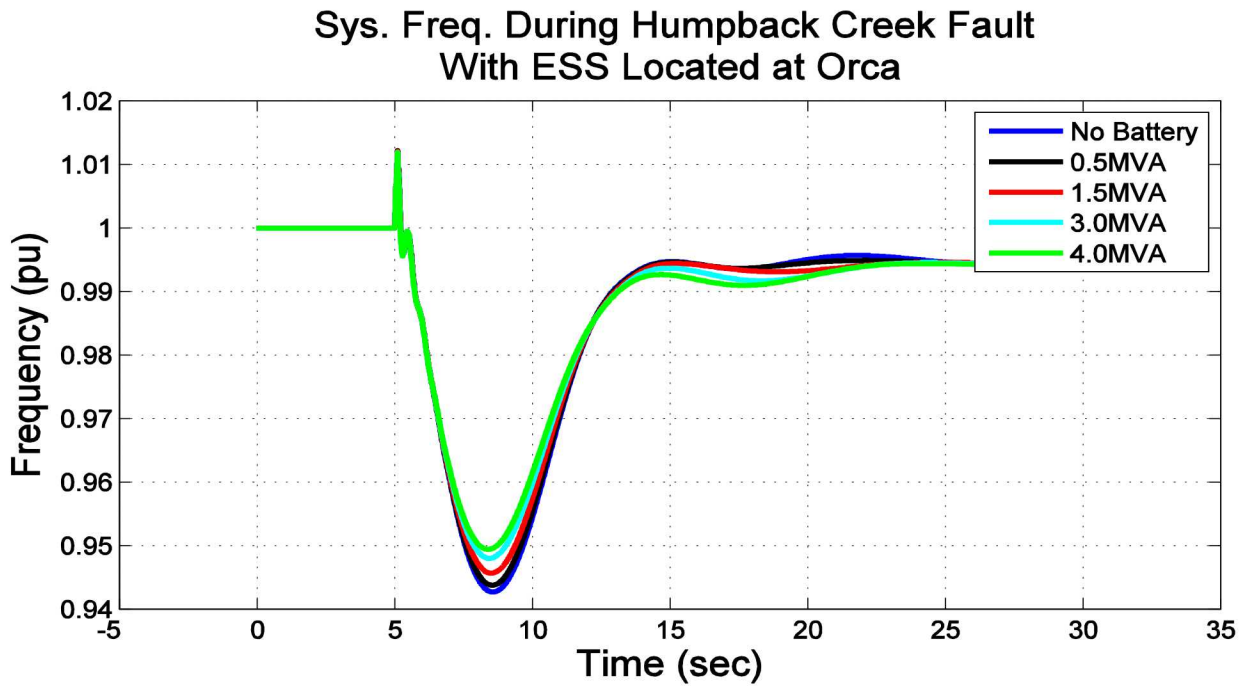

Figure 192 – System Frequency with varying ESS MVA ratings at Orca Substation during fault along Humpback Creek feeder

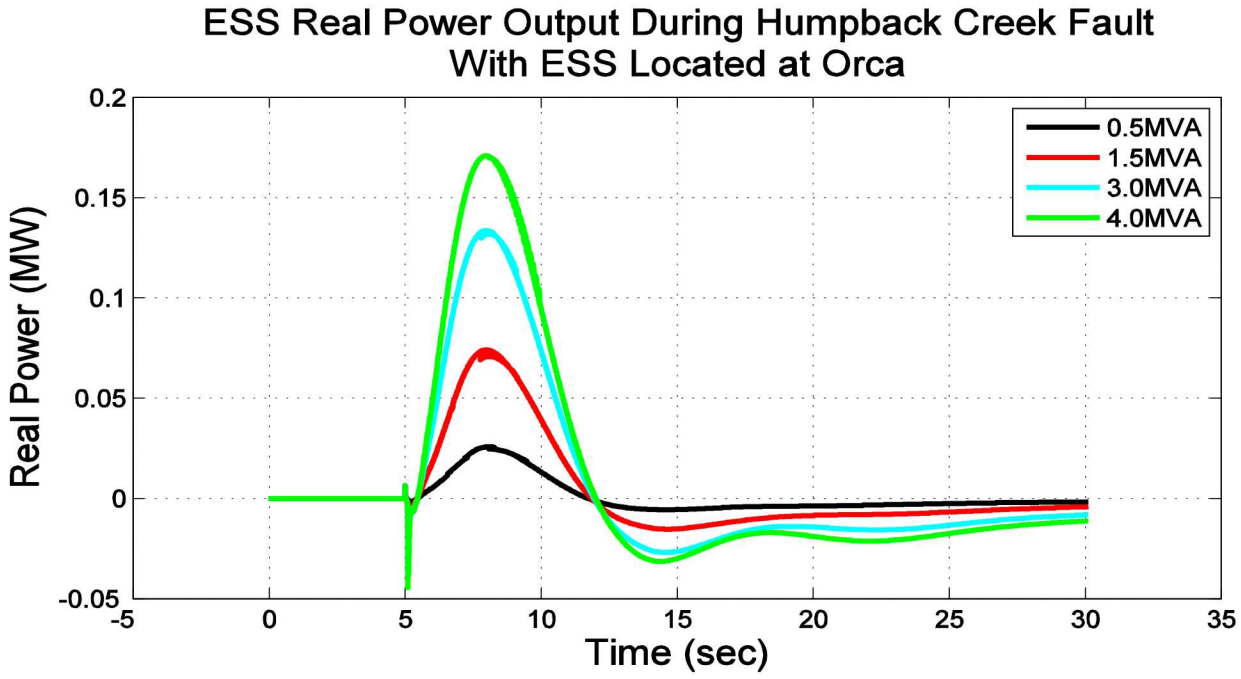

Figure 193 – Real power output of various ESS MVA ratings at Orca Substation during fault along Humpback Creek feeder

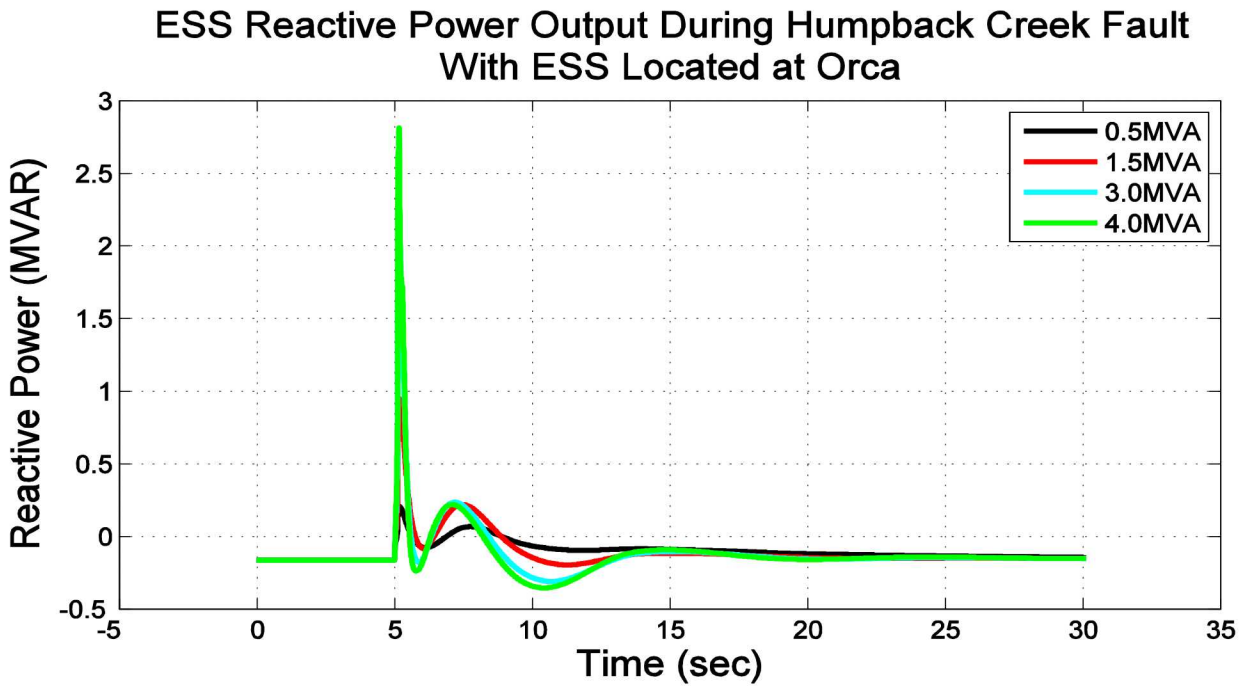

Figure 194 – Reactive` power output of various ESS MVA ratings at Orca Substation during fault along Humpback Creek feeder

ESS located at Eyak Substation during Humpback Creek feeder fault

Figures in this section are results from the PSLF dynamic simulation varying the ESS MVA ratings while located at the Eyak Substation during a fault along the Humpback Creek feeder.

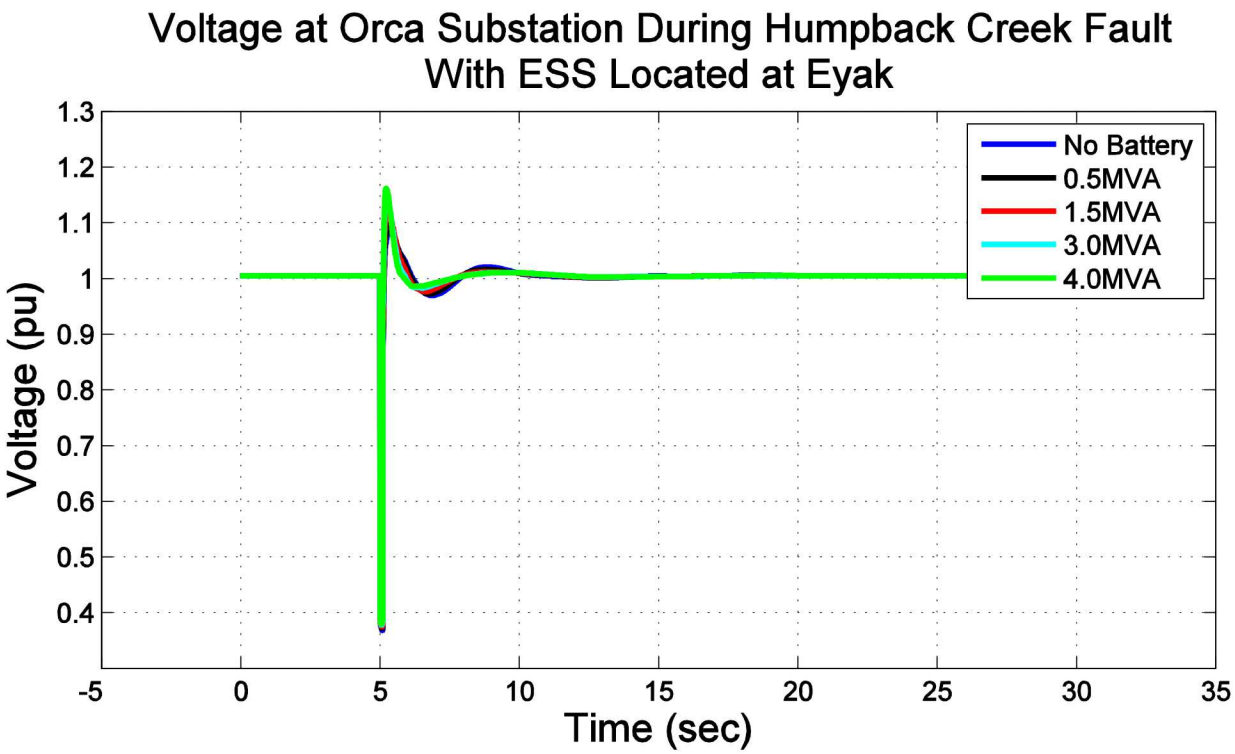

Figure 195 - Voltage at Orca Substation with varying ESS MVA ratings at Eyak Substation during fault along Humpback Creek feeder

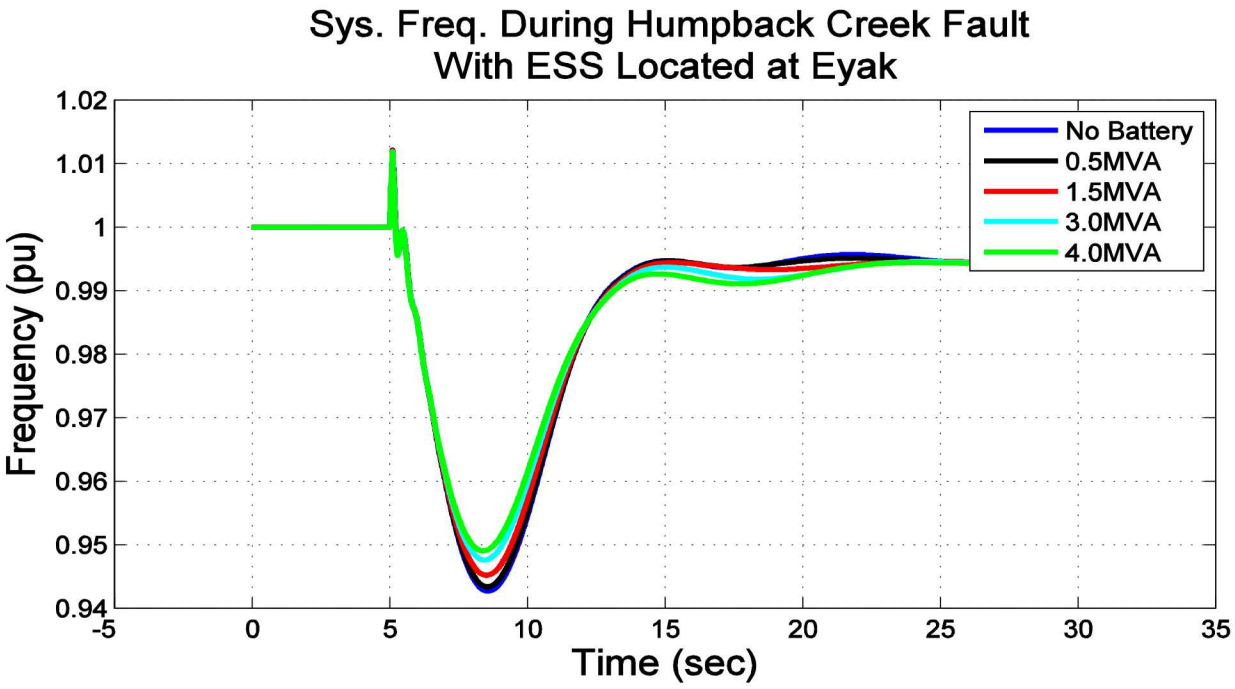

Figure 196 – System Frequency with varying ESS MVA ratings at Eyak Substation during fault along Humpback Creek

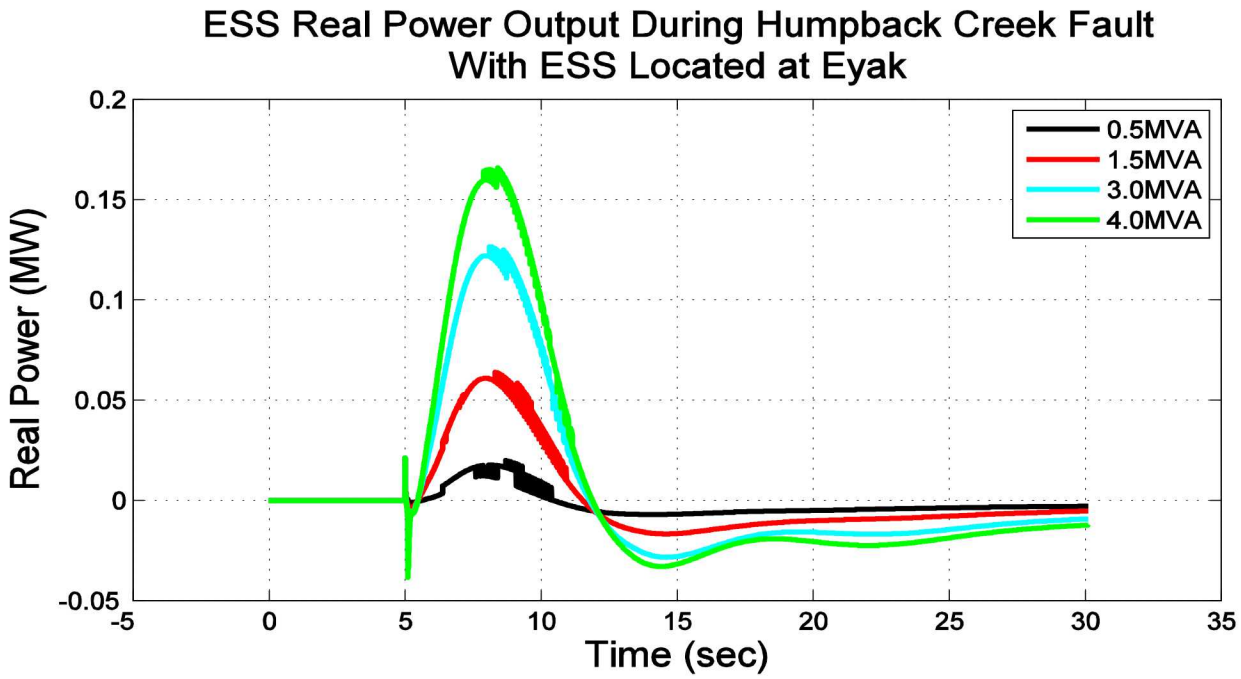

Figure 197 - Real power output of various ESS MVA ratings at Eyak Substation during fault along Humpback Creek feeder

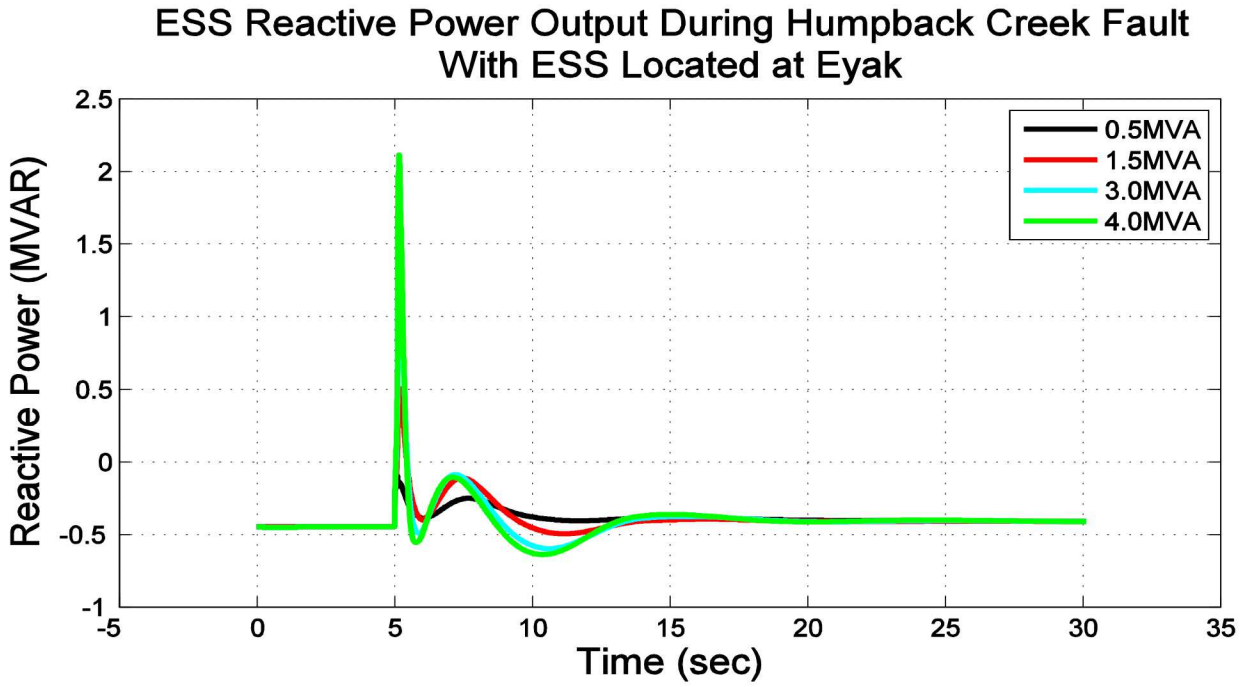

Figure 198 – Reactive power output of various ESS MVA ratings at Eyak Substation during fault along Humpback Creek feeder

ESS located at Main Hospital during Humpback Creek feeder fault

Figures in this section are results from the PSLF dynamic simulation varying the ESS MVA ratings while located at the Main Hospital during a fault along the Humpback Creek feeder.

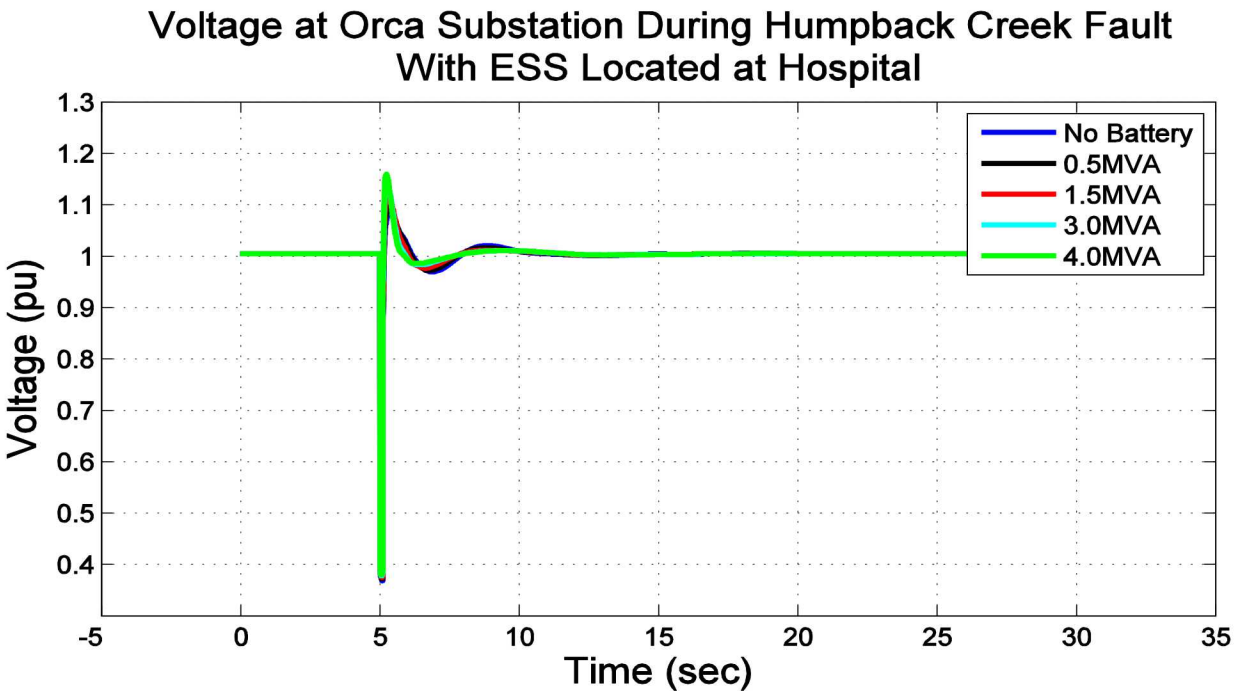

Figure 199 - Voltage at Orca Substation with varying ESS MVA ratings at Main Hospital during fault along Humpback Creek feeder

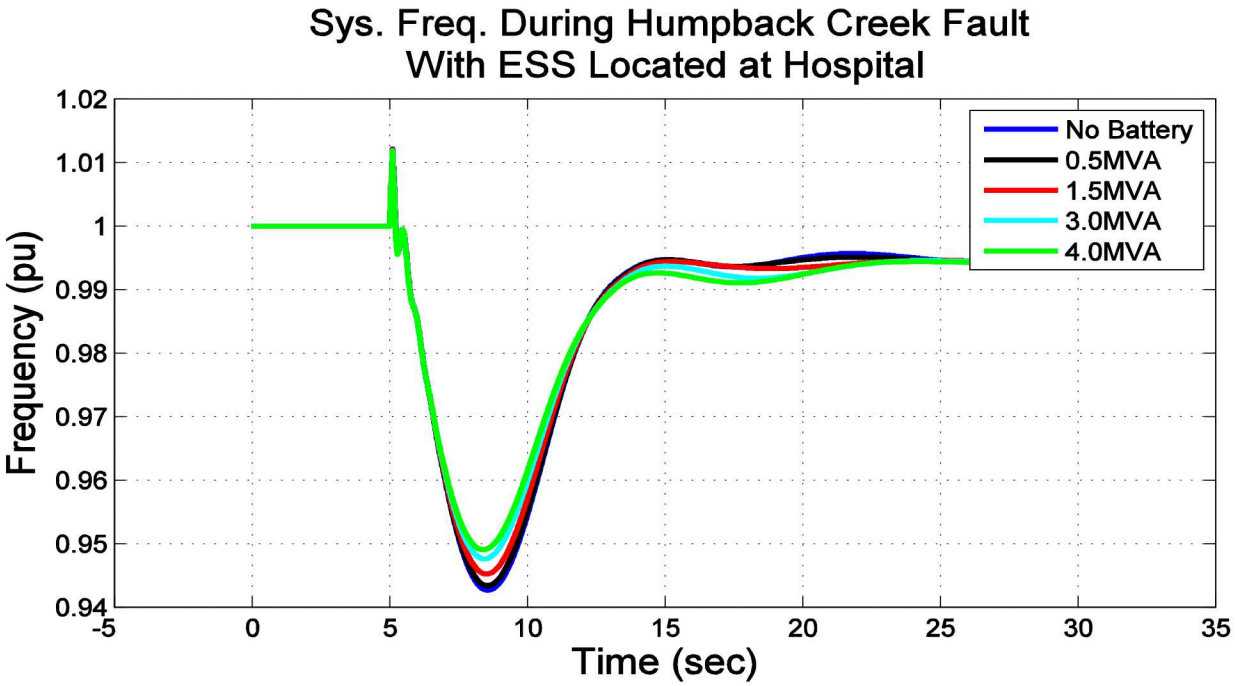

Figure 200 – System Frequency with varying ESS MVA ratings at Main Hospital during fault along Humpback Creek feeder

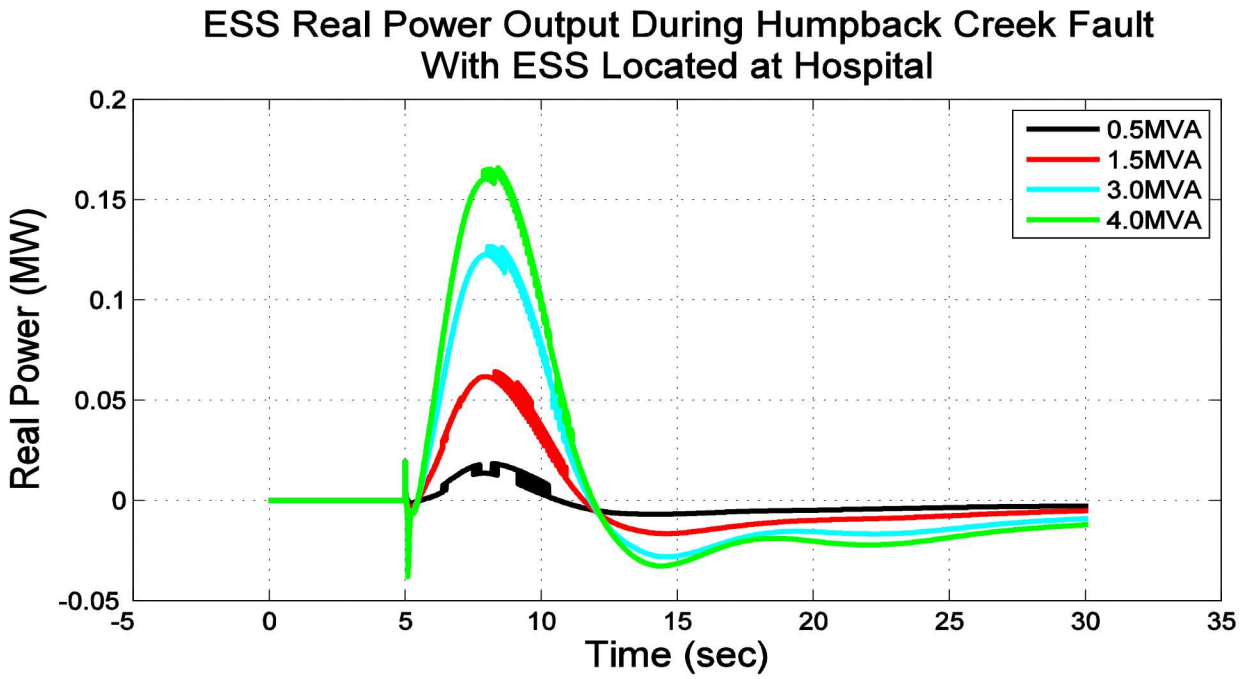

Figure 201 - Real power output of various ESS MVA ratings at Main Hospital during fault along Humpback Creek feeder

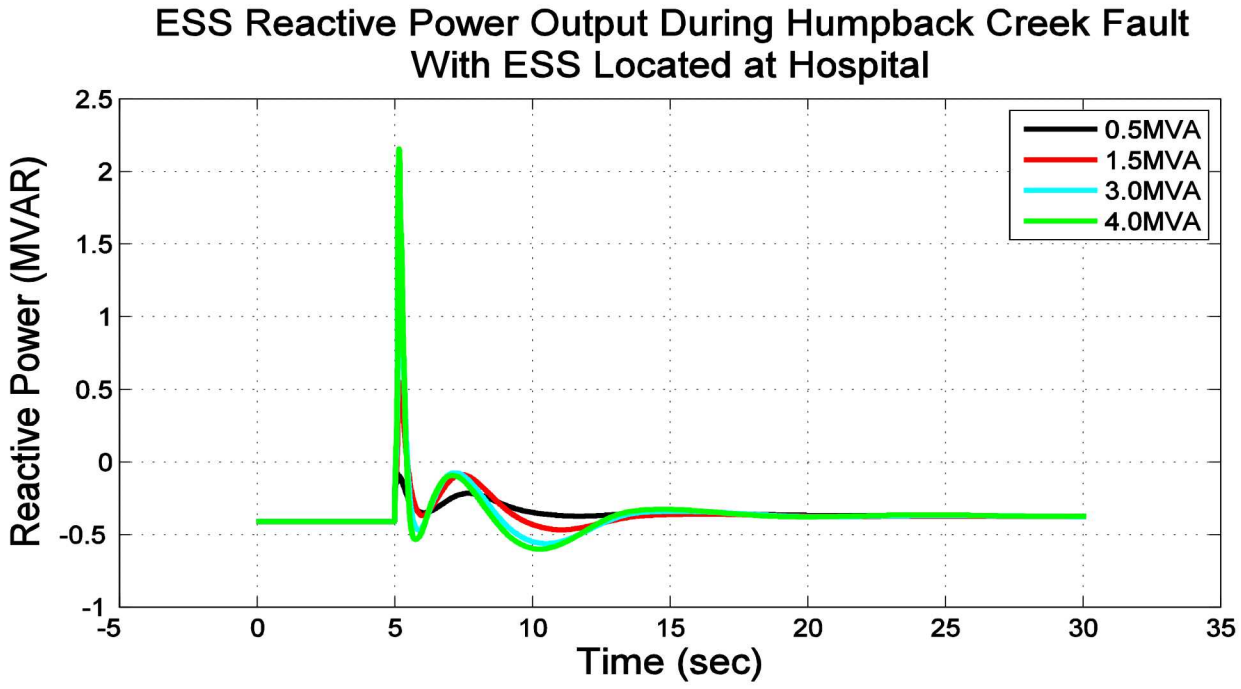

Figure 202 – Reactive power output of various ESS MVA ratings at Main Hospital during fault along Humpback Creek feeder

ESS located at Airport during Humpback Creek feeder fault

Figures in this section are results from the PSLF dynamic simulation varying the ESS MVA ratings while located at the Airport during a fault along the Humpback Creek feeder.

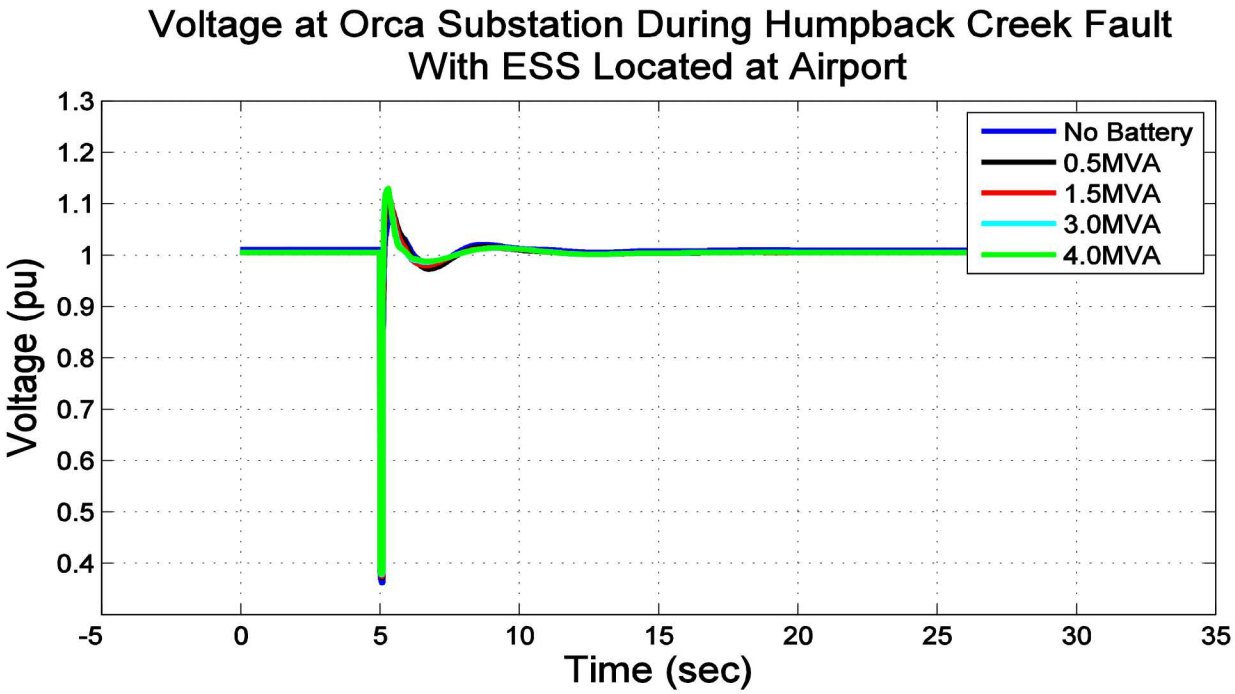

Figure 203 - Voltage at Orca Substation with varying ESS MVA ratings at Airport during fault along Humpback Creek feeder

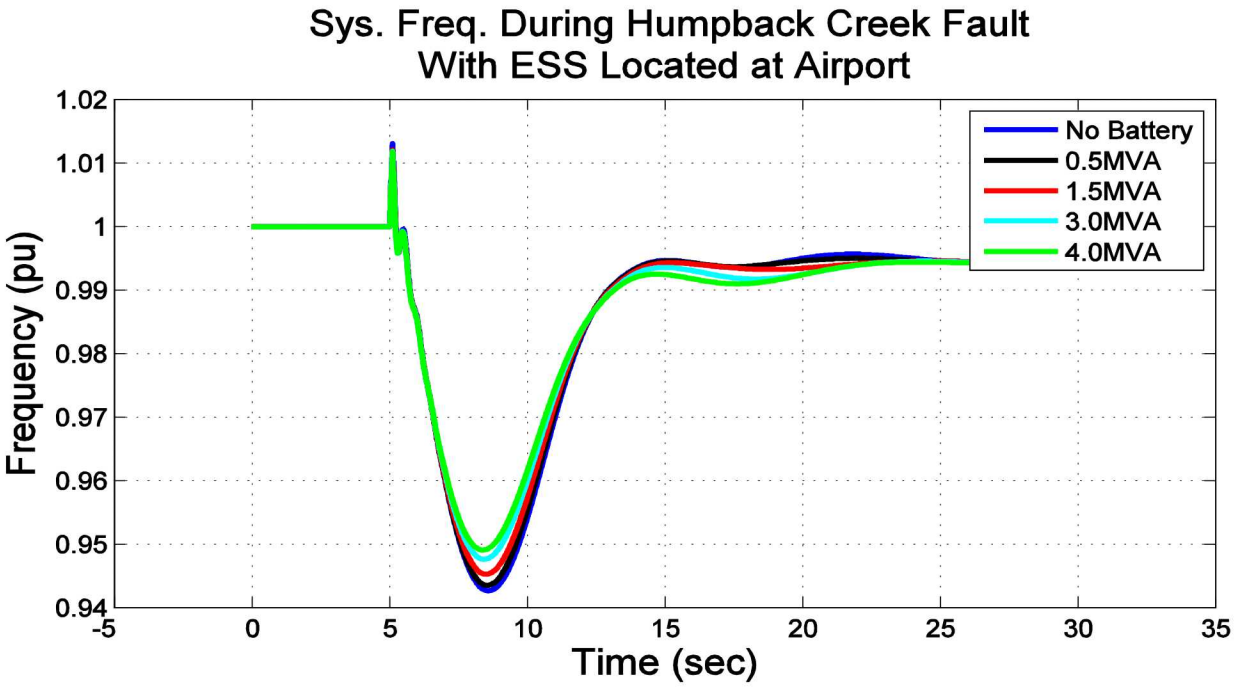

Figure 204 – System Frequency with varying ESS MVA ratings at Airport during fault along Humpback Creek feeder

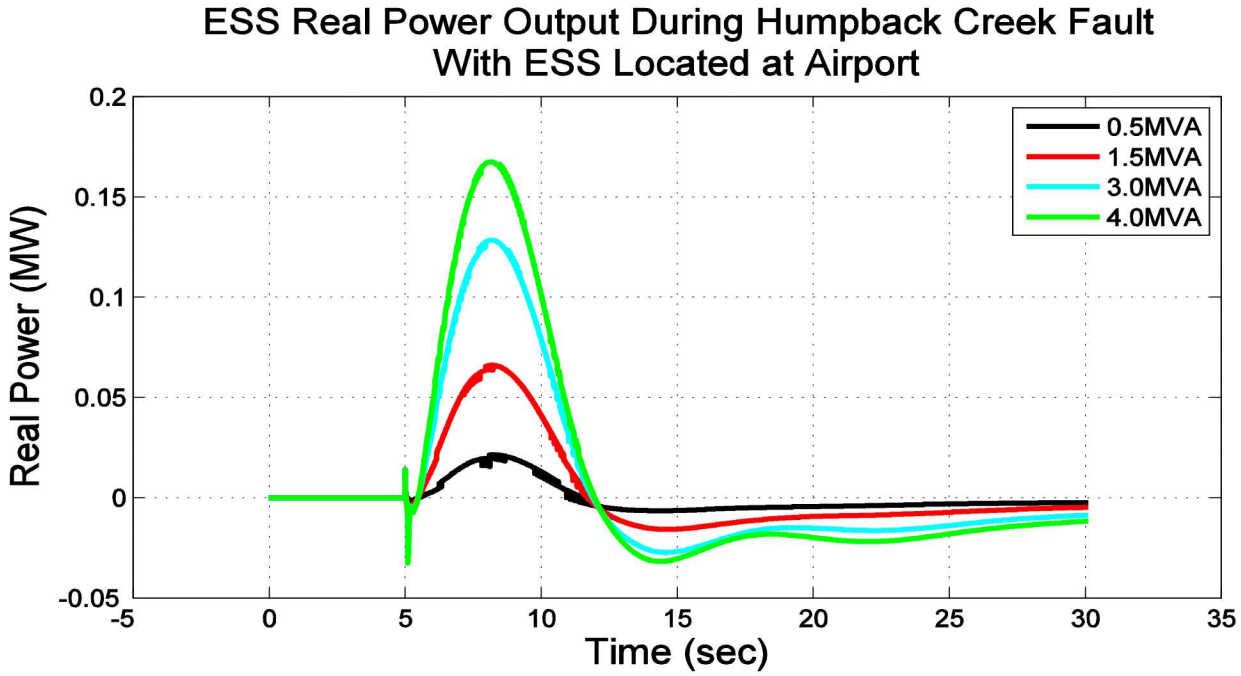

Figure 205 - Real power output of various ESS MVA ratings at Airport during fault along Humpback Creek feeder

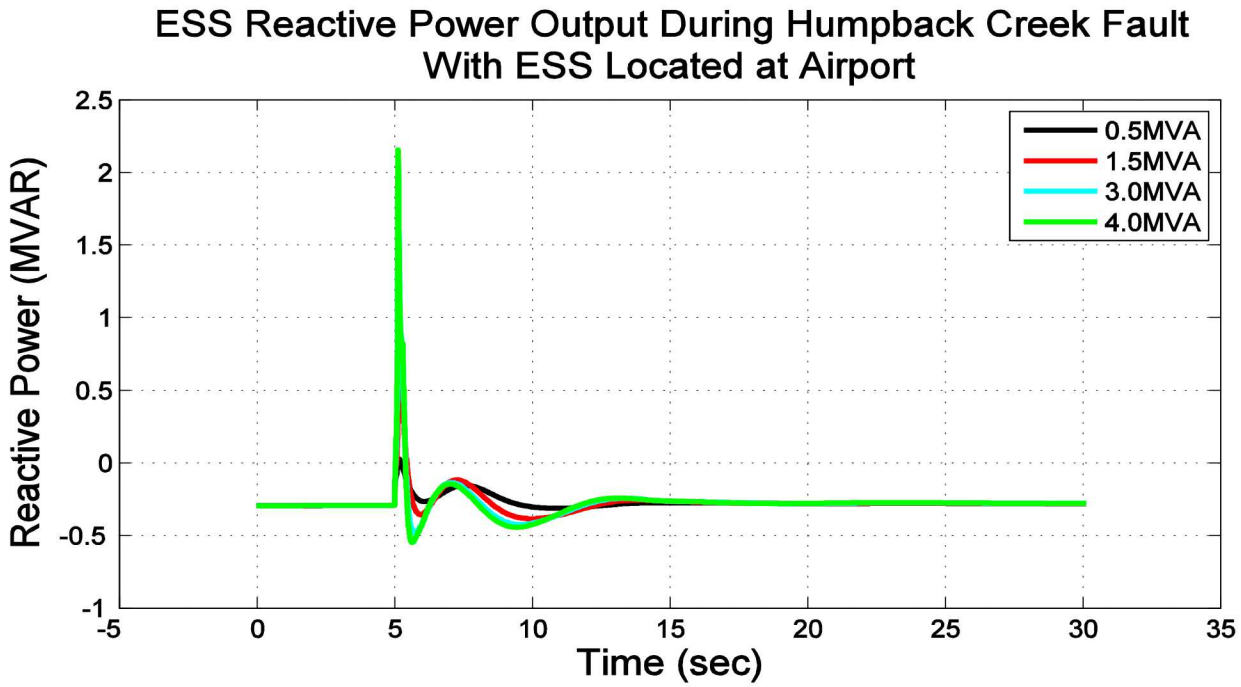

Figure 206 – Reactive power output of various ESS MVA ratings at Airport during fault along Humpback Creek feeder

ESS located at Orca Substation during Main Town feeder fault

Figures in this section are results from the PSLF dynamic simulation varying the ESS MVA ratings while located at the Orca Substation during a fault along the Main Town feeder.

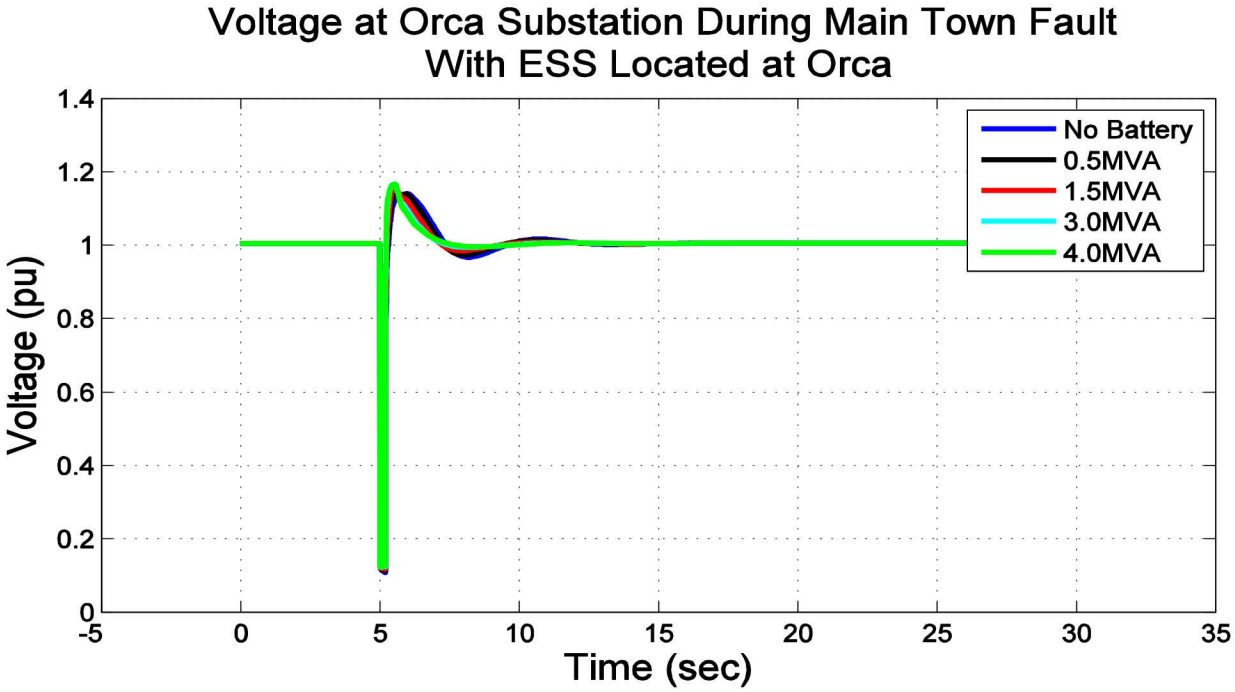

Figure 207 - Voltage at Orca Substation with varying ESS MVA ratings at Orca Substation during fault along Main Town feeder

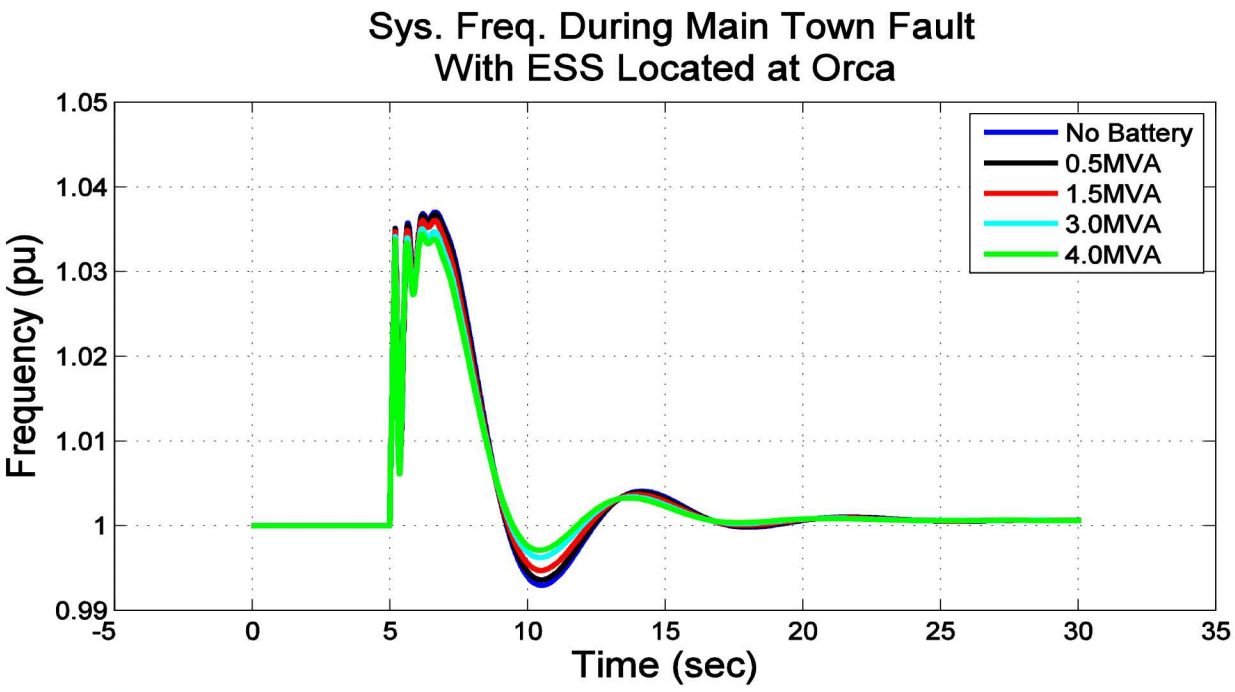

Figure 208 – System Frequency with varying ESS MVA ratings at Orca Substation during fault along Main Town feeder

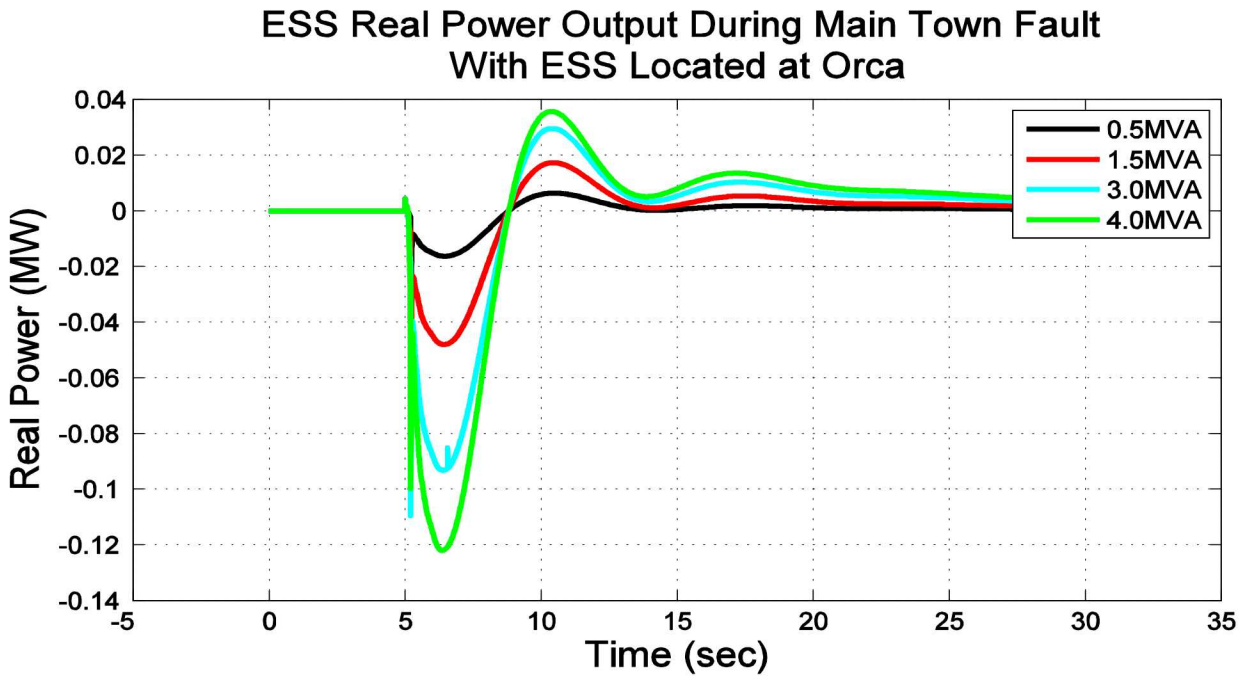

Figure 209 - Real power output of various ESS MVA ratings at Orca Substation during fault along Main Town feeder

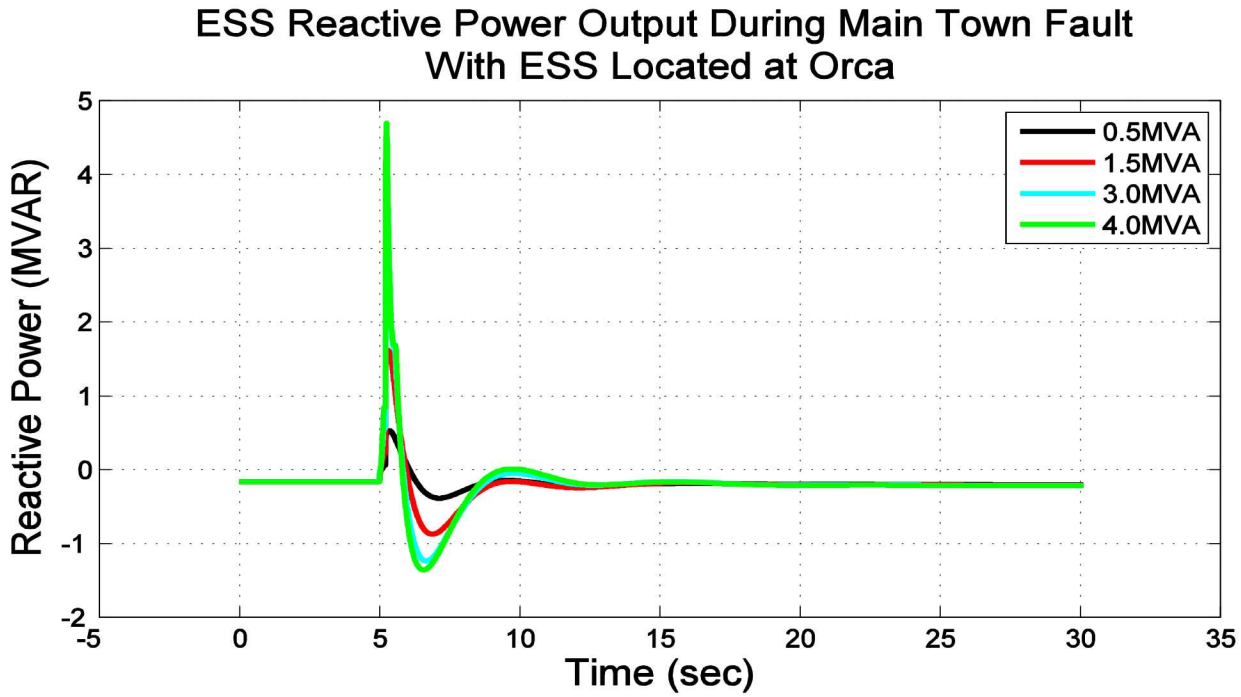

Figure 210 – Reactive power output of various ESS MVA ratings at Orca Substation during fault along Main Town feeder

ESS located at Eyak Substation during Main Town feeder fault

Figures in this section are results from the PSLF dynamic simulation varying the ESS MVA ratings while located at the Eyak Substation during a fault along the Main Town feeder.

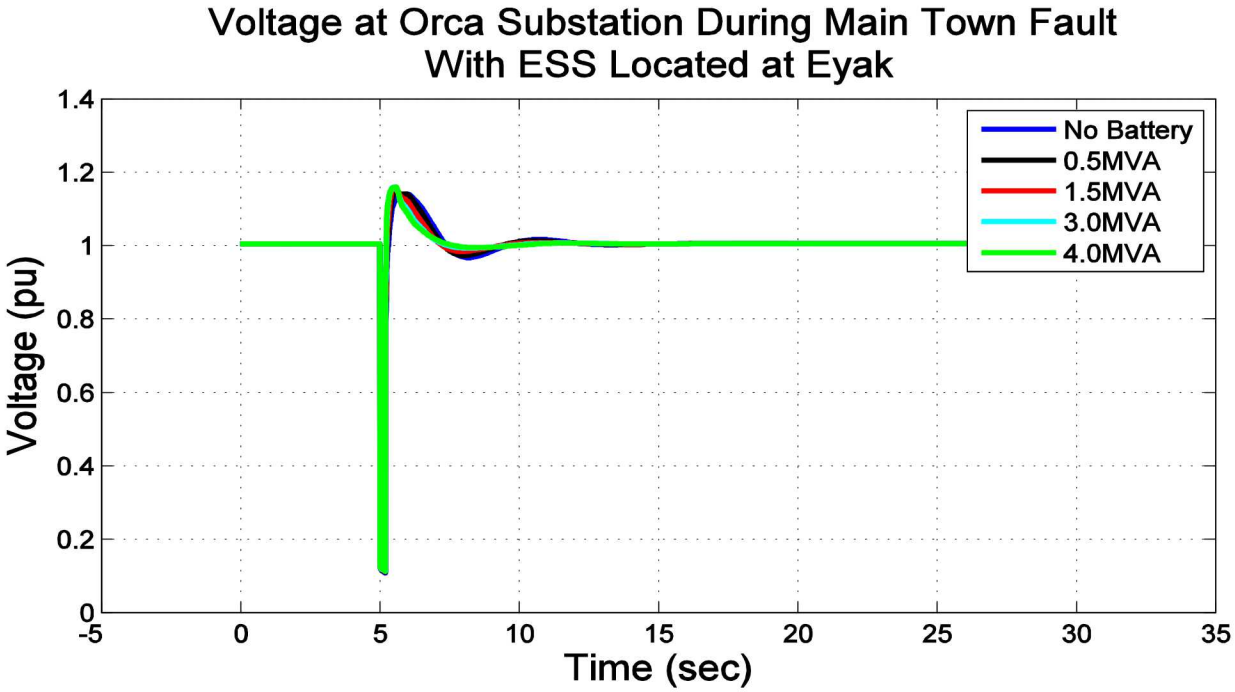

Figure 211 - Voltage at Orca Substation with varying ESS MVA ratings at Eyak Substation during fault along Main Town feeder

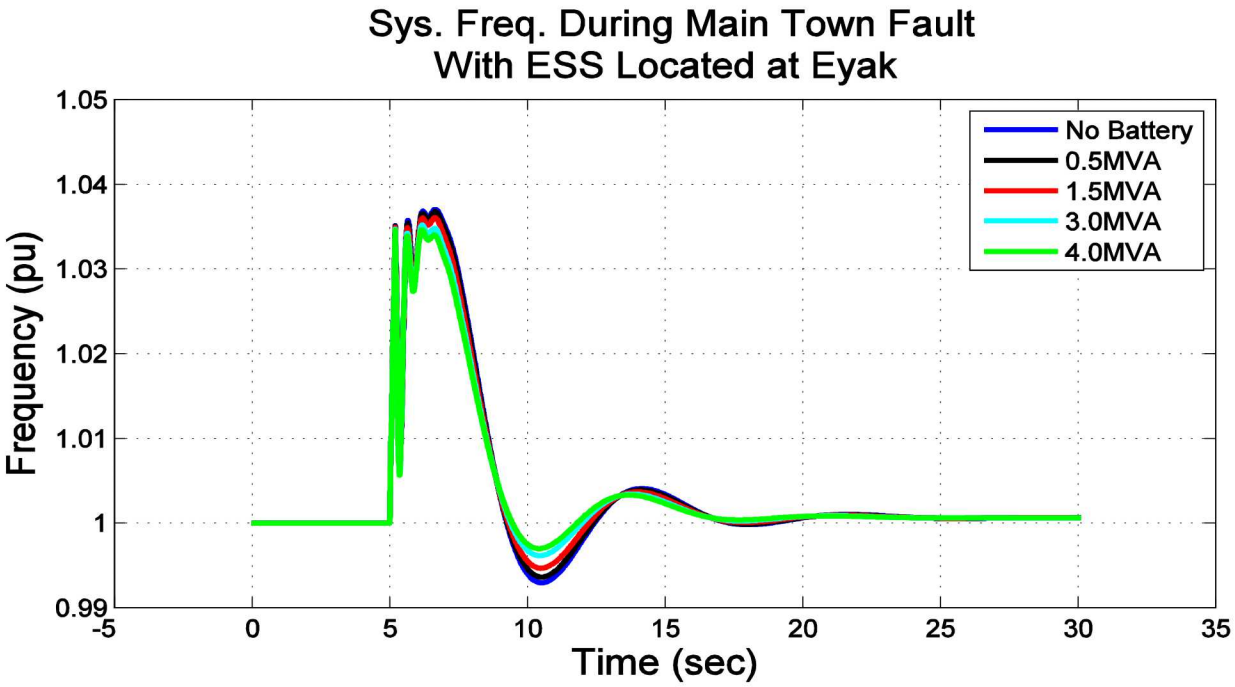

Figure 212 – System Frequency with varying ESS MVA ratings at Eyak Substation during fault along Main Town feeder

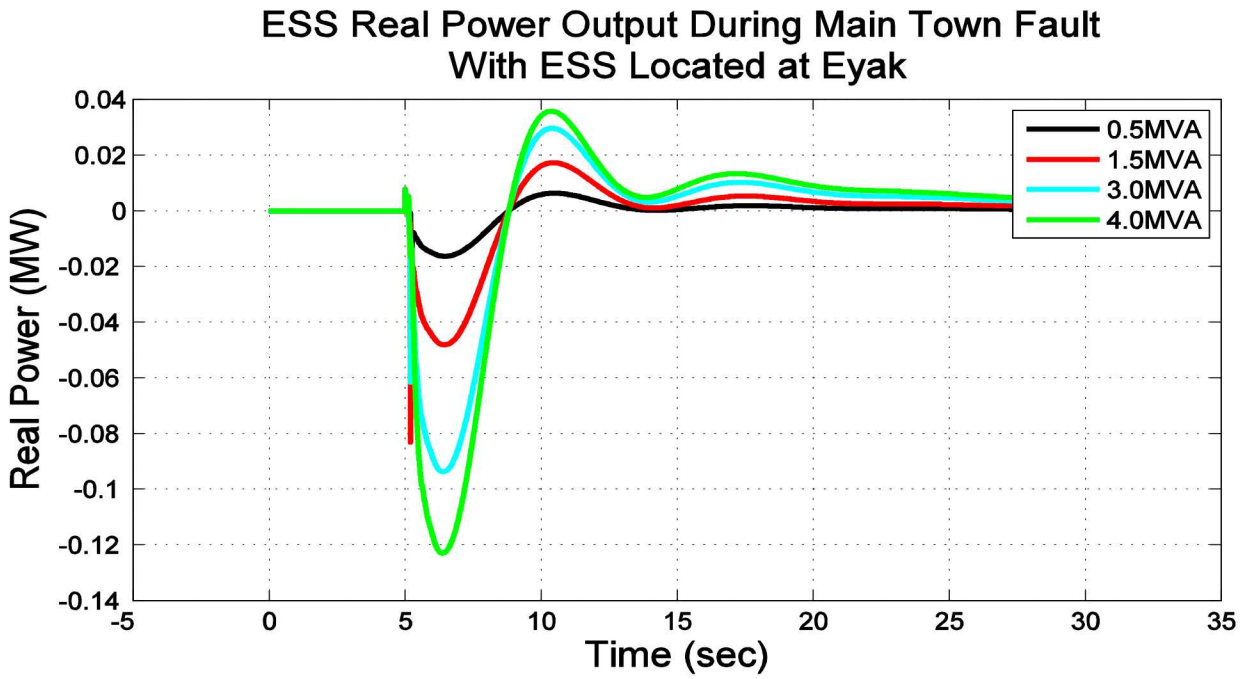

Figure 213 - Real power output of various ESS MVA ratings at Eyak Substation during fault along Main Town feeder

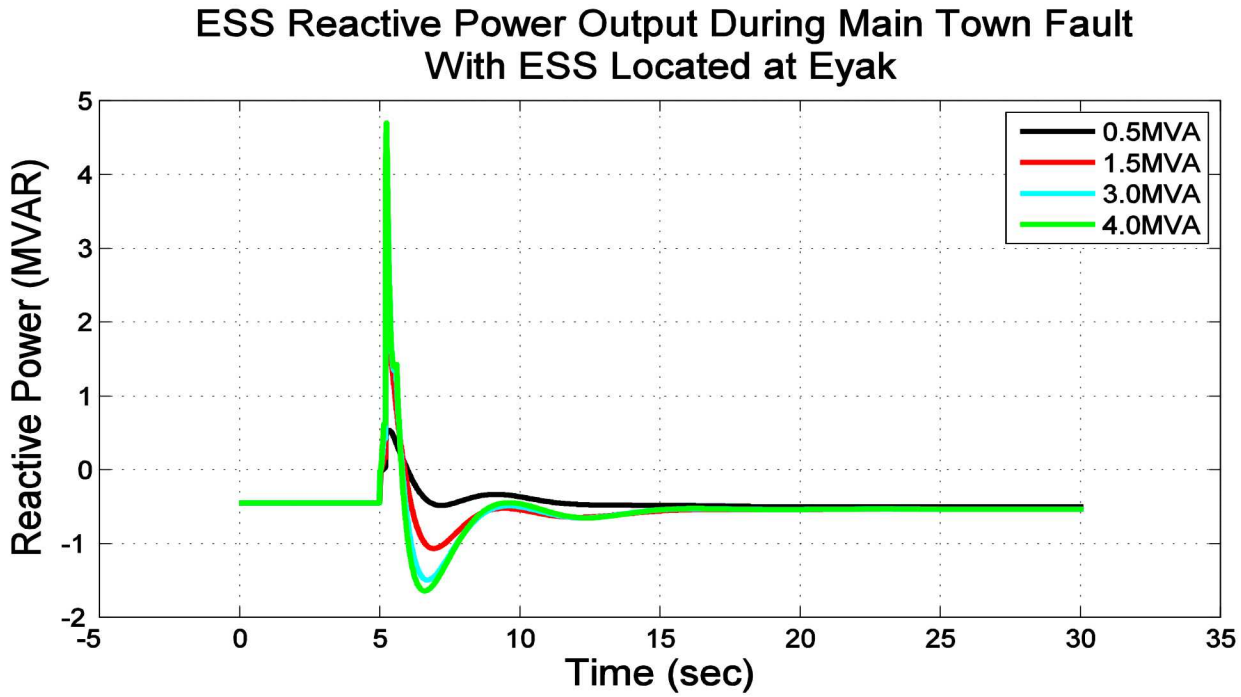

Figure 214 – Reactive power output of various ESS MVA ratings at Eyak Substation during fault along Main Town feeder

ESS located at Main Hospital during Main Town feeder fault

Figures in this section are results from the PSLF dynamic simulation varying the ESS MVA ratings while located at the main Hospital during a fault along the Main Town feeder.

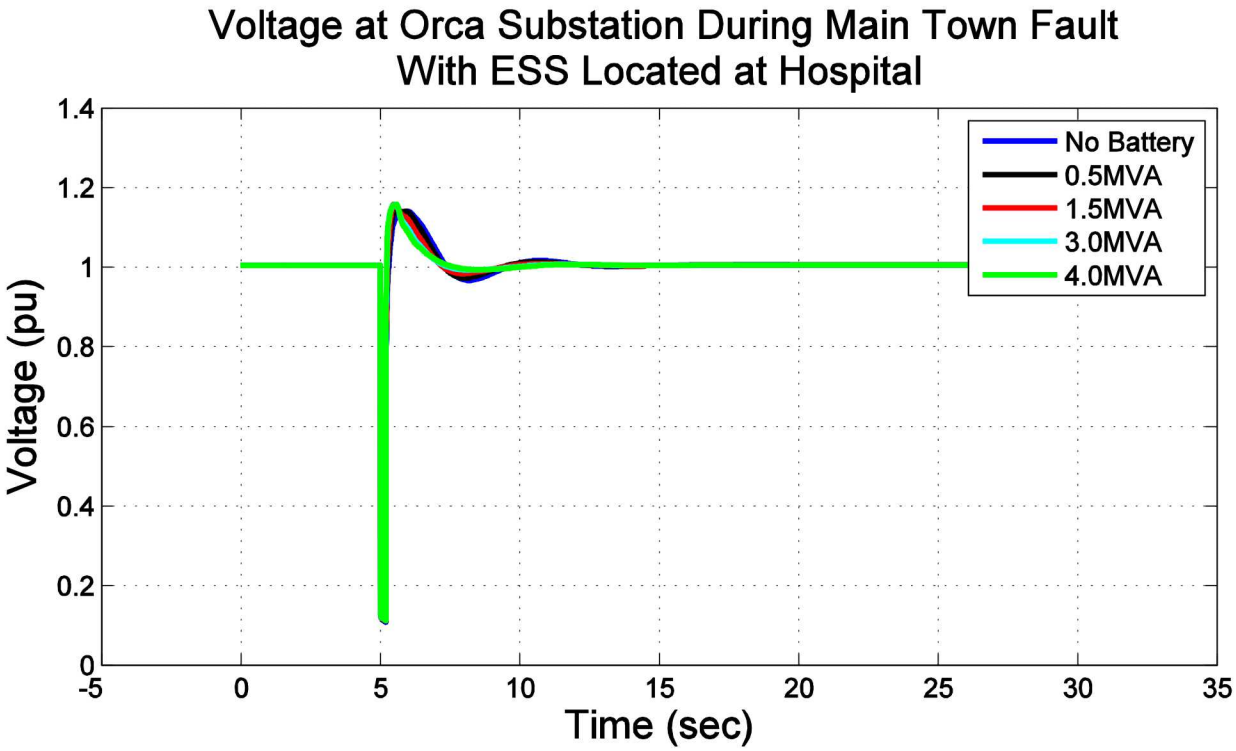

Figure 215 - Voltage at Orca Substation with varying ESS MVA ratings at Main Hospital during fault along Main Town feeder

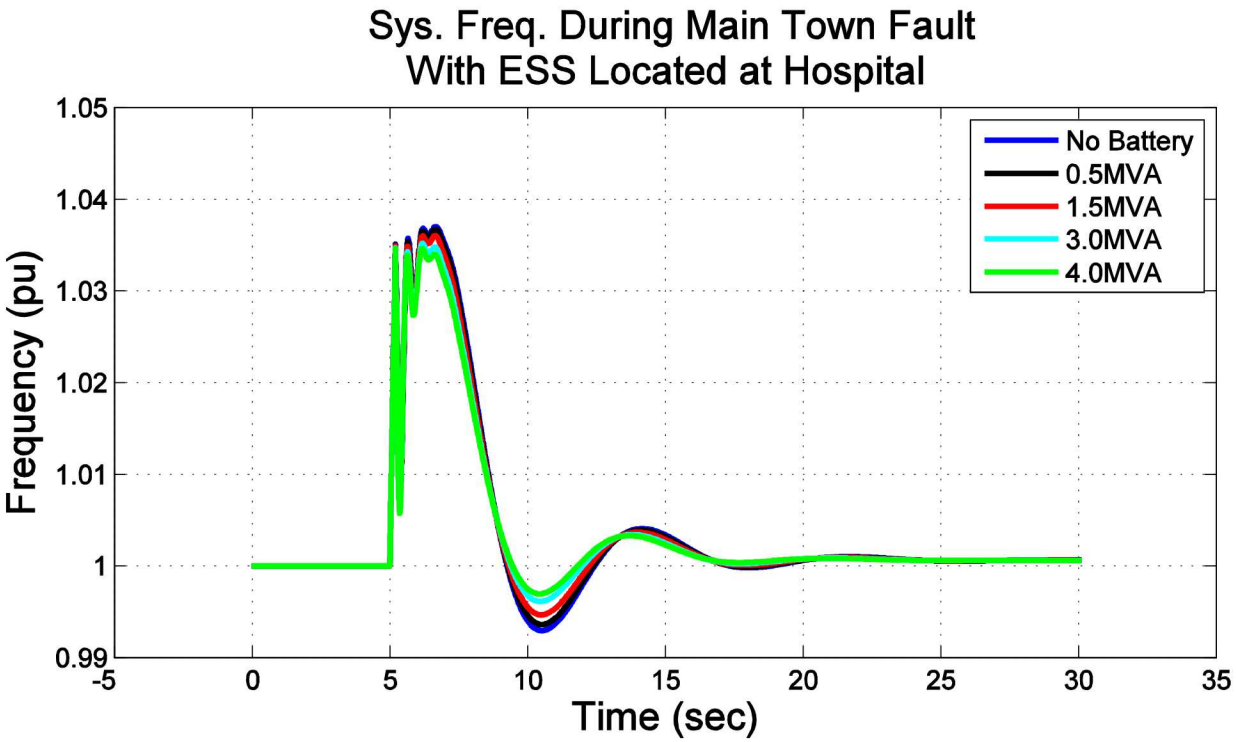

Figure 216 - System Frequency with varying ESS MVA ratings at Main Hospital during fault along Main Town feeder

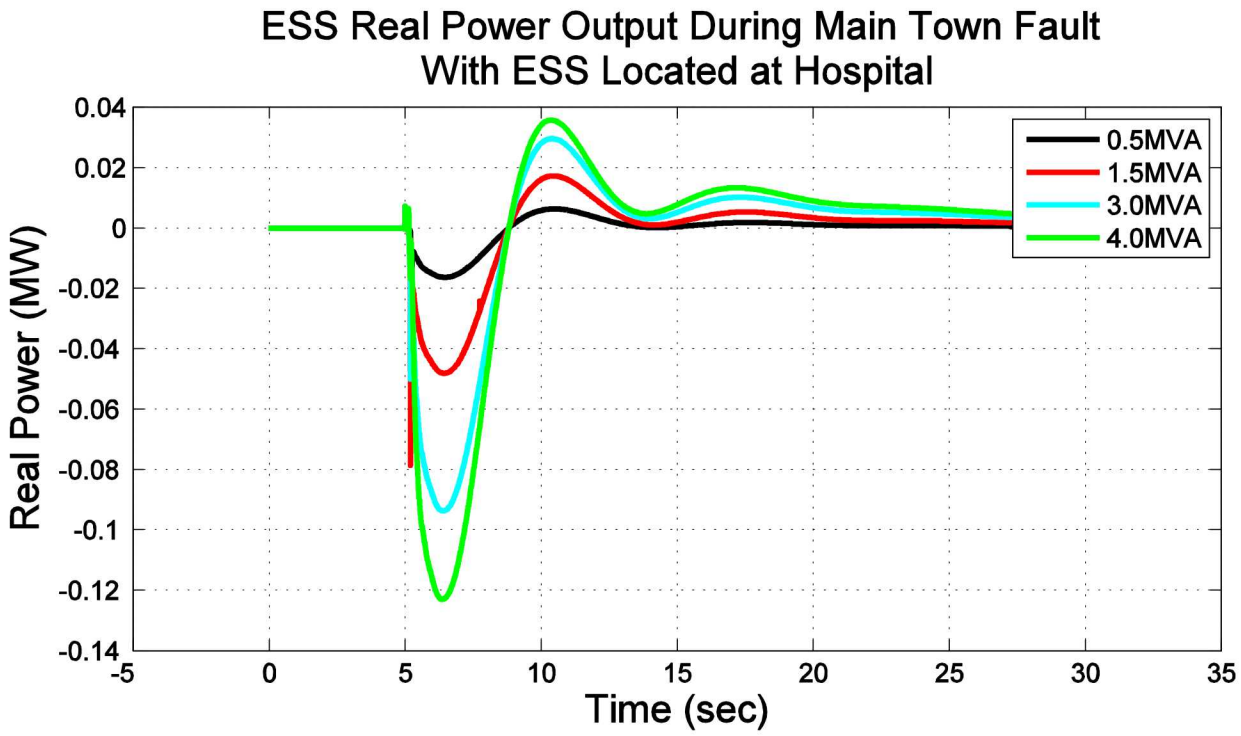

Figure 217 - Real power output of various ESS MVA ratings at Hospital during fault along Main Town feeder

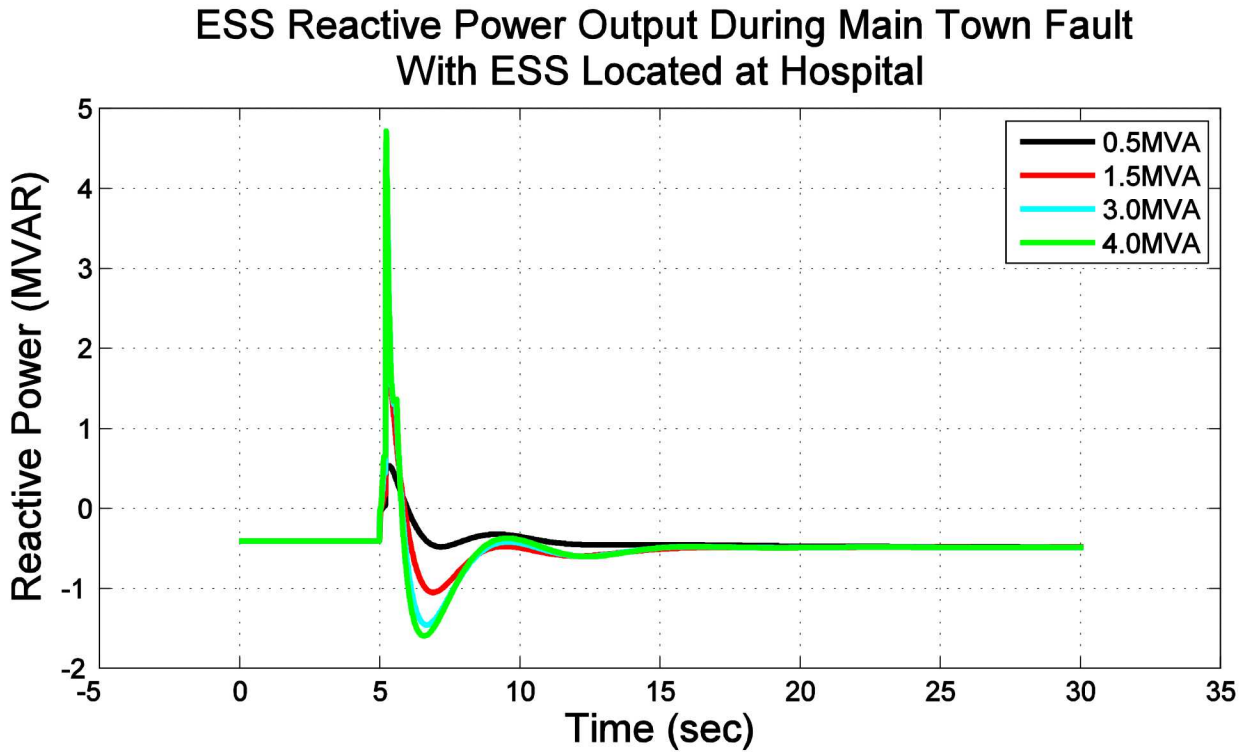

Figure 218 - Reactive power output of various ESS MVA ratings at Hospital during fault along Main Town feeder

ESS located at Airport during Main Town feeder fault

Figures in this section are results from the PSLF dynamic simulation varying the ESS MVA ratings while located at the Airport during a fault along the Main Town feeder.

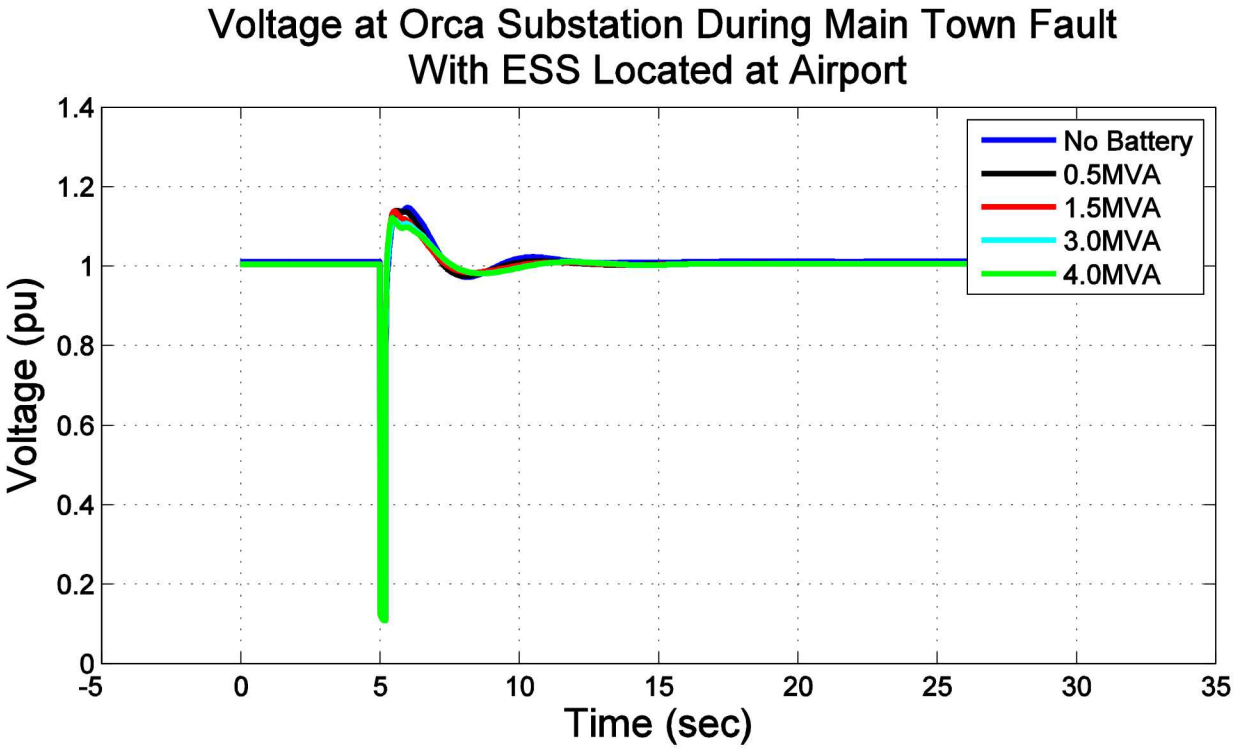

Figure 219 - Voltage at Orca Substation with varying ESS MVA ratings at Airport during fault along Main Town feeder

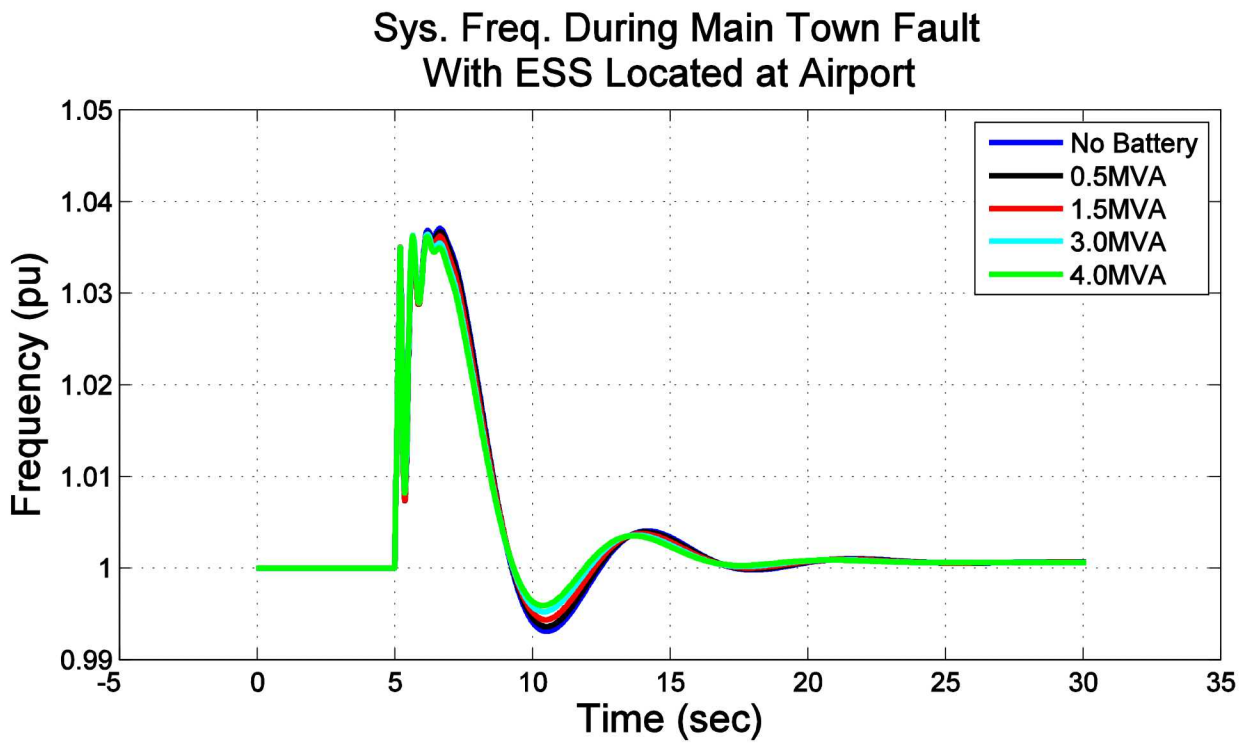

Figure 220 - System Frequency with varying ESS MVA ratings at Airport during fault along Main Town feeder

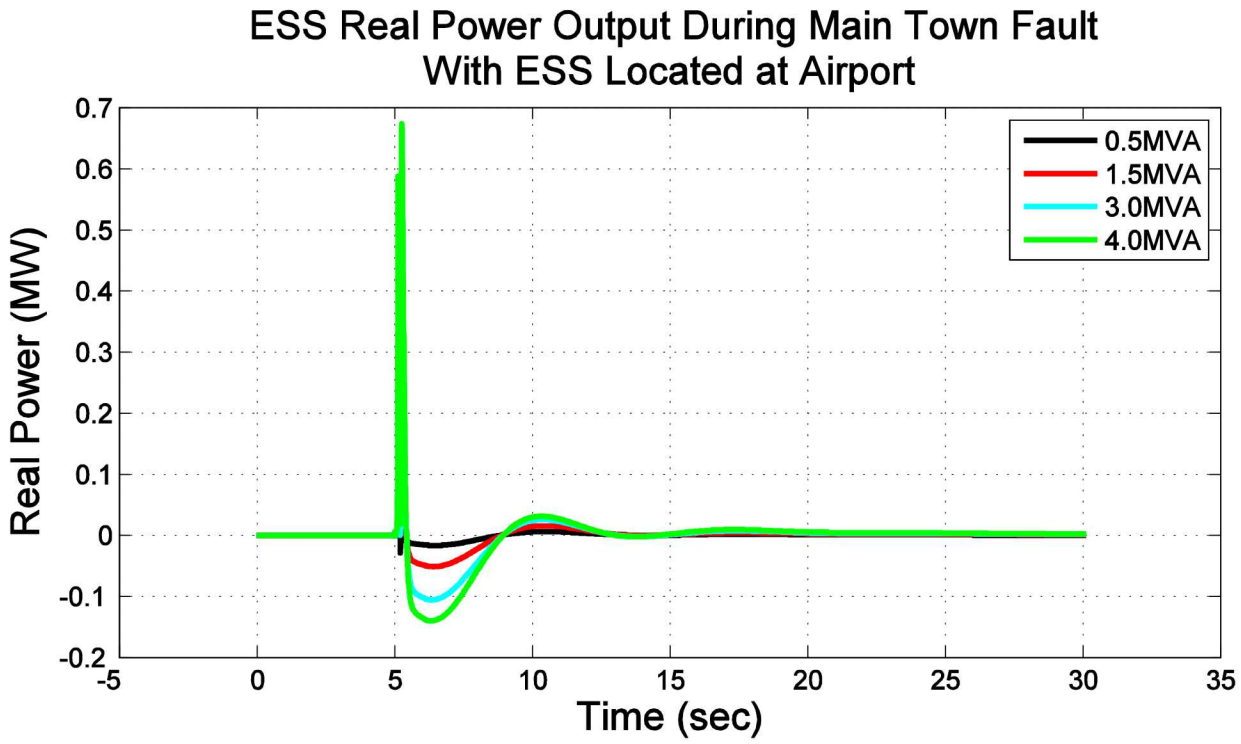

Figure 221 - Real power output of various ESS MVA ratings at Airport during fault along Main Town feeder

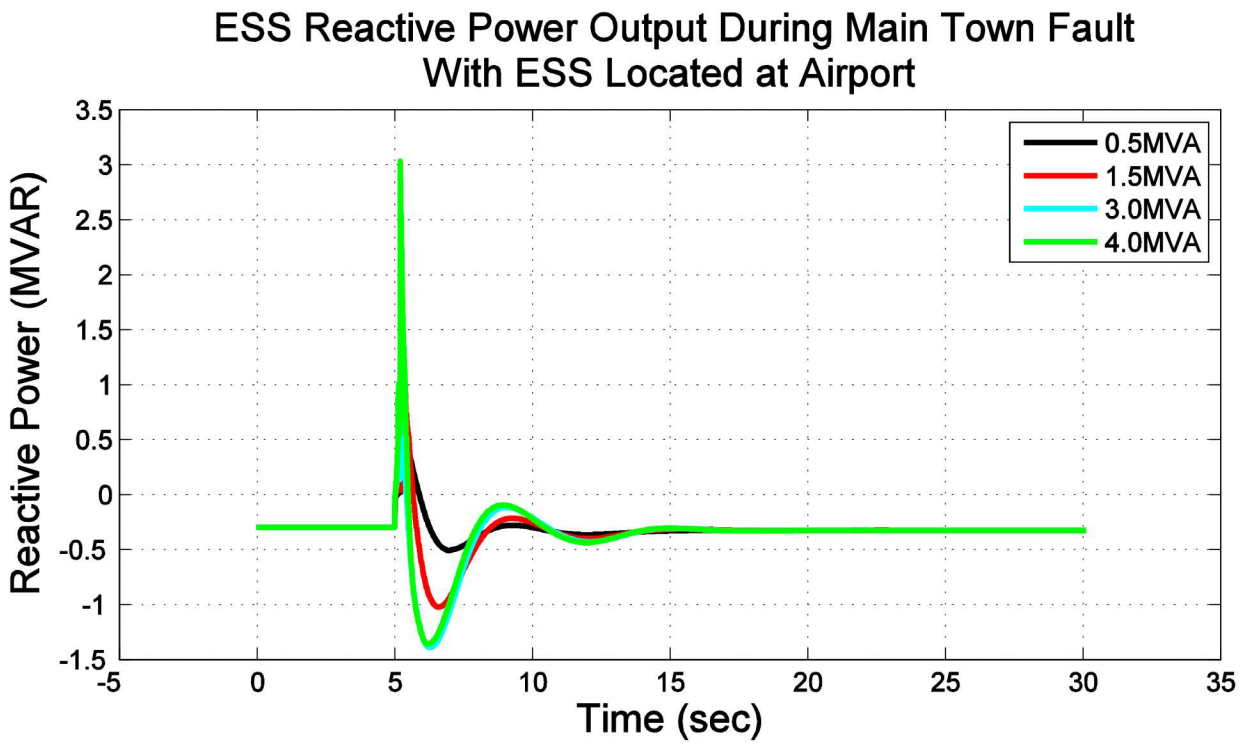

Figure 222 - Reactive power output of various ESS MVA ratings at Airport during fault along Main Town feeder

ESS located at Orca Substation during Lake Avenue feeder fault

Figures in this section are results from the PSLF dynamic simulation varying the ESS MVA ratings while located at the Orca Substation during a fault along the Lake Avenue feeder.

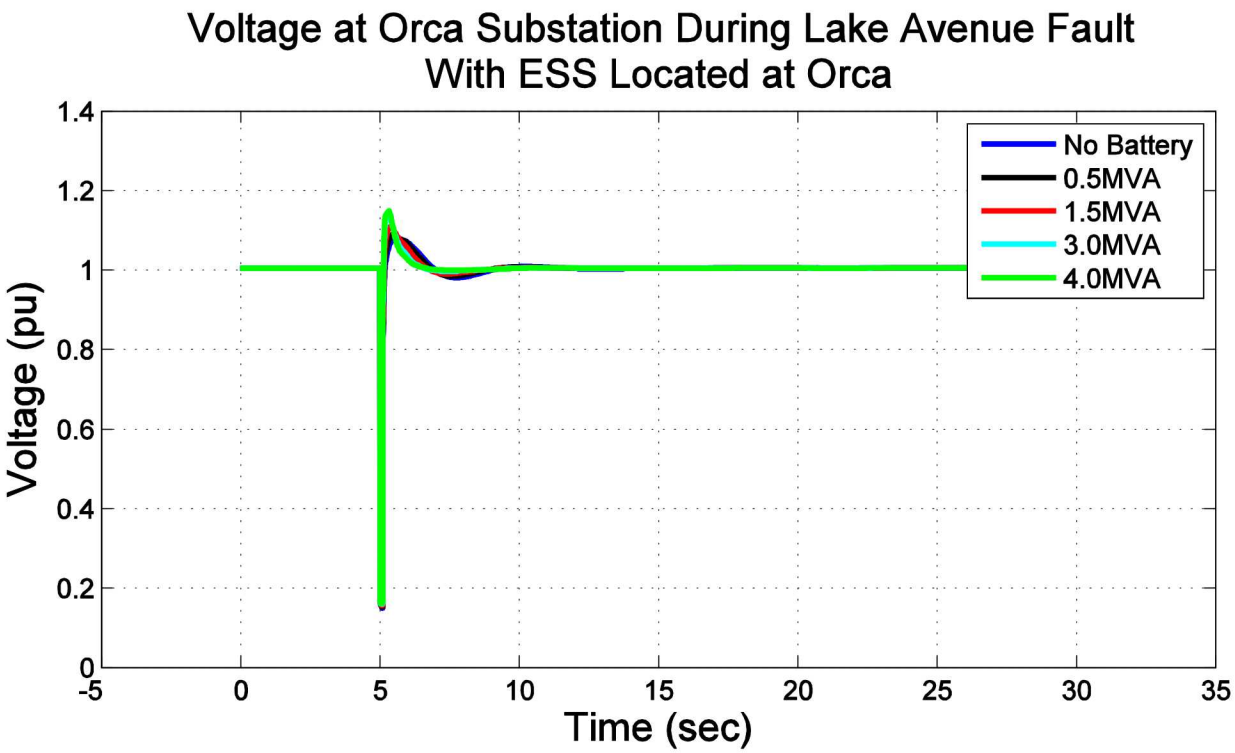

Figure 223 - Voltage at the Orca Substation with varying ESS MVA ratings at Orca Substation during fault along Lake Avenue feeder

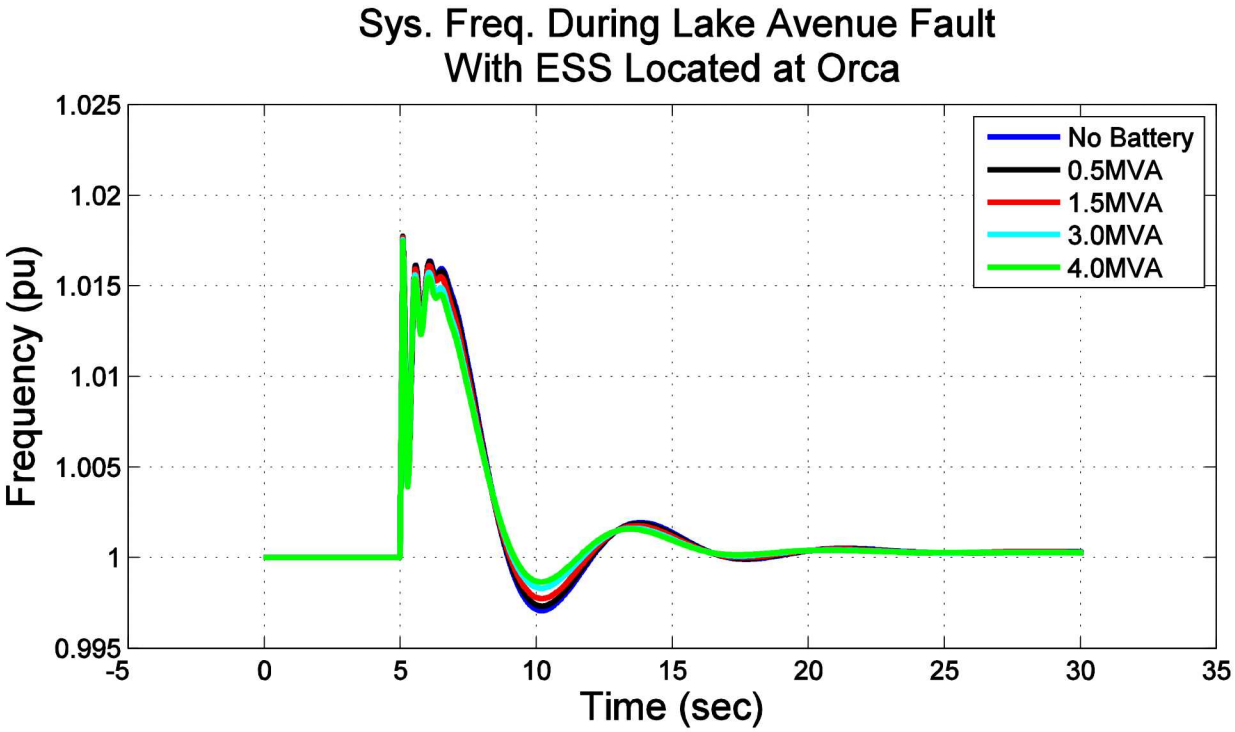

Figure 224 - System Frequency with varying ESS MVA ratings at Orca Substation during fault along Lake Avenue feeder

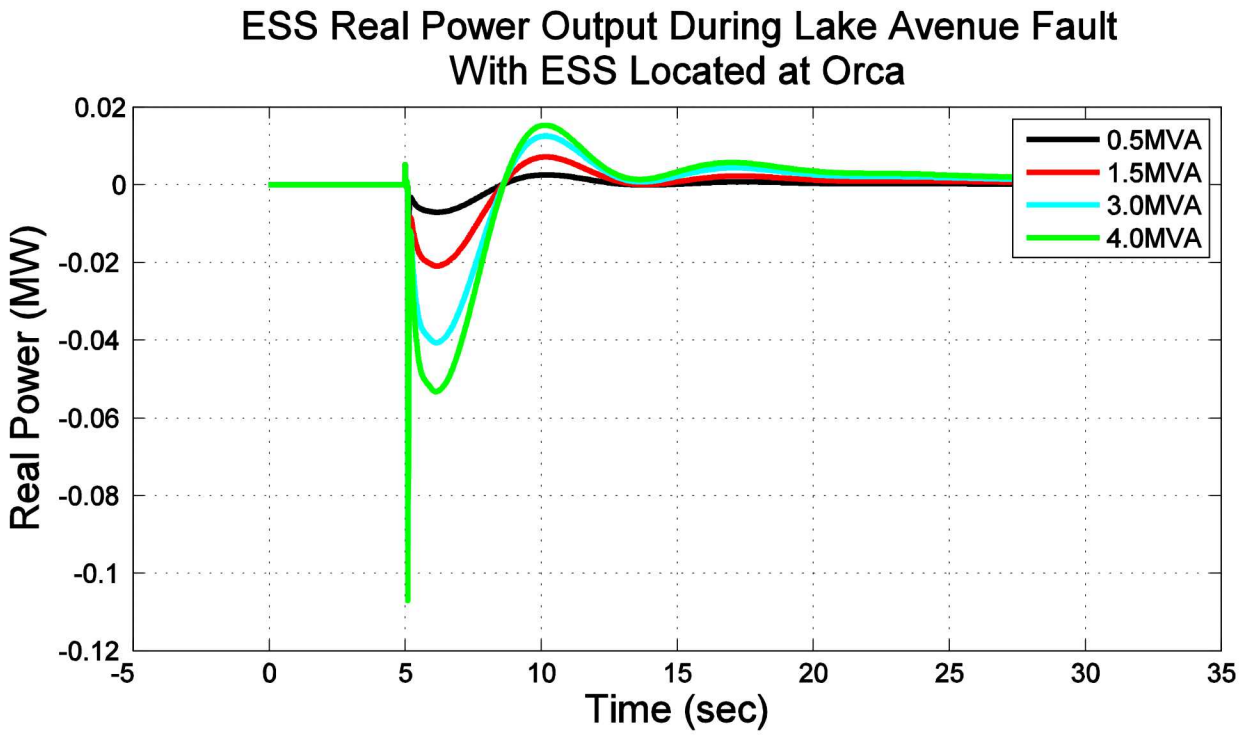

Figure 225 - Real power output of various ESS MVA ratings at Orca Substation during fault along Lake Avenue feeder

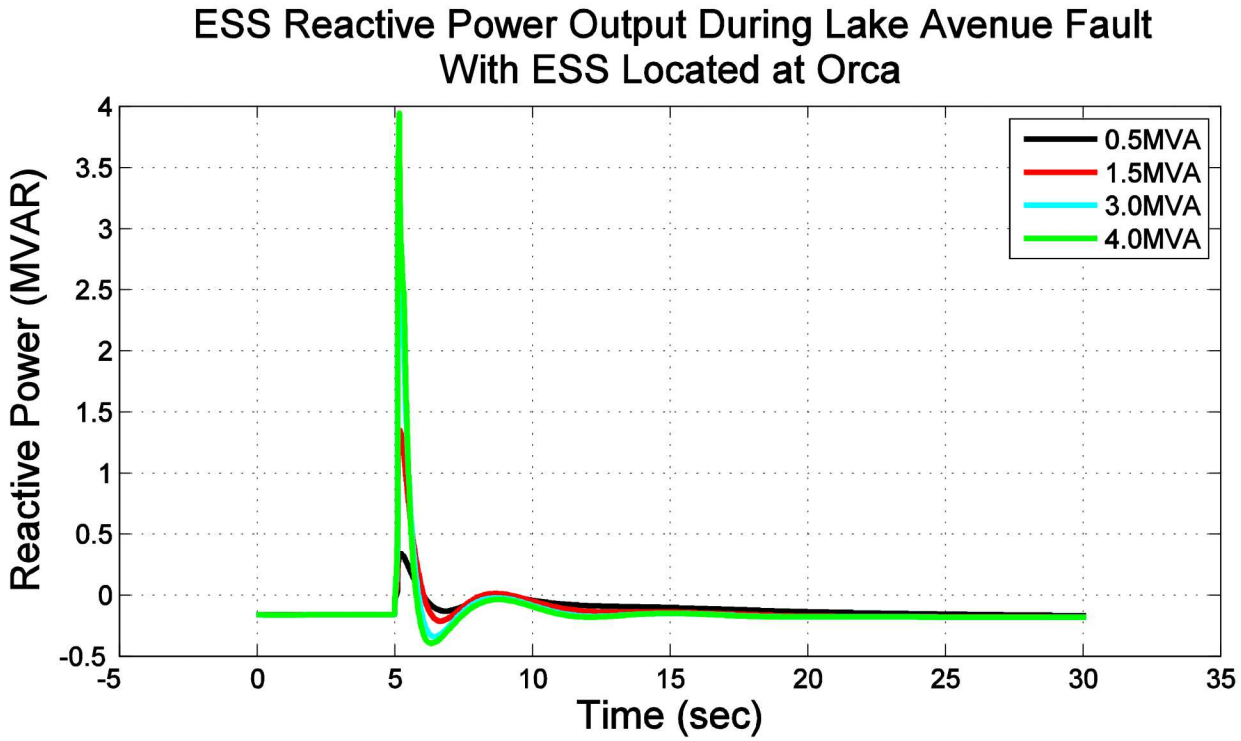

Figure 226 - Reactive power output of various ESS MVA ratings at Orca Substation during fault along Lake Avenue feeder

ESS located at Eyak Substation during Lake Avenue feeder fault

Figures in this section are results from the PSLF dynamic simulation varying the ESS MVA ratings while located at the Eyak Substation during a fault along the Lake Avenue feeder.

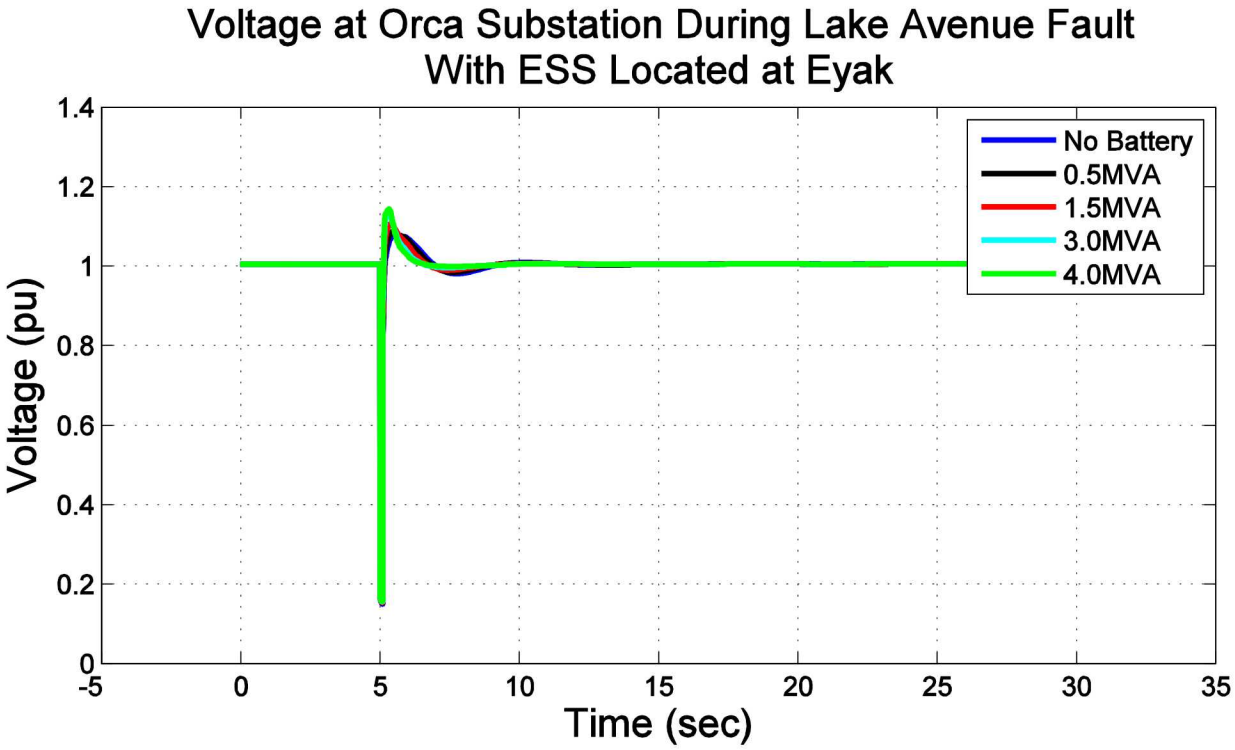

Figure 227 - Voltage at the Orca Substation with varying ESS MVA ratings at Eyak Substation during fault along Lake Avenue feeder

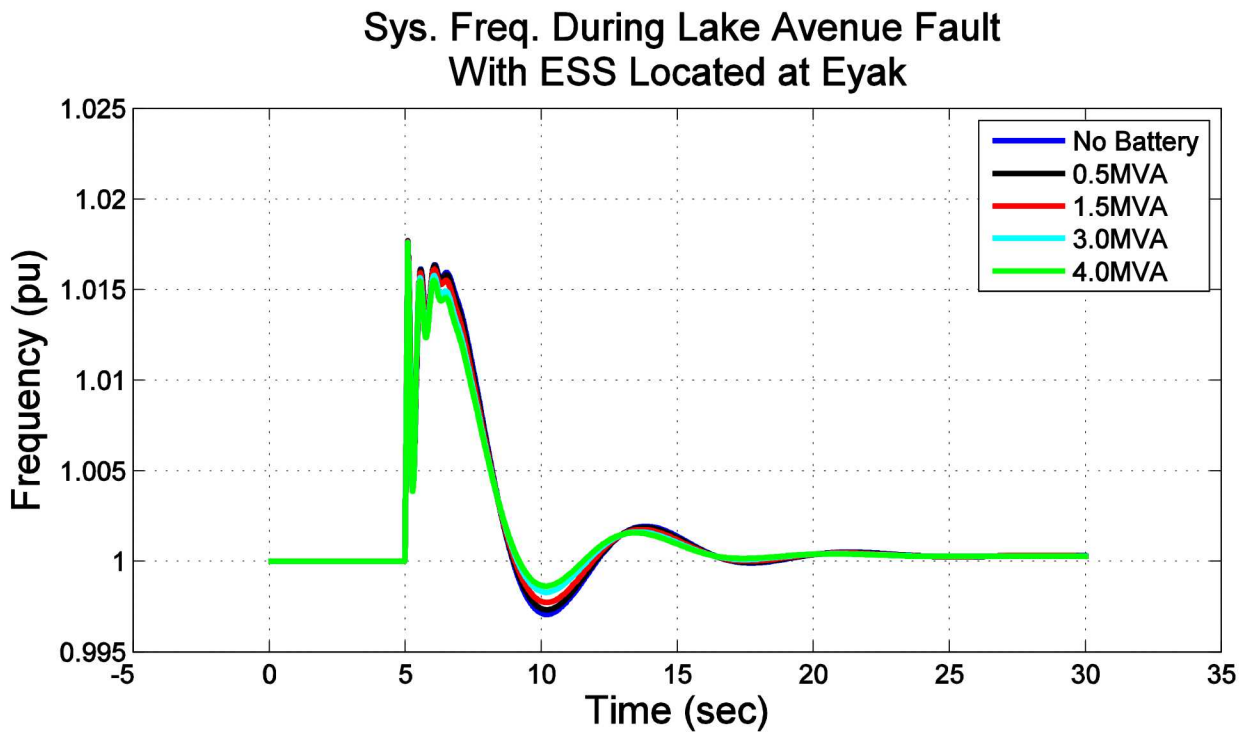

Figure 228 - System Frequency with varying ESS MVA ratings at Eyak Substation during fault along Lake Avenue feeder

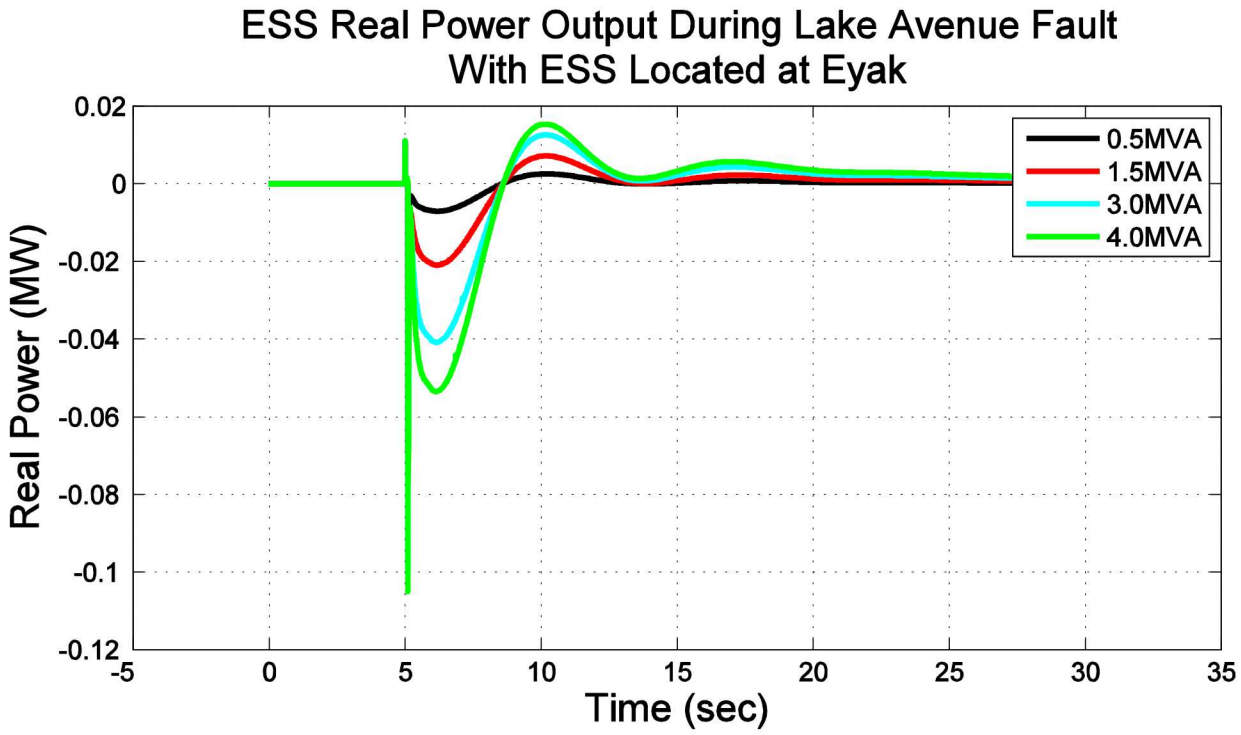

Figure 229 - Real power output of various ESS MVA ratings at Eyak Substation during fault along Lake Avenue feeder

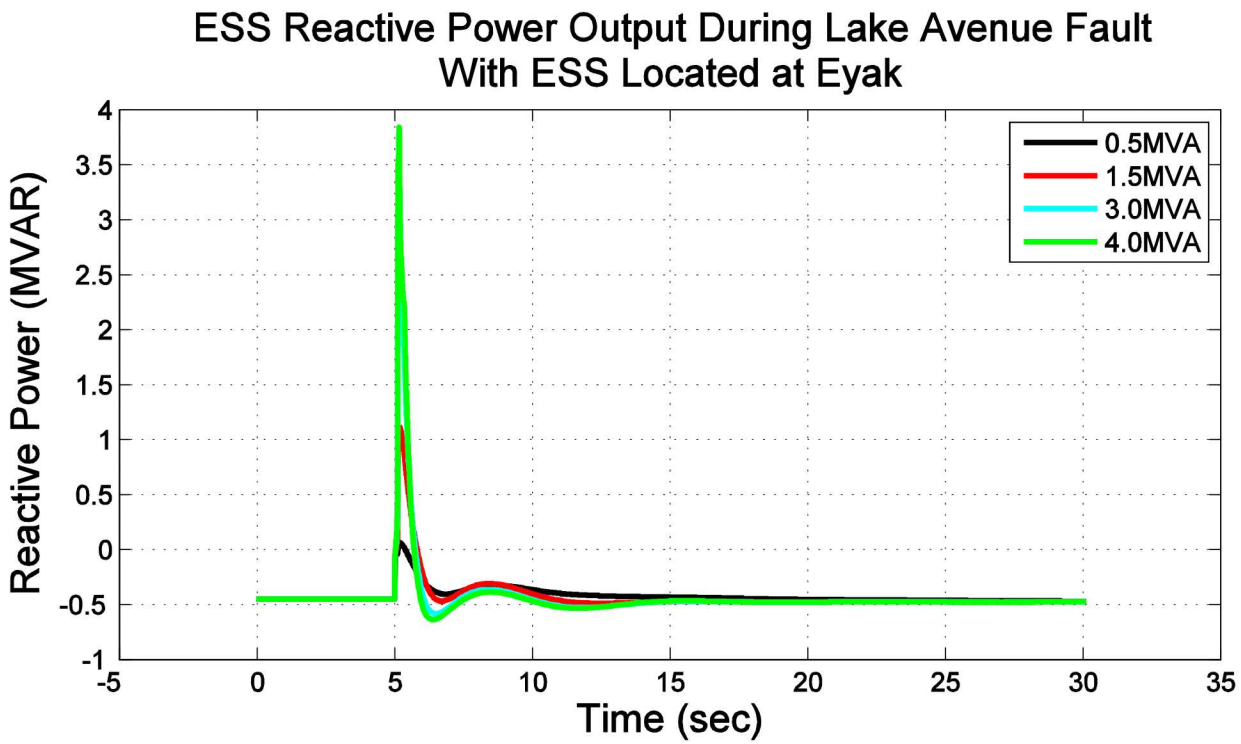

Figure 230 - Reactive power output of various ESS MVA ratings at Eyak Substation during fault along Lake Avenue feeder

ESS located at Main Hospital during Lake Avenue feeder fault

Figures in this section are results from the PSLF dynamic simulation varying the ESS MVA ratings while located at the main Hospital during a fault along the Lake Avenue feeder.

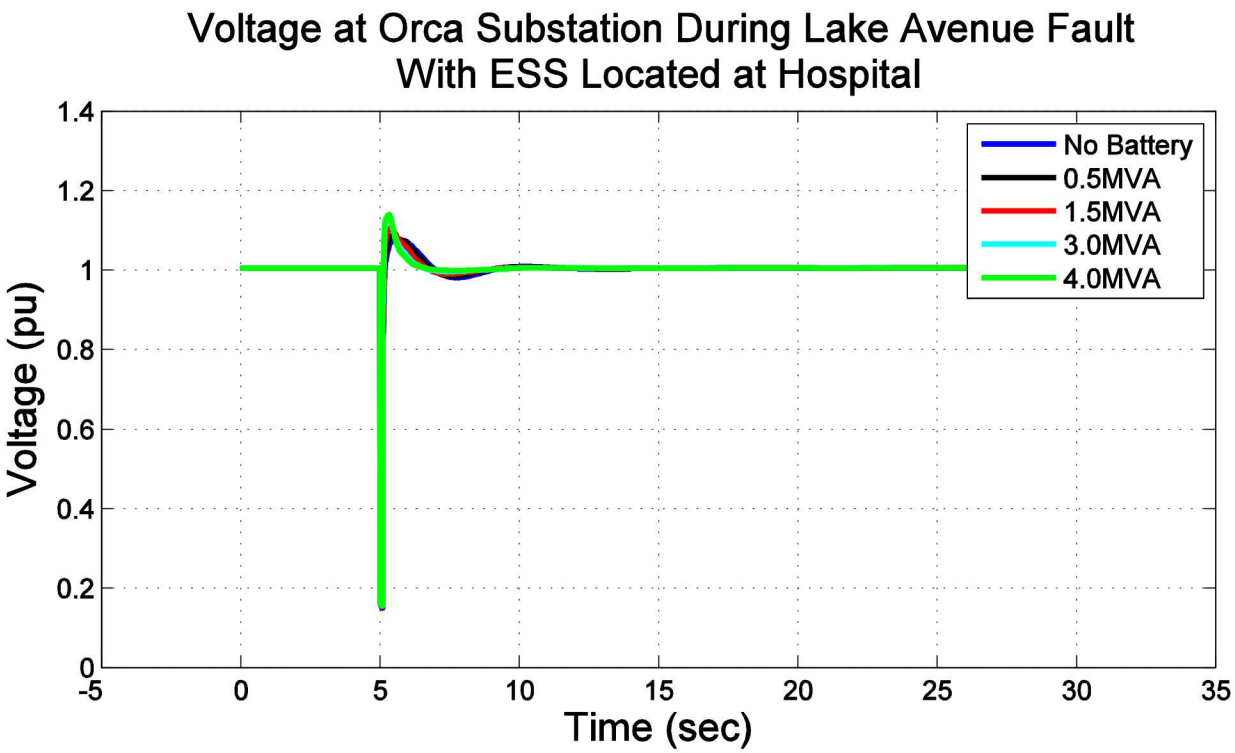

Figure 231 - Voltage at the Orca Substation with varying ESS MVA ratings at Hospital during fault along Lake Avenue feeder

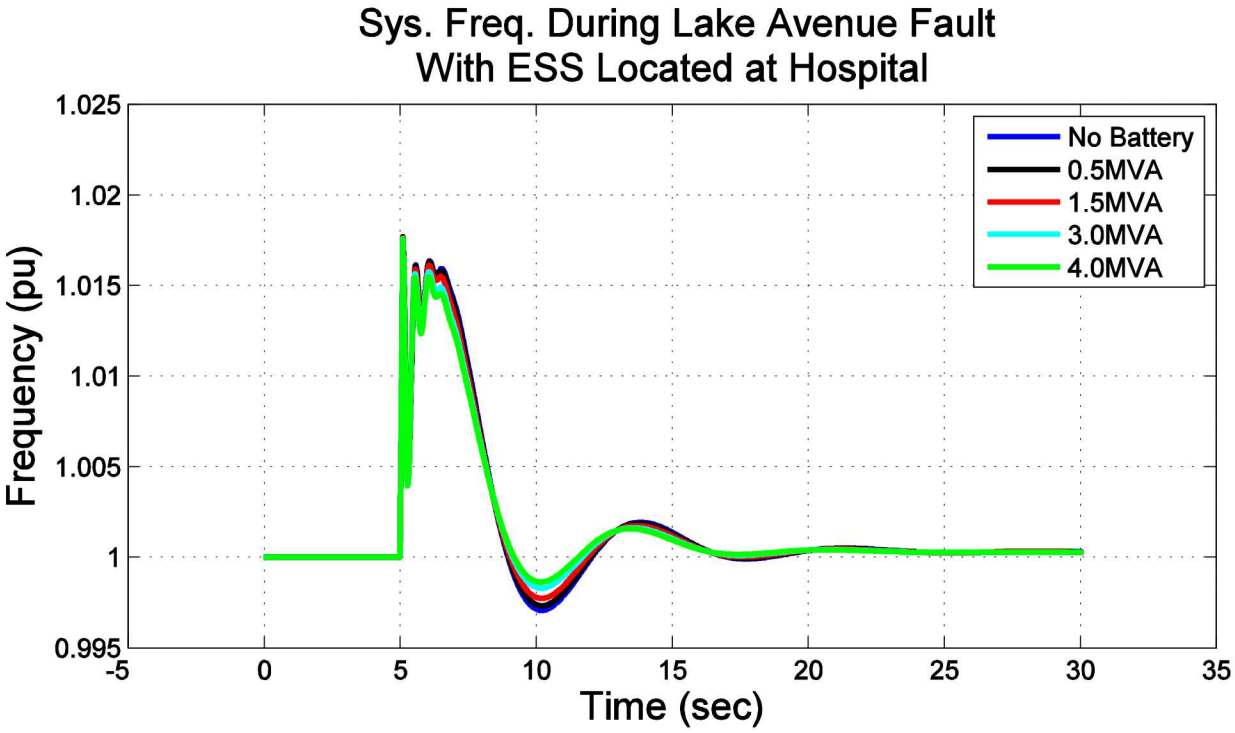

Figure 232 - System Frequency with varying ESS MVA ratings at Hospital during fault along Lake Avenue feeder

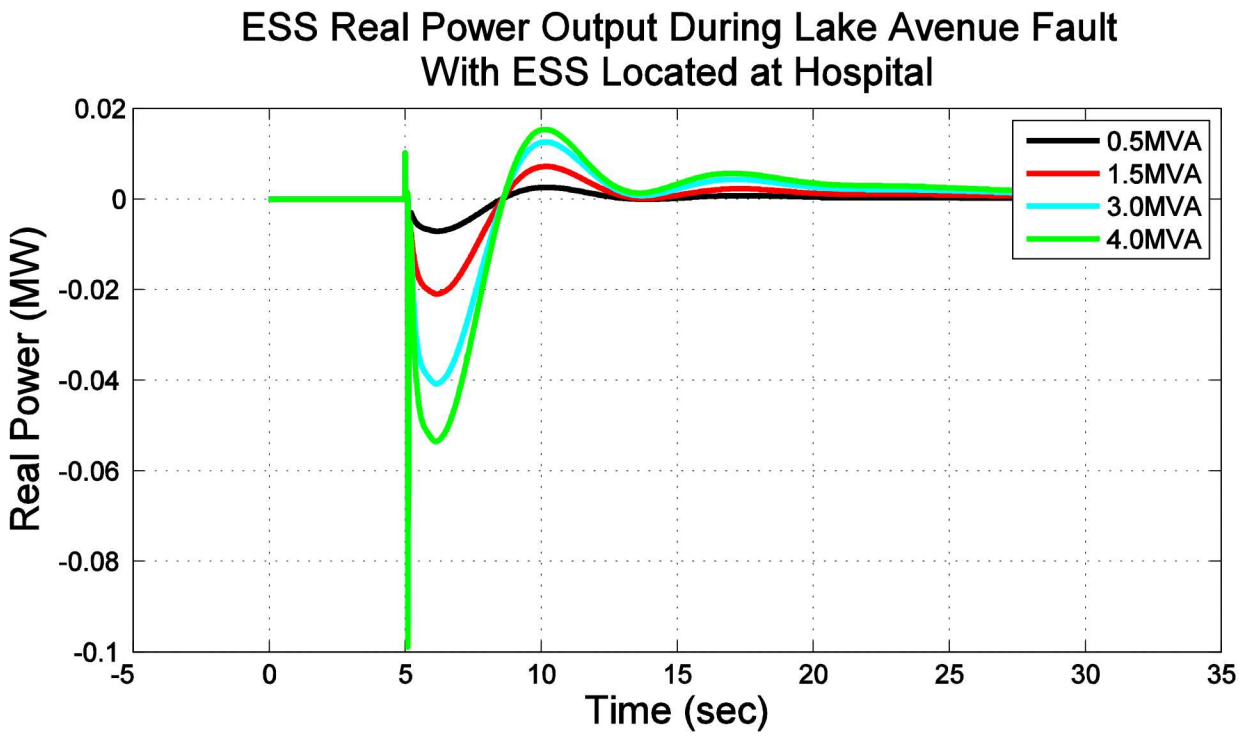

Figure 233 - Real power output of various ESS MVA ratings at Hospital during fault along Lake Avenue feeder

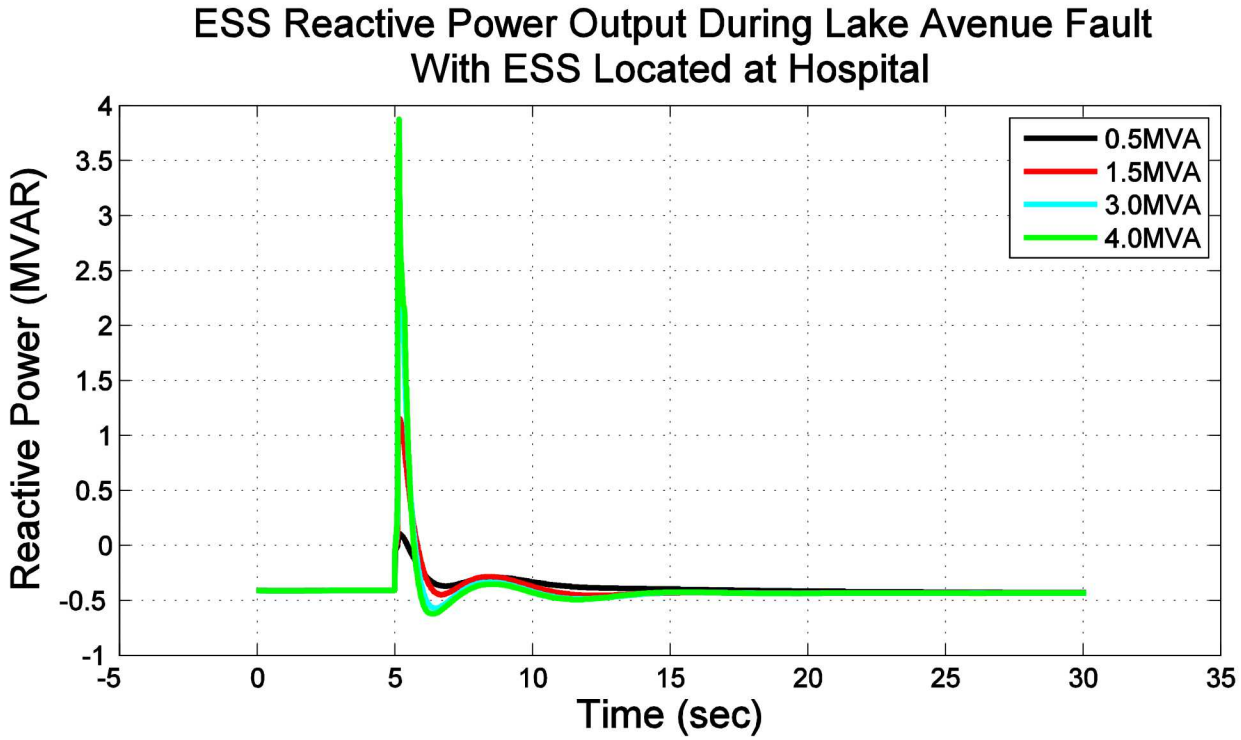

Figure 234 - Reactive power output of various ESS MVA ratings at Hospital during fault along Lake Avenue feeder

ESS located at Airport during Lake Avenue feeder fault

Figures in this section are results from the PSLF dynamic simulation varying the ESS MVA ratings while located at the main Airport during a fault along the Lake Avenue feeder.

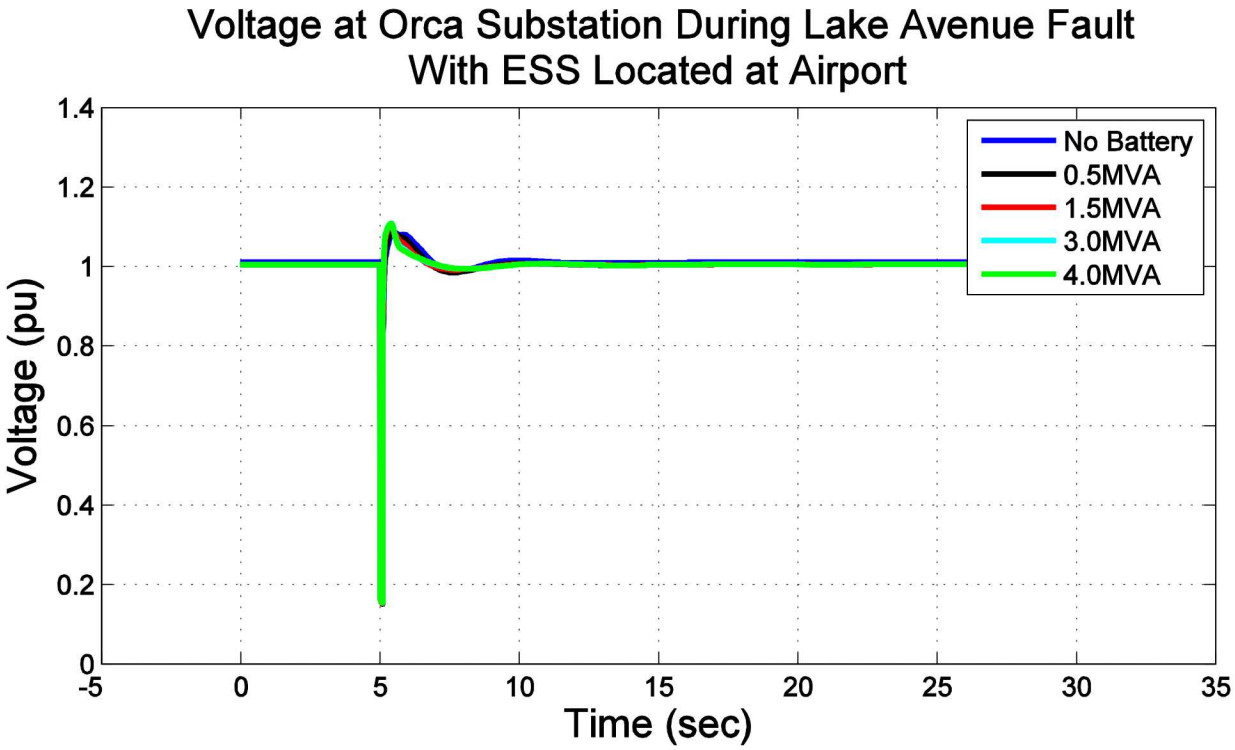

Figure 235 - Voltage at the Orca Substation with varying ESS MVA ratings at Airport during fault along Lake Avenue feeder

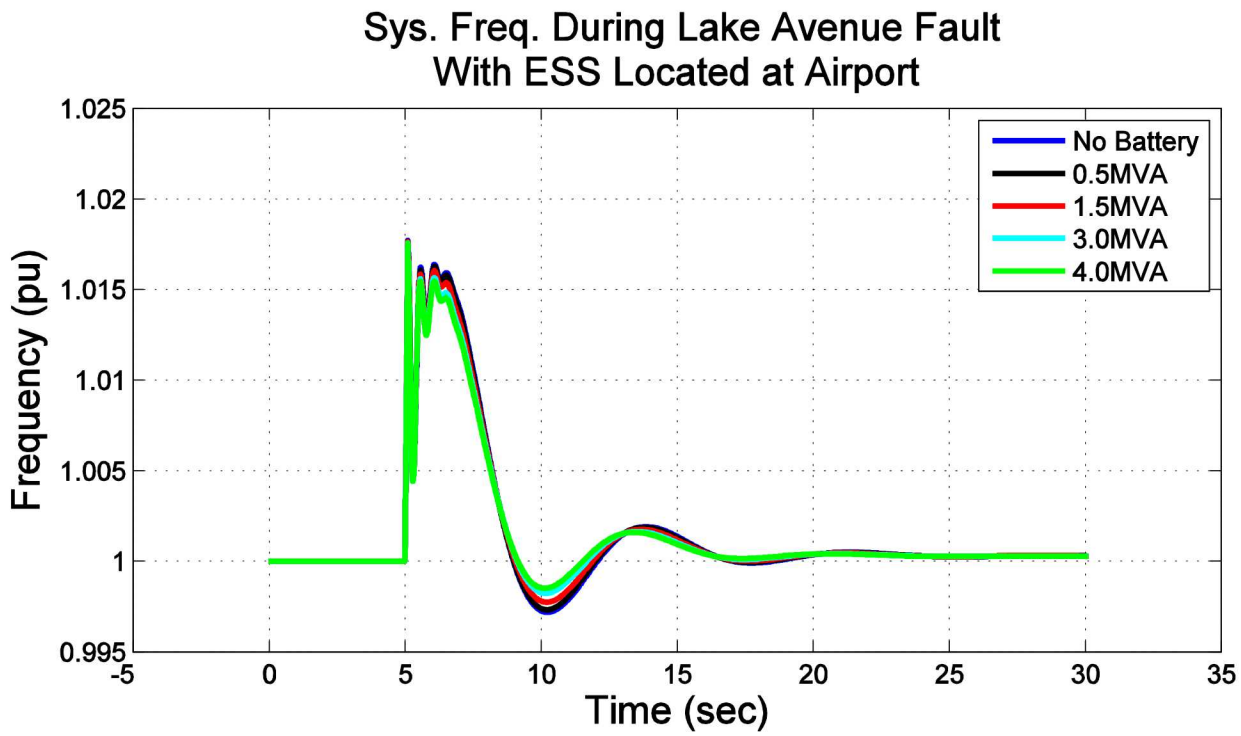

Figure 236 - System Frequency with varying ESS MVA ratings at Airport during fault along Lake Avenue feeder

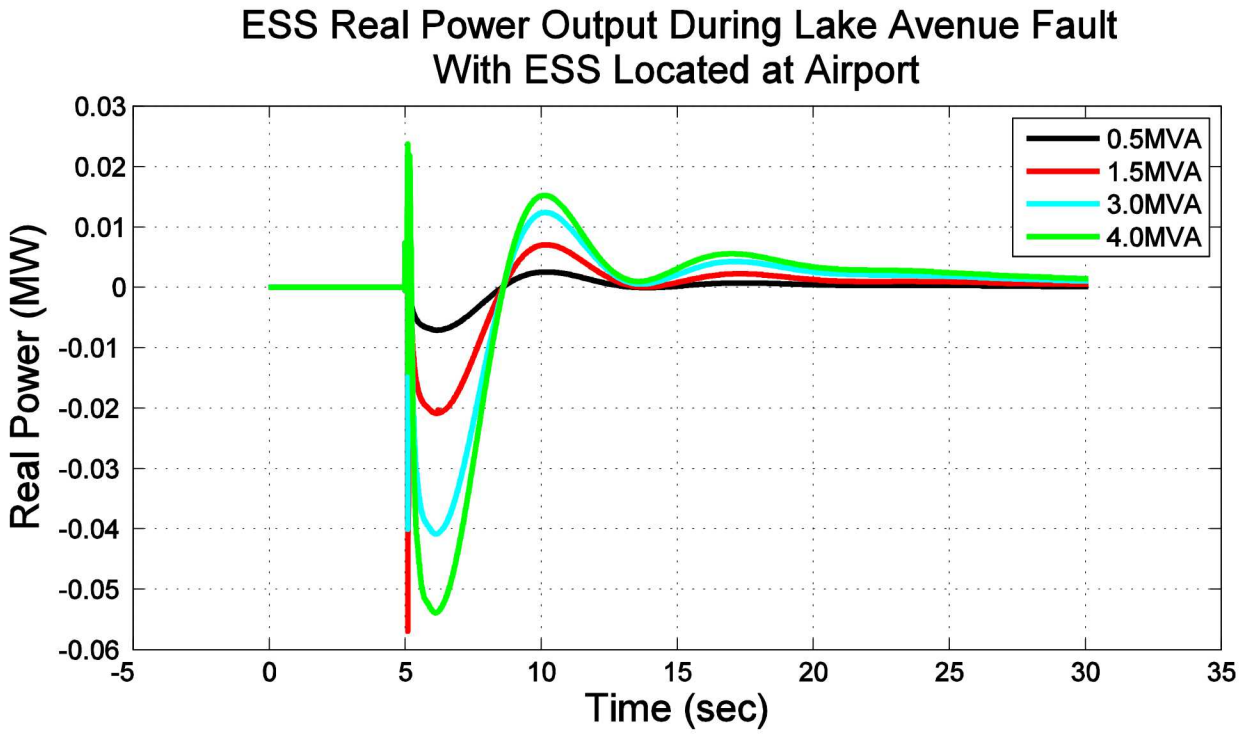

Figure 237 - Real power output of various ESS MVA ratings at Airport during fault along Lake Avenue feeder

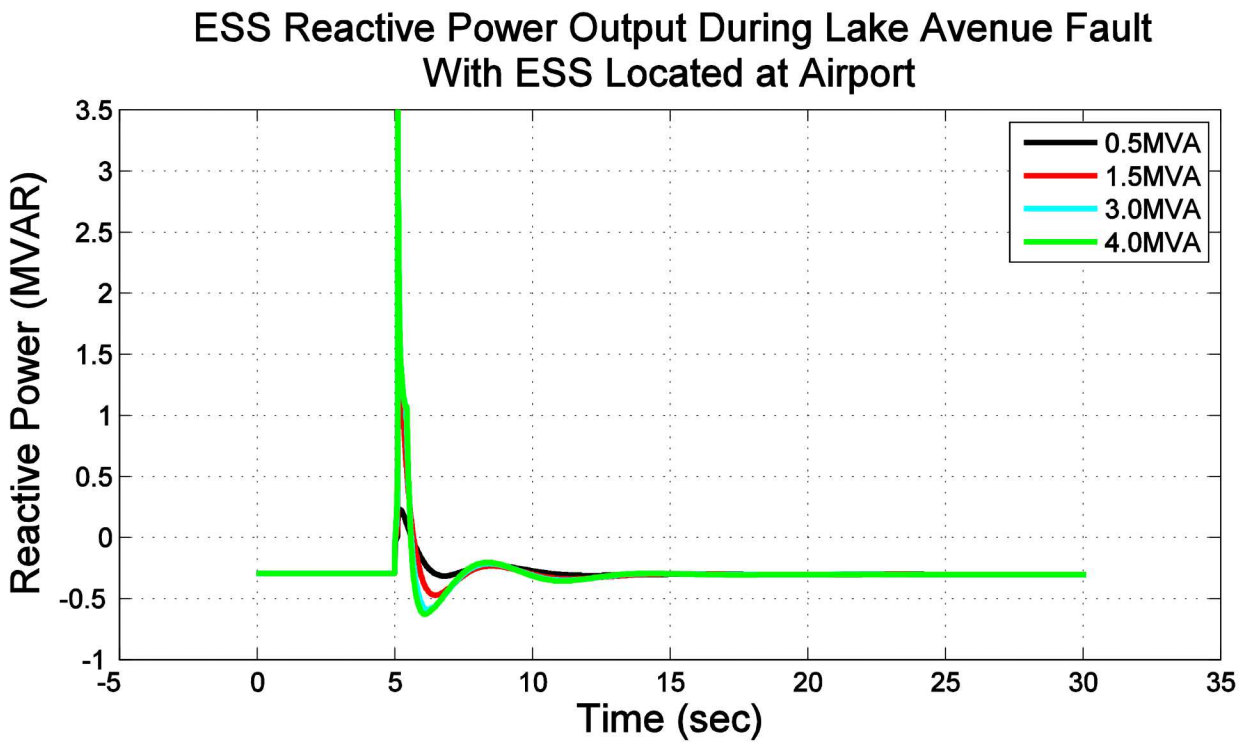

Figure 238 - Reactive power output of various ESS MVA ratings at Airport during fault along Lake Avenue feeder

ESS located at Orca Substation during Generator Trip

Figures in this section are results from the PSLF dynamic simulation varying the ESS MVA ratings while located at the Orca Substation during a generator trip at the Orca Power Plant.

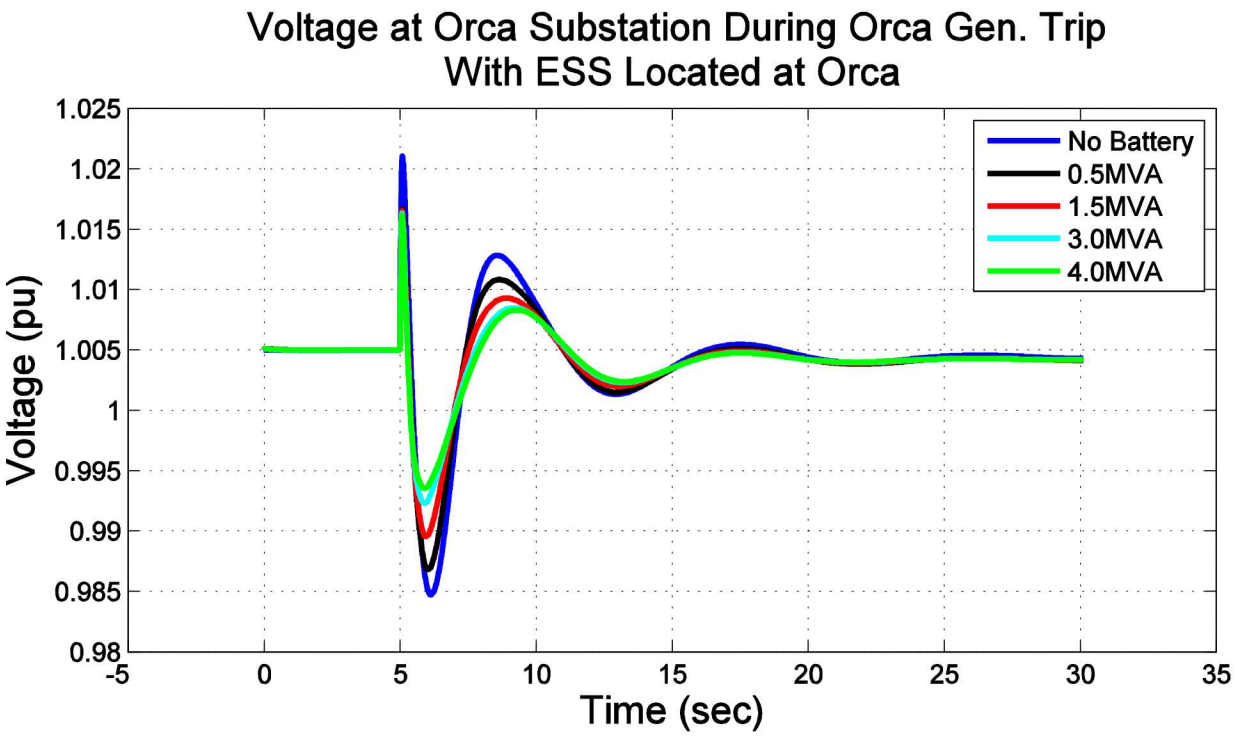

Figure 239 - Voltage at the Orca Substation with varying ESS MVA ratings at Orca Substation during a generator trip

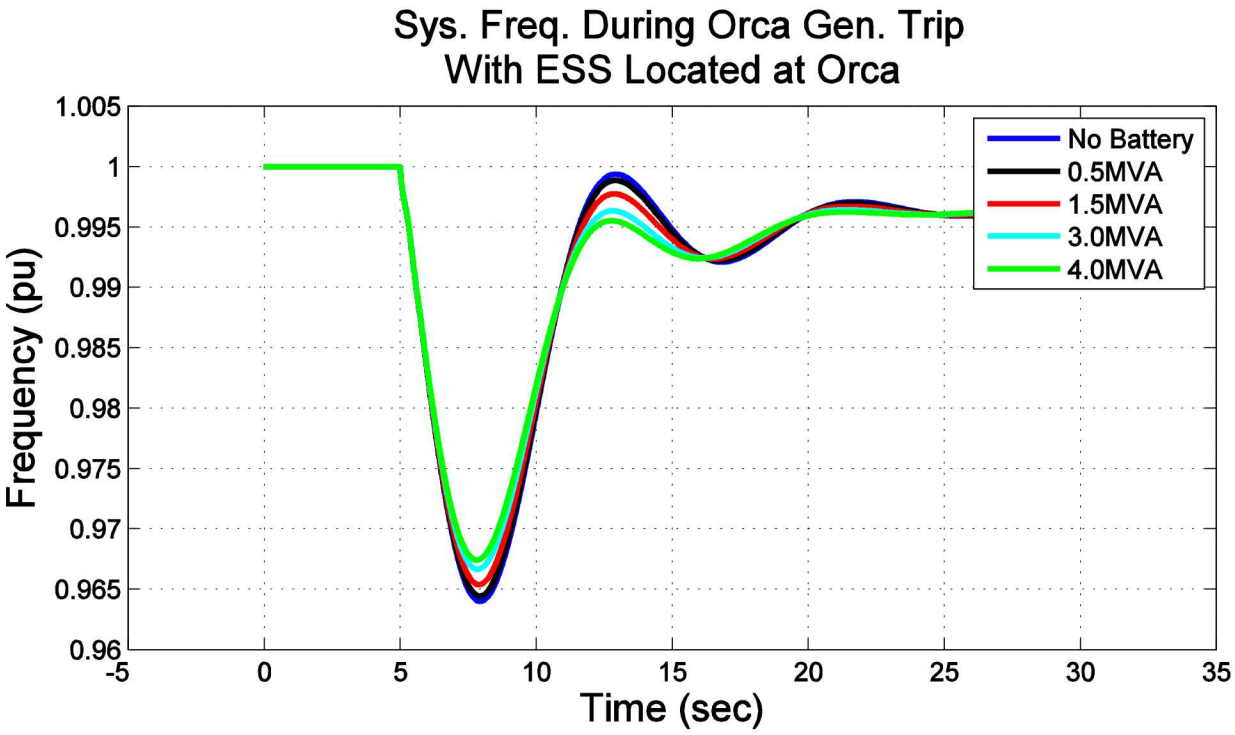

Figure 240 - System Frequency with varying ESS MVA ratings at Orca Substation during a generator trip

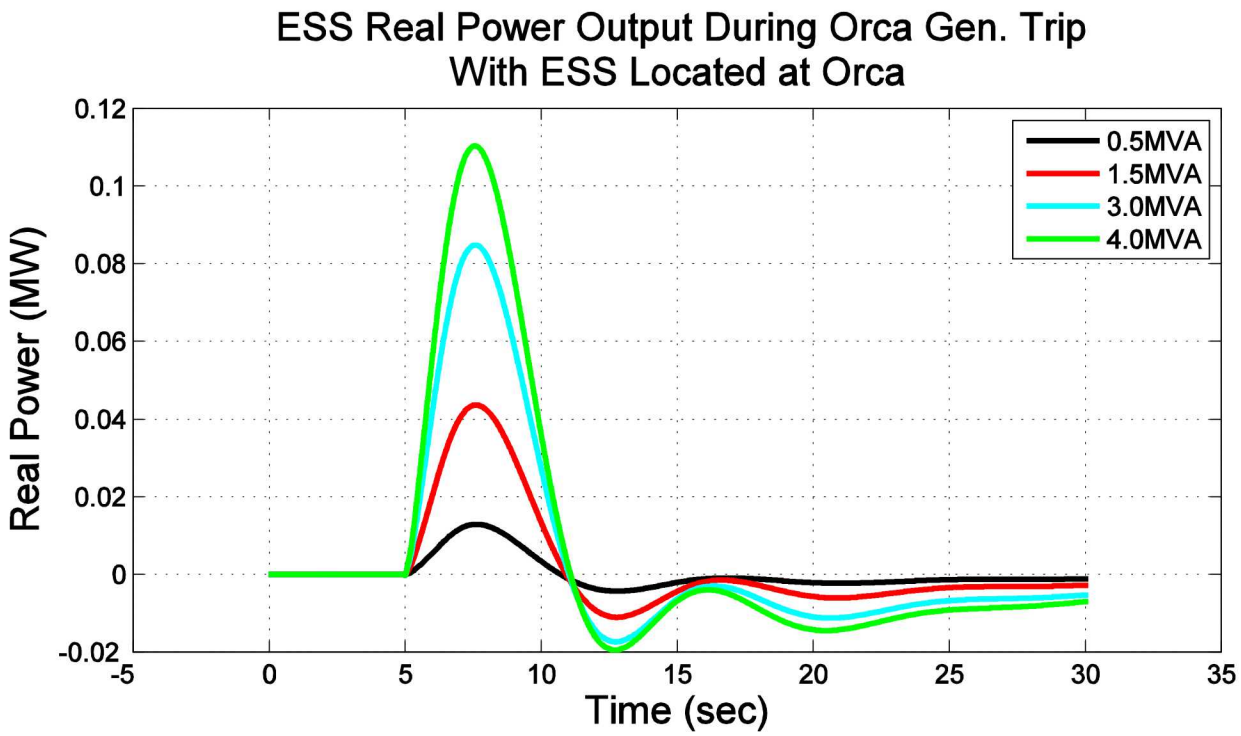

Figure 241 - Real power output of various ESS MVA ratings at Orca Substation during a generator trip

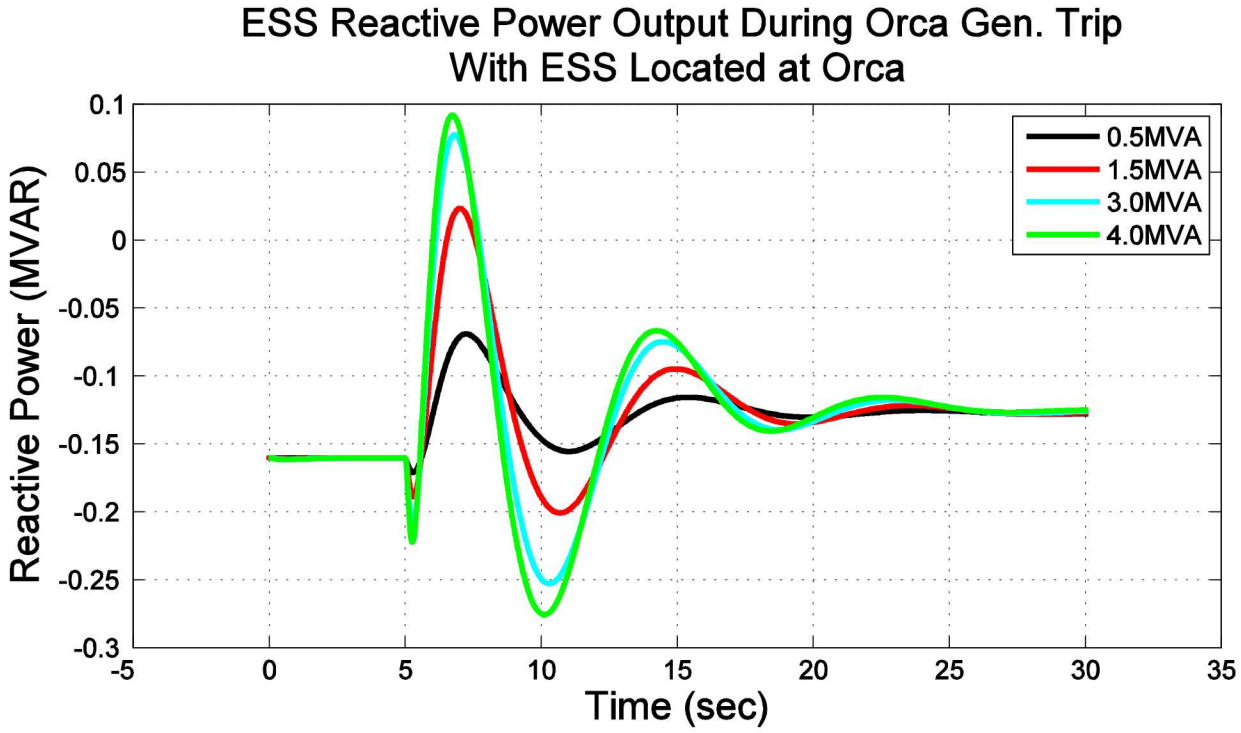

Figure 242 - Reactive power output of various ESS MVA ratings at Orca Substation during a generator trip

ESS located at Eyak Substation during Generator Trip

Figures in this section are results from the PSLF dynamic simulation varying the ESS MVA ratings while located at the Eyak Substation during a generator trip at the Orca Power Plant.

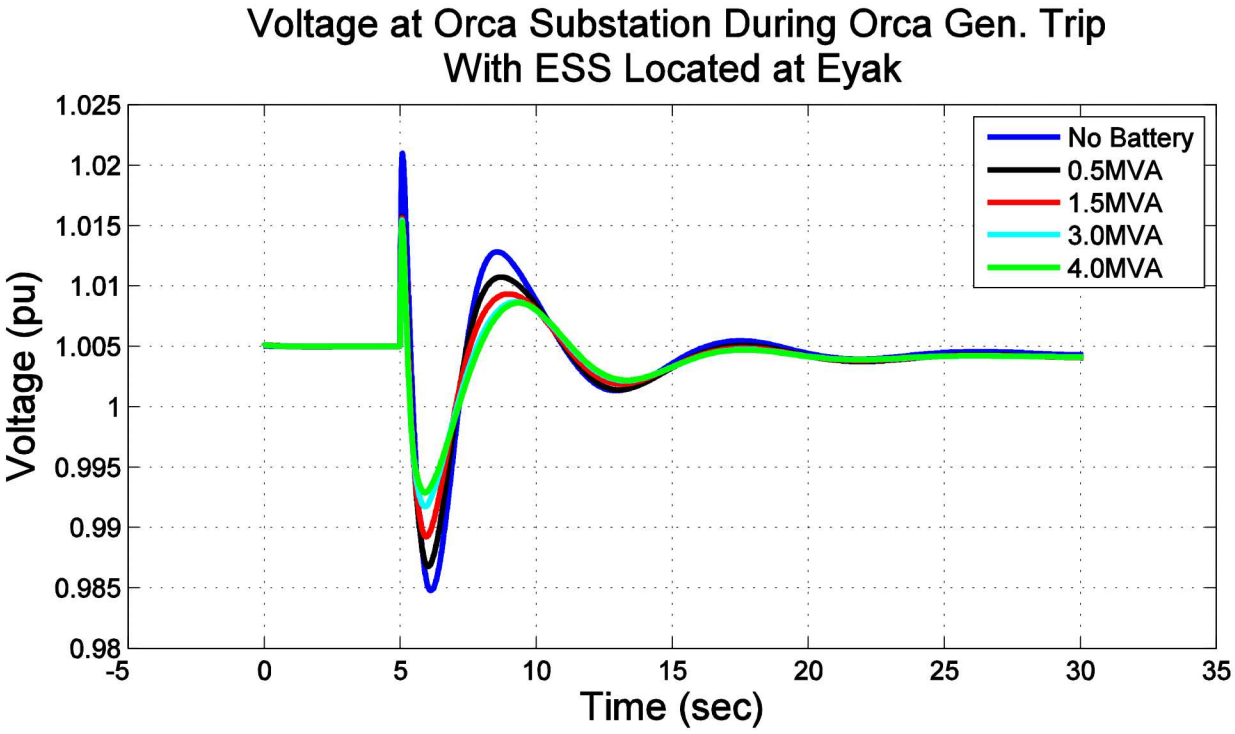

Figure 243 - Voltage at the Orca Substation with varying ESS MVA ratings at Eyak Substation during a generator trip

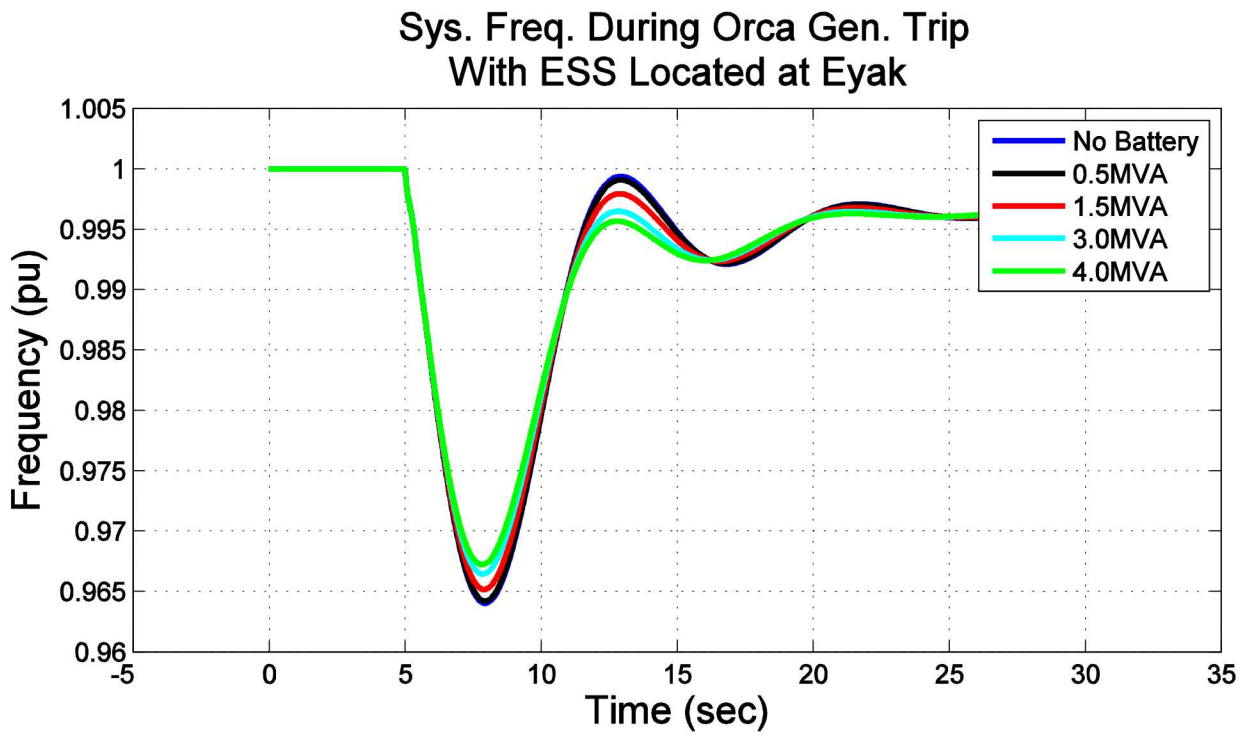

Figure 244 - System Frequency with varying ESS MVA ratings at Eyak Substation during a generator trip

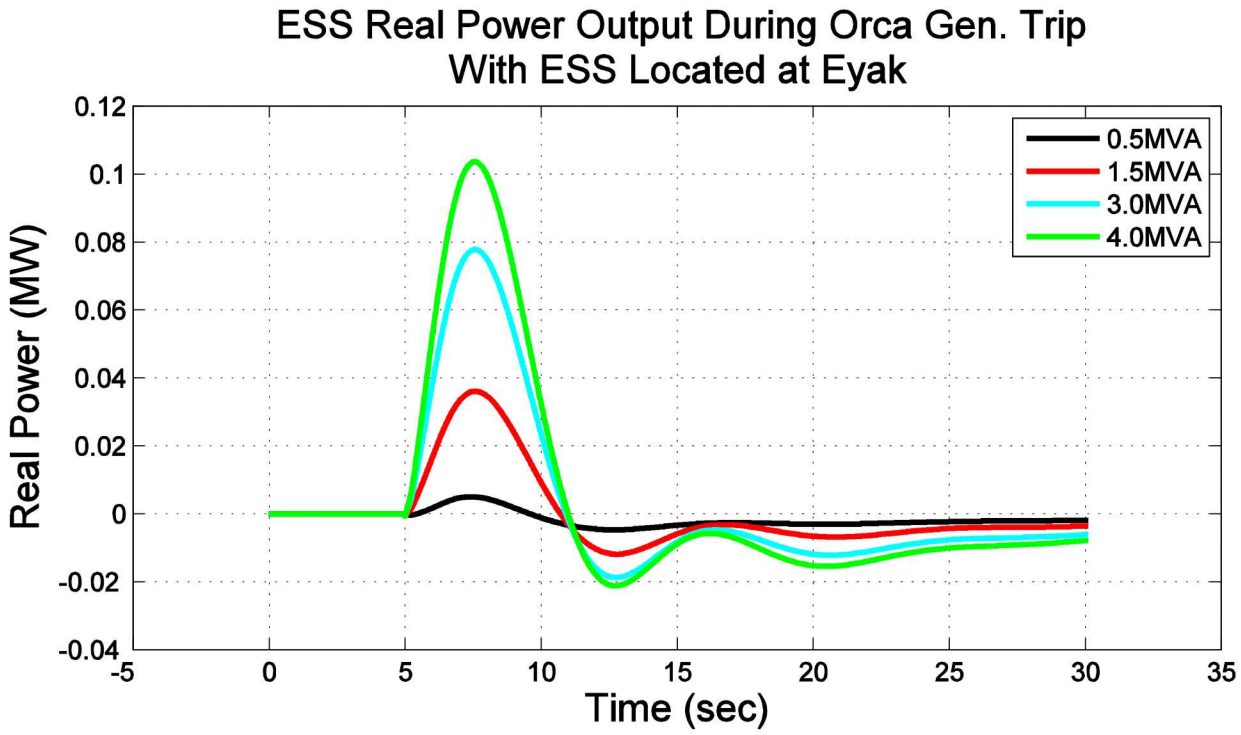

Figure 245 - Real power output of various ESS MVA ratings at Eyak Substation during a generator trip

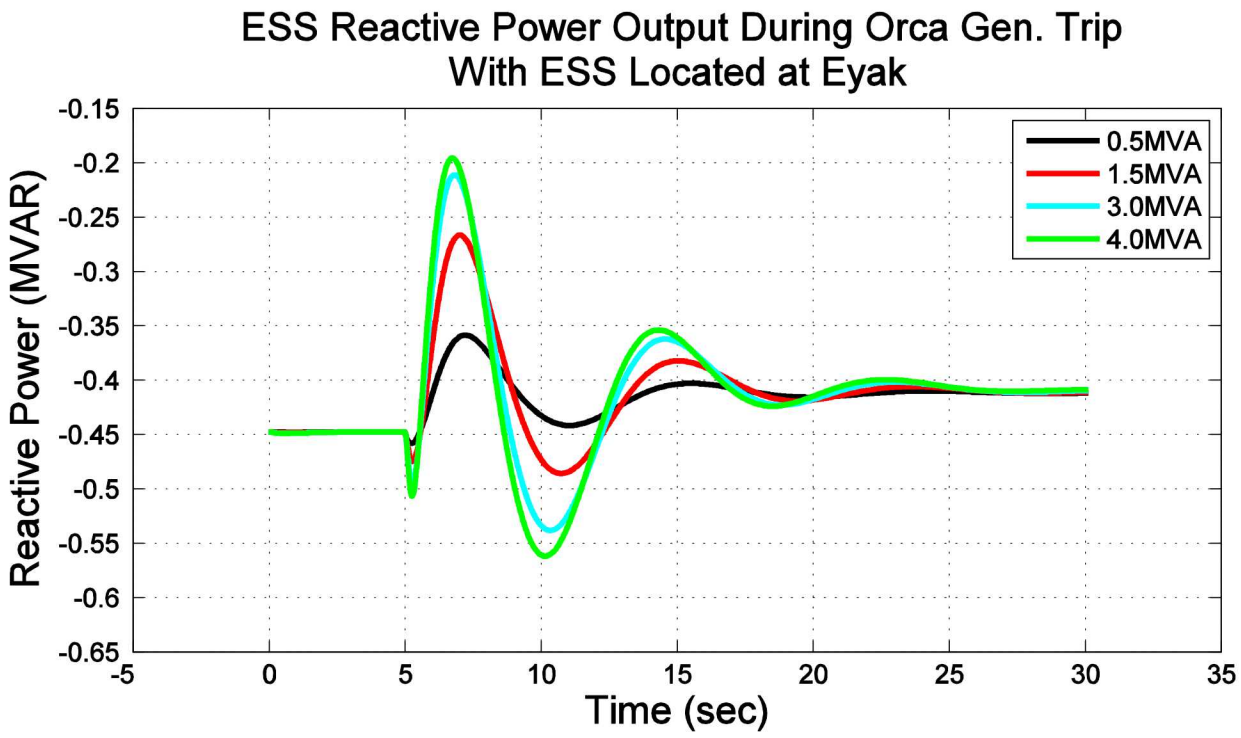

Figure 246 - Reactive power output of various ESS MVA ratings at Eyak Substation during a generator trip

ESS located at Main Hospital during Generator Trip

Figures in this section are results from the PSLF dynamic simulation varying the ESS MVA ratings while located at the main Hospital during a generator trip at the Orca Power Plant.

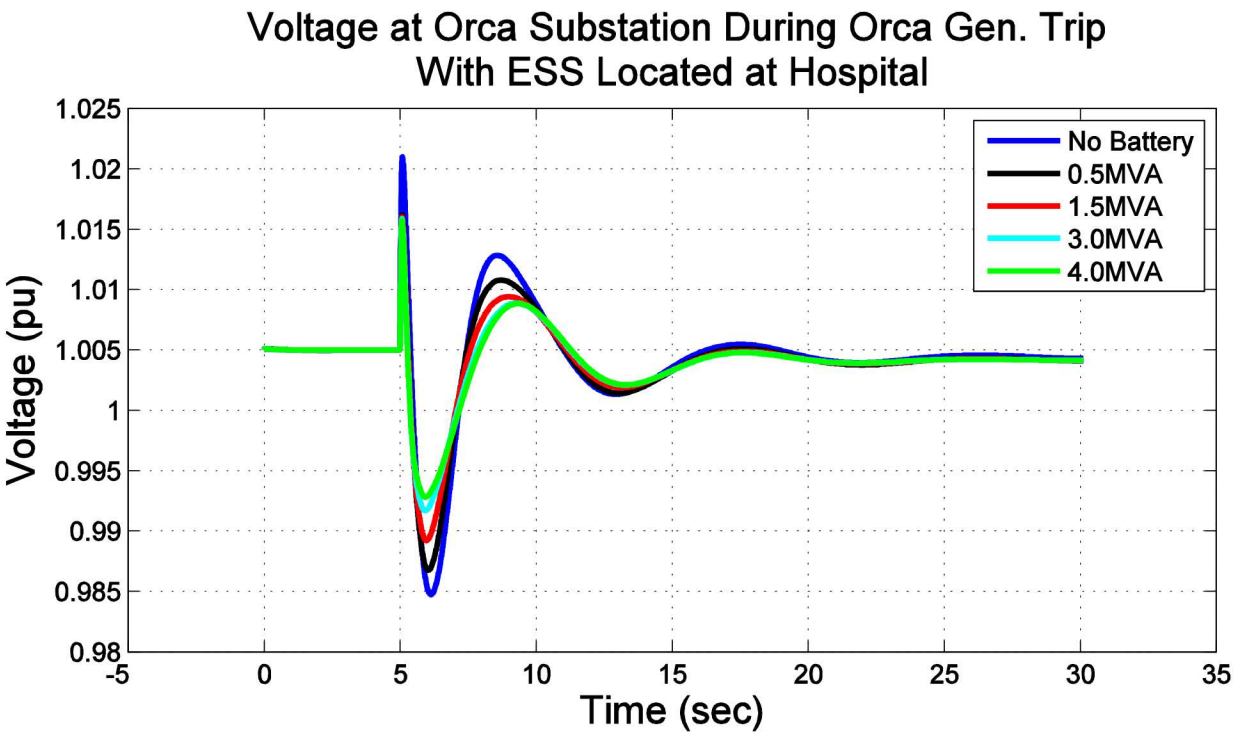

Figure 247 - Voltage at the Orca Substation with varying ESS MVA ratings at Hospital during a generator trip

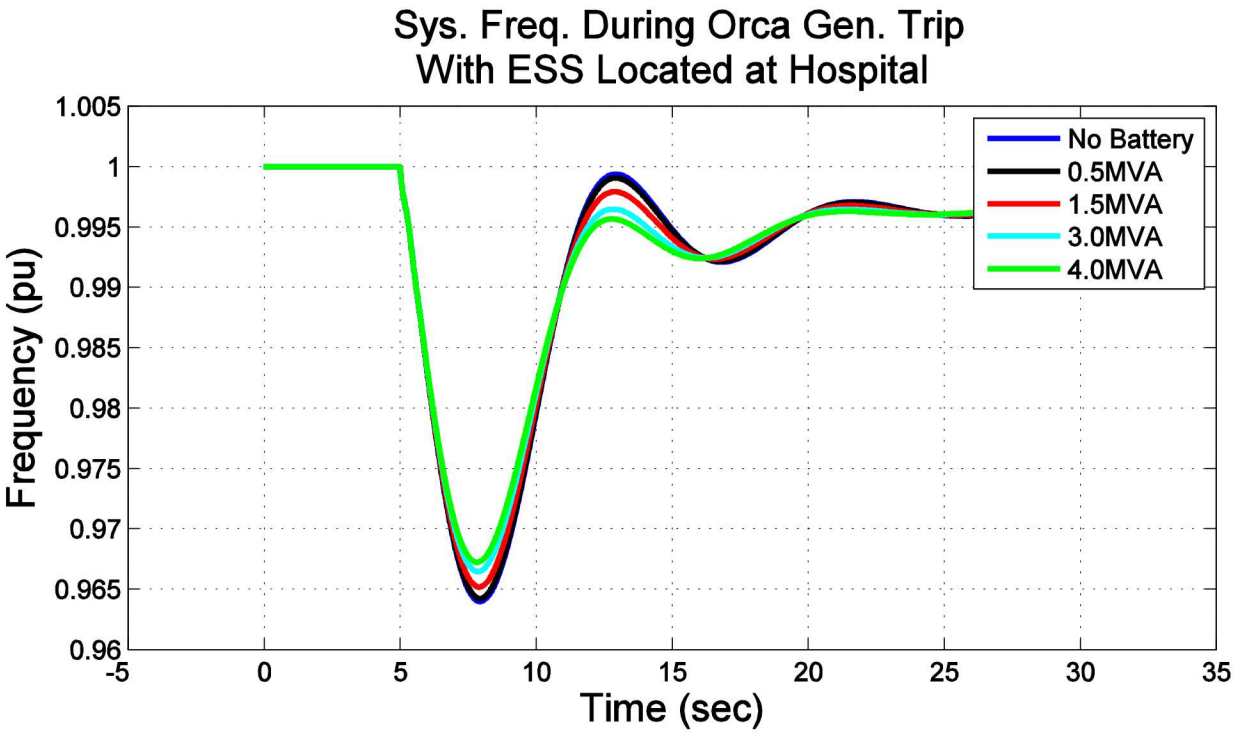

Figure 248 - System Frequency with varying ESS MVA ratings at Hospital during a generator trip

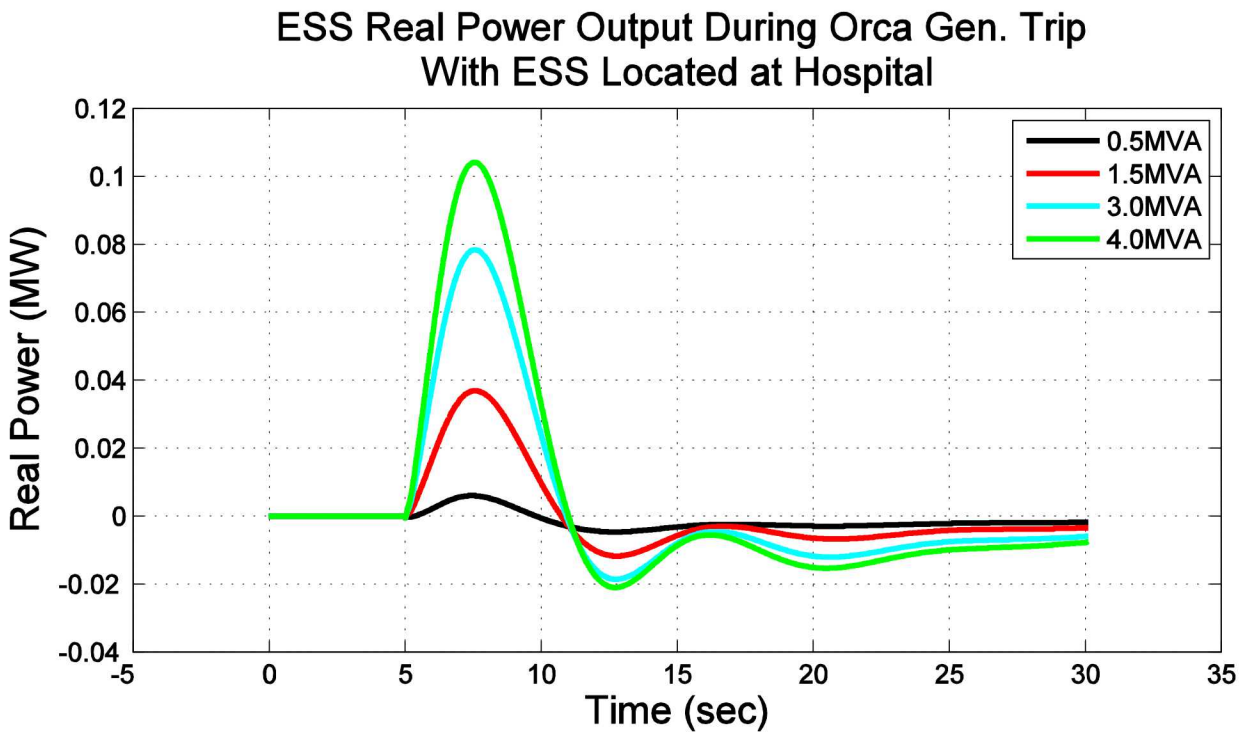

Figure 249 - Real power output of various ESS MVA ratings at Hospital during a generator trip

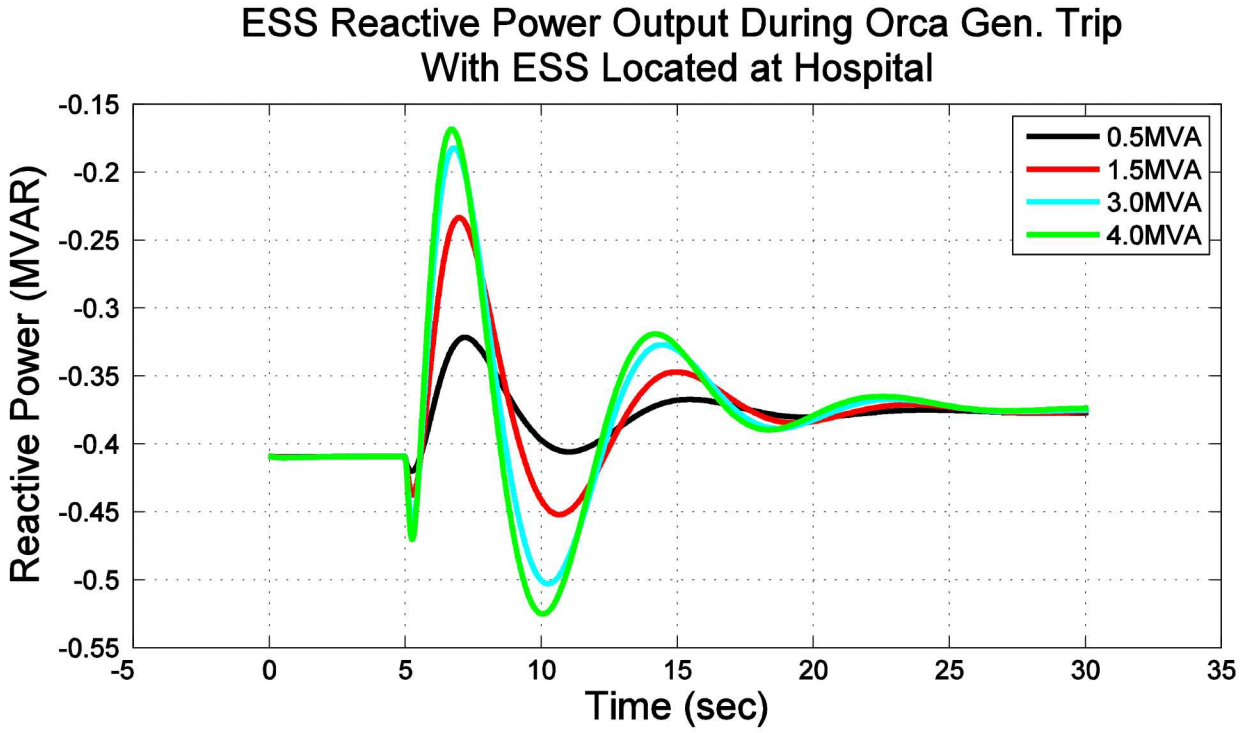

Figure 250 - Reactive power output of various ESS MVA ratings at Hospital during a generator trip

ESS located at Airport during Generator Trip

Figures in this section are results from the PSLF dynamic simulation varying the ESS MVA ratings while located at the Airport during a generator trip at the Orca Power Plant.

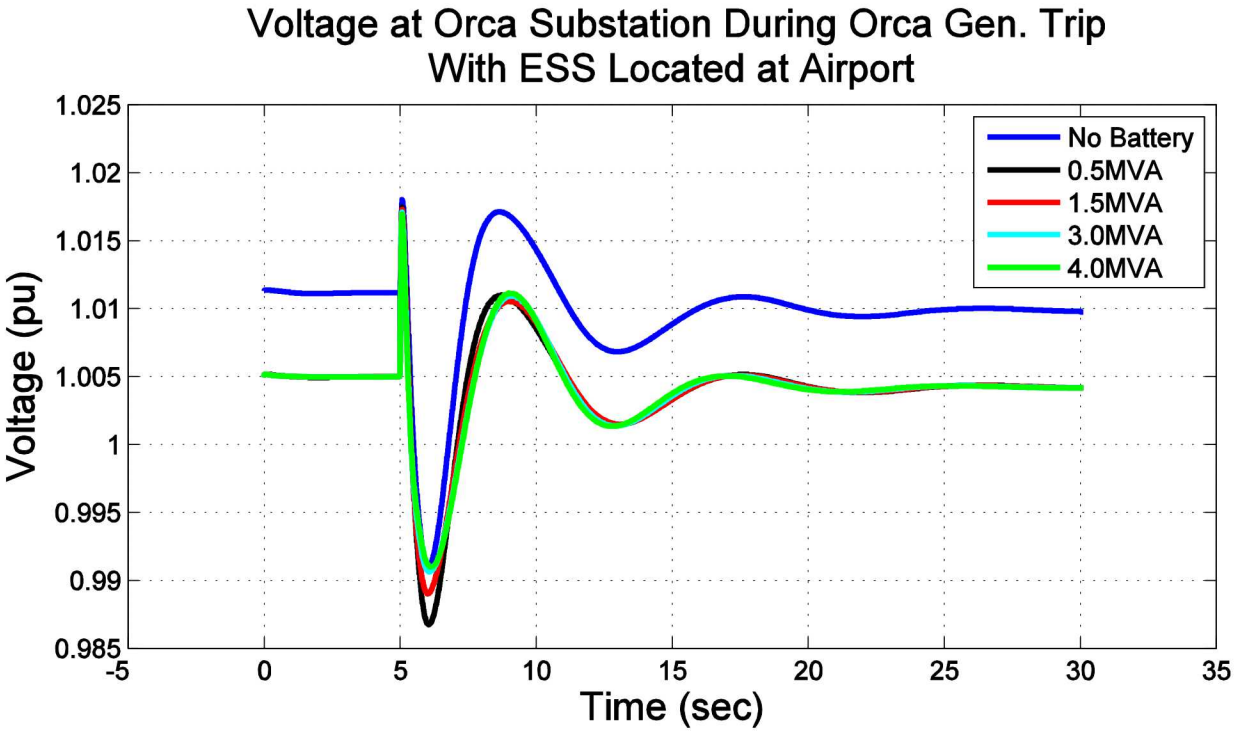

Figure 251 - Voltage at the Orca Substation with varying ESS MVA ratings at Airport during a generator trip

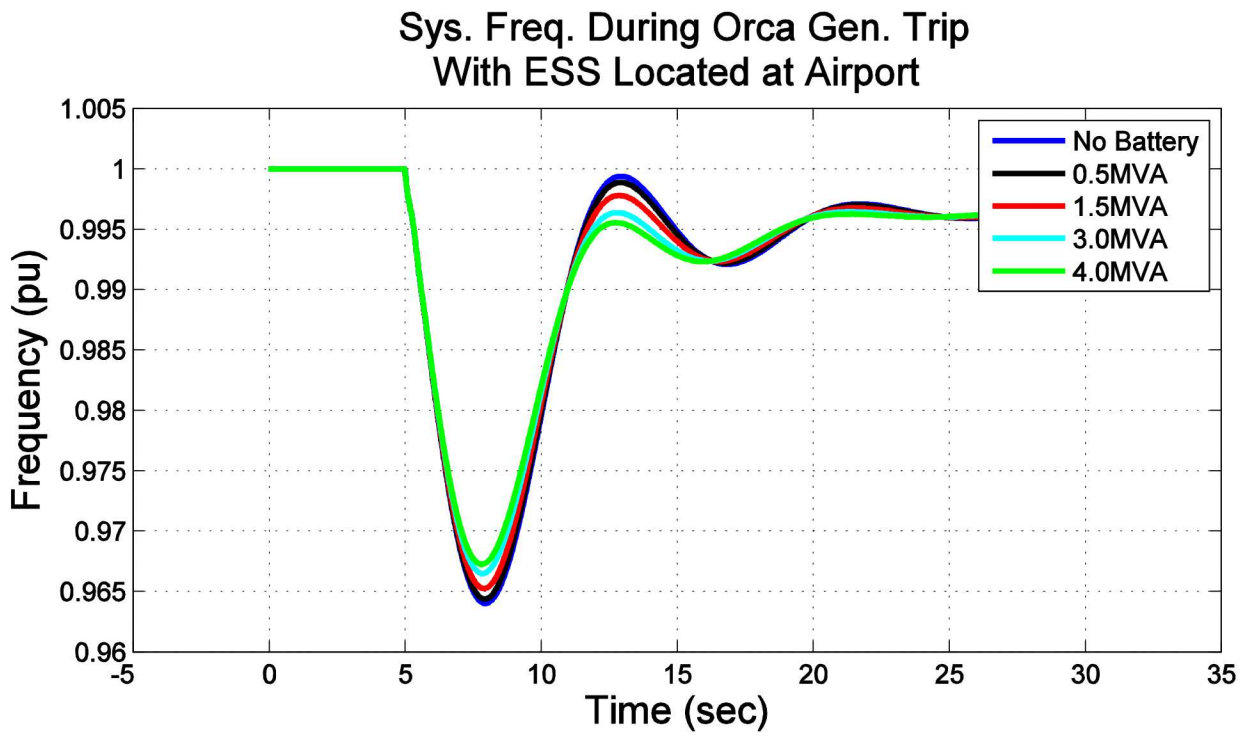

Figure 252 - System Frequency with varying ESS MVA ratings at Airport during a generator trip

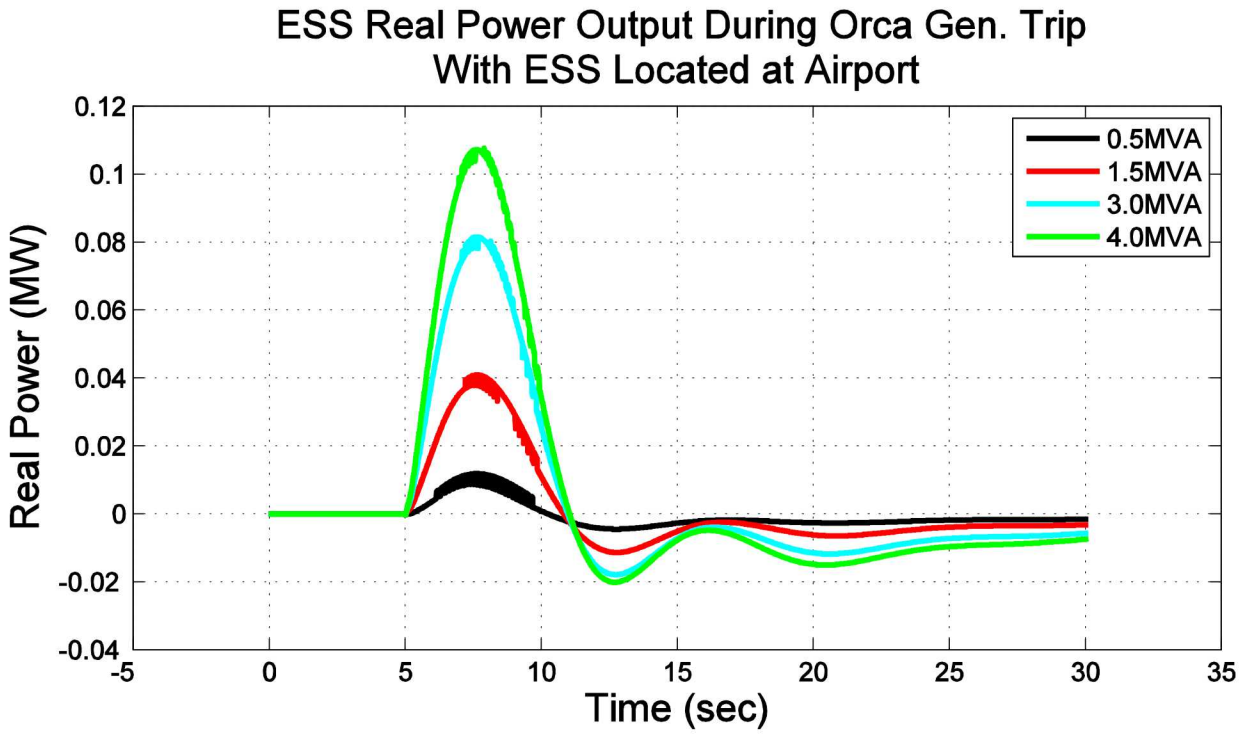

Figure 253 - Real power output of various ESS MVA ratings at Airport during a generator trip

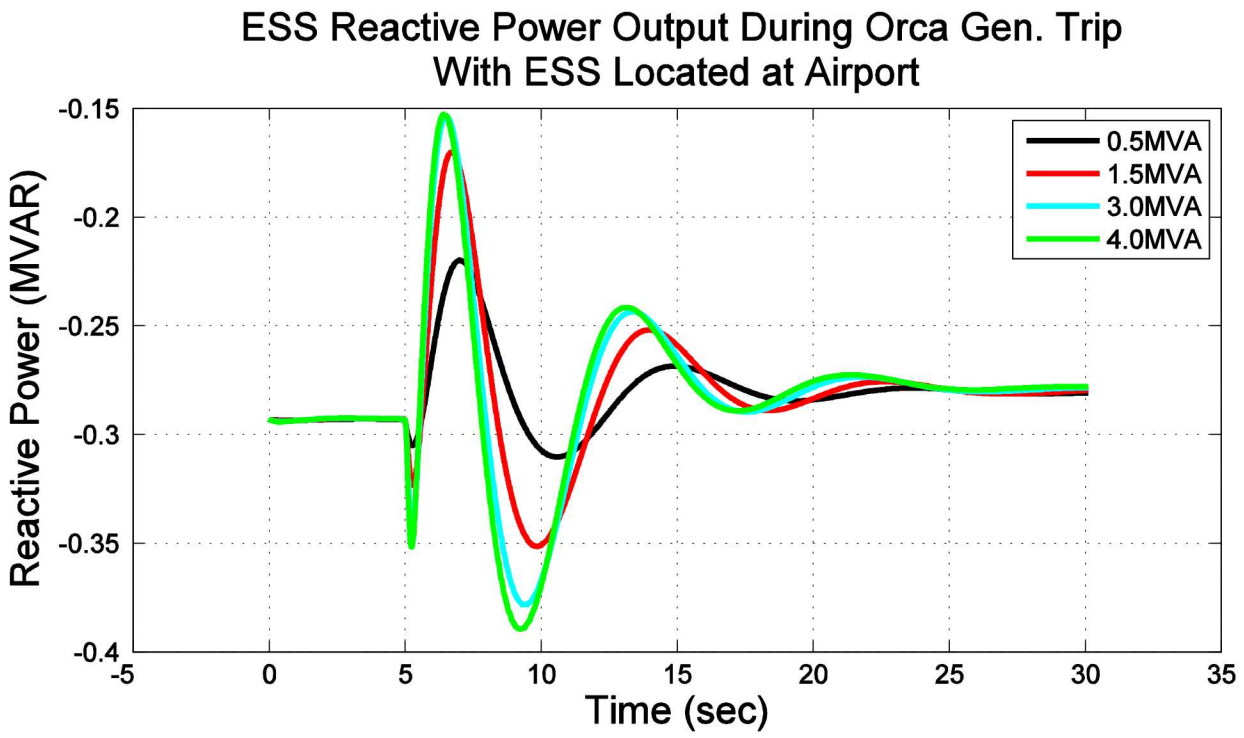

Figure 254 - Reactive power output of various ESS MVA ratings at Airport during a generator trip

Comparison of Energy Storage Location

It was shown through the graphical result s above that the MVA rating of the ESS did not have a significant effect on the dampening of the transient stability. The next analysis investigated was to determine if the placement of the ESS within the CEC grid made a difference in the dampening of the transients. This section has the results from the dynamic simulation comparing a single energy storage rating at various locations during different transient conditions.

0.5 MVA ESS During Electrical Transient

A PSLF simulation was performed with the ESS rating set to 0.5 MVA, placed in one of four locations within the CEC Grid, and one of four electrical transient was applied. The same rated MVA ESS was then moved to another one of the four locations and the same electrical transient was simulated. This simulation was run two more times with the same rated MVA ESS in the other two locations. Locations of the ESS were based off the input from CEC in regards to available space which were the Orca Substation, Eyak Substation, Main Hospital, and Airport. Electrical transient that were performed are fault along the Humpback Creek Feeder, fault along the Main Town feeder, fault along the Lake Avenue feeder and a generator trip at the Orca Power Plant. The figures below show the results from the simulations comparing the 0.5 MVA ESS at the different locations during various electrical transients.

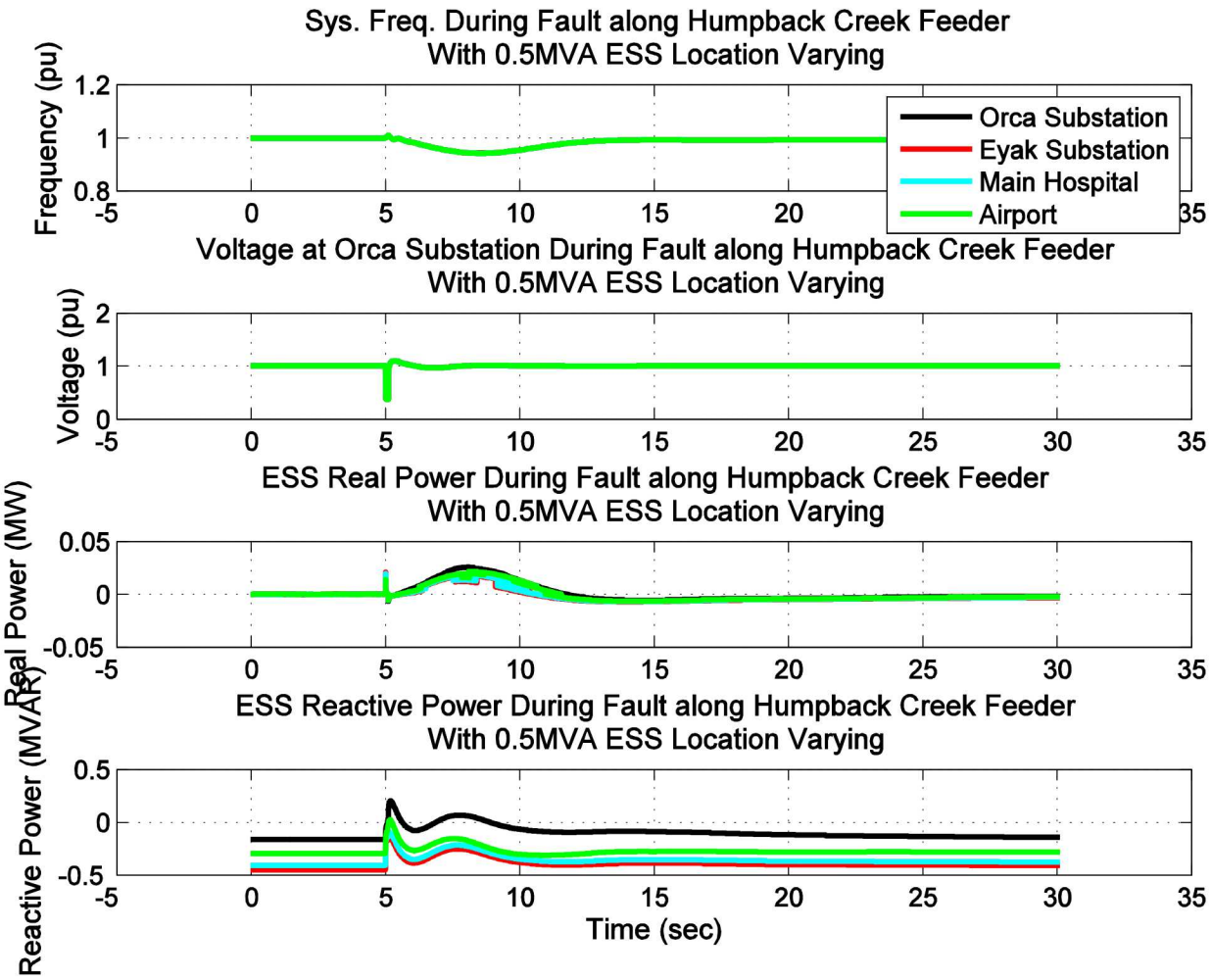

Figure 255 - Dynamic simulation results of 0.5MVA ESS at various locations during Humpback Creek feeder fault

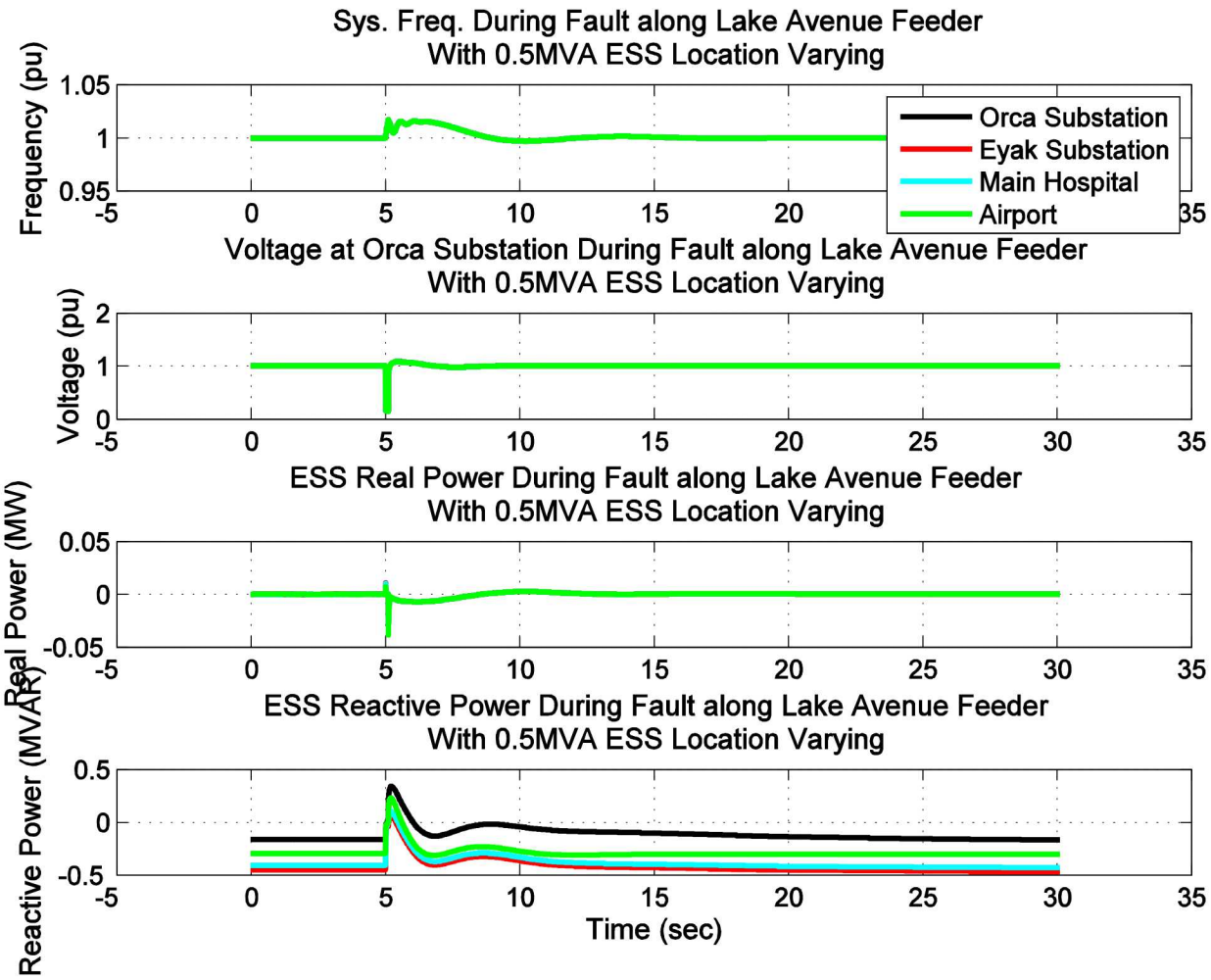

Figure 256 - Dynamic simulation results of 0.5MVA ESS at various locations during Lake Avenue feeder fault

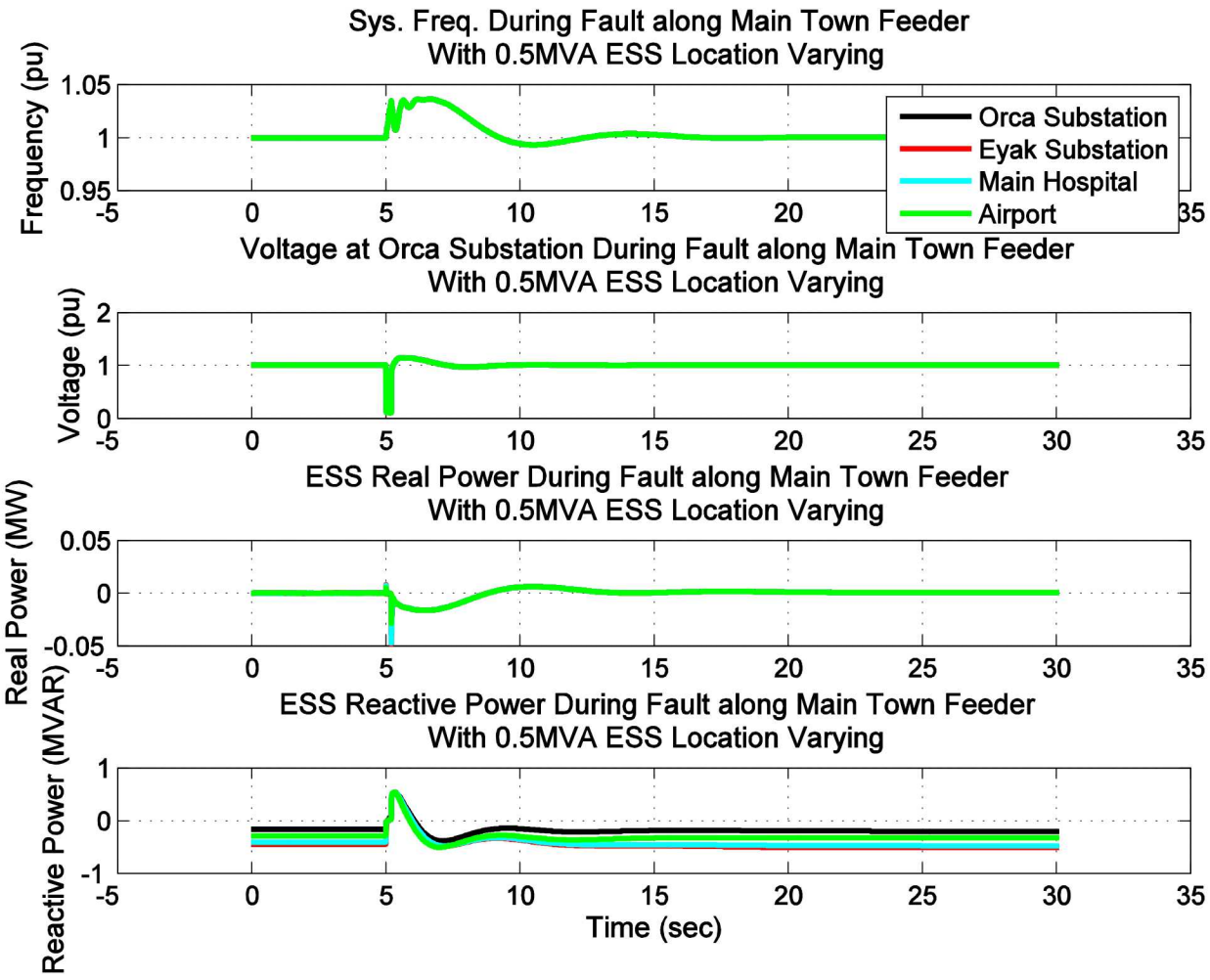

Figure 257 - Dynamic simulation results of 0.5MVA ESS at various locations during Main Town feeder fault

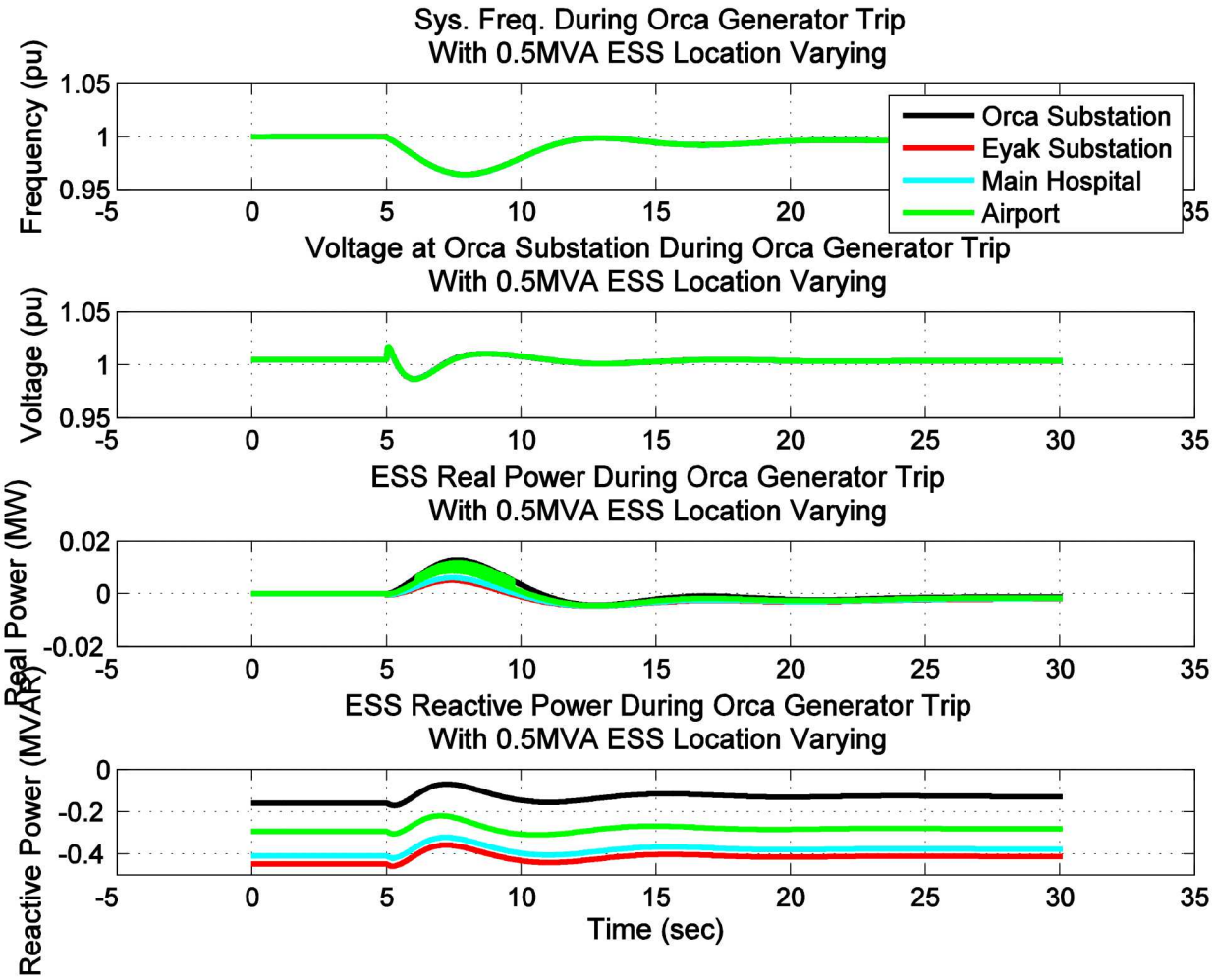

Figure 258 - Dynamic simulation results of 0.5MVA ESS at various locations during generator trip

1.0 MVA ESS During Electrical Transient

A PSLF simulation was performed with the ESS rating set to 1.0 MVA, placed in one of four locations within the CEC Grid, and one of four electrical transient was applied. The same rated MVA ESS was then moved to another one of the four locations and the same electrical transient was simulated. This simulation was run two more times with the same rated MVA ESS in the other two locations. Locations of the ESS were based off the input from CEC in regards to available space which were the Orca Substation, Eyak Substation, Main Hospital, and Airport. Electrical transient that were performed are fault along the Humpback Creek Feeder, fault along the Main Town feeder, fault along the Lake Avenue feeder and a generator trip at the Orca Power Plant. The figures below show the results from the simulations comparing the 1.0 MVA ESS at the different locations during various electrical transients.

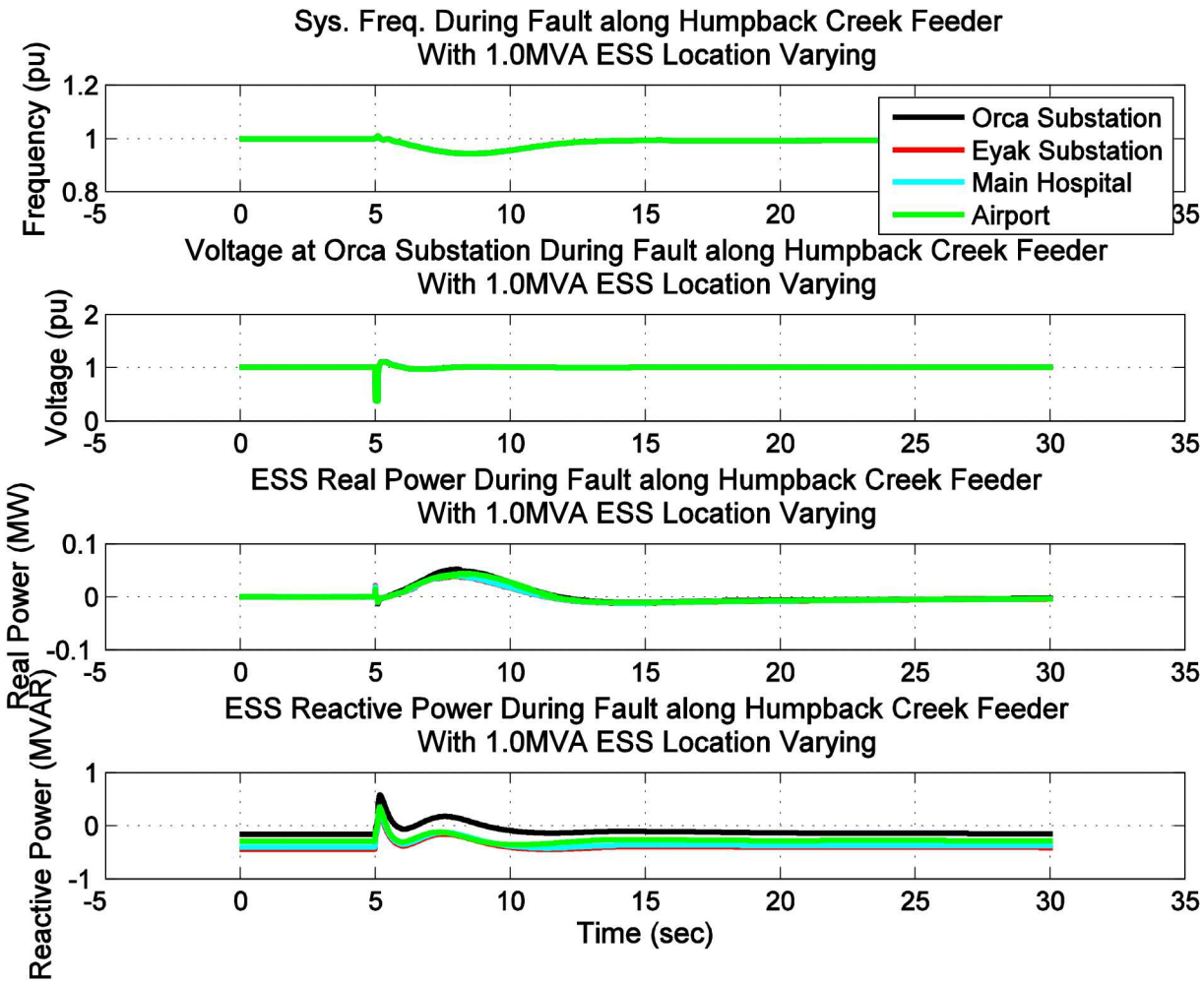

Figure 259 - Dynamic simulation results of 1.0MVA ESS at various locations during Humpback Creek feeder fault

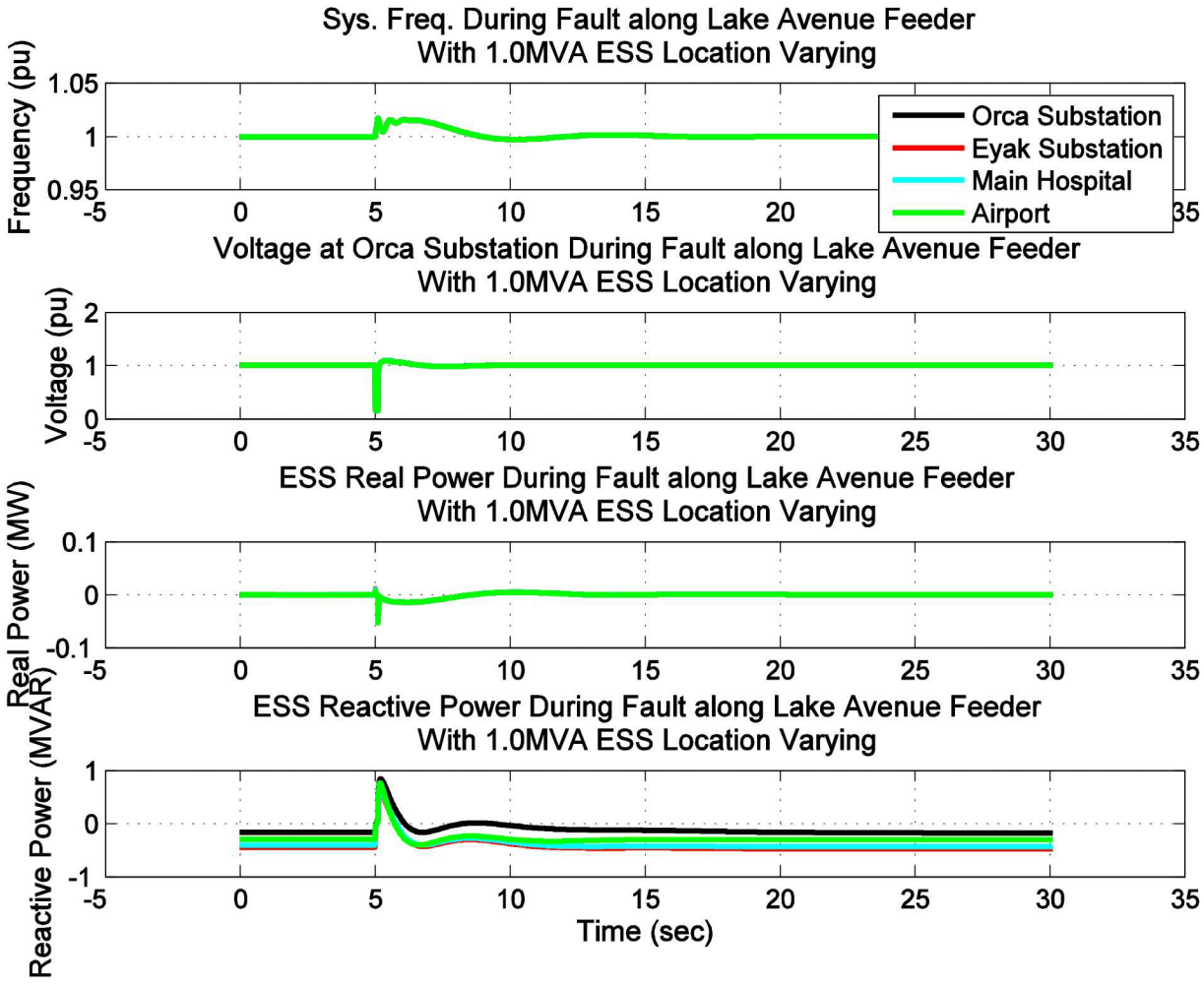

Figure 260 - Dynamic simulation results of 1.0MVA ESS at various locations during Lake Avenue feeder fault

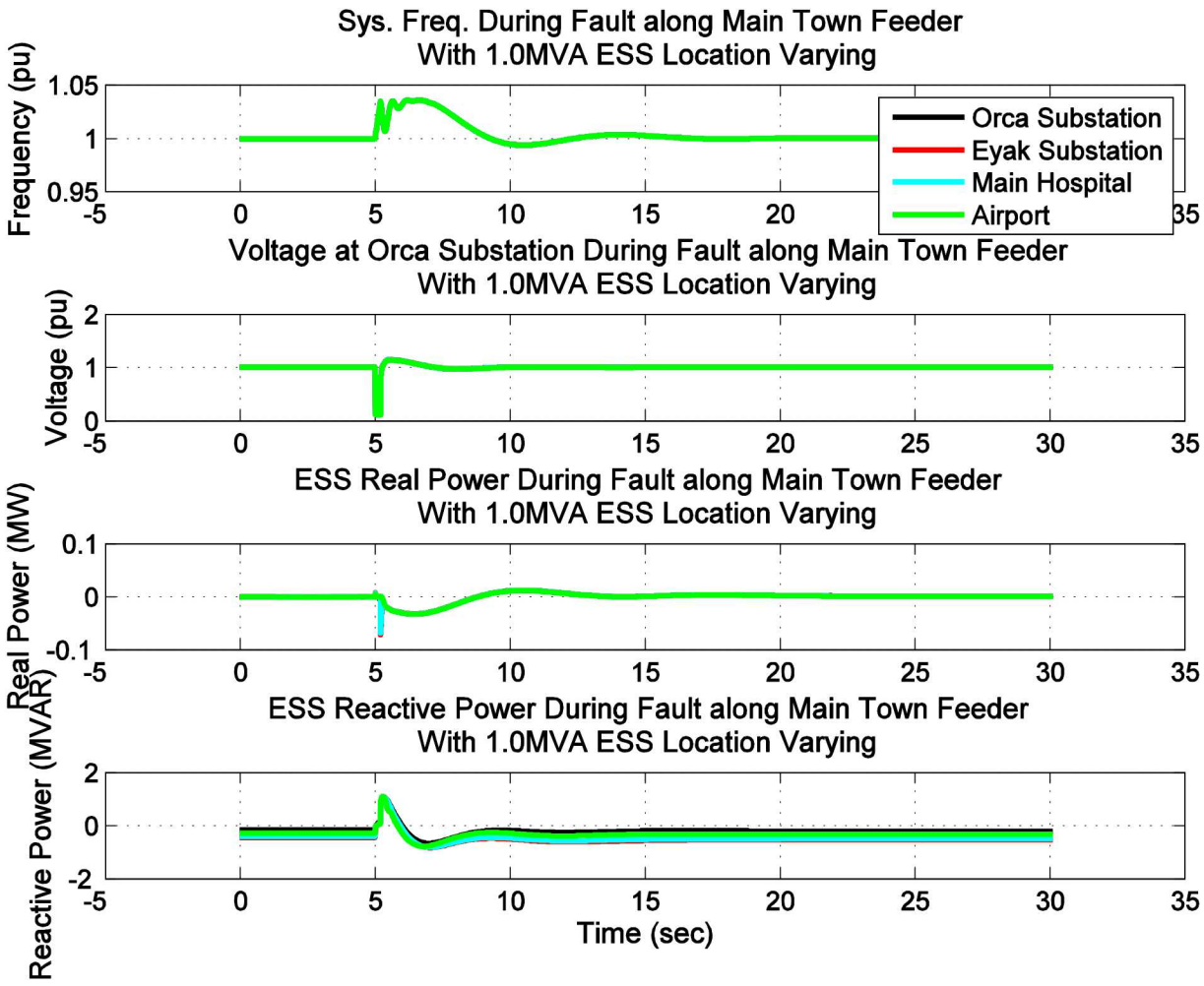

Figure 261 - Dynamic simulation results of 1.0MVA ESS at various locations during Main Town feeder fault

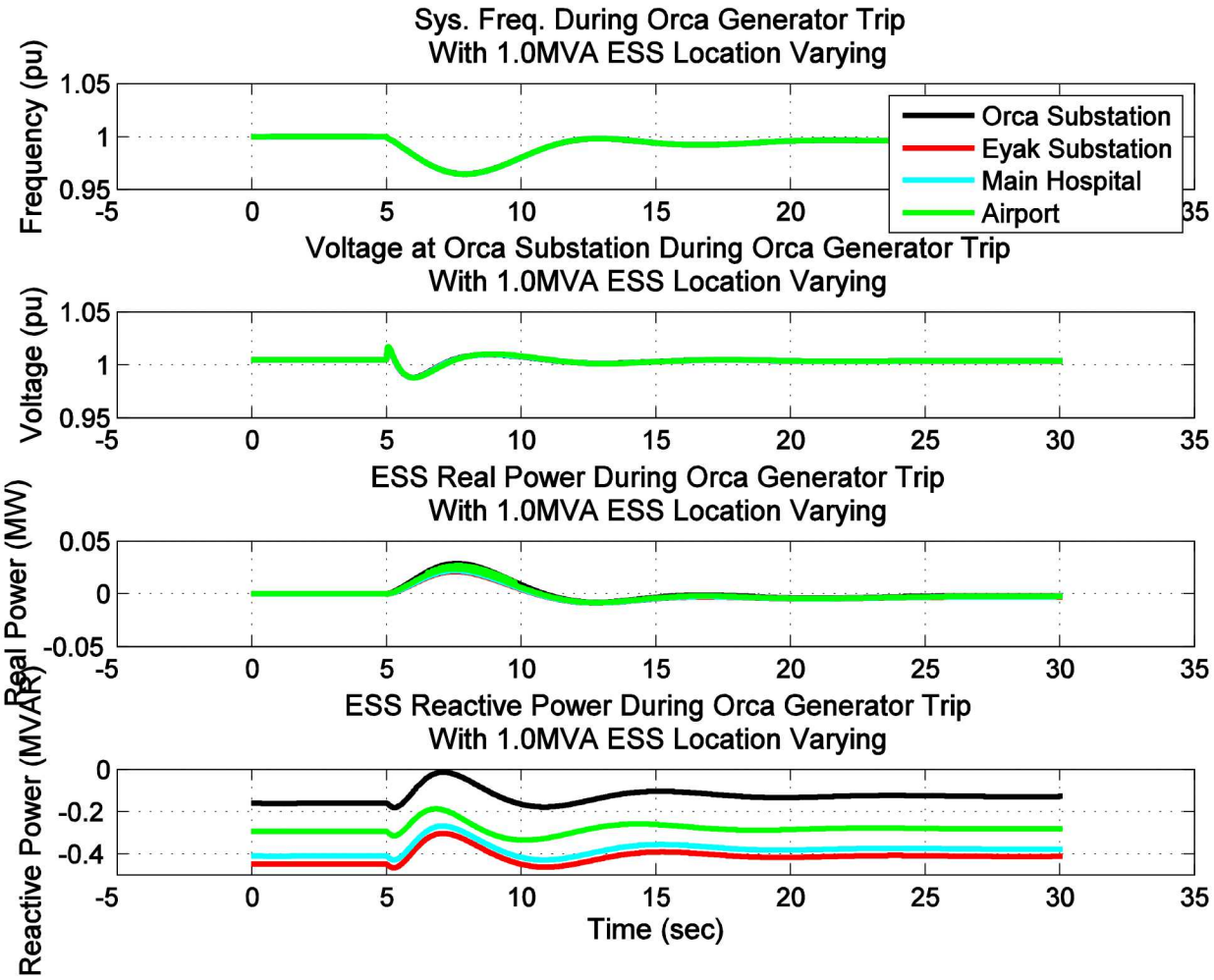

Figure 262 - Dynamic simulation results of 1.0MVA ESS at various locations during generator trip

1.5 MVA ESS During Electrical Transient

A PSLF simulation was performed with the ESS rating set to 1.5 MVA, placed in one of four locations within the CEC Grid, and one of four electrical transient was applied. The same rated MVA ESS was then moved to another one of the four locations and the same electrical transient was simulated. This simulation was run two more times with the same rated MVA ESS in the other two locations. Locations of the ESS were based off the input from CEC in regards to available space which were the Orca Substation, Eyak Substation, Main Hospital, and Airport. Electrical transient that were performed are fault along the Humpback Creek Feeder, fault along the Main Town feeder, fault along the Lake Avenue feeder and a generator trip at the Orca Power Plant. The figures below show the results from the simulations comparing the 1.5 MVA ESS at the different locations during various electrical transients.

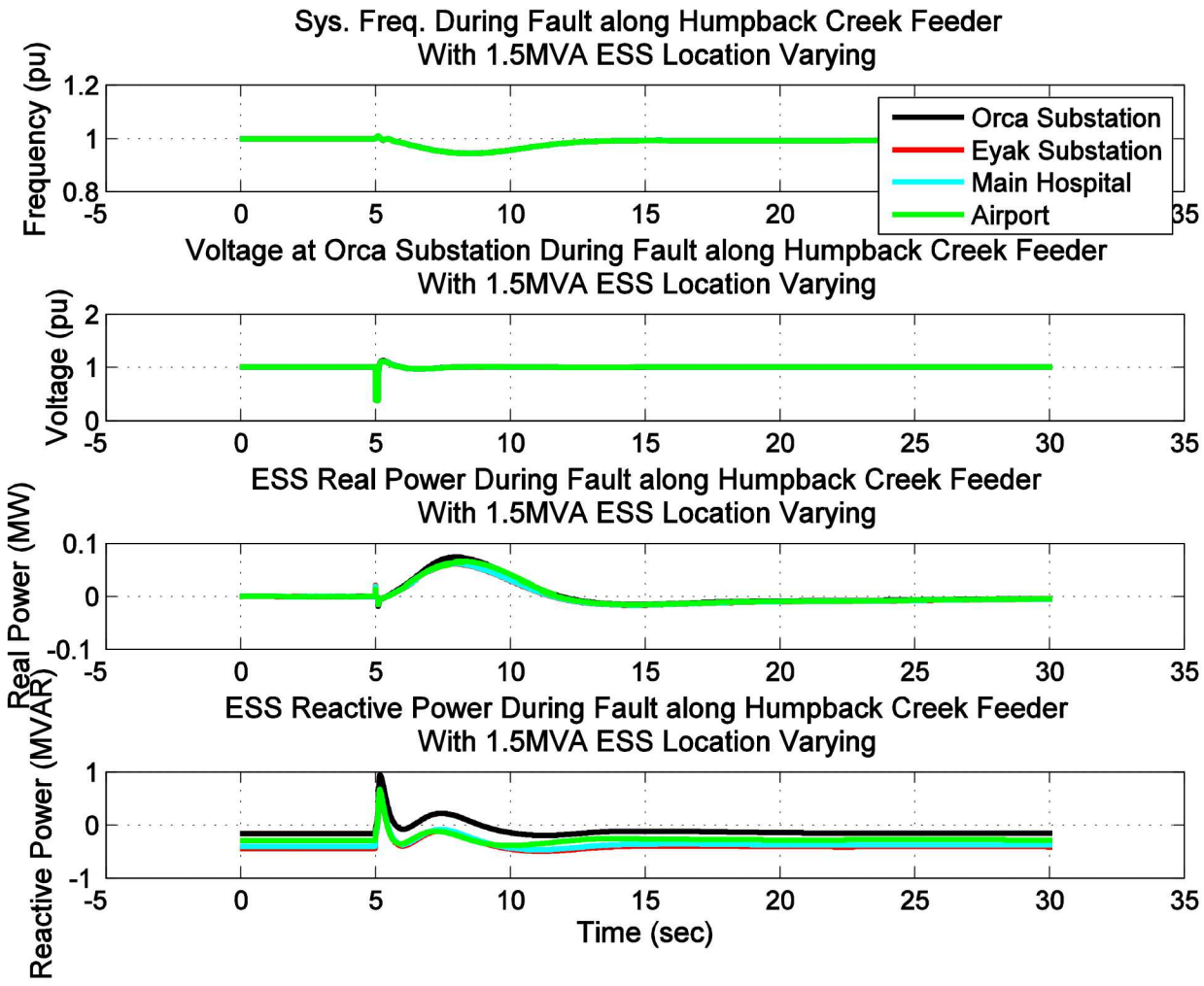

Figure 263 - Dynamic simulation results of 1.5MVA ESS at various locations during Humpback Creek feeder fault

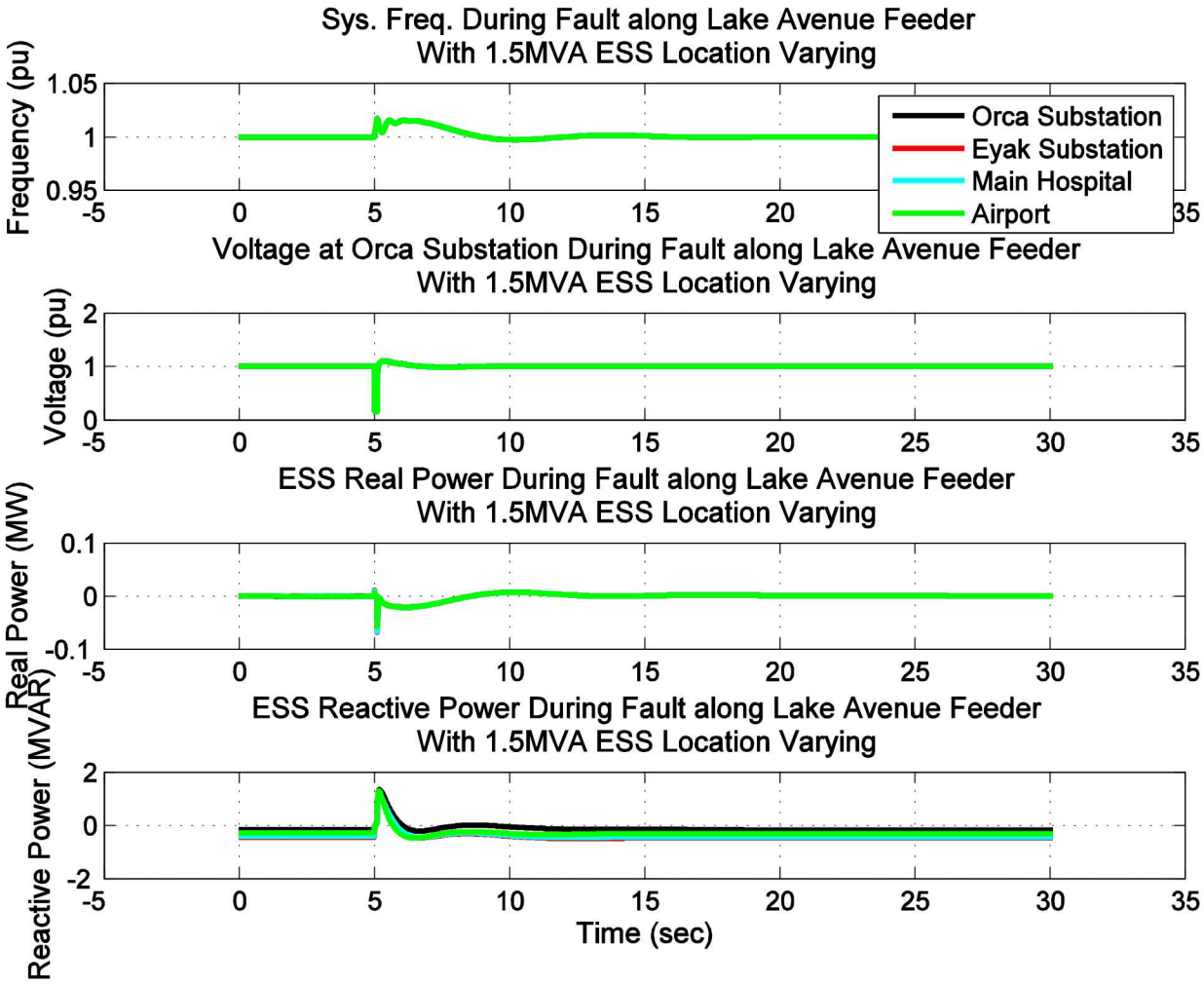

Figure 264 - Dynamic simulation results of 1.5MVA ESS at various locations during Lake Avenue feeder fault

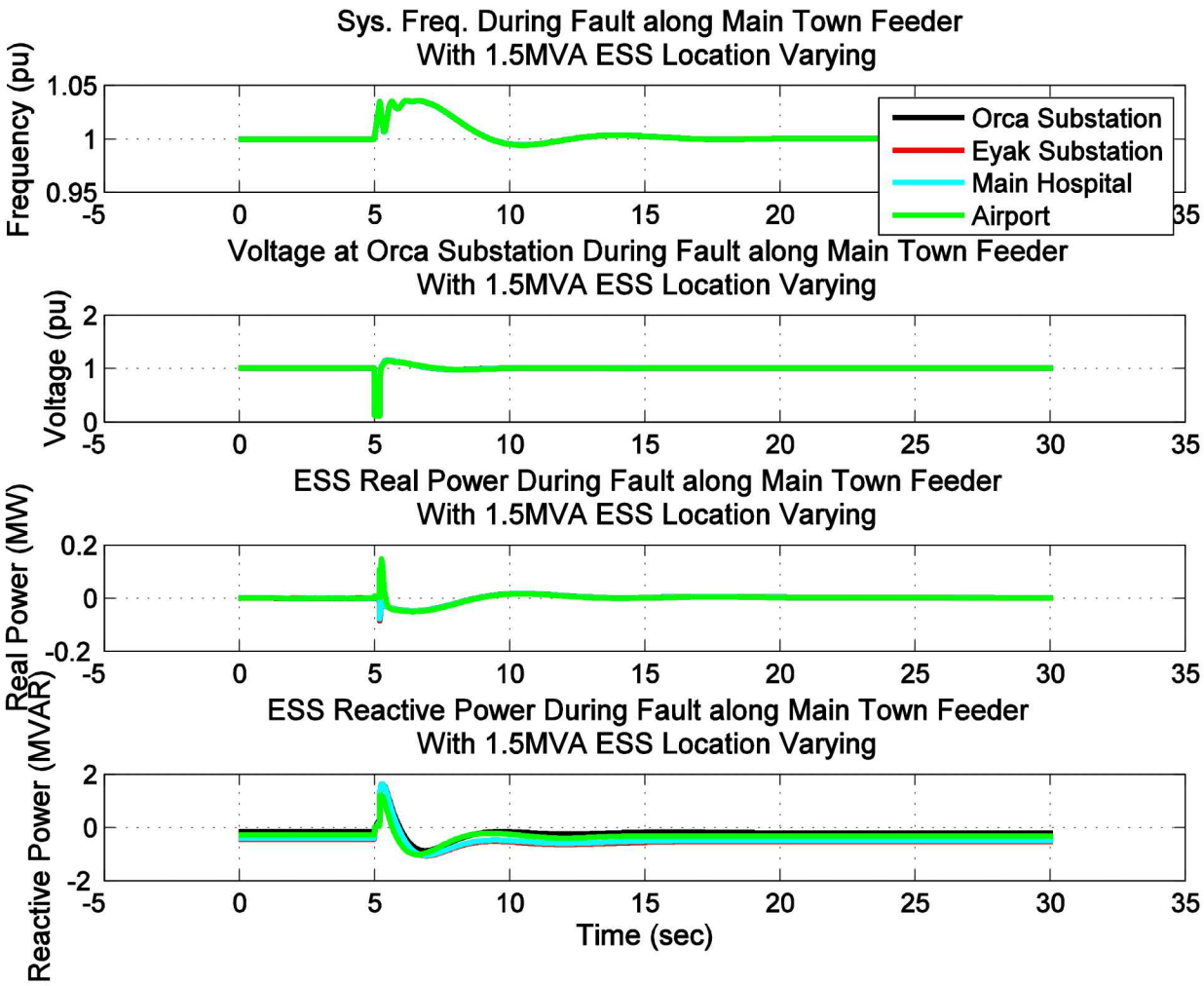

Figure 265 - Dynamic simulation results of 1.5MVA ESS at various locations during Main Town feeder fault

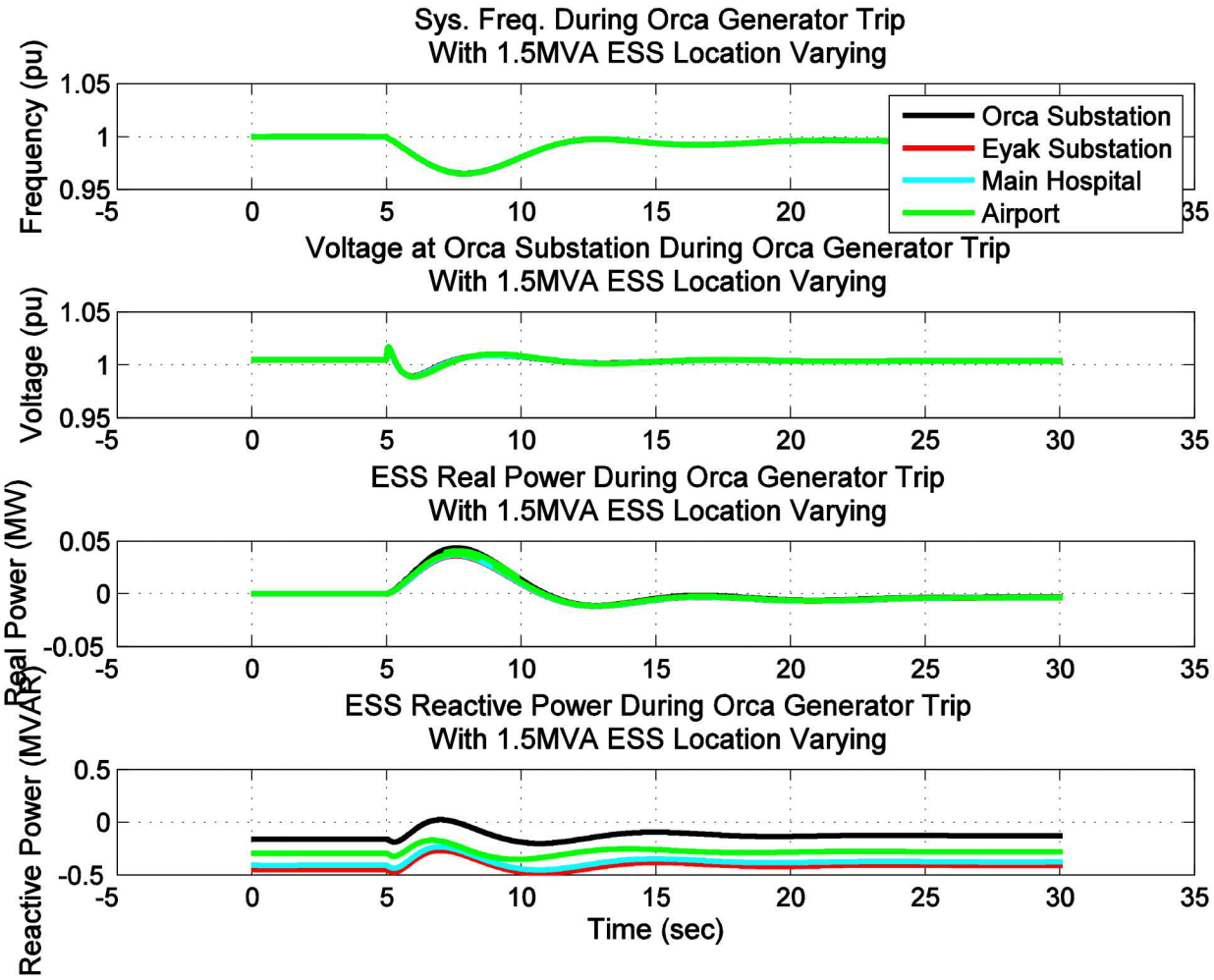

Figure 266 - Dynamic simulation results of 1.5MVA ESS at various locations during a generator trip

2.0 MVA ESS During Electrical Transient

A PSLF simulation was performed with the ESS rating set to 2.0 MVA, placed in one of four locations within the CEC Grid, and one of four electrical transient was applied. The same rated MVA ESS was then moved to another one of the four locations and the same electrical transient was simulated. This simulation was run two more times with the same rated MVA ESS in the other two locations. Locations of the ESS were based off the input from CEC in regards to available space which were the Orca Substation, Eyak Substation, Main Hospital, and Airport. Electrical transient that were performed are fault along the Humpback Creek Feeder, fault along the Main Town feeder, fault along the Lake Avenue feeder and a generator trip at the Orca Power Plant. The figures below show the results from the simulations comparing the 2.0 MVA ESS at the different locations during various electrical transients.

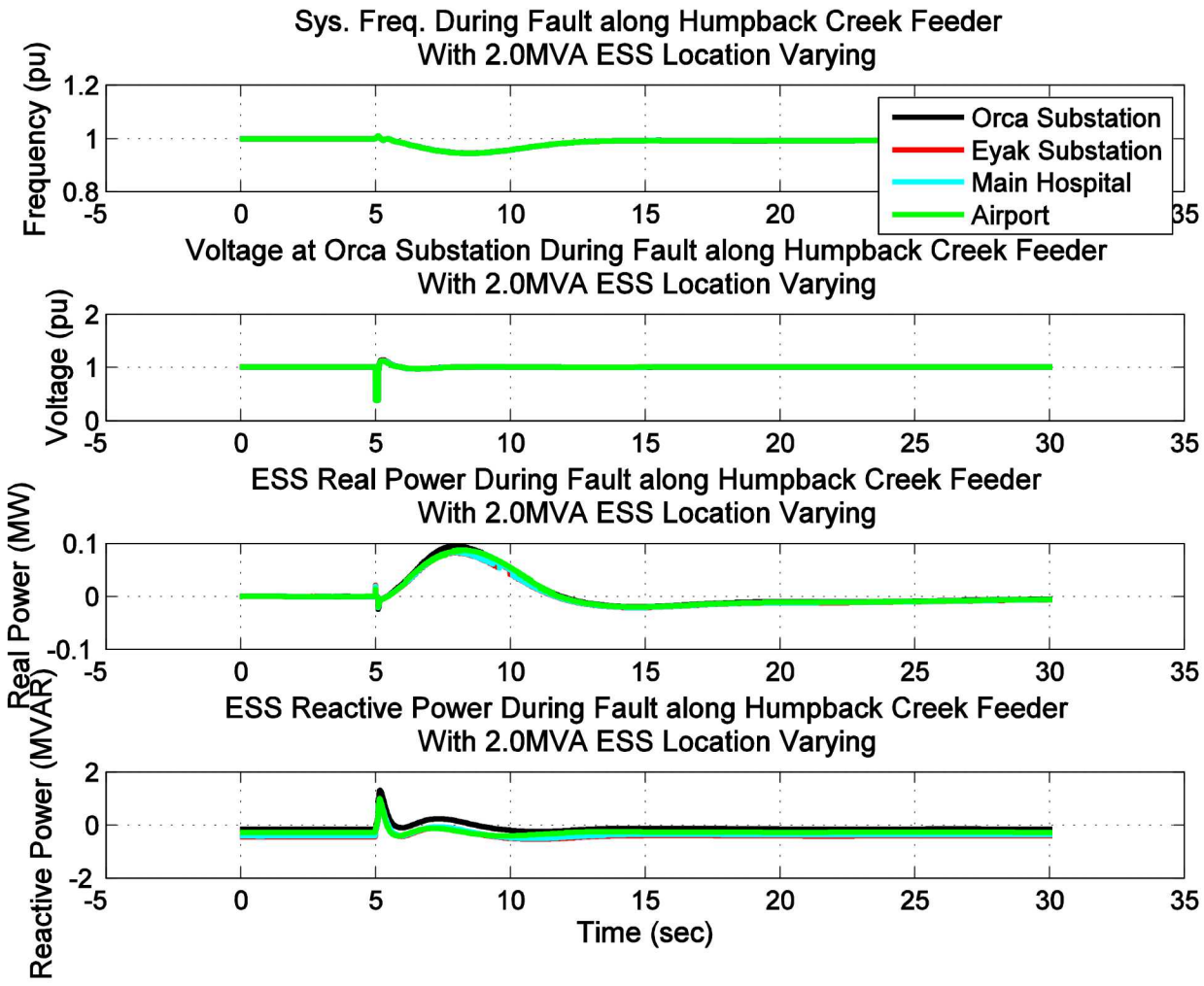

Figure 267 - Dynamic simulation results of 2.0MVA ESS at various locations during Humpback Creek feeder fault

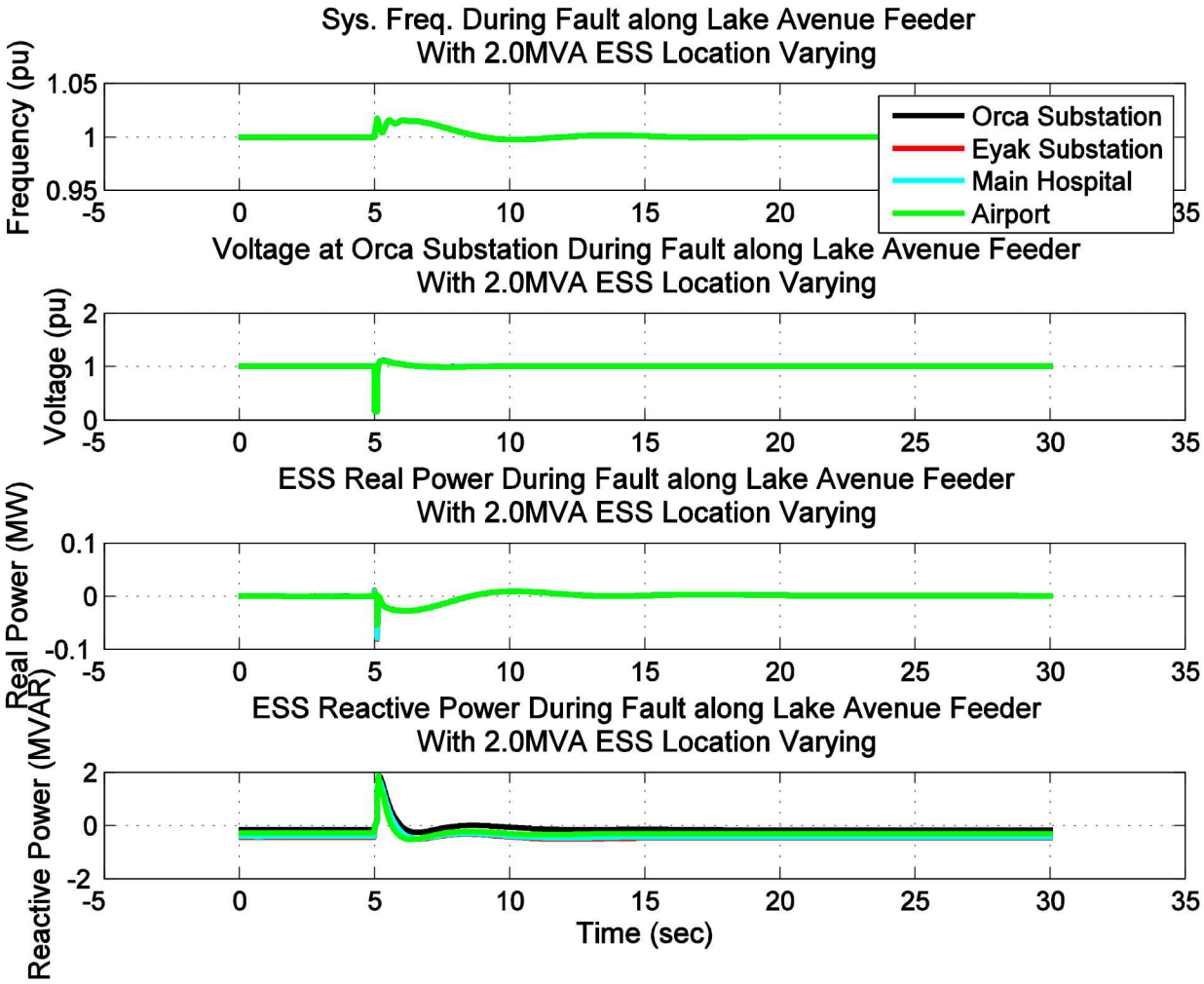

Figure 268 - Dynamic simulation results of 2.0MVA ESS at various locations during Lake Avenue feeder fault

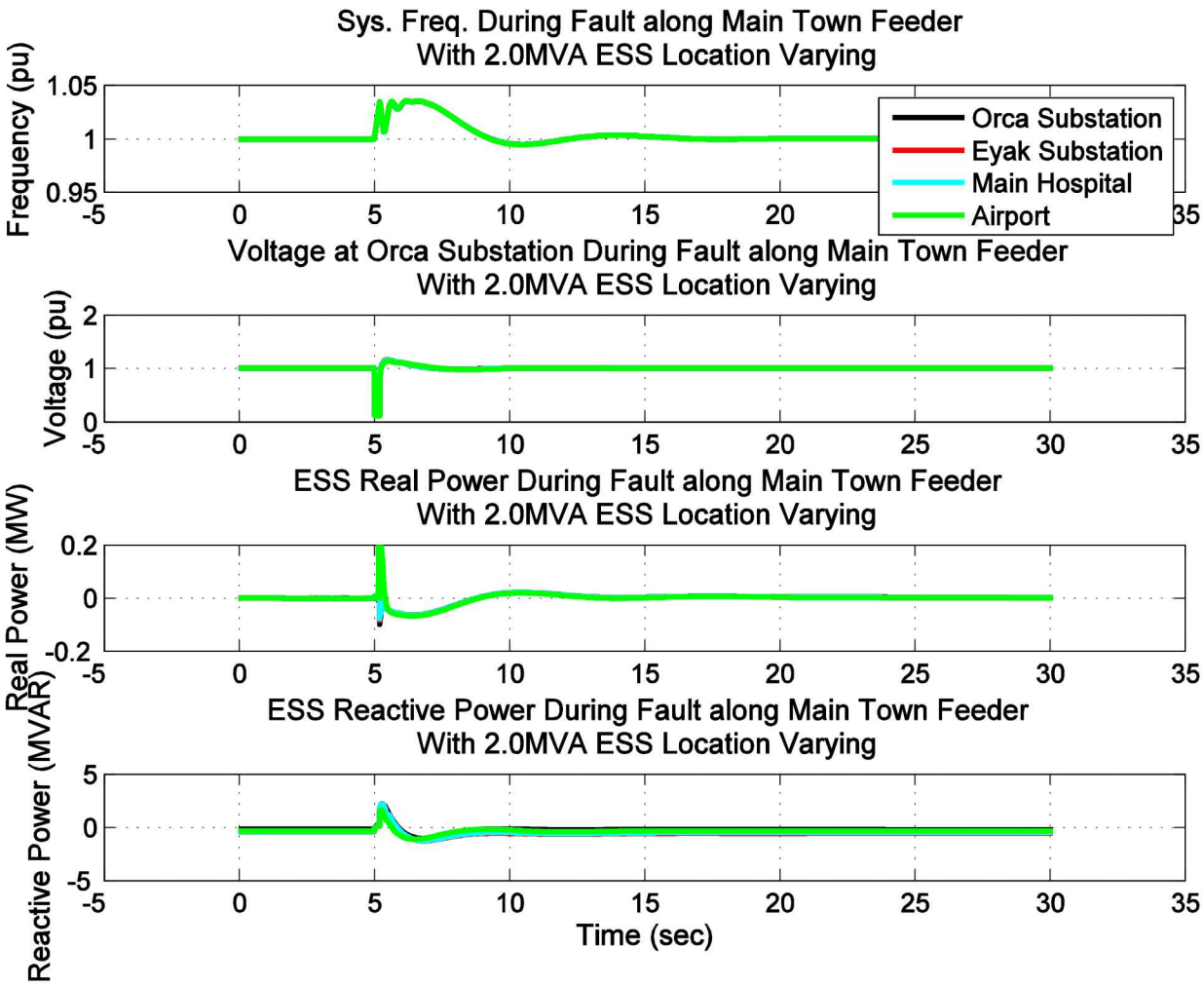

Figure 269 - Dynamic simulation results of 2.0MVA ESS at various locations during a Main Town feeder fault

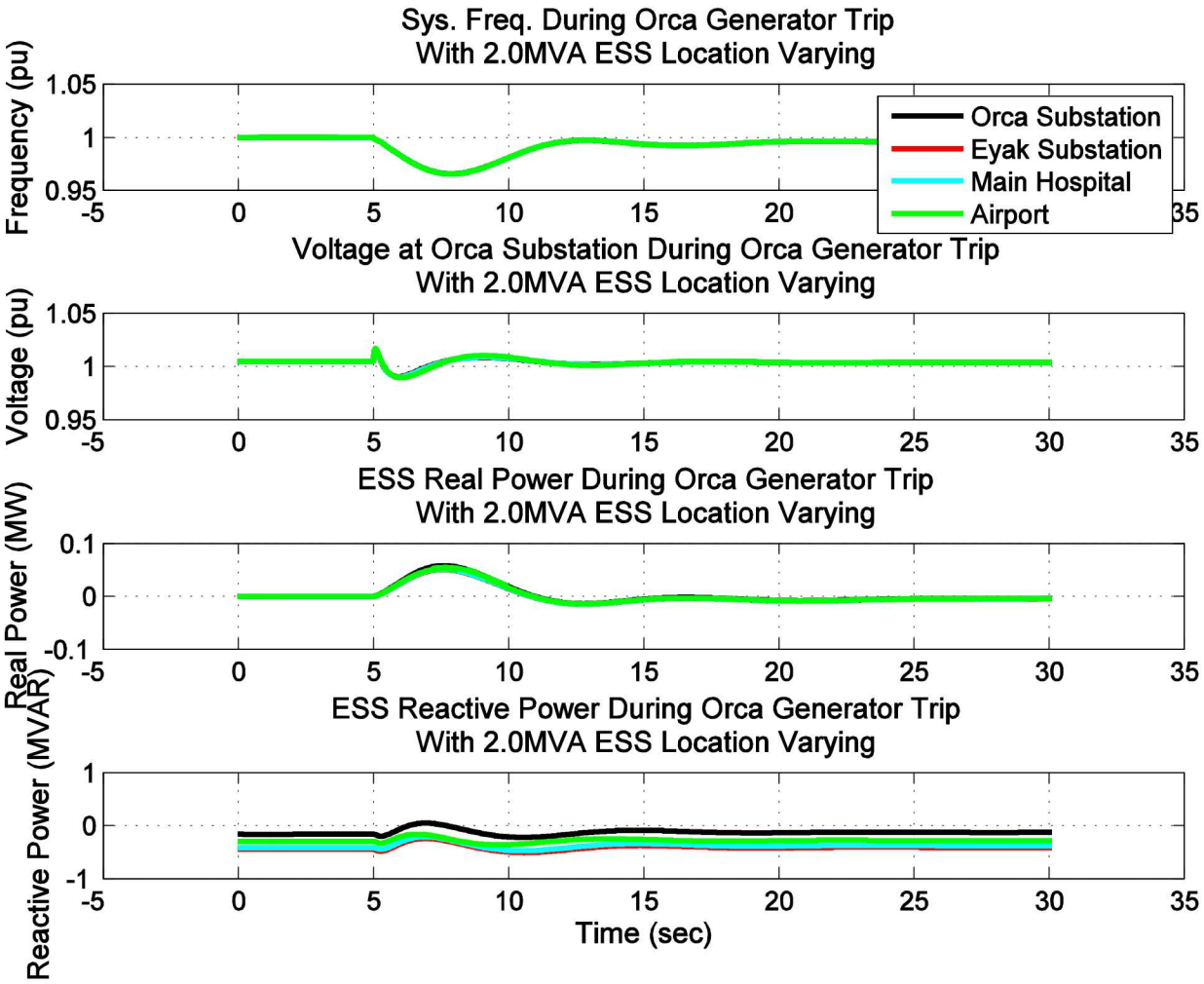

Figure 270 - Dynamic simulation results of 2.0MVA ESS at various locations during a generator trip

Results

3.0 MVA ESS During Electrical Transient

A PSLF simulation was performed with the ESS rating set to 3.0 MVA, placed in one of four locations within the CEC Grid, and one of four electrical transient was applied. The same rated MVA ESS was then moved to another one of the four locations and the same electrical transient was simulated. This simulation was run two more times with the same rated MVA ESS in the other two locations. Locations of the ESS were based off the input from CEC in regards to available space which were the Orca Substation, Eyak Substation, Main Hospital, and Airport. Electrical transient that were performed are fault along the Humpback Creek Feeder, fault along the Main Town feeder, fault along the Lake Avenue feeder and a generator trip at the Orca Power Plant. The figures below show the results from the simulations comparing the 3.0 MVA ESS at the different locations during various electrical transients.

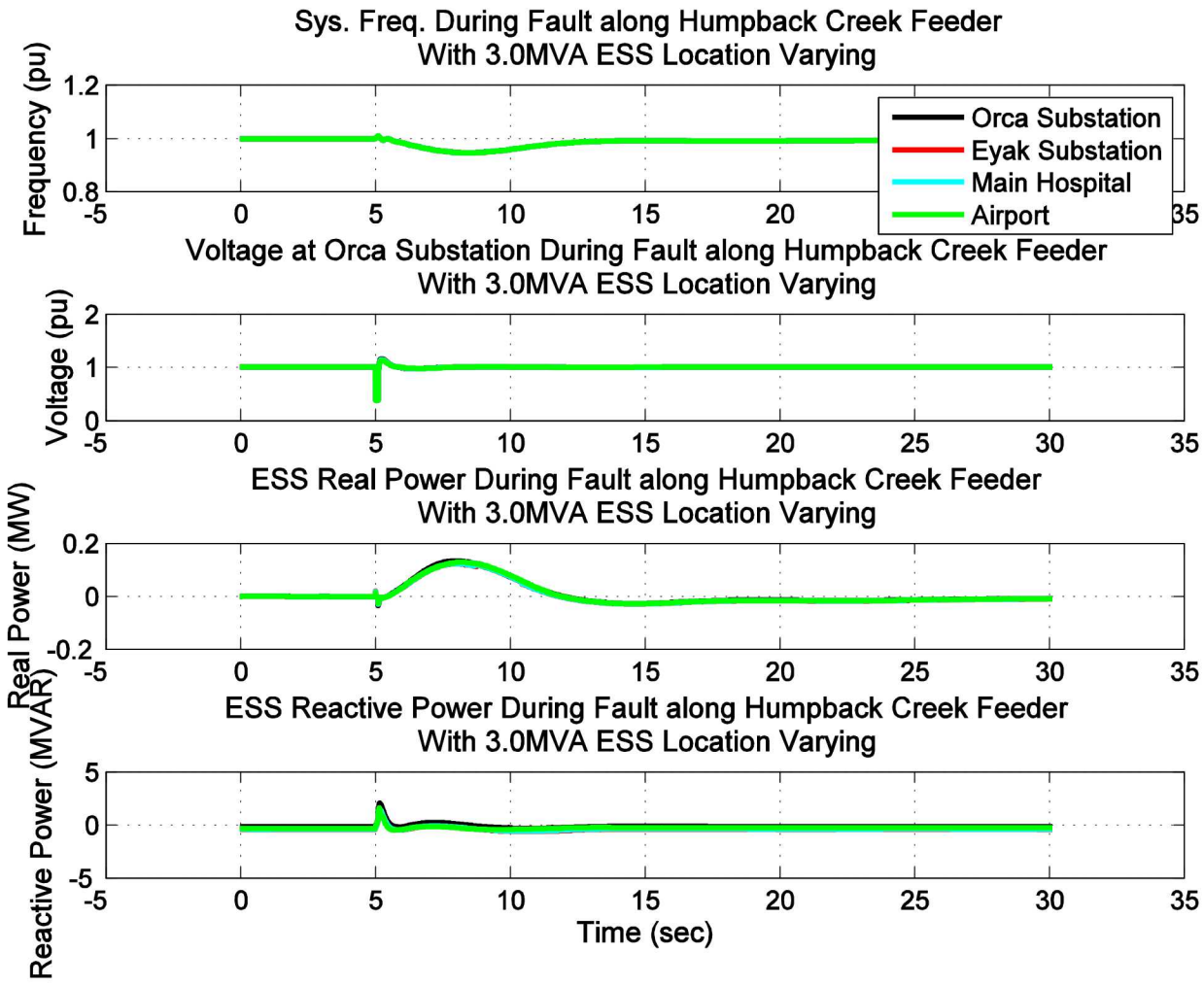

Figure 271 - Dynamic simulation results of 3.0MVA ESS at various locations during a Humpback Creek feeder fault

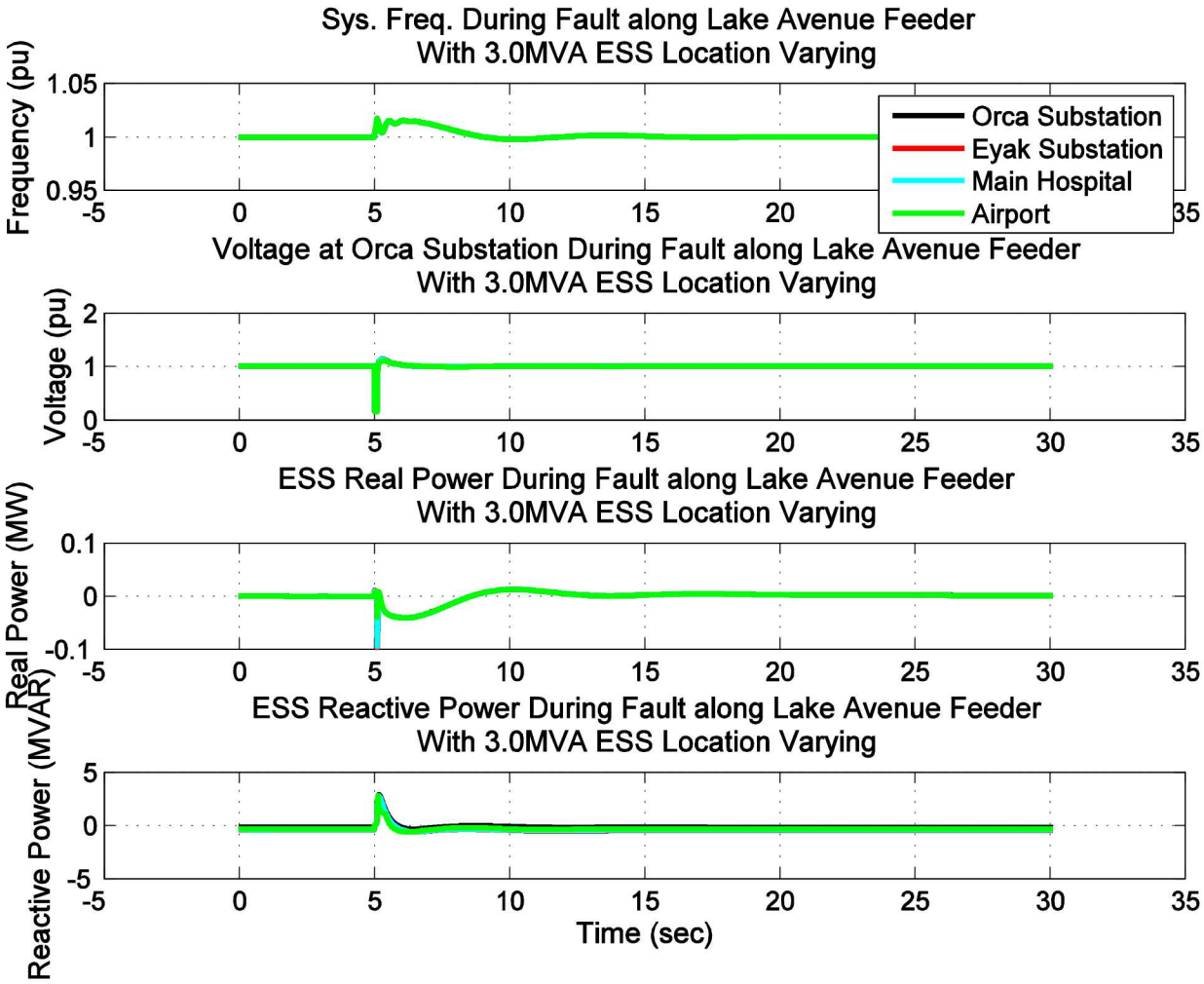

Figure 272 - Dynamic simulation results of 3.0MVA ESS at various locations during a Lake Avenue feeder fault

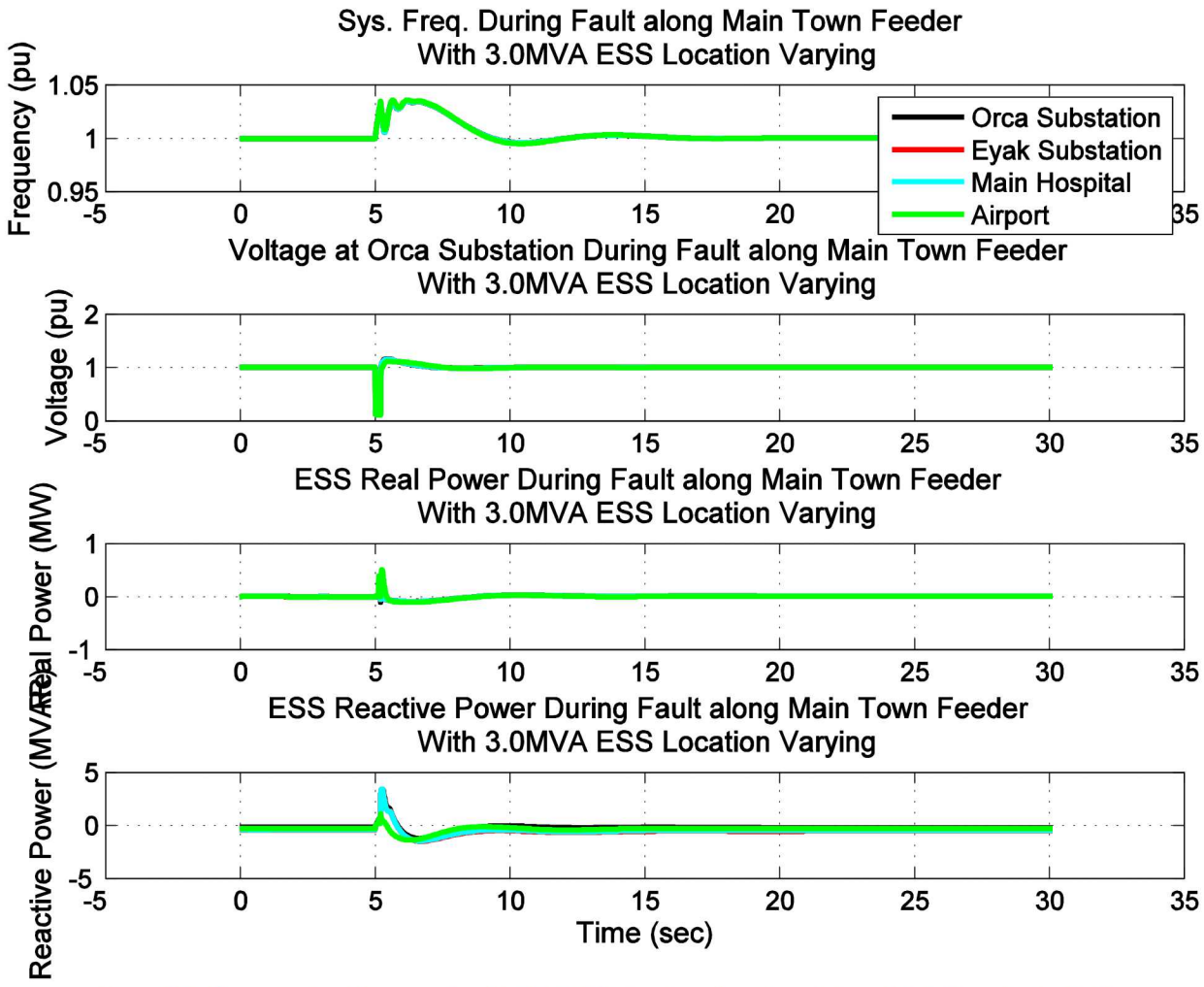

Figure 273 - Dynamic simulation results of 3.0MVA ESS at various locations during a Main Town feeder fault

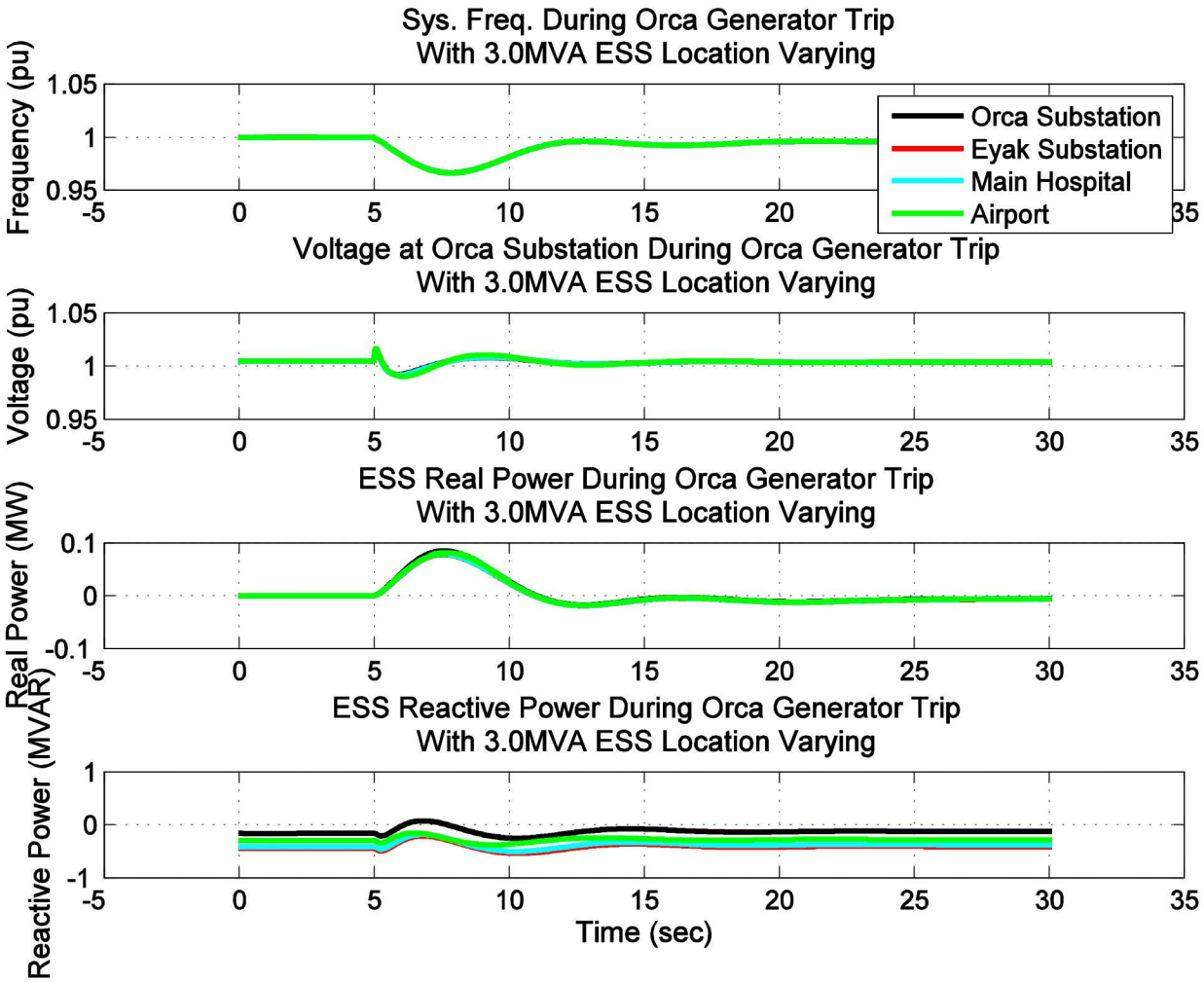

Figure 274 - Dynamic simulation results of 3.0MVA ESS at various locations during a generator trip

4.0 MVA ESS During Electrical Transient

A PSLF simulation was performed with the ESS rating set to 4.0 MVA, placed in one of four locations within the CEC Grid, and one of four electrical transient was applied. The same rated MVA ESS was then moved to another one of the four locations and the same electrical transient was simulated. This simulation was run two more times with the same rated MVA ESS in the other two locations. Locations of the ESS were based off the input from CEC in regards to available space which were the Orca Substation, Eyak Substation, Main Hospital, and Airport. Electrical transient that were performed are fault along the Humpback Creek Feeder, fault along the Main Town feeder, fault along the Lake Avenue feeder and a generator trip at the Orca Power Plant. The figures below show the results from the simulations comparing the 4.0 MVA ESS at the different locations during various electrical transients.

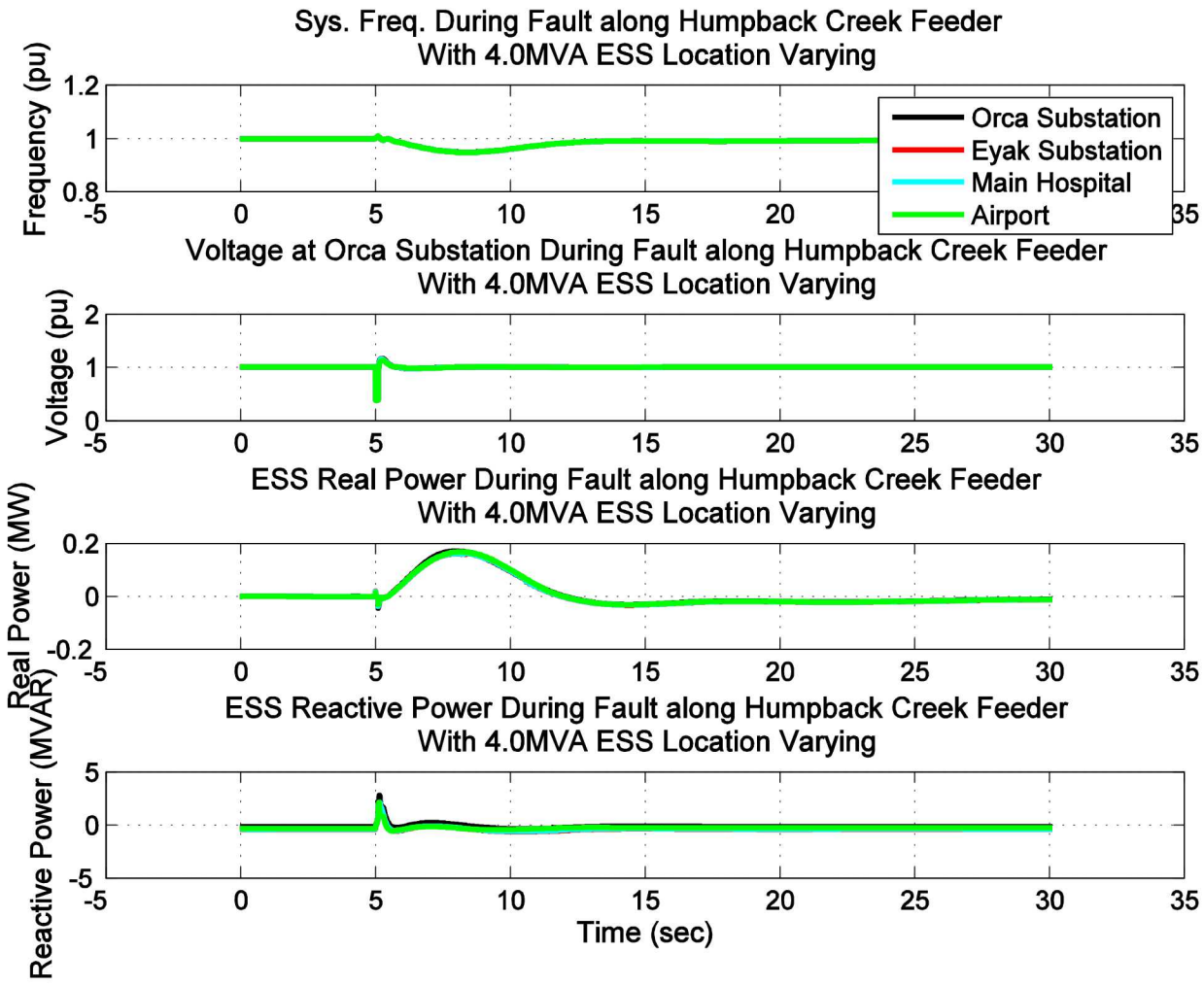

Figure 275 - Dynamic simulation results of 4.0MVA ESS at various locations during a Humpback Creek feeder fault

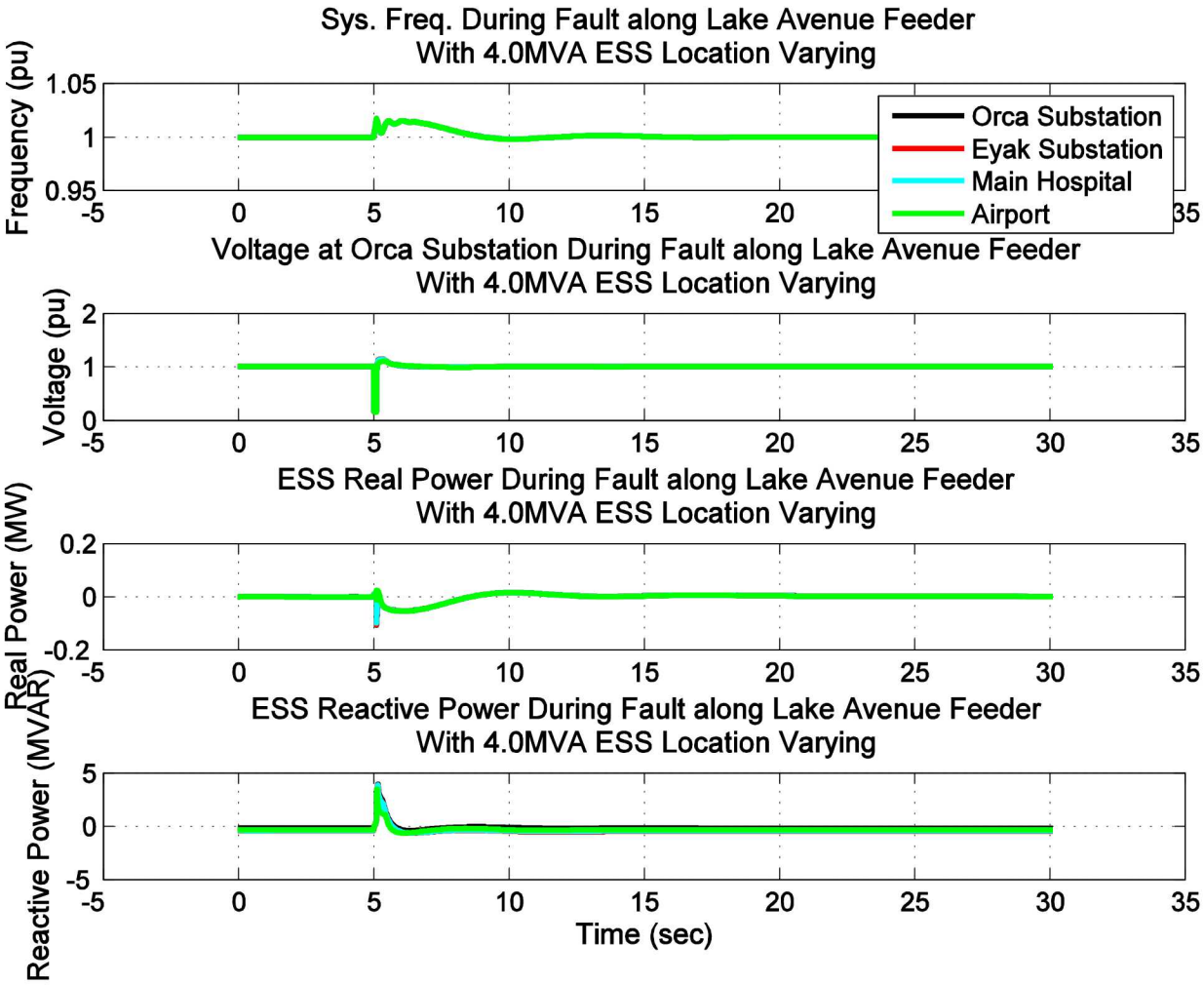

Figure 276 - Dynamic simulation results of 4.0MVA ESS at various locations during a Lake Avenue feeder fault

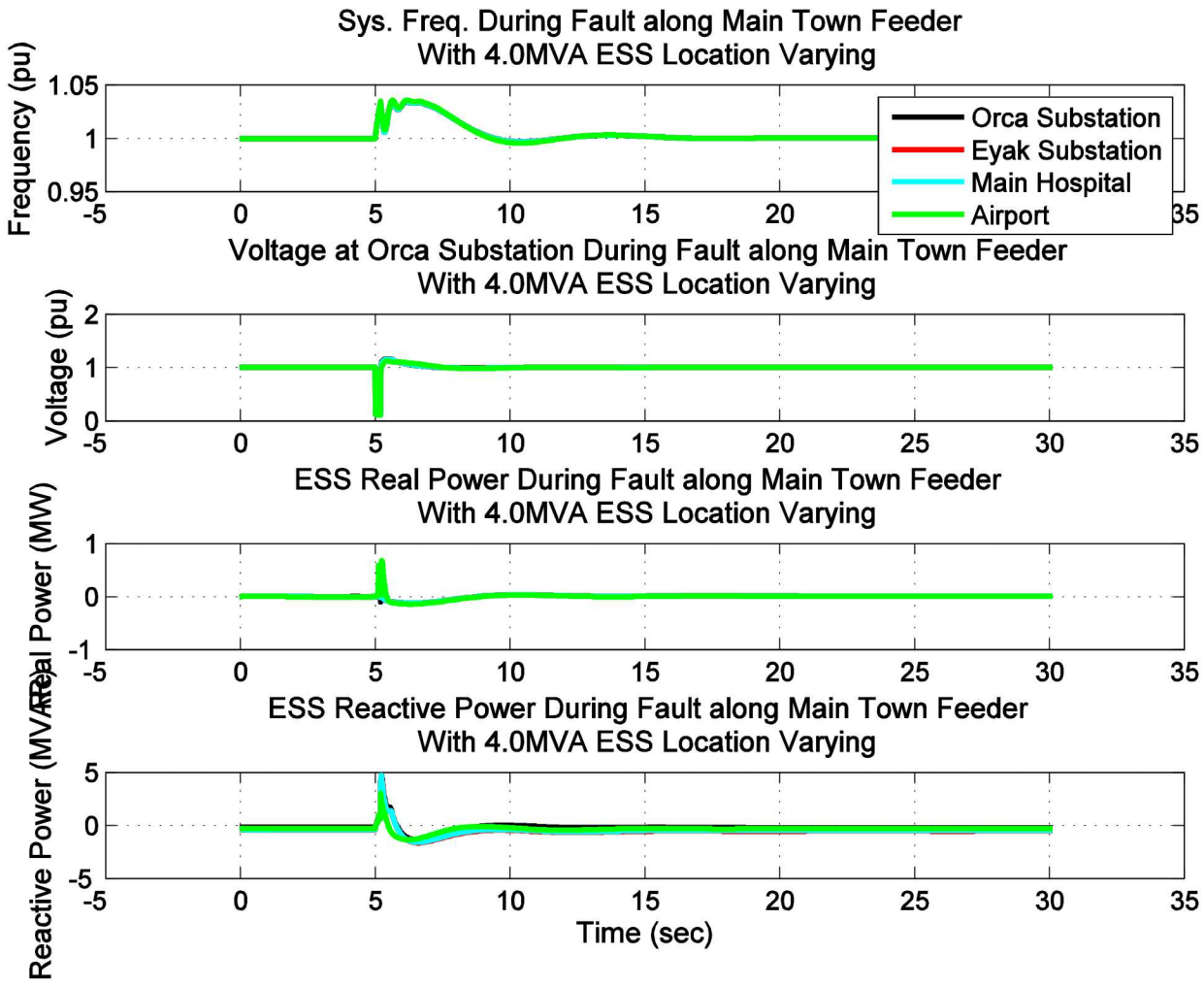

Figure 277 - Dynamic simulation results of 4.0MVA ESS at various locations during a Main Town feeder fault

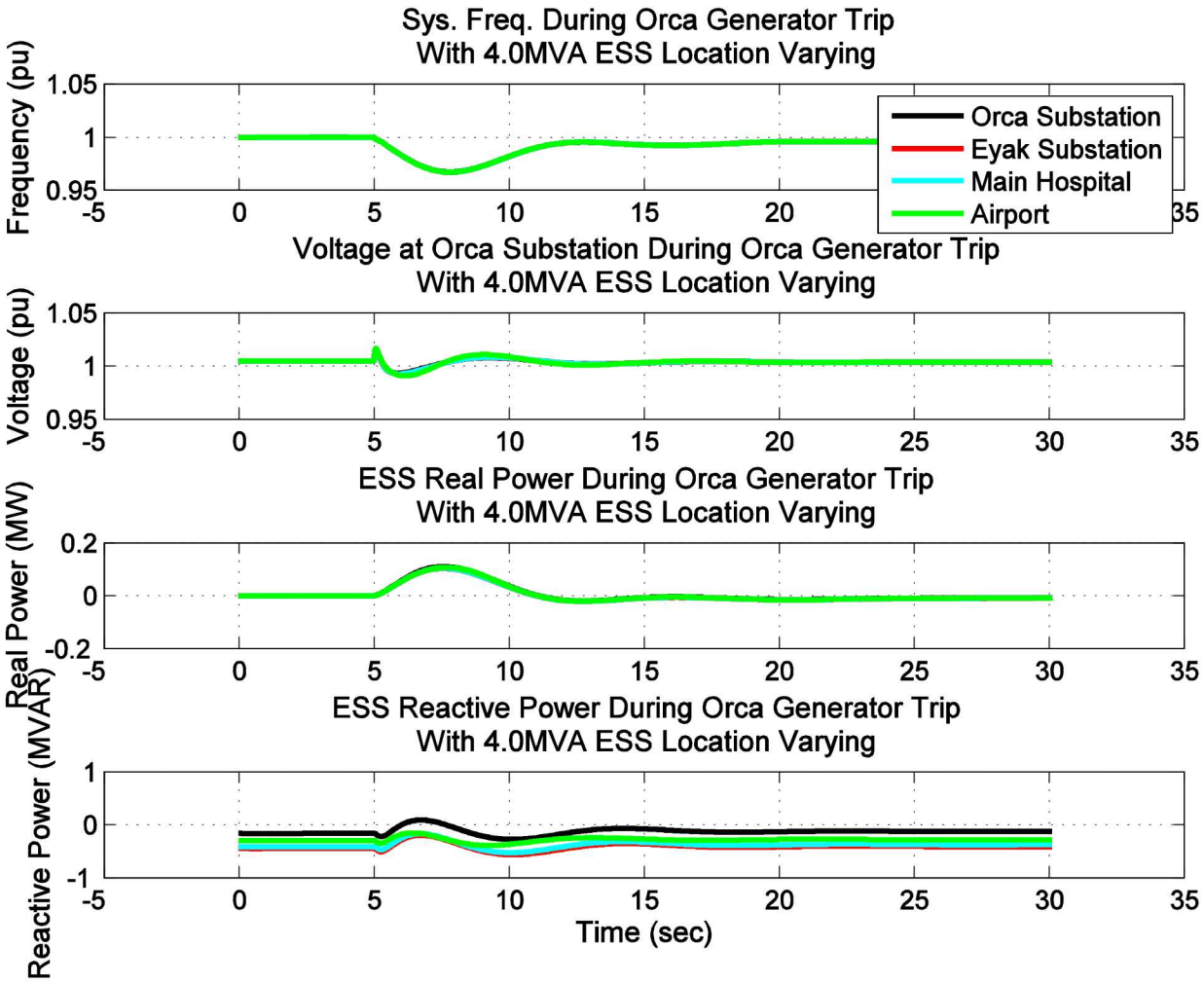

Figure 278 - Dynamic simulation results of 4.0MVA ESS at various locations during a generator trip

Results

Increasing the MVA rating of the ESS did not have a significant damping effect during the faults or generator trip electrical disturbances. Location of the ESS did not have a significant affect as well in damping the electrical transients. Even though the ESS did not provide significant damping of the electrical transients, it did provide some damping and did not harm the CEC electrical grid. Since size and location did not provide significant damping of the electrical transients, the size of the ESS will be based on the energy balance model and the location will be based off societal benefit.

[PAGE LEFT INTENTIONALLY BLANK]

DISTRIBUTION

1 Alaska Center for Energy and Power
University of Alaska Fairbanks
P.O. Box 7559-10
Fairbanks, Alaska 99775-5910

2 Cordova Electric Cooperative
705 Second Street
P.O. Box 20
Cordova, Alaska 99574

3	MS1108	Benjamin Schenkman	08811
4	MS1108	Dan Borneo	08811
5	MS1033	Abraham Ellis	08812
6	MS1188	Michael Baca	08813
7	MS1108	Babu Chalamala	08811
8	MS0899	Technical Library	9536 (electronic copy)


Sandia National Laboratories